

Dimensjonering, analyse og testing av inserts i karbonfiber kompositt sandwich chassis

Henrik Haugum

Morten Pløen

Master i produktutvikling og produksjon
Innlevert: september 2014
Hovedveileder: Nils Petter Vedvik, IPM

Norges teknisk-naturvitenskapelige universitet
Institutt for produktutvikling og materialer

THE NORWEGIAN UNIVERSITY
OF SCIENCE AND TECHNOLOGY
DEPARTMENT OF ENGINEERING DESIGN
AND MATERIALS

**MASTER THESIS SPRING 2014
FOR
STUD.TECHN. MORTEN PLØEN**

**DESIGN, ANALYSIS AND TESTING OF JOINTS ON CARBON FIBER COMPOSITE
SANDWICH CHASSIS**

Revolve NTNU shall participate in Formula Student with a carbon fiber composite chassis. The monocoque chassis is based on a sandwich structure design where suspension, gearbox and other parts of the assembly are joined to the sandwich structure by combinations for mechanical and adhesive joints. Inserts are commonly used to carry localized loads in sandwich structures. Analysis and research of the regions of the chassis subjected to concentrated loads will be the main objective of this thesis. Detailed tasks may include

1. Study of insert and sandwich theory
2. Identify the critical load cases on the chassis.
3. Modeling and submodeling of the structure and the joints
4. Finite element analysis
5. Experimental research and testing of load carrying capacity of the structure and the solutions for joints
6. Evaluation of results with respect to traditional insert and sandwich theory
7. Optimization of insert size and geometry
8. Fatigue analysis

The tasks given shall be considered as tentative. A detailed plan shall be made within the first 3 weeks of the project, indicating how the work will be distributed among the members of the project.

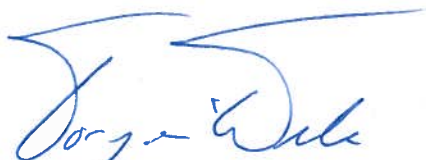
Three weeks after start of the thesis work, an A3 sheet illustrating the work is to be handed in. A template for this presentation is available on the IPM's web site under the menu "Masteroppgave" (<http://www.ntnu.no/ipm/masteroppgave>). This sheet should be updated one week before the Master's thesis is submitted.

Performing a risk assessment of the planned work is obligatory. Known main activities must be risk assessed before they start, and the form must be handed in within 3 weeks of receiving the problem text. The form must be signed by your supervisor. All projects are to be assessed, even theoretical and virtual. Risk assessment is a running activity, and must be carried out before starting any activity that might lead to injury to humans or damage to materials/equipment or the external environment. Copies of signed risk assessments should also be included as an appendix of the finished project report.

The thesis should include the signed problem text, and be written as a research report with summary both in English and Norwegian, conclusion, literature references, table of

contents, etc. During preparation of the text, the candidate should make efforts to create a well arranged and well written report. To ease the evaluation of the thesis, it is important to cross-reference text, tables and figures. For evaluation of the work a thorough discussion of results is appreciated.

The thesis shall be submitted electronically via DAIM, NTNU's system for Digital Archiving and Submission of Master's thesis.



Torgeir Welo
Head of Division



Nils Petter Vedvik
Professor/Supervisor



NTNU
Norges teknisk-
naturvitenskapelige universitet
Institutt for produktutvikling
og materialer

THE NORWEGIAN UNIVERSITY
OF SCIENCE AND TECHNOLOGY
DEPARTMENT OF ENGINEERING DESIGN
AND MATERIALS

**MASTER THESIS SPRING 2014
FOR
STUD. TECHN. HENRIK HAUGUM**

**DESIGN, ANALYSIS AND TESTING OF JOINTS ON CARBON FIBER COMPOSITE
SANDWICH CHASSIS**

Revolve NTNU shall participate in Formula Student with a carbon fiber composite chassis. The monocoque chassis is based on a sandwich structure design where suspension, gearbox and other parts of the assembly are joined to the sandwich structure by combinations for mechanical and adhesive joints. Inserts are commonly used to carry localized loads in sandwich structures. Analysis and research of the regions of the chassis subjected to concentrated loads will be the main objective of this thesis. Detailed tasks may include

1. Study of insert and sandwich theory
2. Identify the critical load cases on the chassis.
3. Modeling and submodeling of the structure and the joints
4. Finite element analysis
5. Experimental research and testing of load carrying capacity of the structure and the solutions for joints
6. Evaluation of results with respect to traditional insert and sandwich theory
7. Optimization of insert size and geometry
8. Fatigue analysis

The tasks given shall be considered as tentative. A detailed plan shall be made within the first 3 weeks of the project, indicating how the work will be distributed among the members of the project.

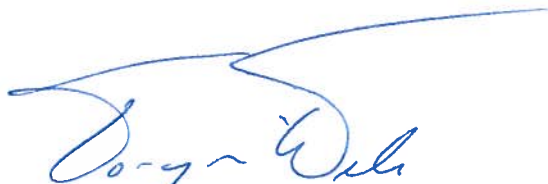
Three weeks after start of the thesis work, an A3 sheet illustrating the work is to be handed in. A template for this presentation is available on the IPM's web site under the menu "Masteroppgave" (<http://www.ntnu.no/ipm/masteroppgave>). This sheet should be updated one week before the Master's thesis is submitted.

Performing a risk assessment of the planned work is obligatory. Known main activities must be risk assessed before they start, and the form must be handed in within 3 weeks of receiving the problem text. The form must be signed by your supervisor. All projects are to be assessed, even theoretical and virtual. Risk assessment is a running activity, and must be carried out before starting any activity that might lead to injury to humans or damage to materials/equipment or the external environment. Copies of signed risk assessments should also be included as an appendix of the finished project report.

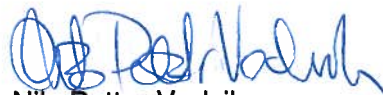
The thesis should include the signed problem text, and be written as a research report with summary both in English and Norwegian, conclusion, literature references, table of

contents, etc. During preparation of the text, the candidate should make efforts to create a well arranged and well written report. To ease the evaluation of the thesis, it is important to cross-reference text, tables and figures. For evaluation of the work a thorough discussion of results is appreciated.

The thesis shall be submitted electronically via DAIM, NTNU's system for Digital Archiving and Submission of Master's thesis.



Torgeir Welo
Head of Division



Nils Petter Vedvik
Professor/Supervisor



NTNU
Norges teknisk-
naturvitenskapelige universitet
Institutt for produktutvikling
og materialer

THE NORWEGIAN UNIVERSITY
OF SCIENCE AND TECHNOLOGY
DEPARTMENT OF ENGINEERING DESIGN
AND MATERIALS

**MASTER THESIS SPRING 2014
FOR
STUD.TECHN. MORTEN PLØEN**

**DESIGN, ANALYSIS AND TESTING OF CARBON FIBER COMPOSITE SANDWICH
CHASSIS FOR REVOLVE NTNU**

Revolve NTNU shall participate in Formula Student with a carbon fiber composite chassis. Design and analysis of the chassis with regards to strength and stiffness is key for making a safe and fast car. The monocoque chassis is based on a sandwich structure design where suspension, gearbox and other parts of the assembly are joined to the sandwich structure by combinations of mechanical and adhesive joints. Inserts are commonly used to carry localized loads in sandwich structures. Analysis and research of the regions of the chassis subjected to concentrated loads along with optimization of the chassis with respect to FSAE regulations and overall stiffness/strength will be the focus of this thesis. The goal of this thesis should be to make a substantial contribution for Revolve NTNUs coming chassis designs.

The thesis may include the following tasks/goals:

1. Study of insert and sandwich theory
2. Identify the critical load cases on the chassis.
3. Finite element analysis of chassis with respect to overall stiffness and strength.
4. Layup optimization for weight and overall stiffness and strength.
5. Experimental research and testing of load carrying capacity of the structure and the solutions for joints.
6. Evaluation of results with respect to traditional insert and sandwich theory
7. Design of insert size and geometry
8. Manufacture of monocoque chassis

The tasks given shall be considered as tentative. A detailed plan shall be made within the first 3 weeks of the project, indicating how the work will be distributed among the members of the project.

Three weeks after start of the thesis work, an A3 sheet illustrating the work is to be handed in. A template for this presentation is available on the IPM's web site under the menu "Masteroppgave" (<http://www.ntnu.no/ipm/masteroppgave>). This sheet should be updated one week before the Master's thesis is submitted.

Performing a risk assessment of the planned work is obligatory. Known main activities must be risk assessed before they start, and the form must be handed in within 3 weeks of receiving the problem text. The form must be signed by your supervisor. All projects are to be assessed, even theoretical and virtual. Risk assessment is a running activity, and must be

carried out before starting any activity that might lead to injury to humans or damage to materials/equipment or the external environment. Copies of signed risk assessments should also be included as an appendix of the finished project report.

The thesis should include the signed problem text, and be written as a research report with summary both in English and Norwegian, conclusion, literature references, table of contents, etc. During preparation of the text, the candidate should make efforts to create a well arranged and well written report. To ease the evaluation of the thesis, it is important to cross-reference text, tables and figures. For evaluation of the work a thorough discussion of results is appreciated.

The thesis shall be submitted electronically via DAIM, NTNU's system for Digital Archiving and Submission of Master's thesis.

The contact person is (navn på veileder i utlandet, bedrift eller lignende)

Torgeir Welo
Head of Division

Nils Petter Vedvik
Professor/Supervisor



ABSTRACT

The work presented in this thesis, has been carried out as a comprehensive work on different aspects of the development of a monocoque chassis. Design, analysis and production of a Formula Student monocoque chassis are the main topics in this thesis. Focus have been on describing the approach in the design phase as well as analysis and testing of localized loads on sandwich panels. A production process for the monocoque chassis has also been developed.

A significant part of the work has been design, analysis and testing of localized loads on insert sandwich panels, focused around a race car chassis for Revolve NTNU, with related loads and design challenges. Most of the insert theory described and used in the thesis is based on empirical results. Production of the sandwich structure, including evaluation and validation of the structure is also included as a part of the work.

OBJECTIVES

The overall goal of this thesis is to get a better understanding of how localized loads interact with a sandwich structure, in this case a monocoque chassis. Focus will be on reducing risks and optimize the design of joints on future Revolve NTNU race car chassis. There will be a focus on sandwich technology, insert theory, and adhesive technology.

Detailed tasks for this thesis include:

- Study of insert and sandwich theory
- Identification and analysis of critical loads on the chassis
- Modeling and FEA of the structure and its joints
- Experimental research and testing of load carrying capacity of the structure and its joints
- Evaluation of results
- Fatigue analysis
- Production process of the monocoque chassis

SAMMENDRAG

I arbeidet med denne avhandlingen har det blitt utført et omfattende arbeid på ulike aspekter ved utviklingen av et monocoque chassis designet for å konkurrere i Formula Student. Analyse, dimensjonering og produksjon er hovedtema i denne oppgaven. Fokuset har ligget i å beskrive den tilnærmingen som brukes i designfasen, analyse og testing av lokaliserte laster på sandwichpaneler, samt utvikle en produksjonsprosess for chassiset.

Alt av dimensjonering, analyse og testing er utført på sandwich paneler representativt for et monocoque chassis. Hovedfokuset har vært et racerbilchassis for Revolve NTNU, med tilhørende laster. Monocoque-chassiset er en selvberende konstruksjon hvor hjuloppheng, girkasse, veltebøyler og andre innfestninger går direkte i chassiset som tar opp alle kreftene.

Mye av arbeidet har blitt gjort i analyse og eksperimentell testing av lokaliserte laster på sandwich paneler med såkalte “inserts”, da dette er den mest brukte metoden for å overføre laster inn på et skjærsvakt sandwichpanel.

Eksperimenter og testing har vært en stor del av denne avhandlingen. Den meste av teorien som er beskrevet og brukt i denne oppgaven er også basert på empiriske resultater. Mye av arbeidet har bestått av den faktiske produksjon av strukturen, og tilhørende måling og verifisering av strukturen.

CONTENTS

| | |
|--|-----------|
| CHAPTER 1 BACKGROUND..... | 1 |
| 1.1 FORMULA STUDENT AND REVOLVE NTNU | 1 |
| 1.2 MONOCOQUE CHASSIS | 3 |
| 1.2.1 History | 3 |
| 1.2.2 Pro's and Con's | 5 |
| 1.2.3 Design challenges | 7 |
| CHAPTER 2 CHASSIS LOADS | 8 |
| 2.1 RULE REGULATED LOADS AND ATTACHMENTS..... | 8 |
| <i>Baseline material</i> | 9 |
| 2.1.1 Monocoque General Requirements | 10 |
| 2.2 NON-RULE REGULATED LOADS AND ATTACHMENTS | 12 |
| CHAPTER 3 THEORY | 18 |
| 3.1 SANDWICH THEORY | 18 |
| 3.2 INSERT THEORY | 23 |
| 3.2.1 Out of plane loading | 26 |
| 3.2.2 In-plane loading..... | 27 |
| 3.2.3 Bending and torsional loads | 28 |
| 3.2.4 Total capacity | 29 |
| 3.3 FAILURE MODES..... | 30 |
| 3.3.1 Facesheet yield | 30 |
| 3.3.2 Intracell buckling | 31 |
| 3.3.3 Facesheet wrinkling | 31 |
| 3.3.5 Shear crimping..... | 32 |
| 3.3.6 Core shear..... | 33 |
| 3.3.7 Local indentation | 34 |
| CHAPTER 4 ANALYSIS | 37 |
| | 37 |
| 4.1 MATERIAL ANALYSIS | 37 |
| 4.2 BENDING ANALYSES | 42 |
| 4.3 INSERT ANALYSIS | 44 |
| 4.3.1 Out-of-plane | 45 |

| | |
|---|-----------|
| 4.3.2 <i>Bending</i> | 48 |
| 4.4 TORSIONAL STIFFNESS ANALYSIS..... | 54 |
| CHAPTER 5 TESTING | 58 |
| 5.1 RULE-REGULATED TESTING..... | 58 |
| 5.2 INSERT TESTING | 58 |
| 5.2.1 <i>Test samples</i> | 58 |
| 5.2.2 <i>Test setup and test procedure</i> | 60 |
| 5.2.3 <i>Out of plane test results</i> | 62 |
| 5.2.4 <i>Insert bending test results</i> | 66 |
| 5.2.5 <i>Fatigue testing</i> | 67 |
| CHAPTER 6 EVALUATION | 70 |
| 6.1 VALIDATION OF RESULTS..... | 70 |
| 6.1.1 <i>Evaluation of theoretical and experimental stiffness</i> | 70 |
| 6.1.2 <i>Evaluation of failure loads and failure behavior</i> | 73 |
| 6.1.3 <i>Failure modes</i> | 74 |
| 6.1.4 <i>Sources of error</i> | 75 |
| 6.2 FURTHER DISCUSSION | 75 |
| CHAPTER 7 PRODUCTION | 76 |
| 7.1 INITIAL PROCESS..... | 76 |
| 7.2 PRECISION AND QUALITY..... | 77 |
| 7.3 SANDWICH BONDING..... | 81 |
| 7.3 PRODUCTION EVALUATION..... | 87 |
| CHAPTER 8 CONCLUSION..... | 88 |
| CHAPTER 9 FURTHER WORK..... | 89 |
| CHAPTER 10 REFERENCES..... | 90 |

LIST OF FIGURES

| | |
|--|----|
| Figure 1.1: Events in fomula student | 1 |
| Figure 1.2: KA Borealis R (2012, top) and KA Aquilo R (2013, below) | 2 |
| Figure 1.3: Murphy Moose homebuilt aircraft under construction | 3 |
| Figure 1.4: McLaren mp4/1c | 4 |
| Figure 1.5: Monocoque chassis of Audi R18 | 5 |
| Figure 1.7: Comparison of monocoque chassis and steel space frame | 6 |
| Figure 2.1: Primary structure..... | 8 |
| Figure 2.2: Monocoque side impact | 9 |
| Figure 2.4: Top-view of suspension FE-model | 14 |
| Figure 2.5: Side-view of suspension FE-model | 15 |
| Figure 2.6: Legend for figure 2.4 and 2.5. | 15 |
| Figure 2.7: Resultant reaction forces - 2g brake. | 16 |
| Figure 3.1: Sandwich structure..... | 18 |
| Figure 3.2: Sandwich panel 3pt bending | 19 |
| Figure 3.3: Affected region of local load | 23 |
| Figure 3.4: Potting radius | 25 |
| Figure 3.5: Inclined load on insert | 29 |
| Figure 3.6: Facesheet yield..... | 30 |
| Figure 3.7: Intracell buckling | 31 |
| Figure 3.8: Facesheet wrinkling | 31 |
| Figure 3.9:Shear crimping..... | 32 |
| Figure 3.1: Core shear | 33 |
| Figure 3.11:Shear-loading of core..... | 33 |
| Figure 3.12: Local indentation | 34 |
| Figure 3.13:Compressive and shear loading of core | 34 |
| Figure 3.14: Photographs of a sandwich beam under a 10 mm diameter central roller just prior to peak load and well after the peak load. | 35 |
| Figure 4.0: Different types of weave..... | 39 |
| Figure 4.1: 5056 flexcore | 41 |

| | |
|---|----|
| Figure 4.2: FE-analysis of 3pt bending panel showing max disp. 3.744mm. | 42 |
| Figure 4.3: FE-model of 3pt bending panel with constrains and loads..... | 43 |
| Figure 4.3: Load-displacement curve for different 3pt bending panels | 43 |
| Figure 4.4: Strain plot of the front suspension points on the monocoque, max strain of 0.02 just below front upper fore attachment point. | 44 |
| Figure 4.5: Strain plot of the rear end of the monocoque, max strain of 0.024 in front of rear upper fore attachment point..... | 45 |
| Figure 4.5: Surface to surface gluing | 46 |
| Figure 4.6: out-of-plane simply supported setup..... | 46 |
| Figure 4.7: Stress in ply1, 11-direction. | 47 |
| Figure 4.8: Shear stress in core around insert. | 47 |
| Figure: 4.9: Surface-to-durface gluing & surface-to-surface contact..... | 48 |
| Figure: 4.10: Insert calculation spreadsheet based on ESA insert design handbook. | 49 |
| Figure 4.11: Stress plot of core, insert bending test. | 50 |
| Figure 4.12: Displacement plot of insert bending test. | 51 |
| Figure 4.13: Strain around insert, insert bending test. | 52 |
| Figure 4.14: Bonding simulation, shear stress. | 53 |
| Figure 4.15: Deformation of chassis subjected to torsional load. First iteration with a result of 2200Nm/deg..... | 55 |
| Figure 4.16: Different layup-zones of the monocoque. | 55 |
| Figure 4.17: Torsional analysis with main hoop included, displaying the last iteration with a torsional stiffness of 3247Nm/deg. | 57 |
| Figure 5.1: Test samples from batch 2 after cure. | 59 |
| Figure 5.2: Insert bending test setup (left) and out of plane test setup (right). | 60 |
| Figure 5.3: Load-displacement curve for epoxy-potted insert samples | 62 |
| Figure 5.4: Repetitive testing of sample 6..... | 63 |
| Figure 5.5: Evidence of leaked potting material (left) and core shear failure (right)..... | 63 |
| Figure 5.6: Load-displacement curve for foam-potted out of plane samples, flexcore | 64 |
| Figure 5.8: Shear failure of core in sample OOP 11-3 (left) and sample OOP 14-3 (right) | 65 |
| Figure 5.9: Load-displacement curves for insert bending tests..... | 66 |
| Figure 5.10: Out of plane fatigue testing..... | 68 |
| Figure 5.11: Load-displacement curve for fatigue testing, sample insert bending 4-3..... | 69 |
| Figure 6.1: Experimental and theoretical load-displacement curves, out of plane test..... | 70 |

| | |
|--|----|
| Figure 6.2: Experimental and theoretical load-displacement curve, bending insert test..... | 71 |
| Figure 6.3: Strain plot of insert bending test at 3.8kN | 72 |
| Figure 6.4: Load strain for insert bending test | 72 |
| Figure 6.5: Shear-stress in core at 1.8kN. | 73 |
| Figure 6.6: Load-strain curve for sample OOP 11-3..... | 74 |
| Figure 7.1: Thermocouple readings for monocoque tooling..... | 79 |
| Figure 7.2: Thermocouple readings for monocoque outer facesheet. | 80 |
| Figure 7.3: Layup of tooling prepreg for the composite tool. | 81 |
| Figure 7.4: Machining of moulds | 82 |
| Figure 7.5: Liquid shim of insert..... | 83 |
| Figure 7.6: Cross section view of sandwich with insert..... | 83 |
| Figure 7.7: Layup of inner facesheet onto the core material..... | 84 |
| Figure 7.8: Placing of rohacell foam core in the rear end of the monocoque. | 85 |
| Figure 7.9: Bonding inserts to the outer facesheet in the front end of the monocoque..... | 85 |
| Figure 7.10: Layup of outer face sheet..... | 86 |

LIST OF TABLES

| | |
|---|----|
| Table 2.1: Base materials | 9 |
| Table 2.2: EI requirements | 10 |
| Table 2.3: Some properties of KOG Arctos R | 12 |
| Table 2.4: Wheel loads [N] for different load cases. | 13 |
| Table 2.5: Insert design loads..... | 17 |
| Table 4.1: Weave properties..... | 37 |
| Table 4.2: Properties of prepreg systems | 40 |
| Table 4.3: Properties of different 3pt. Bending panels..... | 42 |
| Table 4.4: Properties of core materials..... | 50 |
| Table 4.5: Typical chassis torsional stiffness FSAE | 54 |
| Table 4.6: Layup for the zones shown in fig. 4.16..... | 56 |
| Table 5.1: Insert test samples | 61 |
| Table 5.2: Out of plane fatigue testing, sample OOP 12-3 | 67 |
| Table 5.3: Bending fatigue testing, sample insert bending 4-3 | 68 |
| Table 7.1: Brief overview of the two most feasible tooling concepts | 76 |
| Table 7.2: Tooling layup and procedure | 78 |



CHAPTER 1

BACKGROUND

1.1 FORMULA STUDENT AND REVOLVE NTNU

Formula Student is a student engineering competition which has been held annually in Europe since 1998. The task is to design, build and compete with a one seated, open wheel, formula style racecar. The competitions take place at different locations all over the world. The largest competitions are held in Germany, Australia, Brazil, UK and the US. Around 200 000 students take part in these competitions every year, making it the largest engineering competition for students worldwide. The competitions encourage use of alternative fuels, hybrid and electric powertrain. The teams are evaluated on different aspects of their project, from the performance of the car to engineering design and cost analysis.

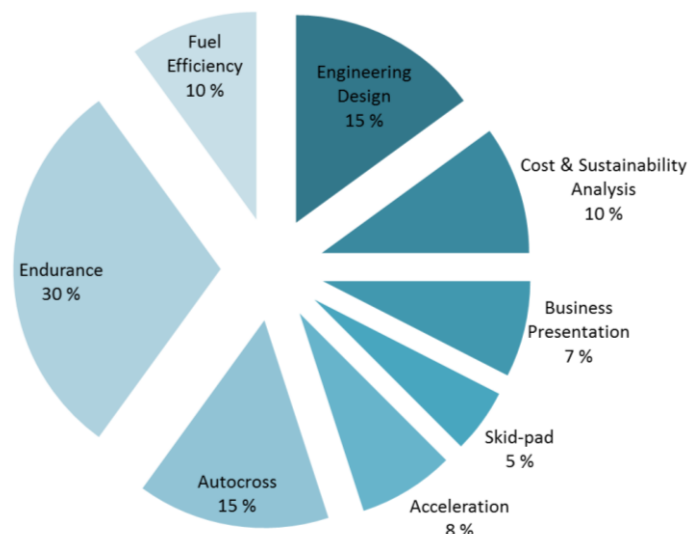


Figure 1.1: Events in fomula student

There are five dynamic and three static events, and the points are divided as shown in figure 1.1. With a maximum score in every event, it is possible to get 1000 points. The static events counts for 30% of the total score, while 70% of the points are achievable through the dynamic events.

Revolve NTNU was founded in 2010, and has participated in Formula Student in 2012 and 2013, with decent results. In 2014, the team will compete in FS UK and FS Germany. The team consists of 46 engineering students from more than ten different study programs and all

five year levels. Revolve NTNU have built their third car during the spring of 2014. Unlike previous years, Revolve NTNU will participate in Formula Student 2014 with a carbon fiber chassis. In addition to the new electric powertrain and the 10 inch wheels, this is one of the most significant changes from the car that was developed for the 2013 season (KA Aquilo R). The two first cars were built around a steel tubular spaceframe chassis, and were equipped with a 600cc internal combustion engine and 13 inch wheels.



Figure 1.2: KA Borealis R (2012, top) and KA Aquilo R (2013, below)

As mentioned, Revolve NTNU has used a tubular steel spaceframe chassis in their earlier cars. This has proven to be a good and reliable solution, so the advantages and disadvantages with a composite monocoque had to be closely evaluated. First of all, the main goal for any Formula Student team is to score as many points as possible in the competitions. This should be reflected in all important design decisions. Other important aspects to keep in mind are the learning outcome for the students and the degree of innovation. Revolve NTNU is always seeking to find new and innovative solutions.

To score as high as possible in the competitions, it is a necessity to have a quick car that can go fast around the track. Two important factors of critical load carrying components in a racecar is weight and stiffness. It is desirable to keep the weight low and have a reasonably high stiffness at the same time. A racecar is always accelerating, braking or turning. Given Newton's second law, $a=F/m$, it is clear that a heavy car would accelerate slower than a light car, given that they have the same traction forces available. A lighter car will also lower the stiffness requirements of load-carrying components. A sandwich structure well suited for structures where weight and high is important. It gives possibility for high stiffness-to-weight ratio, but adds complexity and requires a higher budget. A carbon fiber monocoque has therefor been under development during the Formulas Student 2014-season. The main focus on this thesis is the load carrying structure of the chassis, but there is additional design aspects

included in the thesis to give the reader a more thorough insight into the design of a race car chassis.

1.2 MONOCOQUE CHASSIS

Monocoque (mono- latin for “single”, coque- french for “shell”)

a type of construction (as of a fuselage) in which the outer skin carries all or a major part of the stresses

a type of vehicle construction (as of an automobile) in which the body is integral with the chassis

1.2.1 HISTORY

The monocoque structure has its roots from the early 1920s when a price drop in aluminum material made it possible to meet the demand for stiff, strong and lightweight sheets that could handle the stress due to an increasing power output from the newly designed airplanes. At the end of the Second World War, most high-tech aircrafts were build using a monocoque or semi-monocoque structure.

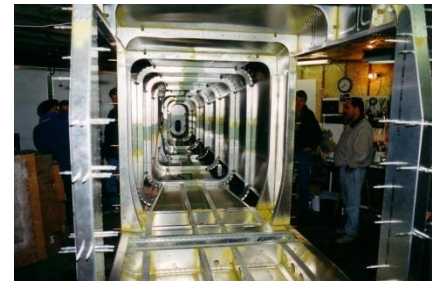


Figure 1.3: Murphy Moose homebuilt aircraft under construction

The use of the monocoque soon progressed into the automotive industry. The first monocoque was introduced I 1923 with the Lancia Lambda, but it wasn't until Nash Motors introduced their model 600 in 1941 that the monocoque actually started to take a hold in the automotive industry. Due to the monocoque structure, Nash Motors produced a vehicle, not only stronger and stiffer, but at the same time 500 pounds lighter than the typical body-on-chassis automobile. Today, monocoque or unibody construction, is so sophisticated in automobile manufacturing that the windshields often make a significant contribution to the structural strength of the vehicle.

The path to the current ‘safety capsule’ Formula One monocoque began in the early 1980s with the adoption of carbon fiber composite materials for chassis manufacture, although in the strict definition of the word, composites had already been in use in motorsport since the 1950s in the form of glass fiber moulded body panels.



Figure 1.4: McLaren mp4/1c

The first Formula One car to race with a composite monocoque chassis was the McLaren M2A in 1965, composed with panels of Mallite, a composite sandwich made from carbon fiber and balsa wood. This was only an early exercise in producing a Mallite monocoque and was the team's first single seater designed by Robin Herd. The car was the base for development of the Formula 1 car and served as a Firestone test vehicle. It used Traco Oldsmobile and Ford V8 engines. McLaren M2A has only competed in non-championship races, but many lessons from its testing were incorporated into the M2B.

McLaren was in 1981 the first Formula One team to send their race cars out on track for the official races with the newly designed composite safety cells. There is still debate as to which team was first to produce a fiber reinforced composite chassis since the Lotus team was secretly carrying out similar research in parallel with McLaren. Lotus followed "cut and fold" methodology simply replacing the pre-bonded aluminium skins with hybrid composite of carbon and kevlar-reinforced epoxy.

While McLaren used a sub-contractor, Hercules Aerospace, for the production of their monocoque, Lotus chose to build theirs in-house. The McLaren monocoque was produced by laying carbon fiber around a positive mould, before applying core materials and the final inner skin of the structure. Lotus opted for using folded sheets of composite material in a similar manner to the way chassis had previously been fabricated using sheet aluminium and aluminium honeycomb.

Two moulds formed the top and bottom half and were bonded together around the bulkheads to form the final composite chassis. As the hard points for the suspension mountings needed to be accurate, and as they were to be attached to the inner skin\bulkhead, the chassis was molded inside out, as explained earlier the male mould was used to lay up the inner skin directly against the mould, removing any variance in sandwich thickness from the final suspension geometry. This resulted in the outer skin being laid up against the honeycomb and not a mould face, hence the outer finish of these chassis were relatively poor.

The main concern for the design of the monocoque in Formula One has been the around impact scenarios of the race car. The CFRP monocoque has proved its incredible ability to resist large impacts. In the Italian Grand Prix of 1981 John Watson lost control over his McLaren and smashed violently into the barriers. He was able to walk away from debris unscathed. This incident went long way to removing any doubts in the minds of those unconvinced of the safety of the carbon fiber composites under strain rate loading in the later years, the energy absorbing properties of composites have made a great contribution of the safety record of the sport.

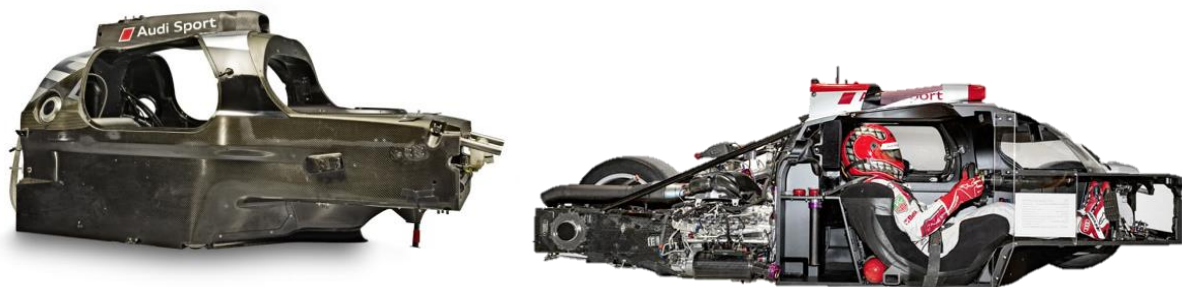


Figure 1.5: Monocoque chassis of Audi R18 LMP

Other teams soon followed the carbon fiber chassis route almost entirely adopting the McLaren molding way.

Then, for the 1983 championship, ATS team D4 racer, under the technical direction of Gustav Brunner, made a female molded chassis taking advantage of the neater external surface of the molded chassis, by also making the monocoques outer skin the primary bodywork for the car and discarding separate bodywork for the large part of the front of the car. Ferrari adopted this design soon after for their first full carbon chassis, the 126C3.

1.2.2 PRO'S AND CON'S

As mentioned, the overall reason for developing a carbon fiber monocoque was the ability to reduce weight while maintaining stiffness and strength. Stiffness is one of the most important parameters when designing our race car chassis as compliance will make the car behave differently under different loads giving the driver a hard time to control the car when suspension parameters constantly is changing. Stiffness and strength are the key elements when designing the chassis for safety. Our drivers are racing the car in excess of 110kph making safety an essential design challenge.

There are however many additional parameters that are changing when a steel tubular spaceframe is replaced by a carbon fiber monocoque. Design complexity, design freedom,

precision, i.e. are just some of them. A radar chart rating steel space frame versus the monocoque chassis is shown in figure 1.8.

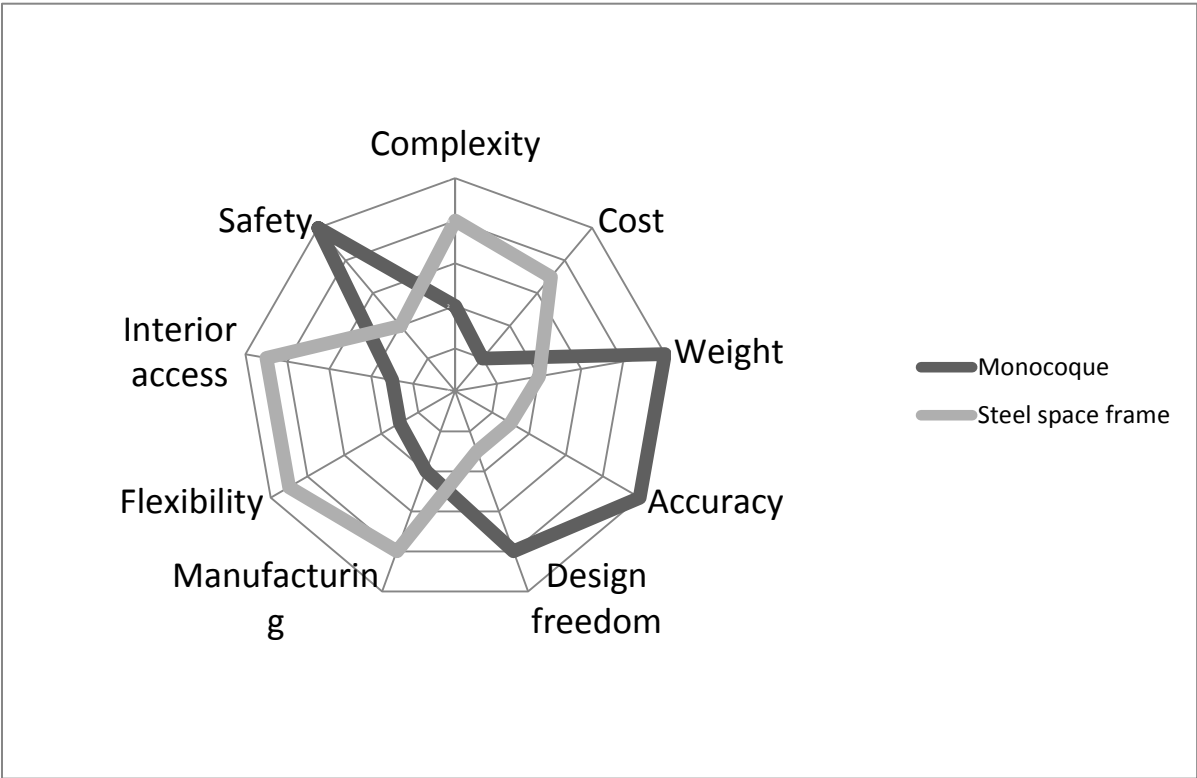


Figure 1.7: Comparison of monocoque chassis and steel space frame

As one can see from the above figures one could see that the monocoque differs substantially from the steel space frames earlier used by Revolve NTNU. One can clearly see that cost has a clear downside with a monocoque compared to the steel frame. The same can be seen from manufacturing and interior access. What the monocoque lacks in flexibility and cost is however returned multiplied in design freedom and accuracy, as Revolve NTNU values these parameters more. Design freedom gives the opportunity to design the monocoque for each load case, for each component and for each function, giving the ability to add stiffness, strength or space where it is desirable. Accuracy in the suspension pickup points is important, in order to obtain a quick and drivable car that behaves the way it is designed to. In addition, the suspension geometry is a critical parameter for the loads reacted into the chassis. A change in suspension geometry will change the load paths into the chassis, which may result in a chassis that is over- or under dimensioned, reducing weight efficiency.

Overall, our most valued parameters/design features such as weight, design freedom, accuracy and safety, are best represented in a monocoque chassis.

1.2.3 DESIGN CHALLENGES

One of the main challenges is how to distribute the loads produced by the accelerating car into the chassis in an appropriate manor. A lightweight sandwich structure most often consists of a weak core making it a challenge to transfer concentrated loads to the sandwich chassis. In order to deal with this, a localized stiffening/strengthening insert is used. There are used a total of 94 inserts in the monocoque produced by Revolve NTNU in 2014.

Some of the loads on the chassis is nearly 100% in-plane or purely compressive, in these cases adhesive joints have been considered, and it might both reduce weight further as well as reducing manufacturing complexity.



CHAPTER 2

CHASSIS LOADS

As the main load-carrying structure of the car, the chassis must be able to handle all loads and external forces reacted into it. For a Formula Student chassis, the chassis loads can be divided into two categories, loads regulated by the rules of the competition, and non-regulated loads. Most of the rule regulated areas of the monocoque are safety related, such as the impact structure and seat belt attachments. These parts of the structure require specific tests to prove that the required load capacity is reached. Loads reacted through the suspension and drivetrain are the most important non-regulated loads acting on the chassis.

2.1 RULE REGULATED LOADS AND ATTACHMENTS

The chassis needs to meet the requirements set by the FSAE 2014 rules [13]. This involves rules for cockpit space and opening as well as requirements for stiffness and strength for different zones of the chassis. The regulations are a significant restriction for the chassis design in Formula student, and it is therefore important to be familiar with the rules. A chassis that does not meet the requirements will not be able to attend in any competition.

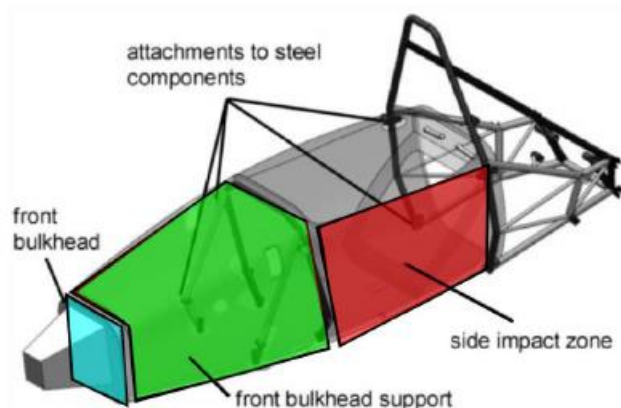


Figure 2.1: Primary structure

Side Impact Zone:

The area of the side of the car extending from the top of the floor to 350 mm (13.8 inches) above the ground and from the Front Hoop back to the Main Hoop.

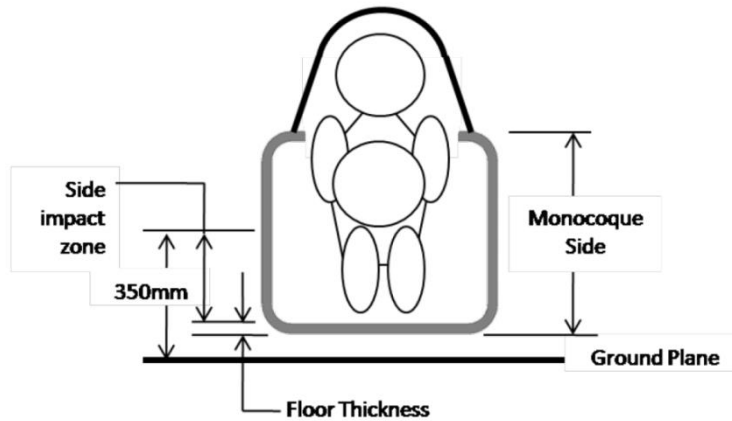


Figure 2.2: Monocoque side impact

Front Bulkhead:

A planar structure that defines the forward plane of the Major Structure of the Frame and functions to provide protection for the driver’s feet.

BASELINE MATERIAL:

Most of the regulations with regards to structural integrity demand results to be compared with a baseline steel tubular space frame. The baseline material properties can be found in the table on the right hand side.

| Baseline Steel Tube Dimensions | Ø25.4x1.6mm | Ø25.4x1.25mm |
|---------------------------------------|-----------------------------|------------------------|
| Application | Front Bulkhead, Side Impact | Front Bulkhead Support |
| D - Outer diameter | 25.4mm | 25.4mm |
| R – Outer radii | 12.7mm | 12.7mm |
| t – Thickness | 1.6mm | 1.25mm |
| d – Inner diameter | 22.2mm | 22.9mm |
| A – Tube cross section area | 119.6mm ² | 94.8mm ² |

Table 2.1: Base materials

2.1.1 MONOCOQUE GENERAL REQUIREMENTS

All equivalency calculations must prove equivalency relative to steel grade SAE/AISI 1010.

T3.30

When specified in the rules, the EI of the monocoque must be calculated as the EI of a flat panel with the same composition as the monocoque about the neutral axis of the laminate. The curvature of the panel and geometric cross section of the monocoque must be ignored for these calculations.

Note: Calculations of EI that do not reference T3.30 may take into account the actual geometry of the monocoque.

Monocoque Front Bulkhead Support

- In addition to proving that the strength of the monocoque is adequate, the monocoque must have equivalent EI to the sum of the EI of the six (6) baseline steel tubes that it replaces.
- The EI of the vertical side of the front bulkhead support structure must be equivalent to at least the EI of one baseline steel tube that it replaces when calculated as per rule T3.30 Monocoque Buckling Modulus.

Monocoque Side Impact

- In addition to proving that the strength of the monocoque is adequate, the side of the monocoque must have equivalent EI to the sum of the EI of the three (3) baseline steel tubes that it replaces.
- The side of the monocoque between the upper surface of the floor and 350 mm above the ground (Side Impact Zone)

must have an EI of at least 50% of the sum of the EI of the three (3) baseline steel tubes that it replaces when calculated as per Rule T3.30 Monocoque Buckling Modulus.

| Area | EI requirement |
|------------------------|------------------------|
| Front Bulkhead Support | 8322[Nm ²] |
| Side Impact | 5106[Nm ²] |
| Impact sone | 2553[Nm ²] |
| Laminate Test | 1702[Nm ²] |

Table 2.2: EI requirements

Monocoque Driver's Harness Attachment Points

- The monocoque attachment points for the shoulder and lap belts must support a load of 13 kN before failure.
- The monocoque attachment points for the anti-submarine belts must support a load of 6.5 kN before failure.
- If the lap belts and anti-submarine belts are attached to the same attachment point, then this point must support a load of 19.5 kN before failure.

In addition there are several complementary rules that need proof by physical testing. The following are the most important:

1. "Teams must build a representative section of the monocoque side impact zone (defined in T3.34) side as a flat panel and perform a 3 point bending test on this panel. They must prove by physical test that a section 200mm x 500 mm has at least the same properties as a baseline steel side impact tube (See T3.4.1 "Baseline Steel Materials") for bending stiffness and two side impact tubes for yield and ultimate strength..."
"If laminates with a lay-up different to that of the side-impact structure are used then additional physical tests must be completed for any part of the monocoque that forms part of the primary structure. The material properties derived from these tests must then be used in the SES for the appropriate equivalency calculations..."
2. "Perimeter shear tests must be completed by measuring the force required to push or pull a 25mm diameter flat punch through a flat laminate sample.
The sample, measuring at least 100mm x 100mm, must have core and skin thicknesses identical to those used in the actual monocoque and be manufactured using the same materials and processes..."
FBHS \geq 4kN, Side impact = 7.5kN
3. The monocoque attachment points for the shoulder and lap belts must support a load of 13 kN before failure. The monocoque attachment points for the anti-submarine belts must support a load of 6.5 kN before failure.
The strength of lap belt attachment and shoulder belt attachment must be proven by physical test where the required load is applied to a representative attachment point where the proposed layup and attachment bracket is used.

There are several other rules and regulations that dictate the design of the monocoque, but these are the most relevant. The complete set of rules can be found in [13]

2.2 NON-RULE REGULATED LOADS AND ATTACHMENTS

One of the most important tasks of a racecar chassis is to have appropriate strength and stiffness in the regions around the suspension attachments. Excessive compliance in these areas will be carried on into the suspension components, resulting in inadequate wheel angles and loss of grip. When designing a chassis, it is important to know the external forces and their effect on the chassis. While the regulated loads give a straight forward load case, the same cannot be said for the suspension loads. To identify the forces reacted into the chassis via the suspension links, it is necessary to know the loads generated into the tires, also known as the wheel loads. With information about the tires, total mass of the car, center of gravity height, aerodynamic downforce and expected worst case shock loads from bumps on the road surface, it is possible to make a good estimate of the wheel loads in different driving situations. It should be mentioned that the wheels are highly dynamic, and fully understanding of the tire is a complicated field. Thus, it is necessary to do some simplifications when analyzing the different load cases.

| | |
|-----------------------------------|----------------|
| Weight [kg] | 180 kg |
| Overall dimensions L/W/H [mm] | 3095/1416/1220 |
| Wheelbase [mm] | 1600 |
| Track (front/rear) [mm] | 1200/1170 |
| Center of gravity height [mm] | 220 |
| % of static weight on rear wheels | 54 |
| Downforce @ 80km/h [N] | 1440 |
| Max motor power [kW] | 85 |

Table 2.3: Some properties of KOG Arctos R

Based on the information given in table 2.3, tire test data and data collected during testing with the previous car built by Revolve NTNU in 2013, a set of realistic load cases were established. The load cases are indicated by the number of g-forces acting on the center of mass to equal the applied load from the wheels. The reference load is the force acting on the car in a stationary condition, which would be equal to one time the gravity, 1g.

- 3g bump (vertical force)
- 2g turn (lateral force)
- 2g braking (longitudinal force)
- 2g turn with 2g bump (lateral and vertical force)
- 2g braking with 2g bump (longitudinal and vertical force)

| Wheel loads | 3g bump | | | 2g turn | | | 2g turn 3g bump | | | 2g brake | | | 2g brake 3g bump | | |
|-------------|---------|---|------|---------|------|------|-----------------|------|------|----------|---|------|------------------|---|------|
| | X | Y | Z | X | Y | Z | X | Y | Z | X | Y | Z | X | Y | Z |
| Front left | 0 | 0 | 1798 | 0 | 1890 | 1143 | 0 | 1890 | 2340 | -1750 | 0 | 1058 | -1750 | 0 | 2256 |
| Front right | 0 | 0 | 1798 | 0 | 455 | 260 | 0 | 455 | 1458 | -1750 | 0 | 1058 | -1750 | 0 | 2256 |
| Rear left | 0 | 0 | 2027 | 0 | 2100 | 1285 | 0 | 2100 | 2636 | -700 | 0 | 411 | -700 | 0 | 1762 |
| Rear right | 0 | 0 | 2027 | 0 | 481 | 275 | 0 | 481 | 1626 | -700 | 0 | 411 | -700 | 0 | 1762 |

Table 2.4: Wheel loads [N] for different load cases.

The wheel loads for the different load cases are calculated and given in table 2.4. X is longitudinal direction, Y is lateral direction and Z is vertical direction. The suspension geometry dictates how these wheel loads are reacted further into the chassis. KOG Arctos R, the car built by Revolve NTNU in 2014, is equipped with a pullrod actuated double wishbone suspension both front and rear. This means that the wheel assembly is connected to the chassis via an upper and a lower wishbone, also called A-arms. A pullrod attached to the upper wishbone connects the wheel assembly to the spring and damper via a moment transferring component called a bellcrank. The front wheel is steered by the steering rod, and the tie rod prevents the rear wheels from steering.

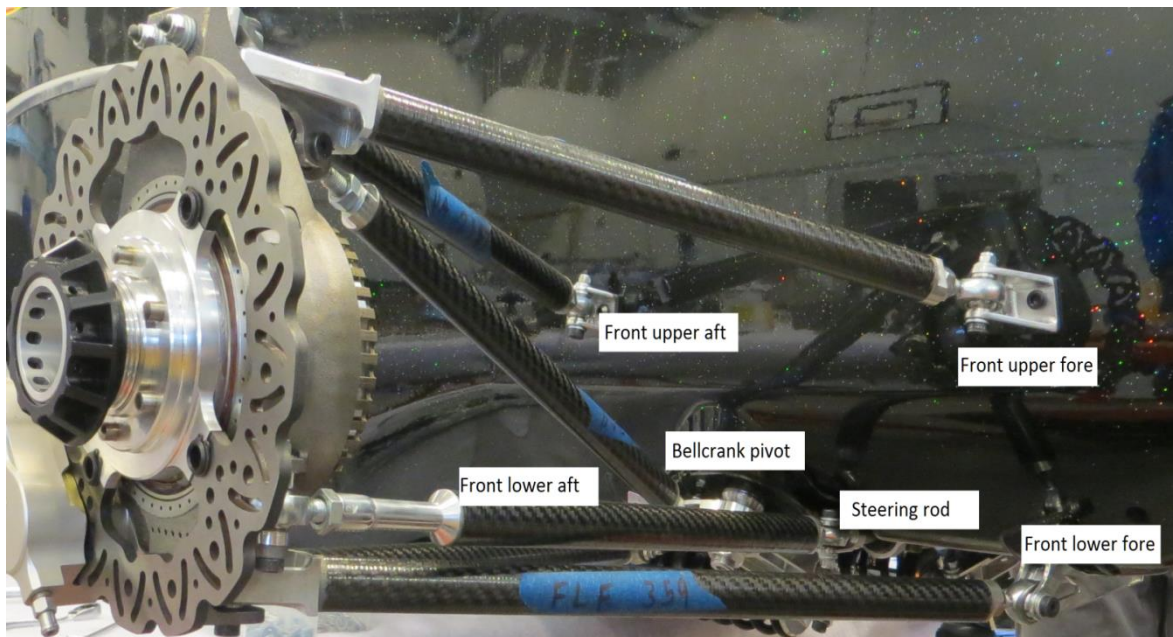


Figure 2.3: Illustration the chassis attachment points for the front suspension. (Damper attachment not visible)

A non-linear finite element analysis based on a parametric point-line model of the left side of the suspension was developed to identify the forces reacted into the chassis. The analysis was done in NX Nastran. As a result of the relatively large deformations from the spring and damper, the analysis was required to be non-linear. The model is designed with a node in each contact point, using 1D-elements to connect them. The entire wheel assembly, including the tire, rim, upright and hub are modeled with RBE2-elements. RBE2-elements connect two nodes with infinite stiffness by forcing the degree of freedom at both nodes to be equal. The wheel assembly will then act as a rigid connection between the ground and the suspension links, which includes wishbones, pull rod and steering rod. The same method is used for the bellcrank, the connection between pull rod and damper. Bellcrank and wheel assembly will in reality deform under load, but the impact of this on the chassis loads is assumed to be negligible.

The suspension links are modeled with CROD-elements, which is 1D-elements with zero rotational stiffness. This means that only axial forces will be transferred through the suspension links, and they are for this use added an infinite axial stiffness. The damper and spring are modeled as an elastic spring, viscous effects from the damper are neglected. The remaining free ends of the system are constrained appropriately, as shown in figure 2.4 and 2.5. Wheel loads for the different load cases are applied in the lower node of the RBE2 elements in the wheel assembly, which is the center of the tire contact patch.

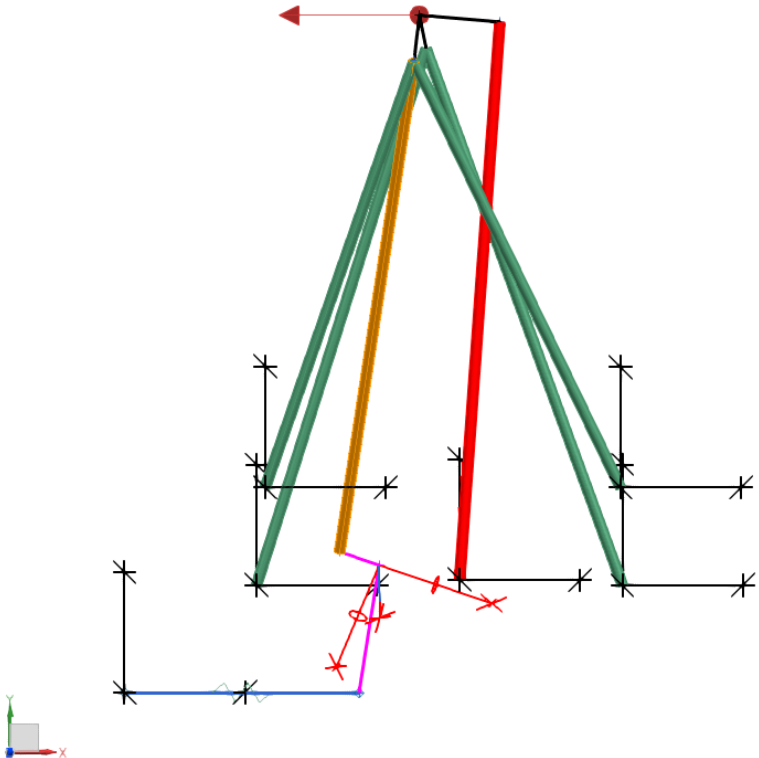


Figure 2.4: Top-view of suspension FE-model

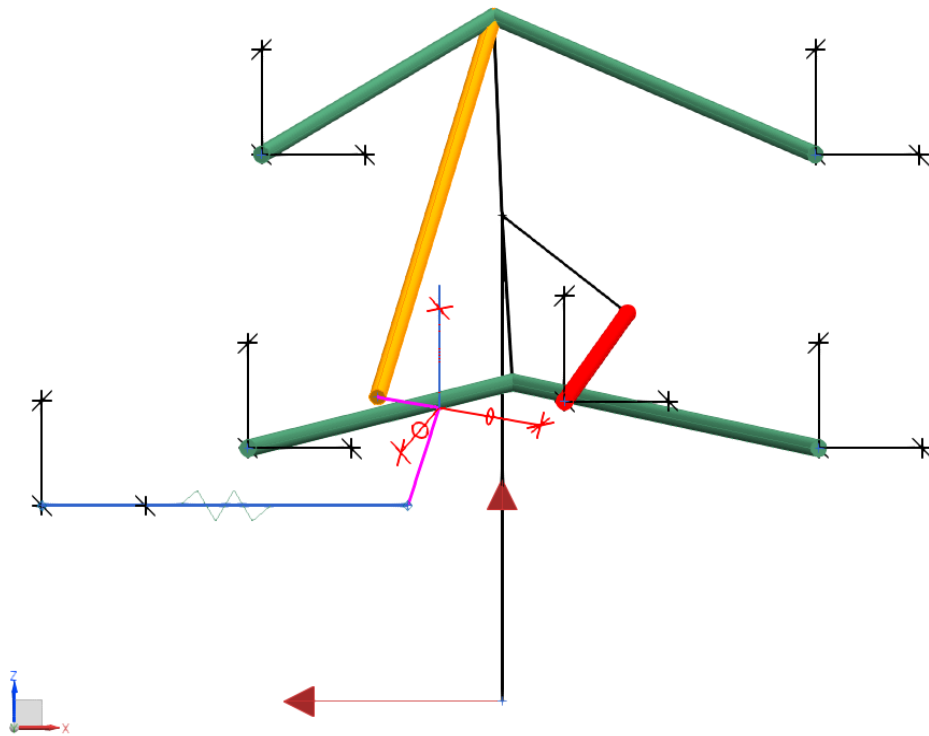


Figure 2.5: Side-view of suspension FE-model










| Constraints and loads: | | Link: | Element: |
|---|----------------------------------|--|----------|
|  | Fixed translation |  Wishbones | Crod |
|  | Free rotation in bellcrank plane |  Steering rod | Crod |
|  | Loads |  Pullrod | Crod |
| | |  Spring | Celas1 |
| | |  Wheel assembly | RBE2 |
| | |  Bellcrank | RBE2 |

Figure 2.6: Legend for figure 2.4 and 2.5.

The reaction forces from the constraints between suspension components and chassis are found from the finite element analysis, and are by equilibrium identical to the forces acting on

the monocoque. Second order effects from deformations in the chassis are assumed to be negligible. Appendix 13 shows the chassis reaction forces decomposed in the vehicle coordinate system. For each attachment point, the highest loads will be used as the design load, marked with orange in the table. To evaluate the load capacity required for each individual insert, the forces should be decomposed into out of plane and shear load. This requires decomposition of the reaction forces into a local coordinate system. There have not been found an easy way to do this in NX. To find out of plane load, in plane load and bending moment for all attachment points, each of the dimensioning loads were manually transformed into a local coordinate system. The results can be found in table 2.5.

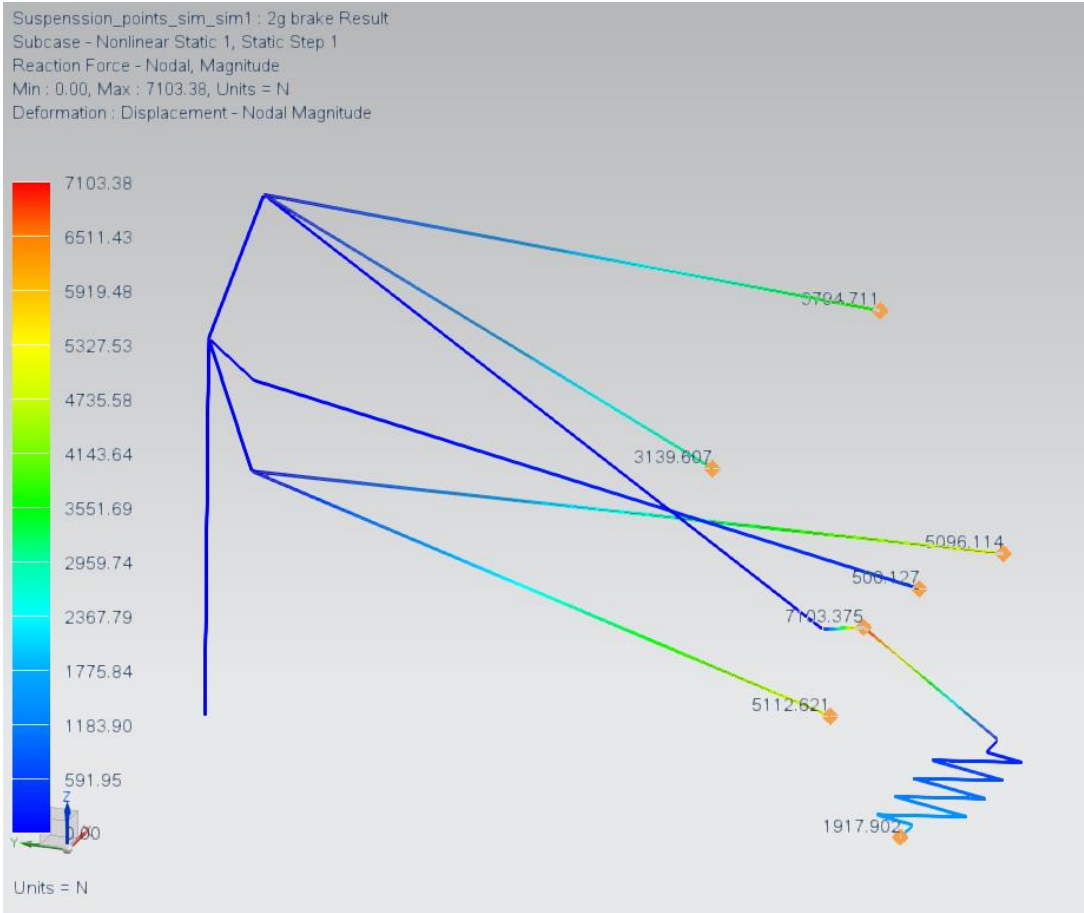


Figure 2.7: Resultant reaction forces - 2g brake.

| Attachment point: | Out of plane load [N]: | In plane load (shear) [N]: | Bending moment [Nm]: |
|-----------------------|------------------------|----------------------------|----------------------|
| Front upper fore | 3509 | 1959 | 0 |
| Front upper aft | 4879 | 2175 | 0 |
| Front lower fore1 | 600 | 2540 | 0 |
| Front lower for 2 | 1895 | 1948 | 0 |
| Front lower aft 1 | 810 | 3935 | 0 |
| Front lower aft 2 | 2337 | 2685 | 0 |
| Rear upper fore | 2982 | 2224 | 0 |
| Rear upper aft | 2422 | 1342 | 0 |
| Rear lower fore | 2452 | 1676 | 0 |
| Rear lower aft | 2078 | 825 | 0 |
| Front bellcrank pivot | 385 | 7393 | 179 |
| Rear bellcrank pivot | 186 | 6581 | 120 |
| Front damper | 0 | 2500 | 0 |
| Rear damper | 0 | 2500 | 0 |

Table 2.5: Insert design loads

Several other attachment points with serious load cases do exist on a race car chassis [30], such as aerodynamic devices, accumulator package and drivetrain. There have been done significant work in the integration of these attachment points, but this will not be included in this thesis.



CHAPTER 3

THEORY

3.1 SANDWICH THEORY

“A structural sandwich is a special form of a laminated composite comprising of a combination of different materials that are bonded to each other so as to utilize the properties of each separate component to the structural advantage of the whole assembly”, The Handbook of Sandwich Construction.

The carbon fiber monocoque will be a light weight sandwich structure with inserts in load intensive attachment points, for example suspension and drivetrain attachments. In addition to weight, focus will be on stiffness in load intensive areas and overall torsional- and bending stiffness. There are several reasons for using sandwich laminate for the chassis structure. If done right, the combined stiffness and weight relations of a sandwich structure is superior to any other type of structure.

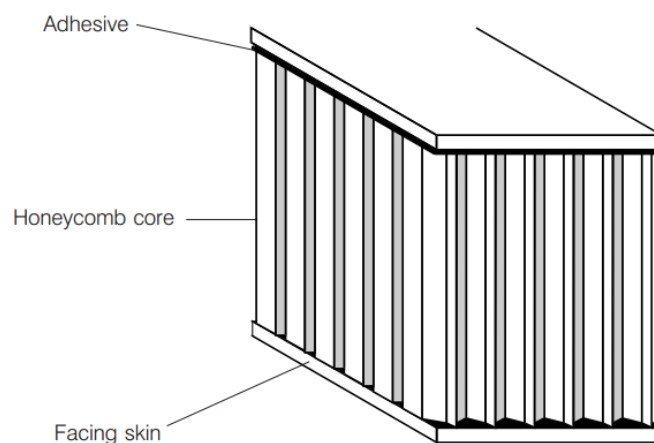


Figure 3.1: Sandwich structure

A sandwich panel is composed by a thick core material with stiff face skins bonded on each side. The core is normally a low strength and density material, typical core materials can be different types of foams or a honeycomb material. Laminates of glass or carbon fiber are commonly used as skin materials, but it is also possible to use thin sheet metal. The object of the core is to resist the shear loads and hereby increase the stiffness of the structure by giving the panel a thickness and holding the face sheets apart. When subjected to bending, the face sheets will be in tension and compression. As shown in fig. 2, deflection of a sandwich beam is made up of both bending and shear deflection. The amount of deflection from shear deformation in a sandwich laminate depends on the core shear stiffness and the core thickness.

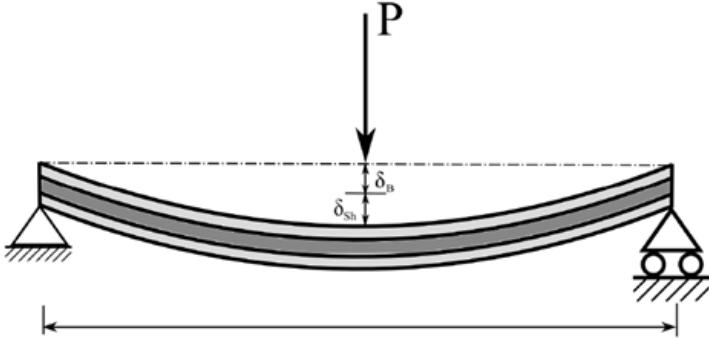


Figure 3.2: Sandwich panel 3pt bending

By doing some simplifications and ignoring higher order effects, one can assume classical beam theory to apply. This will be good enough to give approximations, but will not be completely realistic. It should be clear that the classical theory ignores local geometrical effects close to point loads or support regions. Classical theory also ignores the effects of unsymmetrical laminates. The derived differential equations for a sandwich beams are as follows:

$$D_s d^4 \frac{wb}{dx^4} = 0 \text{ (ordinary beam theory)} \quad \frac{dw_s}{dx} = \frac{-F}{2A_s G_c} \text{ (shear deformation)} \quad (EQ3.1)$$

By applying the boundary conditions for a 3pt bending test, one get the equations for the displacements on the beam mid-point.

$$\delta_{Tot} = \delta_B + \delta_{Sh} = \frac{Pl^3}{48D} + \frac{Pl}{4S} \quad (EQ3.2)$$

$$D = EI = \frac{Eftfh^2b}{2} \quad (EQ3.3) \quad S = bhGc$$

$$(EQ3.4)$$

As seen from equation 3, core thickness is the factor that has the largest impact on bending stiffness. The bonded connection between core and skin makes the sandwich components act as one unit with high stiffness. Another important feature is that the panel has uniform stiffness along its whole area, as long as it stays undamaged.

The bending induces tensile- and compression stresses in the face sheets, while the core will be subjected to shear stresses. Relations between stresses and other parameters are shown in equations 6 and 8. If the core material has low shear strength, a likely failure mode is that core shear failure. If core shear strength is high, it is more likely that the upper face sheet will fail in compression.

$$\sigma_f = \frac{M}{htfb} = \frac{Pl}{4htfb} \quad (EQ3.5)$$

$$\tau_C = \frac{F}{hb} = \frac{P}{2hb} \quad (EQ3.6)$$

Assuming the assumptions laminate theory to apply, the stiffness matrix is given by equation 3.7:

$$\begin{bmatrix} N \\ M \end{bmatrix} = \begin{bmatrix} A & B \\ B & D \end{bmatrix} \begin{bmatrix} \varepsilon \\ \kappa \end{bmatrix} \quad (EQ3.7)$$

Assuming the assumptions laminate theory to apply, for a sandwich laminate, the matrixes A, B and D are determined by the face sheet stiffness matrixes Af, Bf, Df and the core thickness:

$$[A_s] = 2[A_f]$$

$$[B_s] = 0$$

$$[D_s] = \frac{1}{2} h[A_f] + 2[D_f] + 2h[B_f] \quad (EQ3.8)$$

For layups that are symmetrical, Bf=0, making the sandwich balanced. The face sheet matrixes Af, Bf and Df can be calculated by first finding the plane stress stiffness matrix for one layer of the face sheet material:

$$\begin{bmatrix} \sigma_1 \\ \sigma_2 \\ \tau_{12} \end{bmatrix} = \begin{bmatrix} Q_{11} & Q_{12} & 0 \\ Q_{12} & Q_{22} & 0 \\ 0 & 0 & Q_{66} \end{bmatrix} \begin{bmatrix} \varepsilon_1 \\ \varepsilon_2 \\ \gamma_{12} \end{bmatrix} \quad (EQ3.9)$$

$$Q_{11} = Q_{22}(E_2 = E_1) = \frac{E_1}{1 - \nu_{12}\nu_{21}} \quad Q_{12} = \frac{\nu_{12}E_1}{1 - \nu_{12}\nu_{21}} \quad Q_{66} = G \quad (EQ3.10)$$

In order to calculate the ply stiffness matrix, $[\bar{Q}]$, for a ply orientation, it is necessary to do a 2D transformation about the 3-axis:

$$\begin{bmatrix} \sigma_x \\ \sigma_y \\ \tau_{xy} \end{bmatrix} = \begin{bmatrix} \bar{Q}_{xx} & \bar{Q}_{yx} & 0 \\ \bar{Q}_{xy} & \bar{Q}_{yy} & 0 \\ 0 & 0 & \bar{Q}_{ss} \end{bmatrix} \begin{bmatrix} \varepsilon_x \\ \varepsilon_y \\ \gamma_{xy} \end{bmatrix} \quad (EQ3.11)$$

$$[\bar{Q}] = [T\sigma]^{-1}[Q][T\varepsilon] \quad (EQ3.12)$$

$$[T\sigma] = \begin{bmatrix} c^2 & s^2 & 2cs \\ s^2 & c^2 & -2cs \\ -cs & cs & c^2 - s^2 \end{bmatrix} \quad [T\varepsilon] = \begin{bmatrix} c^2 & s^2 & cs \\ s^2 & c^2 & -cs \\ -2cs & 2cs & c^2 - s^2 \end{bmatrix} \quad (EQ3.13)$$

The remaining stress coefficients can then be calculated:

$$\begin{aligned} \bar{Q}_{xx} &= Q_{11}c^4 + 2(Q_{12} + 2Q_{66})c^2s^2 + Q_{22}s^4 \\ \bar{Q} &= (Q_{11} + Q_{22} - 4Q_{66})c^2s^2 + Q_{12}(c^4 + s^4) \\ \bar{Q}_{yy} &= Q_{11}s^4 + 2(Q_{12} + 2Q_{66})s^2c^2 + Q_{22}c^4 \\ \bar{Q}_{xs} &= \bar{Q}_{ys} \\ \bar{Q}_{ss} &= (Q_{11} + Q_{22} - 2Q_{12} - 2Q_{66})c^2s^2 + Q_{66}(c^4 - s^4) \end{aligned} \quad (EQ3.14)$$

The face sheet stiffness elements [Af], [Bf] and [Df] can be calculated from equation 3.15:

$$\begin{aligned} A_{ij} &= \sum_{k=1}^n Q_{ij,k}(h_k - h_{k-1}) \\ B_{ij} &= \frac{1}{2} \sum_{k=1}^n Q_{ij,k}(h_k^2 - h_{k-1}^2) \\ D_{ij} &= \frac{1}{3} \sum_{k=1}^n Q_{ij,k}(h_k^3 - h_{k-1}^3) \end{aligned} \quad (EQ3.15)$$

One can use this to calculate the stiffness matrix of the face sheets and thereby find the stiffness matrix for the whole sandwich laminate.

3.2 INSERT THEORY

“An insert is a local change in stiffness and strength of the sandwich panel, the purpose of which is to distribute a localized load in an appropriate manner”, The Handbook of Sandwich Construction.

It should be noted that the insert capacity calculations presented is largely based on empirical results. Trials have been performed by different organizations and institutions, and the formula will vary among different educational and commercial circles. As solid and reliable organizations, the handbooks and design manuals for both The European Space Agency and Boeing has been used.

By its very nature, sandwich panels handle concentrated loads poorly as the face skins usually are very thin while the core is typically weak. That combinations cause a lack of ability in efficiently transferring localized loads into the structure. With the load cases applied on the monocoque chassis, one will notice almost all the loads applied to the monocoque could be considered as point/concentrated loads. With this in mind a need for designing an efficient method for transferring localized loads to the structure was found.

Consider a localized or concentrated load on a sandwich panel. At any place surrounding the load the conditions of equilibrium must be fulfilled. If we denote the circumference of a closed section around the insert, Π , and we note the out of plane load as P , see figure below 7. Then the transverse forces along the distance Π must equal $(-)\Pi Q$. As the radius of the section is increased, the length of Π increases and it follows that T decreases. At this early stage one could see that the reaction force needed to resist localized loads is inversely proportional to the radius of the section. For loads resulting in moments, the reaction force T will be inversely proportional to r^2 . These dependencies indicate that the affected zone is rather small, and that in future calculations and simulations; it is generally no need for a calculation model for the entire panel.

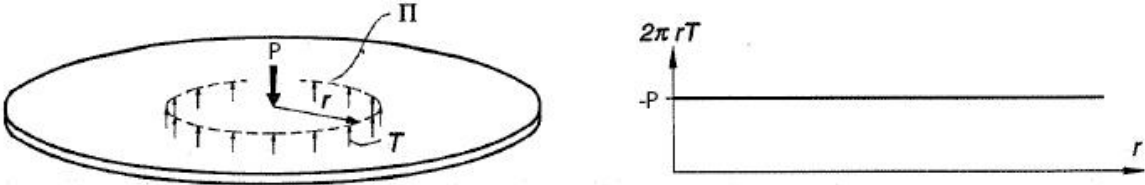


Figure 3.3: Affected region of local load

In order to introduce a concentrated load (either in-plane or out-of-plane) into a honeycomb sandwich structure, the use of solid inserts has been widely adopted. This provides a physical connection between both skins and thereby allows the load to diffuse from the point of application.

The general problem of analyzing sandwich panels which are loaded through inserts is complex due to the fact that the different parts of the structure interact in complex ways in the regions close to the inserts. Local changes in the sandwich structure is mainly responsible for this complexity, and as an example we could point to the fact that the individual face sheets of the panel tend to bend about their own neutral planes, rather than the sandwich's neutral plane.

With this in mind classical antiplane theory cannot be used in analyzing arbitrary external loads. However, there is an exception when the load case of the insert is normal (tensile or compressive loading) to the sandwich panel. Then the active failure mode is nearly always shear rupture of the honeycomb core with the interface between the potting material and the honeycomb cells. The peak shear stress is located at exactly this point, and classical antiplane theory is sufficiently accurate to analyze the shear stress component.

Thus we can estimate the static load-carrying capability of an insert/sandwich panel with tensile or compressive loading. [4]

The shear modulus of the core influence the way in which the load is transmitted through the insert and how it is distributed between face sheets and core. The higher the stiffness of the face sheets compared to the core stiffness, the higher load contribution of the face sheets, and vice versa.

According to ESA measurements [4 p.93] the shear modulus given by the suppliers/manufacturers in both L and W direction are too high, and cannot be used in load bearing capability calculations. The shear modulus varies with loading and tends to decrease as a result of non-linearity.

Instead, an effective shear modulus, G_c^* is used.

$$G_c^* = \frac{G_w}{3} \quad (EQ3.16)$$

Core strength is an important factor in analyzing inserts loaded in compression or tension. The axial load through the insert must be absorbed as shear. Since the honeycomb material is not symmetrical, and there is 72% additional single foils in the L-direction, the effective core shear strength,

$$\tau_{c,crit} = 1.36 \cdot \tau_{W,crit} \quad EQ(3.17)$$

The potting and insert radius is of importance to evaluate as this dictates the total area for the load to be distributed to. As the insert is lightweight while potting material is relatively heavy, it is most efficient to have the effective potting radius close to the insert radius.

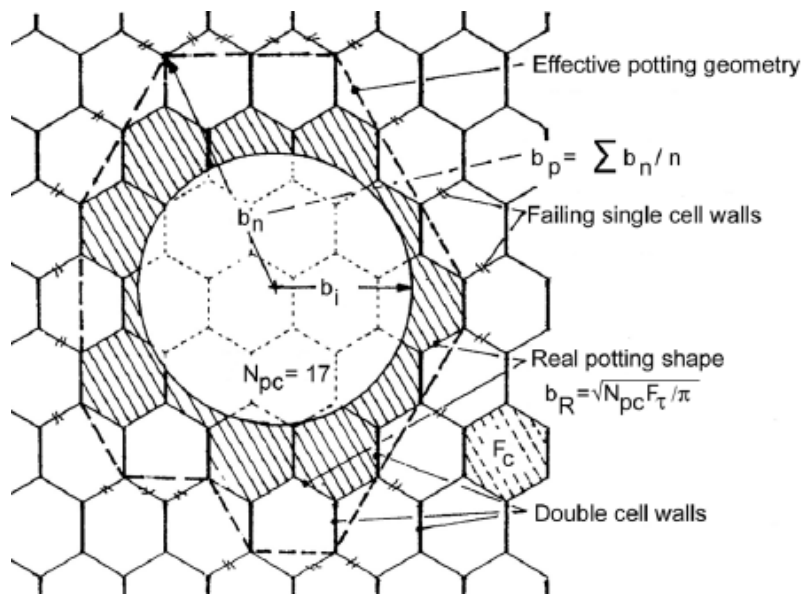


Figure 3.4: Potting radius

The effective potting radius takes into account the fact that the double cell walls next to the potting is both stronger and stiffer than the single cell was. These double cell walls generally do not fail, and is simplified as part of the potting material. b_p is thus defined as the average distance of the nearest single cell walls surrounding the potting material from the center of the insert.

$$b_p = \frac{1}{n} \sum b_n \quad EQ(3.18)$$

Since the actual potting radius depends on the radius, cell size and the positions of the insert center will be a minimum effective potting radius, $b_{p,min}$, which is given by:

$$b_{p,min} = 0.9b_i \cdot 0.7S_c \quad EQ(3.19)$$

Where b_i = insert radius, S_c = core cell size.

In addition there is a typical value, or one could calculate the real potting radius. Using the minimum value is chosen to give a reasonable margin of safety, and will this give the most conservative calculations.

3.2.1 OUT OF PLANE LOADING

Under out of plane loading, with fully potted or through-the-thickness inserts, the insert will fail from shear rupture by the core surrounding the potting. Shear stresses in the potting material is higher than it is at the edge of the honeycomb, but the shear strength of the potting material is much higher and will thus transfer the shear stresses to the honeycomb before failure. The single foil cell walls in the honeycomb will be especially exposed, and this is typically where the first failure occur.

At this location the core shear stress can be calculated to:

$$\tau_{max} = \tau_c(r = b_p) = \frac{P}{2\pi b_p d} \quad EQ(3.20)$$

$$\rightarrow P = 2\pi b_p d \tau_c \quad EQ(3.21)$$

Eq 21, is valid for both tensile and compressive loads.

It follows that the dimensioning factor for out of plane loading will be the shear strength of the core, $\tau_{c,crit}$.

3.2.2 IN-PLANE LOADING

The honeycomb core cannot transfer in-plane stresses, rather it expands or collapses like an accordion. It follows that in-plane loads are carried by the face sheets. In order to make sure the capability of the insert is high enough, it is important to evaluate the different failure modes of in-plane loads carried by the face sheet. Tension, shear-out, dimpling and bearing are some of the possible failure modes. The formula used for describing in-plane load capacity is based on test data[4], and therefore a proper margin of safety should be applied to make up for the empirical results.

Face dimpling or intra cell buckling is localized instability trait to sandwich panels having honeycomb core. Dimpling is the local buckling of the face sheets within the confinements of one or more cells. This happens in the unbounded regions of the core, while the cell walls provide rigid nodal points. For a given face sheet, the core cell size should be small enough to prevent intra cell buckling. The other way around one should, for a given core, have sufficient thickness/stiffness to prevent buckling.

Physical testing provided the following relation between in-plane loading and shear dimpling [4];

$$Q_D \leq \frac{2}{\pi} b_p t_s K_D \frac{E}{1-\nu^2} \left(\frac{t_s}{s_c} \right)^2 \quad EQ (3.22)$$

Where b_p = potting radius
 t_s = face sheet thickness
 K_D = dimpling coefficient

By examining this equation one could conclude that a reduced cell size would be the most efficient way of increase the critical dimpling load, while maintaining low weight.

For bearing failure, the maximum in-plane load Q approximated:

$$Q_b \leq K_b \frac{2}{\pi} b_i t_s \sigma_{comp} \quad EQ (3.23)$$

Where b_i = insert radius
 K_b = bearing coefficient
 σ_{comp} = compressive strength

With a through-the thickness insert, with symmetrical loads on inner skin and outer skin, the capabilities can be calculated by the following expression:

$$Q_{sst,symmetri} = 2(2t_s b_p \sigma_{yield}) \quad EQ(3.24) \quad Q_{sst,unsymmetri} = 2t_s b_p \sigma_{yield} \quad EQ(3.25)$$

3.2.3 BENDING AND TORSIONAL LOADS

Both torsional and bending loads should be avoided in a sandwich panel through an insert. The best way to introduce a moment or torsional load through insert design is to use coupled inserts. For the sake of the monocoque where bending loads are introduced(bell crank), and there is no room for coupled inserts one should make sure the bracket connected to the face sheet for the attached part is as large as possible, and have at least a diameter equal to the real potting radius.

Maximum torsional load, T_{ss} and maximum bending load respectively is as follows:

$$T_{ss} = 4\pi b_r^2 t_0 \tau_0 \quad EQ(3.26) \quad M_{crit} = P_{crit} b_i \quad EQ(3.27)$$

Where

- T_{ss} = Torsional capacity
- M_{crit} = Bending moment capacity
- t_0 = Foil thickness of core
- τ_0 = Shear strength of cell walls
- b_r = Real potting radius

3.2.4 TOTAL CAPACITY

There is seldom loads that occur as just tensile, compressive, moment or torsional loads. It is therefore of high importance to evaluate the load capacity of the combined loads from all these load cases. For through-the-thickness inserts the shear and moment components should be evaluated into one resultant shear component.

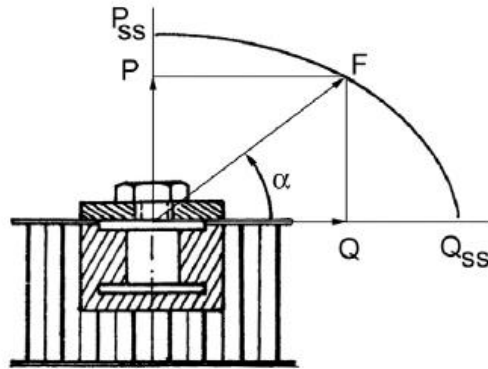


Figure 3.5: Inclined load on insert

With the combined loads of;

- Normal load, P
- Shear, Q
- Bending moment, M
- Torsional moment, T

one could calculate the total capacity of the insert:

$$\left(\frac{P}{P_{crit}}\right)^2 + \left(\frac{Q}{Q_{Stt,unsumm}}\right)^2 + \left(\frac{M}{M_{crit}}\right)^2 + \left(\frac{T}{T_{ss}}\right)^2 \leq 1 \quad (EQ28)$$

where

- P_{ss} = Out of plane capacity
- Q_{ss} = In-plane capacity
- M_{ss} = Bending moment capacity
- T_{ss} = Torsional capacity

3.3 FAILURE MODES

As designers of a complex sandwich structure one of the critical parts to understand are the different failure modes of sandwich panels. Theoretical models using honeycomb mechanics and classical beam theory are described, and eventually evaluated later in chapter 5. This part will have its main focus on a sandwich panel in a three point bending.

Sandwich panels subjected to bending and shear loads, as in a 3-point bending setup, may fail in several ways including compression- or tension failure of the facesheets, wrinkling failure of the facesheet in compression, shear failure of the core, global buckling, local indentation and/or debonding of the core-facesheet interface. Each failure mode has been studied throughout recent years, and this thesis will describe the basic theory behind to failure modes and eventually evaluate and compare analytical results to experimental results.

The failure modes for both honeycomb cores as well as foam cores are presented. The failure modes can mainly be divided into two parts; skin failure and core failure:

3.3.1 FACESHEET YIELD

The maximum stress used for evaluating the yield of the facesheet is taken as

$$\sigma_{max} = \frac{M}{ht_{fb}} = \frac{PL}{4ht_{fb}} \quad EQ(3.5)$$

For easy evaluation of the failure mode a simplification of making the sandwich panel with a symmetrical balanced layup has been done. With the now symmetrical beam the stress is the same in both the compression skin and the tension skin. Skin failure will occur when the axial stresses in either of the skins reach the in-plane strength, σ , of the skin material. With most CFRP materials the weakest link will be the compressive strength, and this will likely be the critical skin assuming a symmetrical layup.

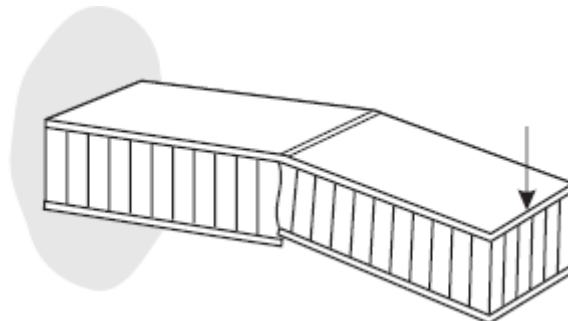


Figure 3.6: Facesheet yield

3.3.2 INTRACELL BUCKLING

Intracell buckling is a failure mode in which a local buckling take place in a honeycomb structure. Intracell buckling is the buckling of the face sheet within one or multiple individual cells of the honeycomb. The failure happens where the facesheets is unsupported by the cell walls. Using classical elastic plate buckling theory for thin plates the critical failure equation for intracell buckling can be derived [22].

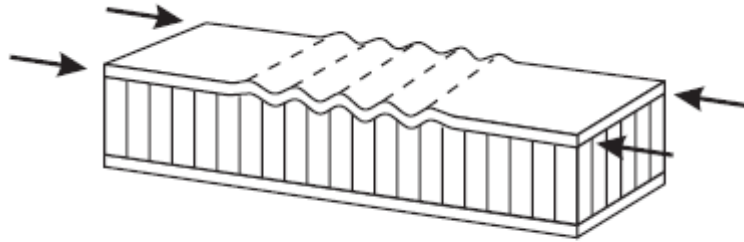


Figure 3.7: Intracell buckling

$$\sigma_{crit} = \frac{2E_f}{(1-\nu^2)} \left(\frac{t_f}{s}\right)^2 \quad \text{EQ(3.29)}$$

This simple intracell dimpling failure estimation can in some cases underpredict the intracell buckling load. Studies of an improved prediction of the intracell buckling in honeycomb sandwich panels can be found at [22]. However, as a first year design team a conservative failure load is favorable, and the extended research on failure modes is not part of this thesis.

3.3.3 FACESHEET WRINKLING

The compression of facesheet can be subjected to an instability mode called wrinkling. Face wrinkling is a buckling mode of the skin with a wavelength greater than the cell width of the honeycomb. [8]

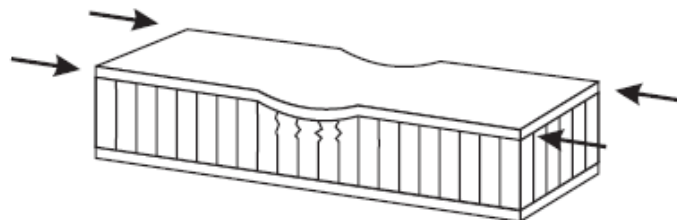


Figure 3.8: Facesheet wrinkling

$$\sigma_{critical} = 0.5 \sqrt[3]{G_c E_c E_f} \quad \text{EQ(3.30)}$$

Sandwich panels using either foam or honeycomb can fail due to core failure. The pertinent failure modes of core will most likely be shear failure or local indentation of the core, both whom will be presented here.

3.3.5 SHEAR CRIMPING

Failure due to shear crimping appears to be a local failure mode, but is really a form of overall buckling where the buckling wavelength is very small. This short wavelength buckle is due to the low shear modulus of the core. The crimping of the sandwich occurs suddenly and usually causes the core to fail in shear at the crimp; it may also cause shear failure in the bond between the facing and core.

The critical shear crimping load can be calculated as;

$$P_{crimp,crit} = t_c G_c b \quad \text{EQ(3.31)}$$

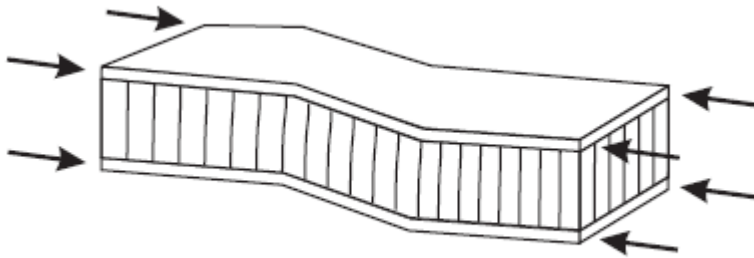


Figure 3.9: Shear crimping

Crimping may also occur in cases where the overall buckle begins to appear and then the crimp occurs suddenly because of severe local shear stresses at the ends of the overall buckle. As soon as the crimp appears, the overall buckle may disappear. Therefore, although examination of the failed sandwich indicates crimping or shear instability, failure may have begun by overall buckling that finally caused crimping.

3.3.6 CORE SHEAR

If one uses simple beam behavior we can assume the shear stress varies in a parabolic way through the skin and the core under 3pt bending. As for the super-lightweight panels usually used in FSAE monocoques, where the facesheets are much stiffer and thinner than the core, the shear stress could be simplified to vary linearly through the facesheets while constant through the core.

When neglecting facesheet contribution, the mean shear stress through the core is given as;

$$\tau_{crit} = \frac{F}{hb} \quad \text{EQ(3.32)}$$

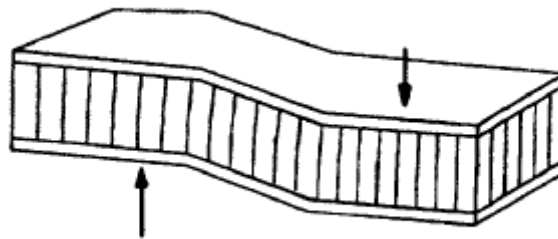


Figure 3.1: Core shear

Facesheets of high modulus is best used in collaboration with cores of high shear modulus. The balance is important to have a high performing effective sandwich panel. If there is little balance between the modulus of the skin and core, one of them will fail before the other is stressed to critical level.

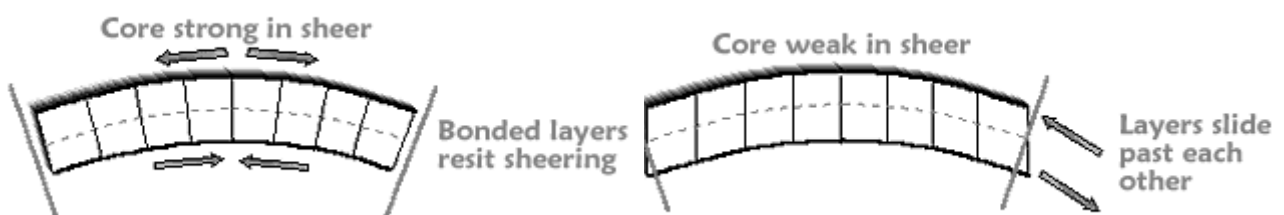


Figure 3.11: Shear-loading of core

3.3.7 LOCAL INDENTATION

Indentation failure is a typical issue that arises from a number of different causes. The typical super-lightweight sandwich panels designed for Formula Student are very sensitive for localized loads. Even handling and low velocity impacts from dropped tools could result in indentation failure of the monocoque.

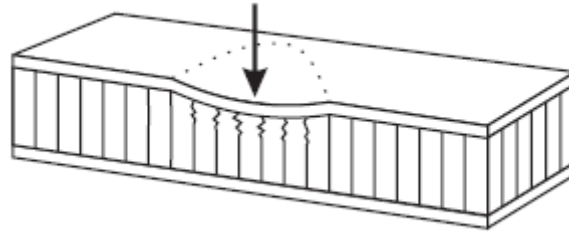


Figure 3.12: Local indentation

The simplest way of evaluating the failure load for indentation on sandwich panels is modeled by taking the critical failure load as the product of the area over which the force is applied and the out-of-plane compressive strength of the core.

$$\sigma_c = \frac{P}{A} \rightarrow P_{crit} = \sigma_c A \quad \text{EQ (3.33)}$$

For the sake of this thesis, the linear model presented in EQ 3.33 will be sufficient due to its limited scope, but in order to understand the indentation failure mode a higher order theory will be briefly presented.

A sandwich panel subjected to indentation loading causes shear and out of plane compressive stresses through the core. To evaluate the core stress, a model combining the the compressive and shear loading is needed.

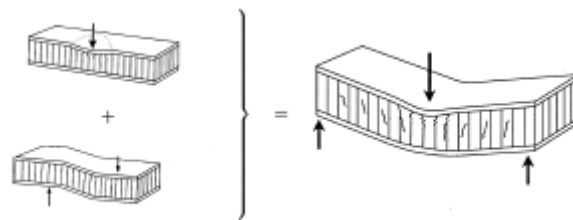


Figure 3.13: Compressive and shear loading of core

From [PS2000] a higher order theory beam theory is described to model the stresses of a honeycomb core due to indentation loading under three-point bending. The theory originally published by Petra sans Sutcliffe [25] presents a linear failure criterion, $\frac{\sigma_{zz}(x)}{\sigma_{cc}} + \frac{\tau_x(x)}{\tau_{cs}} = 1$.

When combining this failure criteria with a model of the distribution of stress through the core, than the failure model for indentation loading can be described. The higher order sandwich beam theory used to model the stress through the core is described in detail by Frostig and Baruch[28].

Frostig and Baruch assume a non-linear way of how the strain/displacement vary through thickness of the core, both in-plane and vertical. The core vertical displacement is assumed to have a quadratic variation in the through-thickness direction. Other core displacements also vary in a non-linear way and the variation can is expressed in terms of a Fourier series. Using simple beam theory, where in-plane core displacements are assumed linear and out-of-plane displacements as constant, we can see the contrast to the higher order theory where the model allows for local changes in core geometry at the loading points.

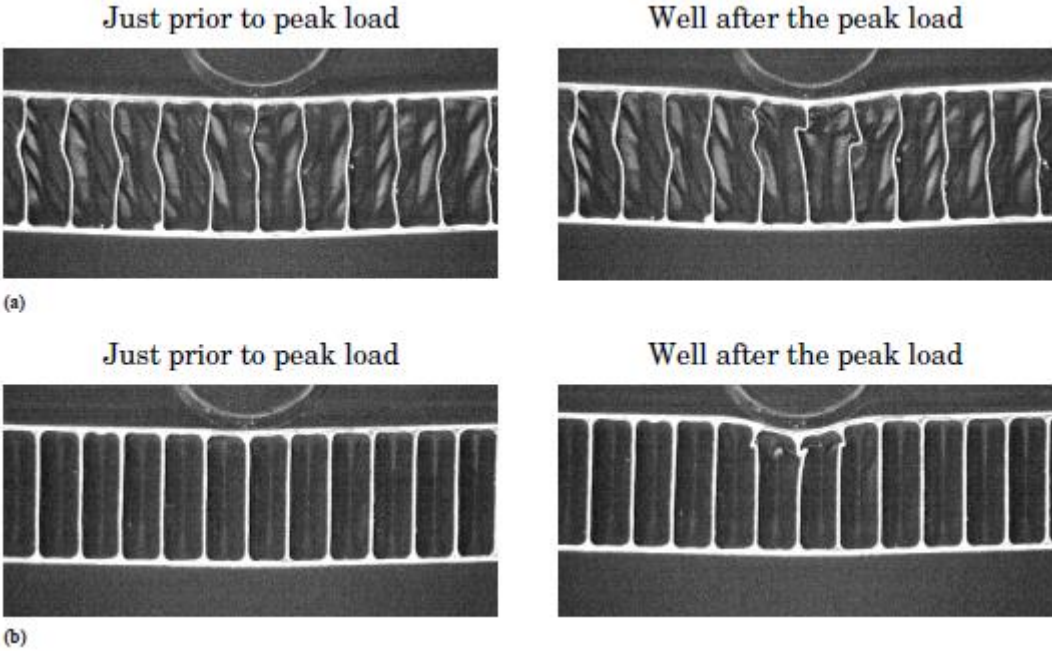


Figure 3.14: Photographs of a sandwich beam under a 10 mm diameter central roller just prior to peak load and well after the peak load.

HOSBT premise/assumption

- The shear stresses in the core are uniform through the height of the core.
- The core vertical displacement varies as a quadratic polynomial in the through-thickness direction, allowing the core to distort and its height to change.
- The core is considered as a 3-D elastic medium, which has out-of-plane compressive and shear rigidity, but negligible resistance to in-plane normal shear stresses.

A non-linear formula can be found in [Indentation failure analysis of sandwich beams], and will give an alternative analytical result for the indentation failure mode. However, a deeper dive into this failure mode is beyond the scope of this thesis and will thus not be explained further.



CHAPTER 4

ANALYSIS

4.1 MATERIAL ANALYSIS

Material choice is one of the most important evaluations in the design of a carbon fiber monocoque. There is a large number of factors which each has its own favorable material characteristics. Mechanical properties of fabric/core, weave, draping and material stability, resin system, fabric-to-core bonding, failure modes and cost are all factors driving the material choice in different directions. Finding a good compromise of all these factors is one of our most important tasks

| Property | Plain | Twill | Satin |
|-------------|-------|-------|-------|
| Stability | **** | *** | ** |
| Drape | ** | **** | ***** |
| Porosity | *** | **** | ***** |
| Smoothness | ** | *** | ***** |
| Balance | **** | **** | ** |
| Symmetrical | ***** | *** | * |
| Low crimp | ** | *** | ***** |

Table 4.1: Weave properties

The monocoque is a structural component needing to withstand high loads and with as small deformations as possible in pick up points. It is also necessary with high impact strength and finally high overall bending- and torsional stiffness.

To provide impact resistance a toughened epoxy resin system is favorable, as it helps to absorb energy during impact. A toughened system with high shear strength will also keep the structure from delaminating under large loads/displacements. With regards to carbon fiber there would be favorable to use a high strength, high modulus fiber/weave as it would provide higher stiffness and strength per weight, as well as providing higher impact resistance.

In order to optimize the material choice one has to determine the most important parameters that will affect the choice. As the regulations of the competition have clearly stated specific requirements regarding strength and stiffness, we would optimize the material choice of these parameters per weight in order to achieve a lightweight, stiff and safe chassis.

Based on the sandwich theory of flat panels (discussed in chapter 3.1) we can see from equation 4.1 that core height, as the only parameter squared, will be the most sensitive parameter and its change will have the largest impact regarding stiffness of the material. One has to take into account that the sandwich panel deflection will consist of both bending deformation and shear deformation. However the shear component of deformation is heavily dependent on the span of the panel, as the bending deformation is dependent on the span cubed, L^3 , while the shear component is dependent on the span¹. As lightweight cores are a likely option, one has to be aware of the shear deformation could be a relatively large contributor to deformation as the low density of the core lead to a low shear modulus for the core.

$$\text{Deflection of flat sandwich panel: } \delta = \frac{Pl^3}{D} + \frac{Pl}{S} = \frac{Pl^3}{0.5*E_f*t_f*h^2*b} + \frac{Pl}{b*h*G_c} \quad \text{EQ (4.1)}$$

Core height is also an important factor for the design of the inserts used in the pick-up points of the monocoque. As seen from the insert theory core height has a linear effect on the out of plane insert capacity, as well as the bending capacity of the insert explained in chapter 3.

The excel spreadsheet seen in appendix 12 calculates a sandwich panels effective stiffness for different a large amount of different cores materials, types, densities, etc. for a given layup and facesheet material. The calculations are based on a sandwich panel subjected to the required loads from the regulations described in chapter 2.1, and the calculated required stiffness. In order to evaluate the different core materials, this deflection is set at maximum, varying only core height for each core configuration. A practical limitation from the manufacturing process of most of the core types only enables us to operate with 1mm increments on core height. Based on the calculated effective stiffness normalized for weight, a selection of core materials could be evaluated for failure modes in addition to its insert capacity influence.

An increase in height will greatly improve a sandwiches ability to resist deformation, but it also comes at a cost. As the race car chassis is the backbone of the car with components to attach both on the outside and inside, a positive change in core height will reduce our ability

to pack the internal components in the car (given a fixed suspension geometry), possibly increasing center of gravity of the car as well as yaw inertia. The increase of core height will also reduce manufacturability as complex curvatures will be more for the honeycomb to conform to the desired shape due to an increased second moment of inertia.

Due to the curvature of the monocoque, a satin- or twill weave fabric would be the best option. Even though this will depend on weave pattern ([2X2], [4X4], etc.), generally a twill weave will have its advantages in good drape ability and high stability of the fabric, while the satin weave will have excellent draping abilities, but lower stability. The plain weave is the worst with regards to draping, but has the highest stability. Practically there is no difference in strength of the fabric based on its weave.

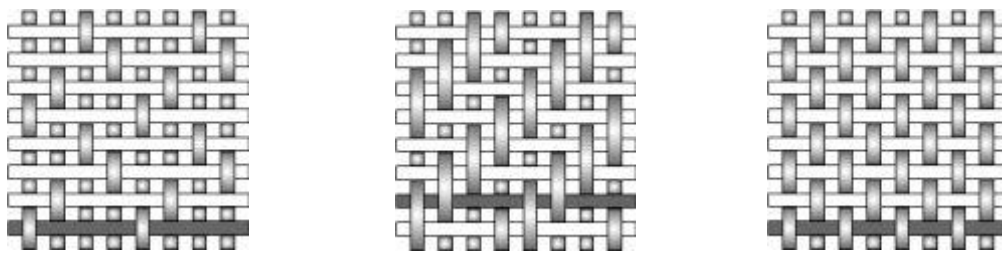


Figure 4.0: Different types of weave

In order to have the appropriate strength and stiffness of the sandwich, an evaluation of the failure modes is critical. The performance of the sandwich structure depends generally on the properties of the face sheets, the core, and the skin-to-core bond. In addition geometrical shape and dimension are contributing factors to the performance of the laminate. Based on the theory from the previous chapter, an excel spreadsheet was made in order to optimize selection of materials. Skin wrinkling, dimpling, shear stress, face stress, bending stiffness, weight etc. was all factors that were evaluated. Weight and bending stiffness was the key dimension factor for choosing materials that “offered” allowable stresses.

Mostly limited by cost, we have chosen a prepreg system from Amber Composites based on the arguments stated above. The E745 is a toughened epoxy resin system, with high specific-energy absorption, developed for impact structures and other mechanically demanding structural applications.

| Property | E745 200g/m² [2X2] Twill IM7 6k 42% r.w. | Hexply 6376 200g/m² | 2040 200g/m² [2X2] Twill M46J 6k 42% r.w. |
|-------------------------|--|--|---|
| Manufacturer | Amber composites | Hexcel | Cytec |
| Fiber weight | 200g | 280g | 200g |
| Tensile strength | 1072MPa | 1005MPa | 694MPa |
| Tensile modulus | 75.9GPa | 67GPa | 125.6GPa |
| Compression strength | 717MPa | 920MPa | 487MPa |
| Compression modulus | 70.6GPa | 67GPa | 101.4GPa |
| ILSS | 70.1MPa | N/A | 58.4MPa |
| In-plane shear strength | 124MPa | N/A | 83.7MPa |
| In-plane shear modulus | 3.9GPa | 2.84GPa | 3.1GPa |
| Cost ratio | 79.2GBP | N/A | 166GBP |
| Cure | 135C | 175C | 180C |
| Comments | Less expensive, short lead time | Expired fiber have been available through KDS. | Expensive, long lead time |

Table 4.2: Properties of prepreg systems

The resin system cures at 135C and has a shelf life of 60 days @RT. Typical applications include F1 nose boxes, side impact structures and generally demanding structural applications.

The fabric with the epoxy system we have ordered is a 2X2 twill weave fabric, with IM7 intermediate modulus fiber. A higher modulus would be favorable, but due to cost and lead time considerations it was considered the best option.

As a result of the curvature of the monocoque chassis in combination with the strength and stiffness requirements, the chosen core material is an aluminum flex core from Hexcel. This combines high strength and stiffness while maintaining low weight and still have excellent drape ability to conform to the curvature of the monocoque. Both aluminum alloy 5052 and 5056 were evaluated, and since the cost was marginally different the choice fell on the 5056 alloy.

Early layup simulations with the 5056 flex core and E745 IM7 twill weave show adequate strength/stiffness with only two top layers, and two bottom layers for most of the monocoque.

The main uncertainty is to meet the regulations with regards to physical perimeter shear test at the side impact zone. It is also some uncertainties associated with insert size and dimensioning where the localized loads from the suspension are fed into the chassis. It is also unknown how the relatively large cockpit opening will affect the overall torsional stiffness.

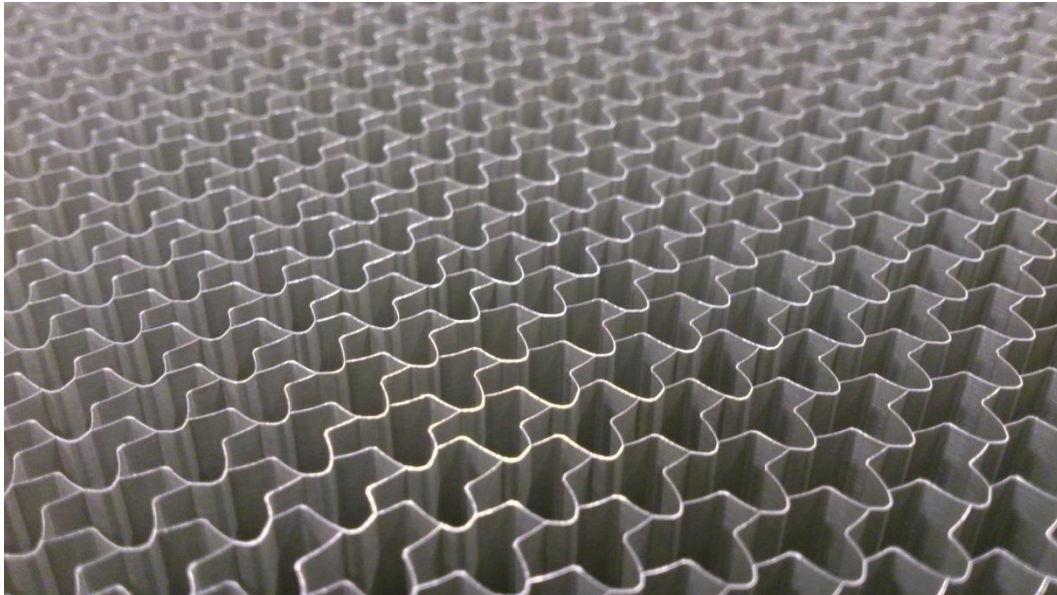


Figure 4.1: 5056 flexcore

4.2 BENDING ANALYSES

Bending analysis was done by finite element analysis in NX Nastran. The sheet model was meshed using 2D elements as this provides good approximations for this type of application. The mesh size was chosen at 5mm, a bigger mesh size could easily have been used with only a small difference in results. The laminate was built up by four different layups, as seen in table 4.3. In order to compare the results to the physical testing, the materials used in the analysis were Hexply 6367, Hexel Flexcore, and the EuroComposites Kevlar core.

| Layup [bottom->top] | Tensile stress bottom skin [Mpa] | Compressive stress top skin [Mpa] | Core shear stress [Mpa] | Deformation [mm] |
|------------------------|-------------------------------------|--------------------------------------|----------------------------|---------------------|
| [90/45/C/90/45/90] | 154,8 | -91,01 | 0,28 | 3,744 |
| [90/45/90/C/45/90] | 91,08 | -154,65 | 0,28 | 3,744 |
| [90/45/C/45/90] | 154,65 | -154,65 | 0,29 | 4,546 |
| [45/90/C/45/90/45] | 59,83 | -42,15 | 0,28 | 4,294 |

Table 4.3: Properties of different 3pt. Bending panels.

The constraint to model was set up to be fixed in DOF1, DOF2 and DOF3 on one end of the panel, while only being fixed in DOF3 at the other end. This would simulate a simply supported beam/panel well. The load was set as a line load at 3269N at the center of the panel, in order to evaluate the panel against the FSAE requirements of maximum 5mm deflection.

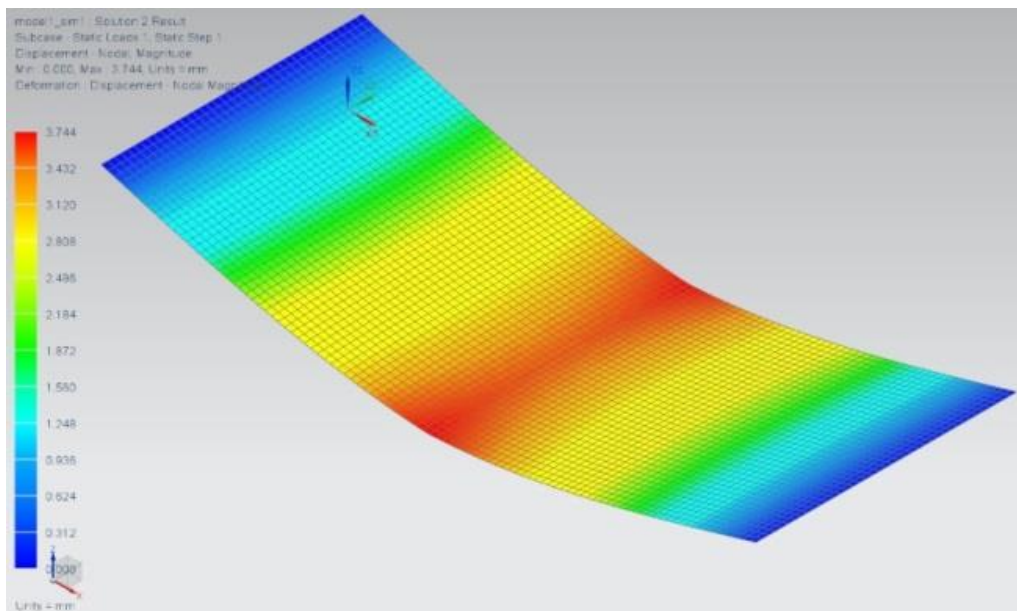


Figure 4.2: FE-analysis of 3pt bending panel showing max disp. 3.744mm.

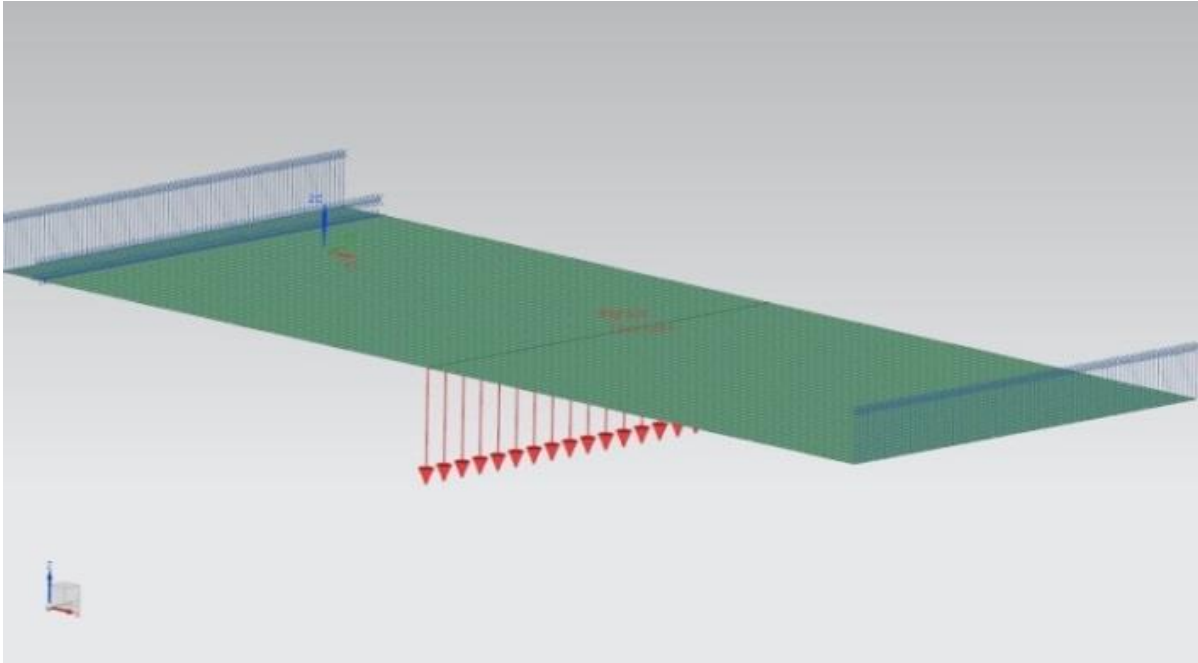


Figure 4.3: FE-model of 3pt bending panel with constraints and loads.

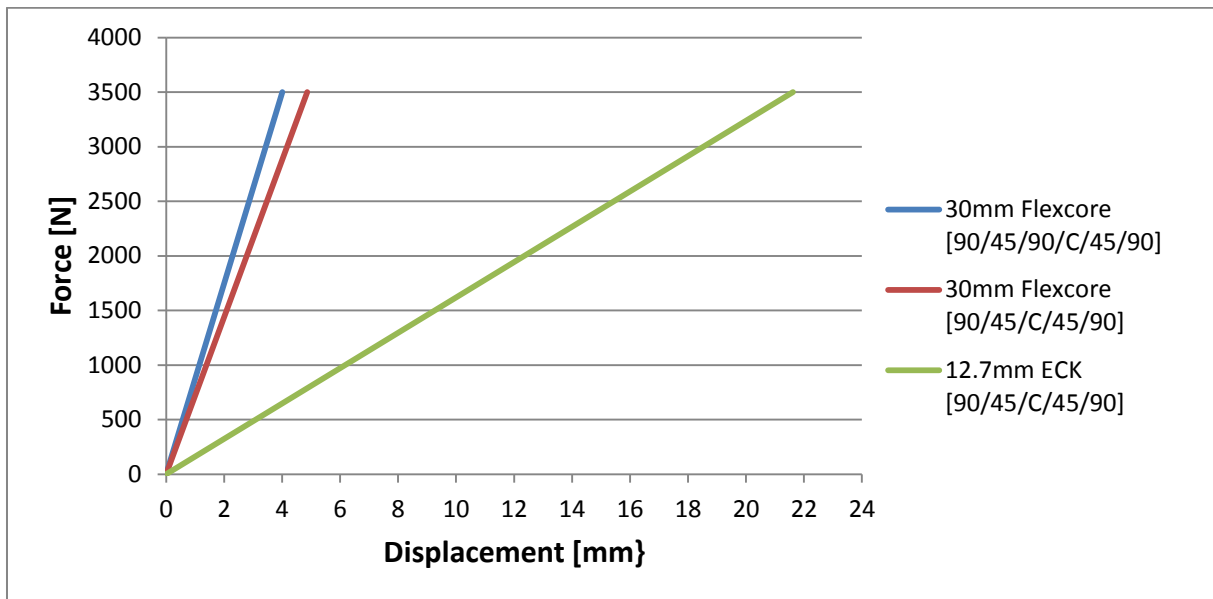


Figure 4.3: Load-displacement curve for different 3pt bending panels

4.3 INSERT ANALYSIS

The inserts was simulated as a 20x20cm sandwich panel using 2D and 3D elements. Ideally we would have simulated the inserts on the full scale monocoque with loads on all inserts at the same time. Although the affected zone is rather small [21], there might be some effects reducing the individual insert capacity as some of the inserts are located rather close to each other, i.e. the affected zones overlap. There is however a testing requirement to the insert design, and a test panel that was easy to produce was chosen, thus allowing us to compare physical testing versus numerical and analytical results.

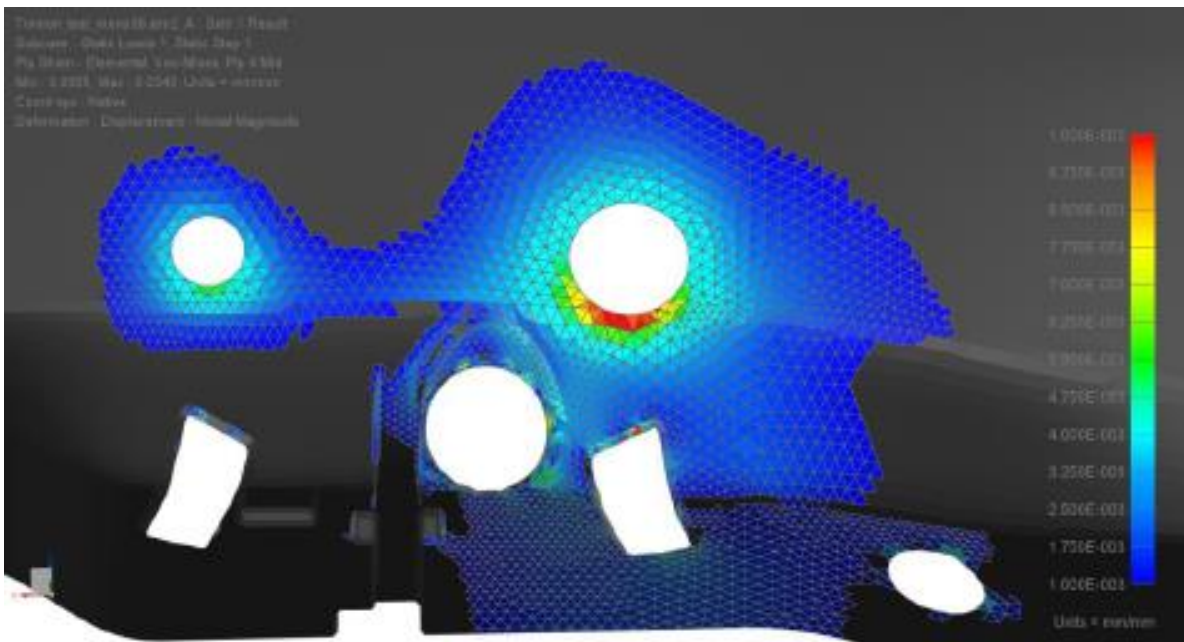


Figure 4.4: Strain plot of the front suspension points on the monocoque, max strain of 0.02 just below front upper fore attachment point.

The 5056 F40 2.1 flexcore from Hexcel, the ECK3.2 72 kevlar hexagonal core from EuroComposites combined with Hexply 6367 prepreg has been the basis for all test model simulations, and test model numerical and analytical calculations.

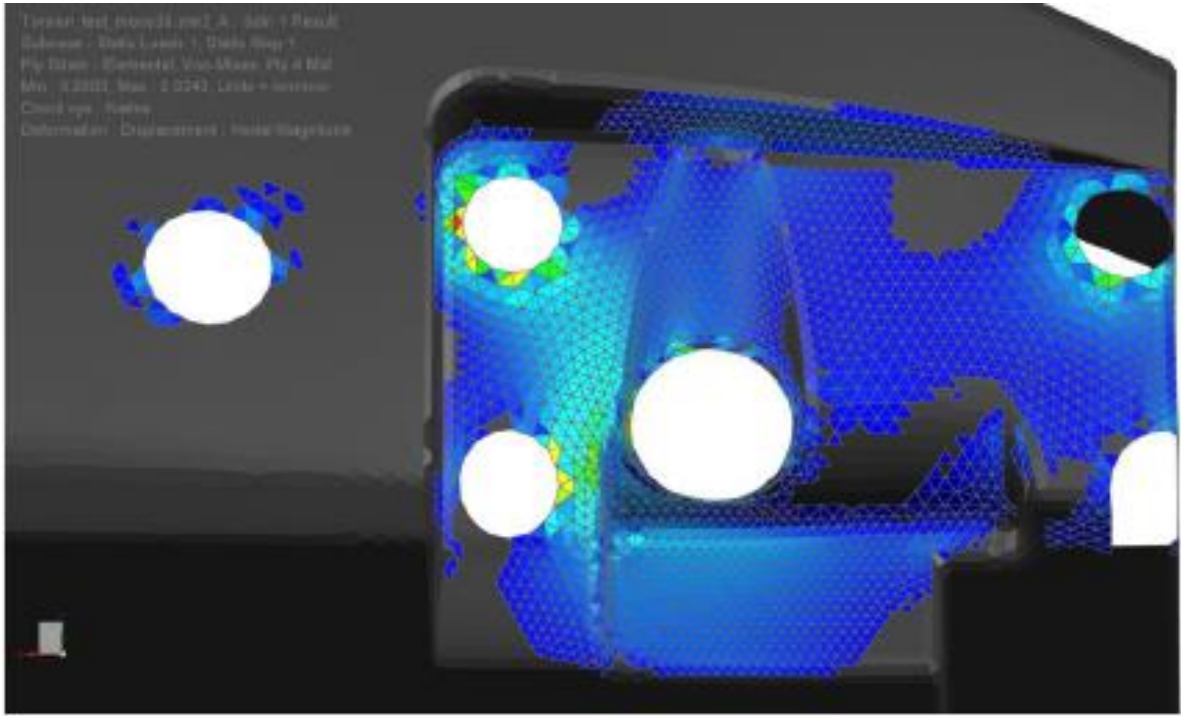


Figure 4.5: Strain plot of the rear end of the monocoque, max strain of 0.024 in front of rear upper fore attachment point.

4.3.1 OUT-OF-PLANE

The out of plane inserts were simulated in NX Nastran. The model consists of both 2D and 3D elements as the shear stress in the adhesive bonding the insert to the core was to be evaluated. Consequently glue results, in addition to the strain results, were opted for in the structural output for the solution. As the failure behavior of the insert panel is interesting, it was initially planned to do non-linear simulations of the insert panels. Unpredictable behavior of the core as well as insufficient knowledge about the core material made it necessary to do some simplifications to obtain results of decent quality. It was therefore decided to do linear finite element analysis and rather observe the failure behavior during the testing of the insert panels.

Facesheets were meshed using a 2D mesh. A rather coarse mesh was used on the panel, while we used mesh control around the insert-core interface to increase accuracy of the model, while still being lightweight. The core and insert were meshed using the same mesh size, but with 3D elements to be able to get the glue results.

The test panel fixture can be seen in the following chapter, but in short it is a square fixture supporting the outside of the panel at its edges, and only constraining the test panel in the Z-direction. Hence, the constraints for the model were chosen to be simply supported at the edges of the panel, only constraining the panel in the Z-direction.

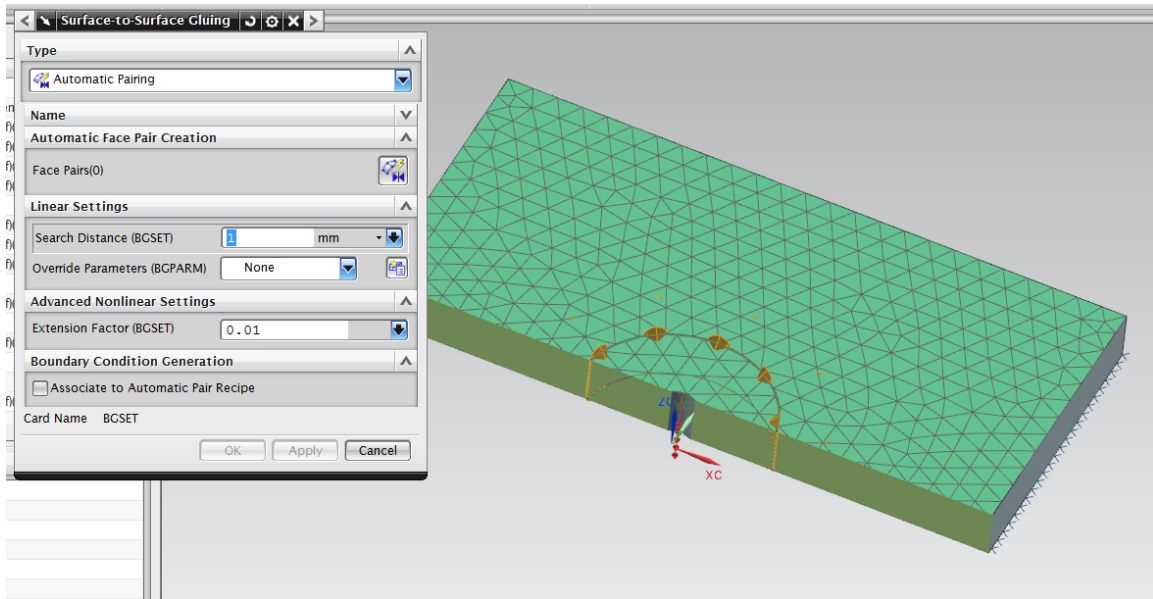


Figure 4.5: Surface to surface gluing

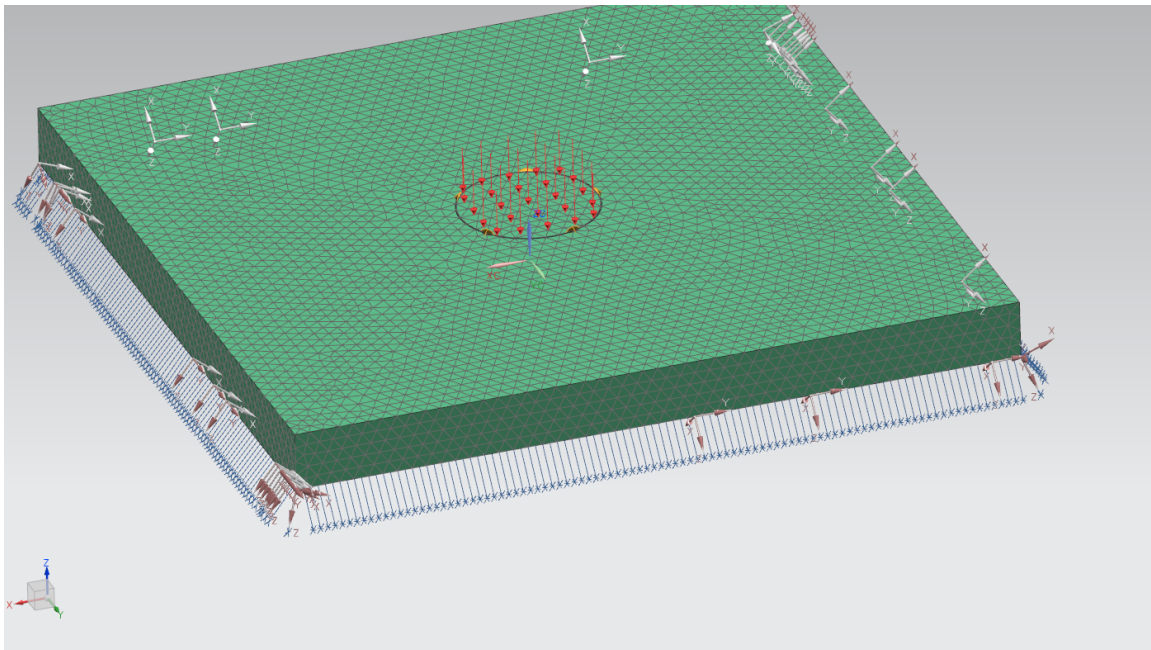


Figure 4.6: out-of-plane simply supported setup

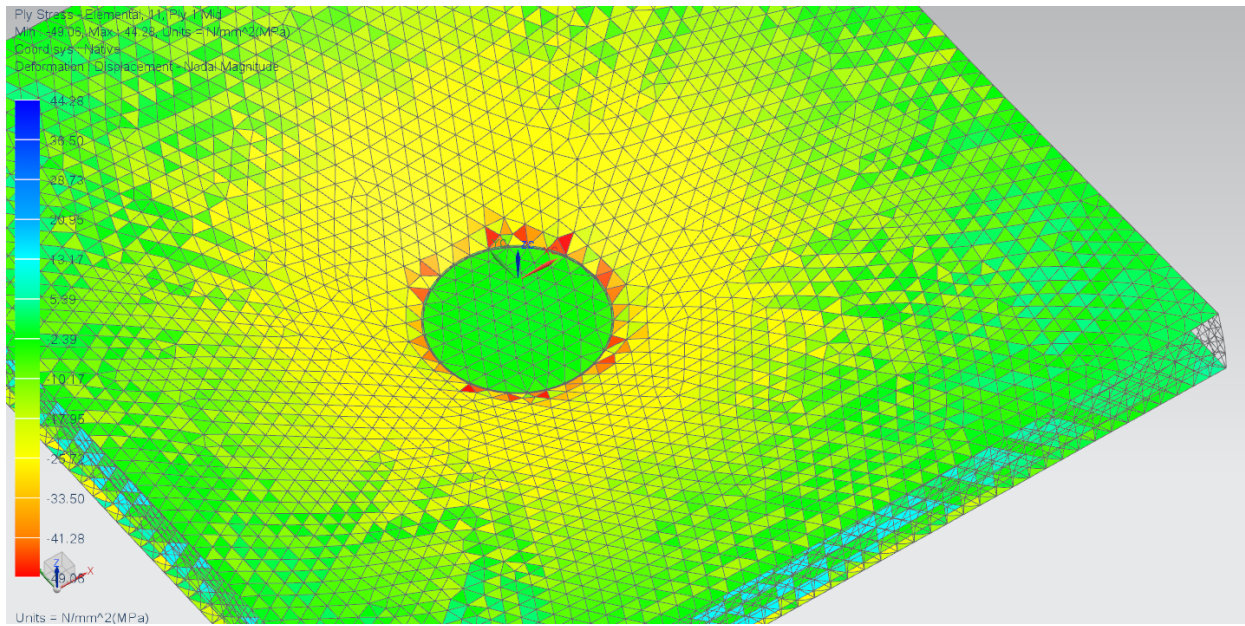


Figure 4.7: Stress in ply1, 11-direction.

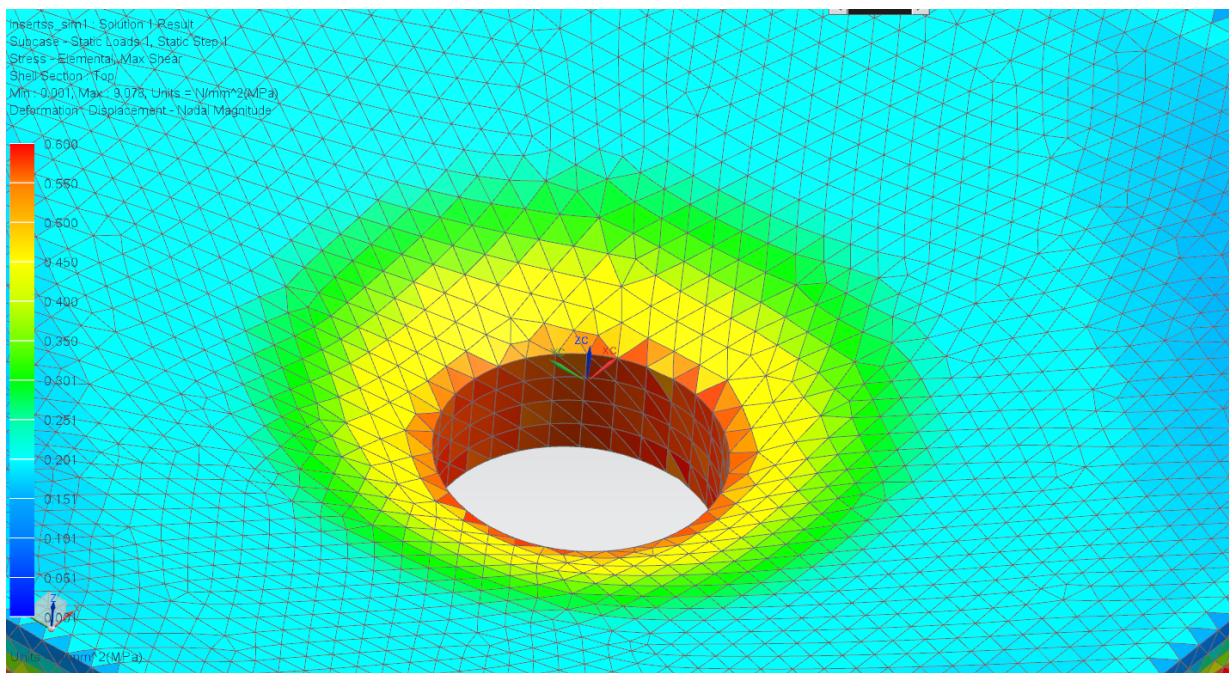


Figure 4.8: Shear stress in core around insert.

Analytical results were also conducted using the formula based upon the Handbook of insert design[4] seen in the previous chapter. A spreadsheet was made in order to evaluate insert dimensions, capacity and having the possibility to see the effects of different core and face sheet materials provided with the material database in the spreadsheet.

FEA analysis showed a deformation of approximately 0.55mm for a load of 1800N on a 50mm insert. The resulting shear forces were approximately 0.6MPa, slightly under core shear strength. Spreadsheet calculations showed a used capacity of 100% for the same load and insert.

4.3.2 BENDING

The out of plane inserts were simulated in NX Nastran. The model consist of both 2D and 3D elements as the shear stress in the adhesive bonding the insert to the core was to be evaluated. In addition the panel consist of an shaft with an interference fit to the insert. This is a model for the bell crank mounting joint on the actual car, and is modeled using surface-to-surface contact between insert and shaft. The load is applied directly to the shaft, and the shaft transfers the load into the sandwich panel through the interference fit to the insert.

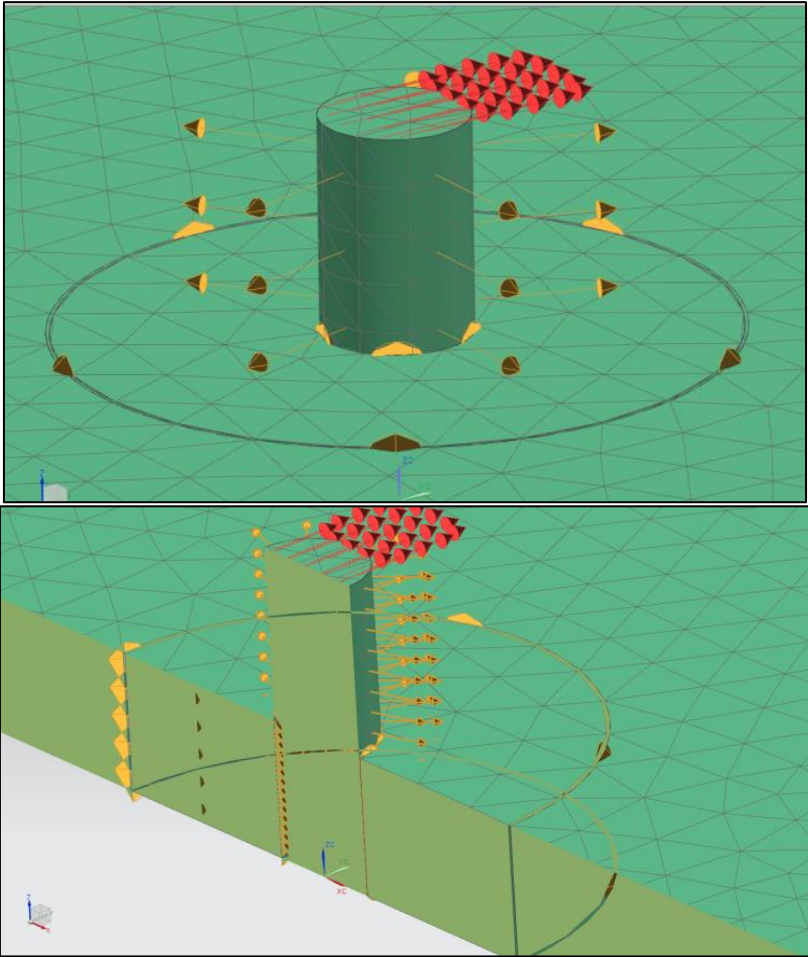


Figure: 4.9: Surface-to-durface gluing & surface-to-surface contact

Constraints that could practically be implemented on the experimental tests was evaluated. A solution constraining the outside edges in all DOF was chosen, as this is easily replicated by using adhesives for the experimental test.

The applied load was chosen to suit the maximum insert capacity found analytically using insert theory. For the bending test the ratio between shear and moment must be decided, and was calculated using;

$$\left(\frac{P}{P_{crit}}\right)^2 + \left(\frac{Q}{Q_{Stt,unsumm}}\right)^2 + \left(\frac{M}{M_{crit}}\right)^2 + \left(\frac{T}{T_{ss}}\right)^2 \leq 1, \text{ where } P=0, M=Q \cdot x \text{ and } T=0.$$

Solving for Q we could find the ratio between shear and moment loads for a given offset on the load, x. The distance was set to give the same shear to moment ratio as the actual race car, $\frac{Q}{M} = 40$. From this, x was set to be 25mm from the center of the test panel.

The following capacity of the 76mm insert used when producing the test panel gave a shear load of 3800N, following a moment of 95Nm, according to ESA calculations.

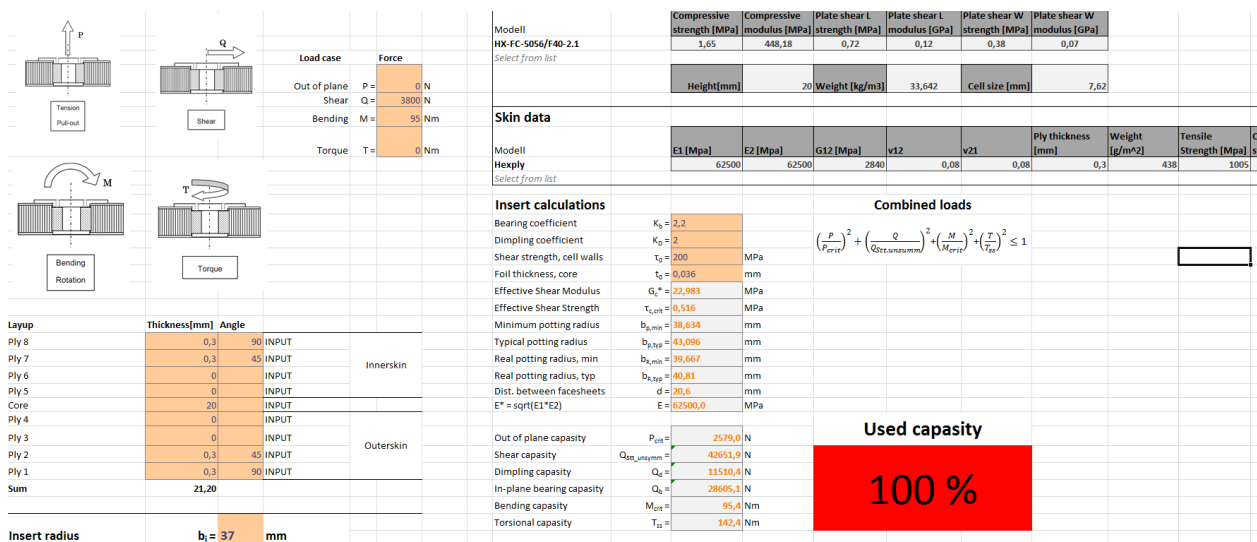


Figure: 4.10: Insert calculation spreadsheet based on ESA insert design handbook.

Numerical simulations show at the applied load that the maximum shear stress in the core is 0.7MPa. The maximum shear stress appears at the core-insert interface. The panel is assumed to yield due to shear rupture of the walls in the honeycomb, occurring at 0,72MPa for the aluminum flexcore. The panel was expected to yield at 100% insert capacity of 3800N in shear, and moment of 95Nm. Based on the fact that numerical results show a stress in the core only 2.8% less than the given shear strength of the core, indications that prove the validity of the analytical results are found.

As seen from table 4.4, the shear strength of the F40 flexcore is 0,72MPa.

| | 5056 F40 2.1 | ECK 3.2 72 |
|------------------------------|--------------|------------|
| Compressive strength [MPa] | 1,65 | 5,59 |
| Compressive modulus [MPa] | 448,18 | 274,5 |
| Plate shear L strength [MPa] | 0,72 | 2,92 |
| Plate shear L modulus [GPa] | 0,12 | 0,183 |
| Plate shear W strength [MPa] | 0,38 | 1,79 |
| Plate shear W modulus [GPa] | 0,07 | 0,108 |

Table 4.4: Properties of core materials

As the produced test panel are equipped with strain gauges the numerical strain results are of great value. As seen from figure 4.13, we can see that the strain is greatest at the core-insert interface. The force is applied in the Y direction, giving a moment about the X-axis. This implies the greatest strain will occur in the Y-direction. The numerical results show a strain of approximately $1.1 \cdot 10^{-3}$ mm/mm in the main direction. Due to budget limitations we have only placed one strain gauge at each panel, and only in the Y direction. A rosette of strain gauges should be used in order to have the complete strain field.

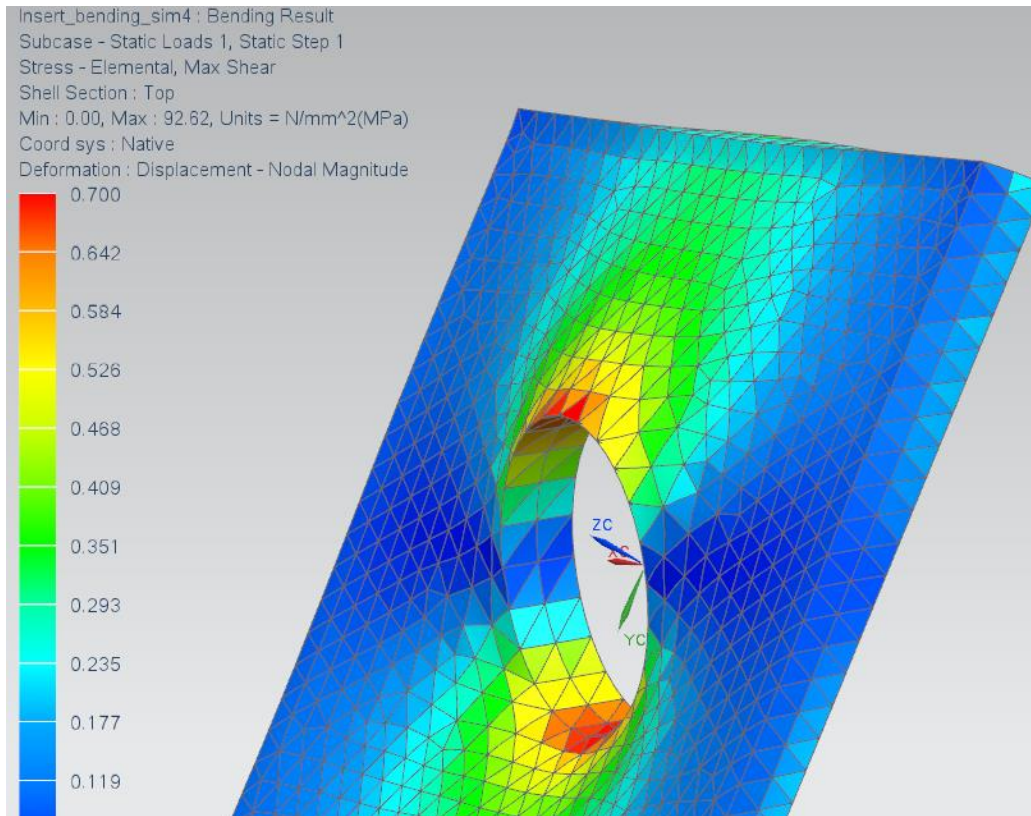


Figure 4.11: Stress plot of core, insert bending test.

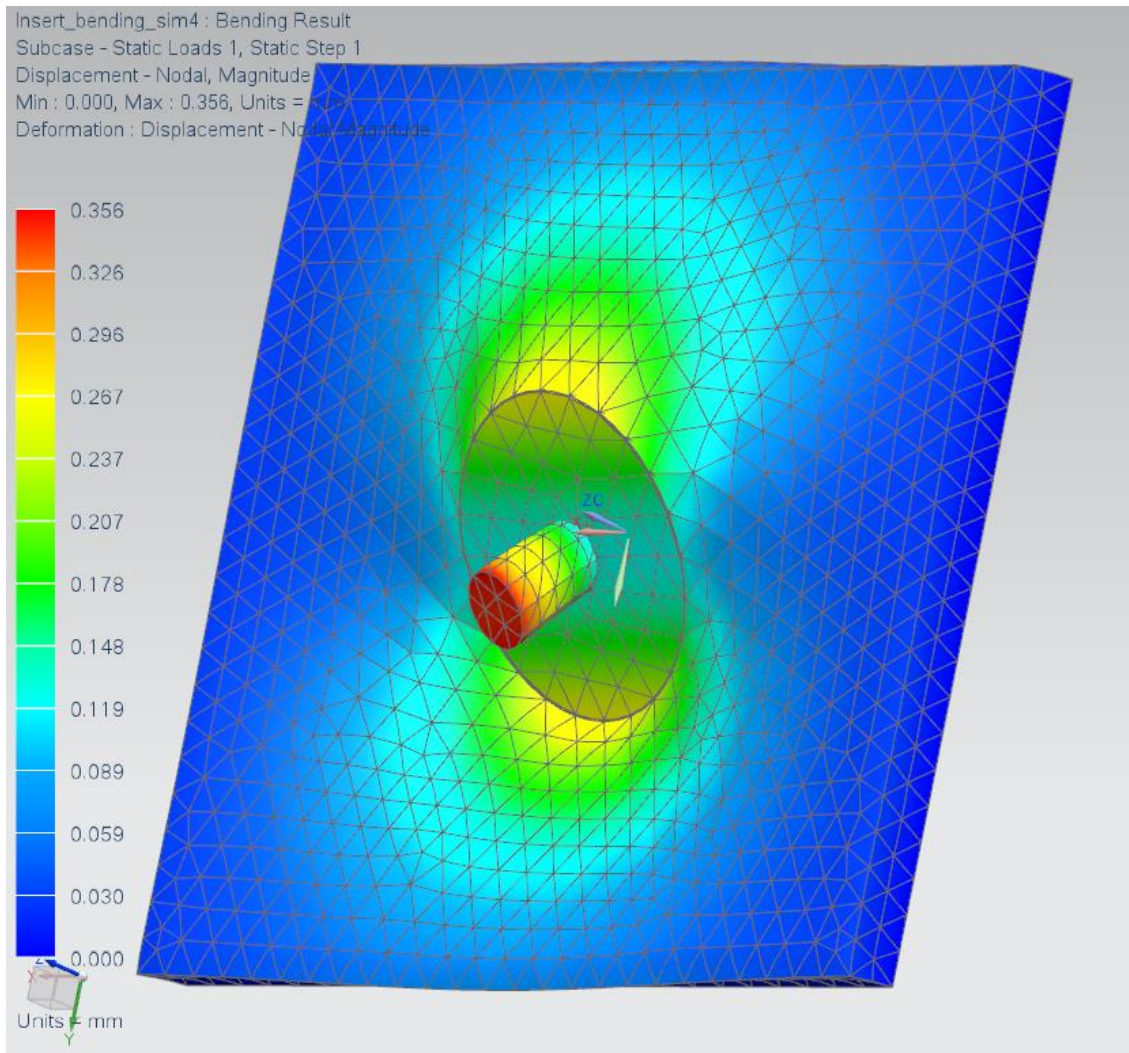


Figure 4.12: Displacement plot of insert bending test.

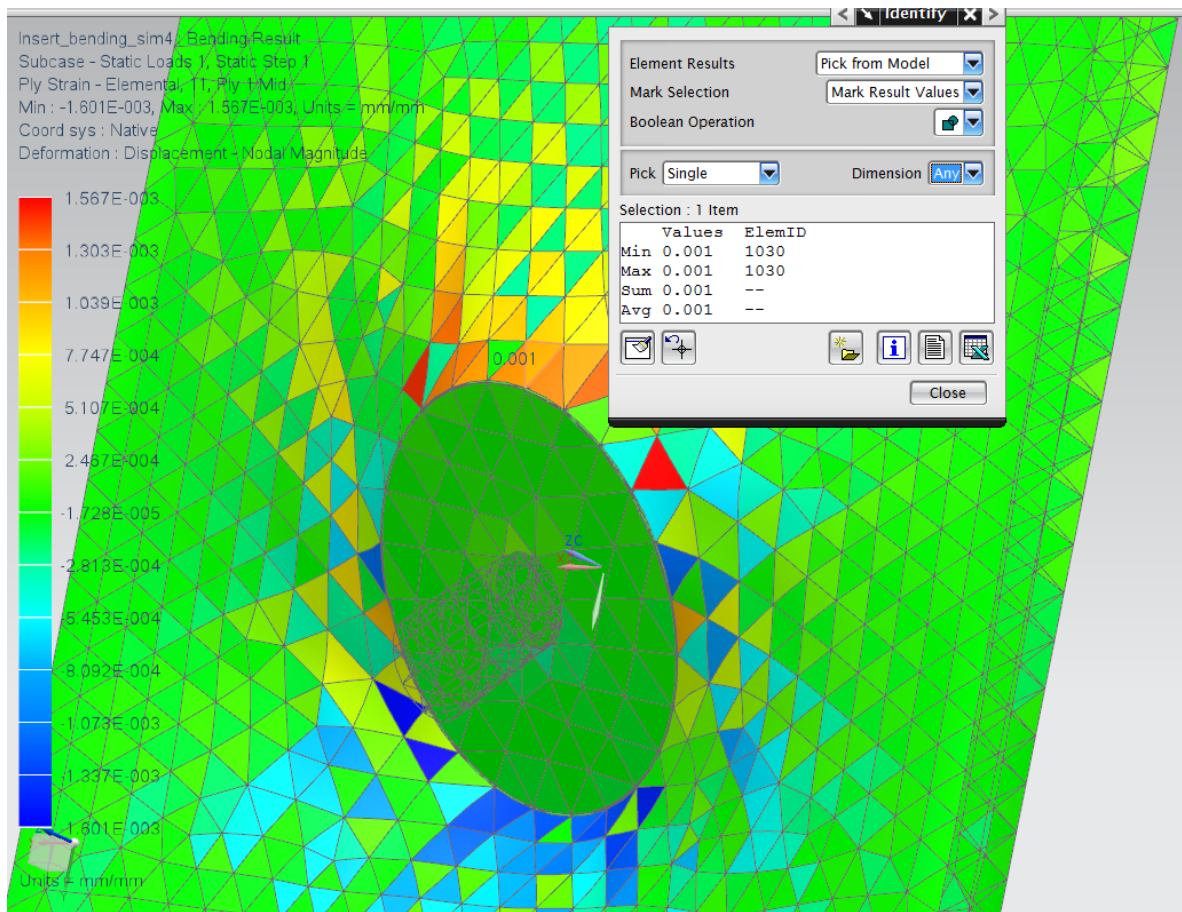


Figure 4.13: Strain around insert, insert bending test.

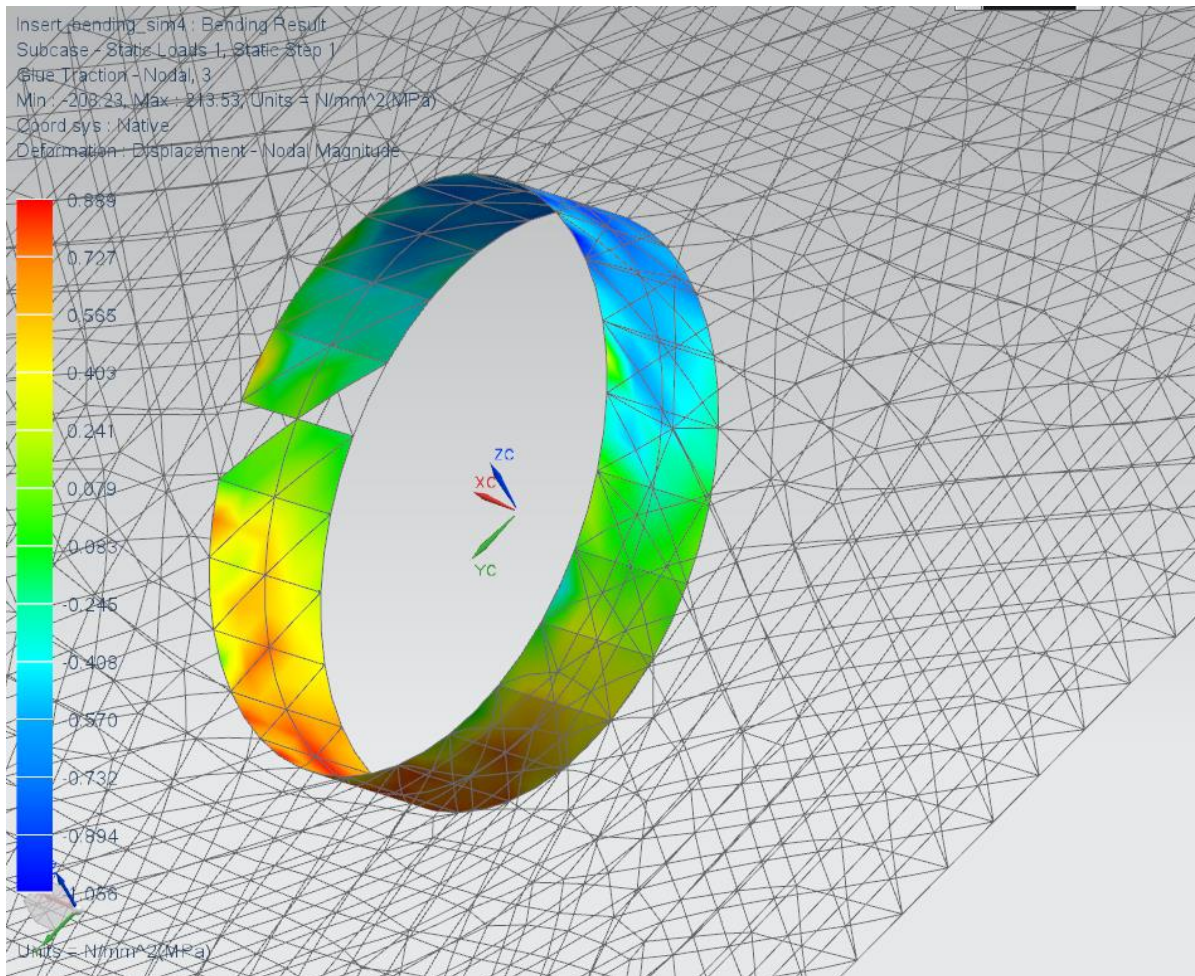


Figure 4.14: Bonding simulation, shear stress.

4.4 TORSIONAL STIFFNESS ANALYSIS

The recommended chassis torsional stiffness is mainly a function of vehicle mass, suspension stiffness and track layout. There is no definitive answer to the question “what is stiff enough?”, but there have been done some research on this topic. Deakin [1] suggests that a torsional stiffness of about 4 times the rolling stiffness of the suspension should be sufficient, which in this case means a little over 2500Nm/deg. A FEA model in NX Nastran was used to analyze the torsional stiffness of the chassis. It is reasonable to assume the chassis to act like a thin shell structure with relatively small deformations. The CAD model was meshed with 2D-elements and the laminate composed by the Amber E745 fiber and Hexcel 5056 flex core. Torsion loads acting on the chassis was modeled by constraining the rear hubs and loading the front suspension in torsion. To avoid complexity and simulation errors, the main hoop with bracings and the front hoop were omitted in the analysis. This gives a quite conservative result, as the hoops are expected to stiffen the structure to some degree. The torsional stiffness can be calculated using the equations given below:

$$K = \frac{T}{\theta} = \frac{PL}{\tan^{-1}\left(\frac{\Delta z_1 + \Delta z_2}{2L}\right)} \quad (\text{EQ29})$$

With:

K=Torsional stiffness

P=Arbitrary applied force

L=Distance from the hub to the centerline of the chassis

Z₁=Displacement of suspension point

Z₂=Displacement of mirroring suspension point

| Car | Mass[kg] | Stiffness [kNm/rad] | Stiffness [Nm/degree] | Specific stiffness [Nm/degree/kg] |
|--------------|----------|---------------------|-----------------------|-----------------------------------|
| FSAE low | 30 | 50 | 872,5 | 29,08 |
| FSAE average | 25 | 120 | 2094 | 83,76 |
| FSAE high | 20 | 300 | 5235 | 261,75 |
| URE05 | 25 | 200 | 3490 | 139,6 |
| Revolve 2014 | 18 | 186 | 3247 | 180,4 |

Table 4.5: Typical chassis torsional stiffness FSAE

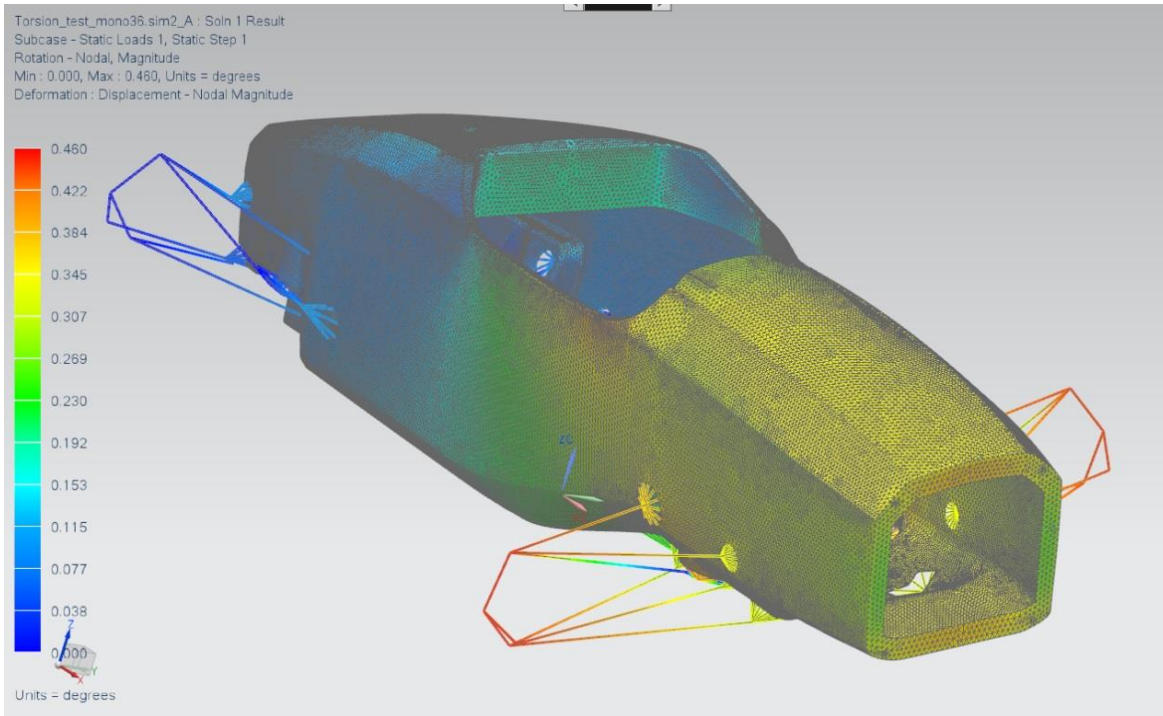


Figure 4.15: Deformation of chassis subjected to torsional load. First iteration with a result of 2200Nm/deg.

As the monocoque is required to comply with several regulations both in terms of stiffness and strength, the monocoque will achieve the lowest weight if the structure is divided into several different zones, each designed accordingly to its own requirements, both regulated and non-regulated.

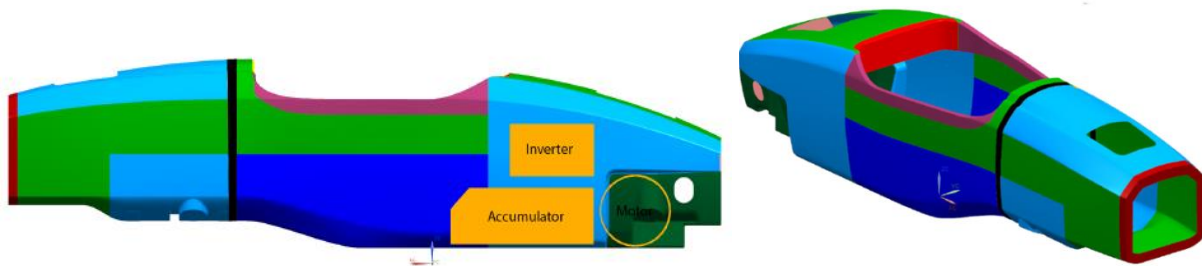


Figure 4.16: Different layout-zones of the monocoque.

It is apparent that a large cockpit opening is an important source of compliance, as well as compliance from the front suspension pickup points. It was experimented with different layups as well as 20 and 30mm core thicknesses for different zones of the chassis. A torsional stiffness of about 2200 Nm/deg was first achieved. Using the regulations and analyzing strain/deformation results a iteration process was begun in order to increase torsional stiffness. The model shows large displacement just at the start of the cockpit opening. It was mainly this area where we focused on iterating through different sandwich thickness' and ply orientation.

The results for the iteration process is presented with the following iterations:

2200Nm/deg, 2347Nm/deg, 2500Nm/deg, 2532Nm/deg, 3247Nm/deg.

| | | | | | | | | | |
|--------------------------|--|------------------------|--|--|-----------------------------|--|---------------------|--|--|
| Light green: | | | | | Purple: | | | | |
| Core: | | 20mm aluminium | | | Core: | | 20mm foam | | |
| Face sheets: | | 0/45 | | | Face sheets: | | 0/45 | | |
| Dark green: | | | | | Red (front bulkhead): | | | | |
| Core: | | 20mm aluminium | | | Core: | | 30mm foam | | |
| Face sheets: | | 0/45/0 | | | Face sheets: | | 0/45/0/45/0/45/0/45 | | |
| Dark blue (side impact): | | | | | Red (shoulder harness bar): | | | | |
| Core: | | 30mm foam | | | Core: | | 40mm foam | | |
| Face sheets: | | 0/45/45/45/0 & 45/45/0 | | | Face sheets: | | 0/45/0/45/0/45 | | |
| Light blue: | | | | | Yellow: | | | | |
| Core: | | 30mm aluminium | | | Core: | | 10mm foam | | |
| Face sheets: | | 0/45 | | | Face sheets: | | 0/45 | | |
| Pink: | | | | | Black: | | | | |
| Core: | | 30mm foam | | | Front hoop | | | | |
| Face sheets: | | 0/45 | | | | | | | |

Table 4.6: Layup for the zones shown in fig. 4.16.

As can be seen from table 4.6, the face sheets will mainly be a two ply 90/45 layup with three plies at zones requiring more stiffness and strength, like the side impact structure and around some suspension mountings.

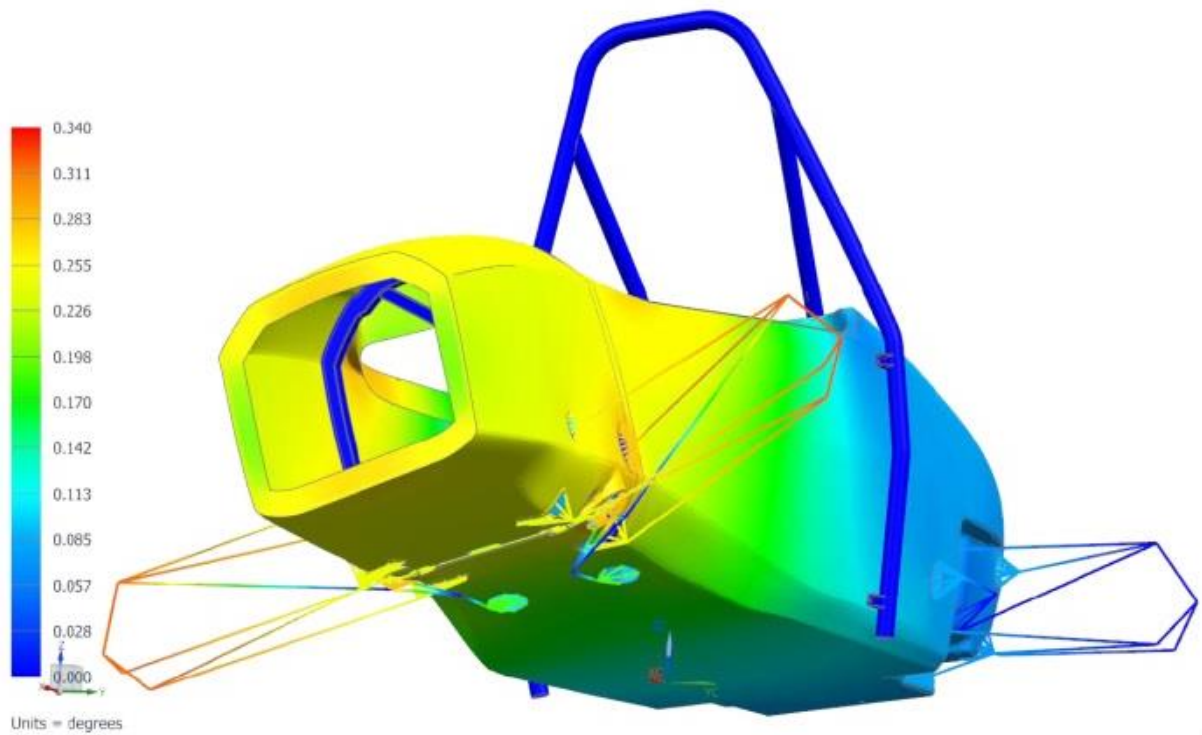
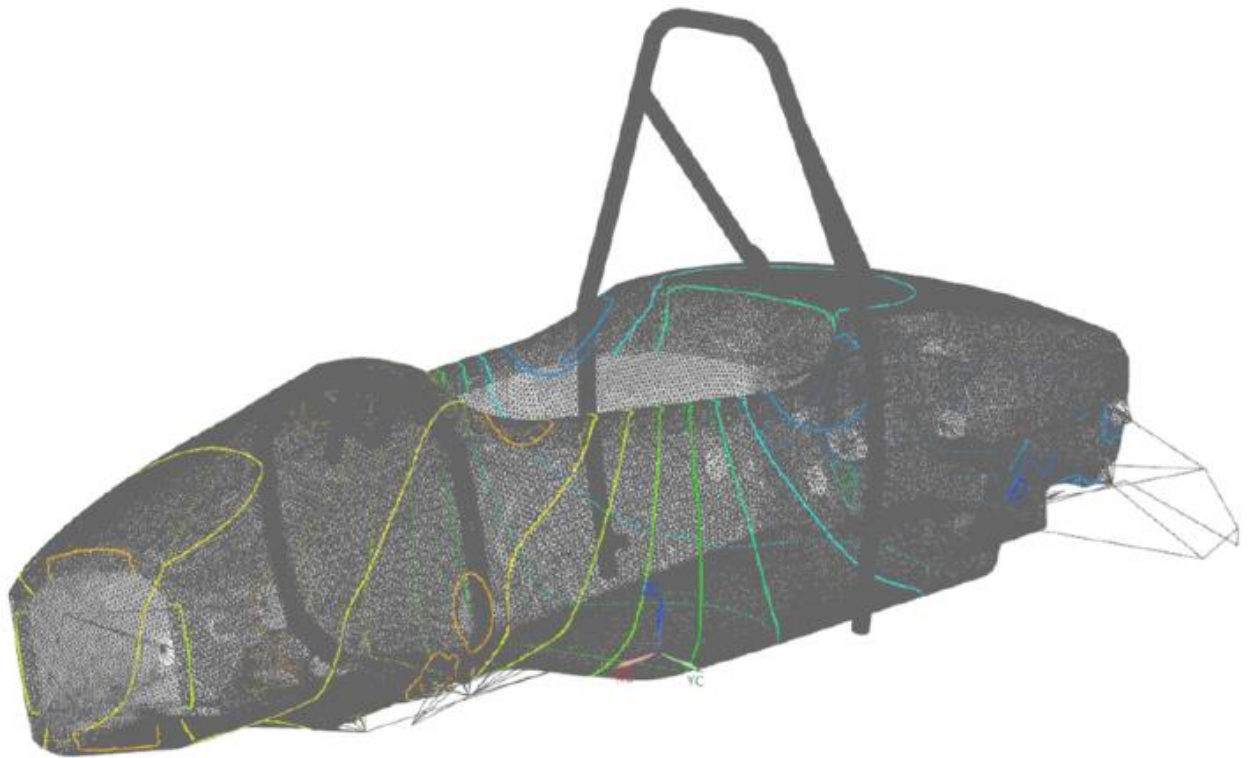


Figure 4.17: Torsional analysis with main hoop included, displaying the last iteration with a torsional stiffness of 3247Nm/deg.



CHAPTER 5

TESTING

5.1 RULE-REGULATED TESTING

There have been carried out a large number of tests to prove that the monocoque chassis is safe compliant with the rules. As explained in chapter 2, there are a wide range of rule regulated testing is required, including seat belt attachments as well as penetration resistance and stiffness of side impact structure. However, the rule-regulated testing is not an important focus in this thesis, and will therefore not be discussed.

5.2 INSERT TESTING

One of the objectives of this thesis is to do experimental research and testing of the local load carrying capacity of the structure, especially the solutions for joints and inserts. This is an important part of the evaluation and validation of the theoretical results, as it will give a basis for comparison between the theory and results collected in practical experiments. As mentioned earlier, local stiffness and strength is important in areas where concentrated loads are reacted into the chassis, for example in all the suspension attachment points.

As the monocoque chassis has a complex geometry with curvature and edges that is complicated and time-consuming to reproduce, it was decided to make flat insert test panels in order to test the load carrying capacity for different combinations of core material, core thickness, insert size and load cases. There has been done finite element analysis on identical insert test panels in NX Nastran, which is described in chapter 4. This analysis, as well as estimated load capacity using the ESA standard for inserts, will be used as a base for evaluation of the results. Although none of the experimental tests are true copies of sections on the monocoque and the loads reacted on it, it is reasonable to assume that the correlation between these experimental results and the analysis done earlier is transferable to the actual cases and analysis done on the chassis.

5.2.1 TEST SAMPLES

As can be seen from table 2.5 in chapter 2, all the chassis attachment points are subjected to a combination of shear, bending moment and out of plane loads. To represent the relevant load cases on the monocoque, there have been done two different types of tests, insert push tests and bending tests. The push test applies pure out of plane load to the test sample, while the bending test induces bending moment and shear force to the sample. The bending tests have a

close relation to the load reacted through the pullrods, which generates bending moment through the bellcrank pivot and into the chassis. The push tests are relevant for the out of plane loads reacted into the chassis, mainly through the wishbones.

All tests are produced and carried out at Department of Engineering Design and Materials at NTNU. There have been produced a total number 18 insert test samples, spread over three batches. It should be mentioned that there were used a different production method for batch number 1 than for batch 2 and 3. Batch number 1, consisting of only push test samples, was produced using a two-step procedure. In this process, the face sheets were cured separately before they were bonded to the core with adhesive film using a heated press. Epoxy was used as insert potting material. Batch 2 and 3 were produced in a one-step procedure where the face sheets were cured directly on the core in vacuum at high temperature. It was desirable to use adhesive film in these tests as well, but it was not available when the tests were produced. Expanding adhesive foam was used as potting material. All inserts used in the test samples are circular and made from medium-density fiberboard (MDF). Carbon fiber inserts are used in the monocoque chassis, but it was decided to use MDF for the test samples to save the cost of expensive carbon fiber material. It should be mentioned that the tests with



Figure 5.1: Test samples from batch 2 after cure.

The out of plane samples are produced as square panels with the dimension 200mmx200mm. There have been used different core materials and insert sizes for these tests. Bending test samples are square 220mmx220mm panels, all five samples are identical. The same layup are

used for all test samples, [0/45/Core/45/0]. Properties of all test samples are listed in table 5.1. Some samples were equipped with strain gauges to measure strain and compare with the analysis. The strain gauges were glued onto the surface of the outer ply oriented in the fiber direction, 5mm outside the edge of the insert.

The tests can be divided into three different test modes. Most of the tests were tested until complete failure.

5.2.2 TEST SETUP AND TEST PROCEDURE

A simple square 175x175mm frame made of circular tubes was used as rig for the out of plane insert tests. The samples were placed on top of the frame, constrained as simply supported in vertical direction. The force is applied through a bracket bolted to the insert, as shown in figure 5.2 below. A speed of 3.5mm/min was used for all out of plane tests.

For the bending tests, a more complex, vertical test rig had to be made. One side of the test panel is bonded to a vertical frame with inner dimensions 200x200mm. The load is then applied to a shaft attached to the panel through a hole in the insert. The load is applied with a distance of 15mm from the face sheet of the panel. This distance gives a suitable relation between bending moment and shear force on the insert. It can also be argued that this relation is of very little importance, as the bending moment is much more critical for the insert than the shear force [4]. The bending tests were run with the same speed as the out of plane tests, 3.5mm/min.

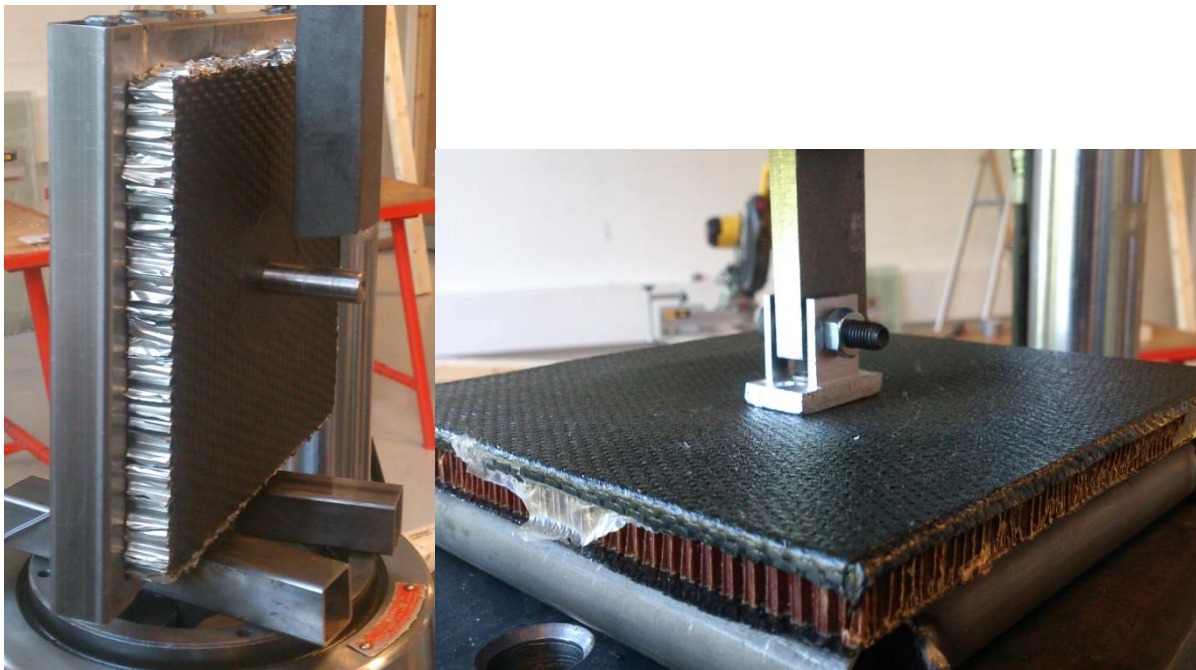


Figure 5.2: Insert bending test setup (left) and out of plane test setup (right).

Most of the samples were tested until complete failure. Some tests were stopped when they had just partly failed, right after the first load peak. This made it possible to identify the first and critical failure mode when inspecting the samples after the test. There have also been done some low cycle fatigue testing to investigate how the samples behaves when they are loaded to the design limits and above the design limits multiple times. As there may be individual variations between the test samples, it will require several tests to generate a consistent base of results for fatigue testing. Because of lack of resources, only one bending test sample and one out of plane test sample were fatigue tested.

| Sample name: | Core thickness: | Core type: | Insert diameter: | Production method: | Potting method: |
|-----------------------|-----------------|--------------------|------------------|--------------------|-----------------|
| Sample 1 Out of Plane | 20mm | HX-FC-5056/F40-2.1 | 50mm | 2-step | Epoxy |
| Sample 2 OOP | 20mm | HX-FC-5056/F40-2.1 | 50mm | 2-step | Epoxy |
| Sample 3 OOP | 30mm | HX-FC-5056/F40-2.1 | 50mm | 2-step | Epoxy |
| Sample 4 OOP | 30mm | HX-FC-5056/F40-3.1 | 50mm | 2-step | Epoxy |
| Sample 5 OOP | 30mm | HX-FC-5056/F40-3.1 | 80mm | 2-step | Epoxy |
| Sample 6 OOP | 30mm | HX-FC-5056/F40-3.1 | 80mm | 2-step | Epoxy |
| Insert OOP 7-2 | 20mm | HX-FC-5056/F40-2.1 | 47mm | 1-step | Adhesive foam |
| Insert OOP 8-2 | 20mm | HX-FC-5056/F40-2.1 | 47mm | 1-step | Adhesive foam |
| Insert OOP 9-2 | 12,7mm | ECK-3.2-72 | 47mm | 1-step | Adhesive foam |
| Insert OOP 10-2 | 12,7mm | ECK-3.2-72 | 47mm | 1-step | Adhesive foam |
| Insert Bending 1-2 | 20mm | HX-FC-5056/F40-2.1 | 76mm | 1-step | Adhesive foam |
| Insert Bending 2-2 | 20mm | HX-FC-5056/F40-2.1 | 76mm | 1-step | Adhesive foam |
| Insert OOP 11-3 | 20mm | HX-FC-5056/F40-2.1 | 47mm | 1-step | Adhesive foam |
| Insert OOP 12-3 | 20mm | HX-FC-5056/F40-2.1 | 47mm | 1-step | Adhesive foam |
| Insert OOP 13-3 | 12,7mm | ECK-3.2-72 | 47mm | 1-step | Adhesive foam |
| Insert OOP 14-3 | 12,7mm | ECK-3.2-72 | 47mm | 1-step | Adhesive foam |
| Insert Bending 2-3 | 20mm | HX-FC-5056/F40-2.1 | 76mm | 1-step | Adhesive foam |
| Insert Bending 4-3 | 20mm | HX-FC-5056/F40-2.1 | 76mm | 1-step | Adhesive foam |
| Insert Bending 5-3 | 20mm | HX-FC-5056/F40-2.1 | 76mm | 1-step | Adhesive foam |

Table 5.1: Insert test samples

5.2.3 OUT OF PLANE TEST RESULTS

The out of plane samples can be divided into two main categories, namely the epoxy-potted samples produced in batch 1 and the foam-potted samples produced in batch 2 and 3. Batch one can be seen as some kind of test-batch, with some different insert sizes and core thicknesses. Because of the potting method, which is unsuitable for monocoque production, these results are not relevant for the monocoque chassis. However, from a more general point of view, it may be interesting to compare different potting techniques.

The out of plane samples in batch two and three are made from two different core materials, where the samples with the Hexcel flexcore honeycomb will be given most of the focus. The samples produced with the kevlar honeycomb are used as a reference.

5.2.3.1 Epoxy-potted inserts

As can be seen from table 5.1, batch 1 consists of six samples. Two samples with 50mm insert and 20mm core, two samples with 50mm insert and 30mm core, two samples with 80mm insert and 30mm core. For the samples with 50mm inserts, one of each sample was tested to complete failure. The other one was tested until failure started to occur and the load-displacement curve began to level out. Load vs. displacement curve for all samples is displayed in figure 5.3. For the samples with 80mm inserts, sample 5 was tested until complete failure, while sample 6 was loaded to its expected limit five times before it was loaded to failure. This made it possible to investigate any signs of weakening in the sample when loaded close to design limit more than once. As shown in figure 5.4, no weakening or softening of the insert panel was found.

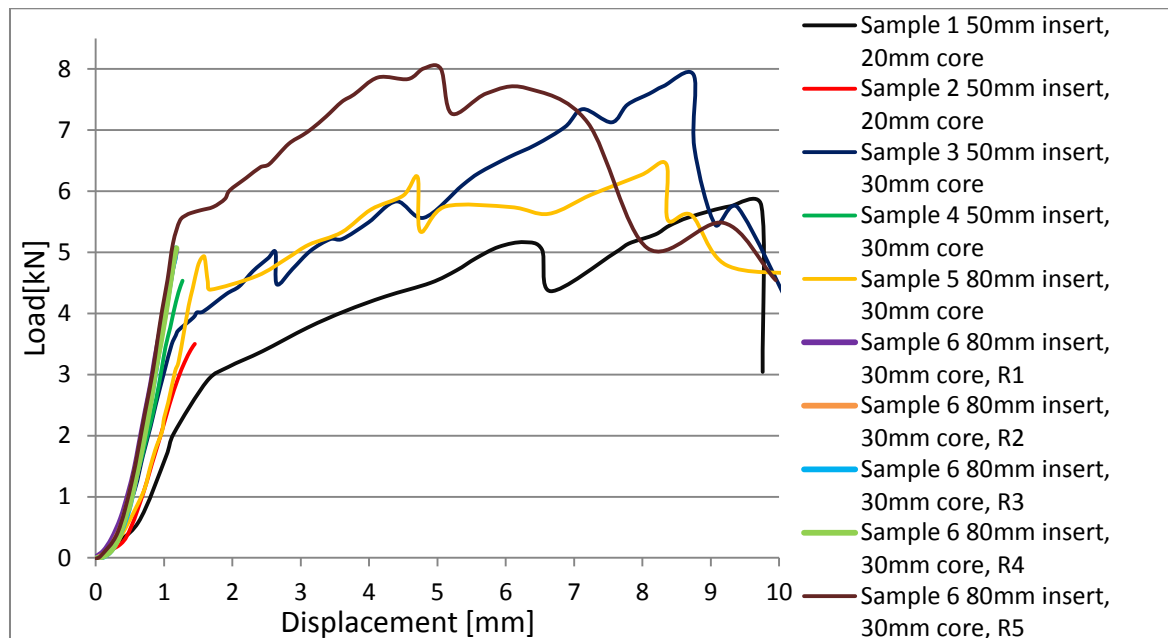


Figure 5.3: Load-displacement curve for epoxy-potted insert samples

From the results displayed in figure 5.3, it can be seen that there are deviations between samples that in theory are identical. This applies particularly for the correlation between sample 1 and 2, and sample 5 and 6. When investigating the samples, it was discovered that potting material had leaked between the core and bottom facesheet. This lead to a smaller bonding surface between insert and core material, which again results in higher shear stresses in the core as the forces has to be transferred over a smaller area. As expected, the leak was worse on sample 1 and 5 than the other samples.

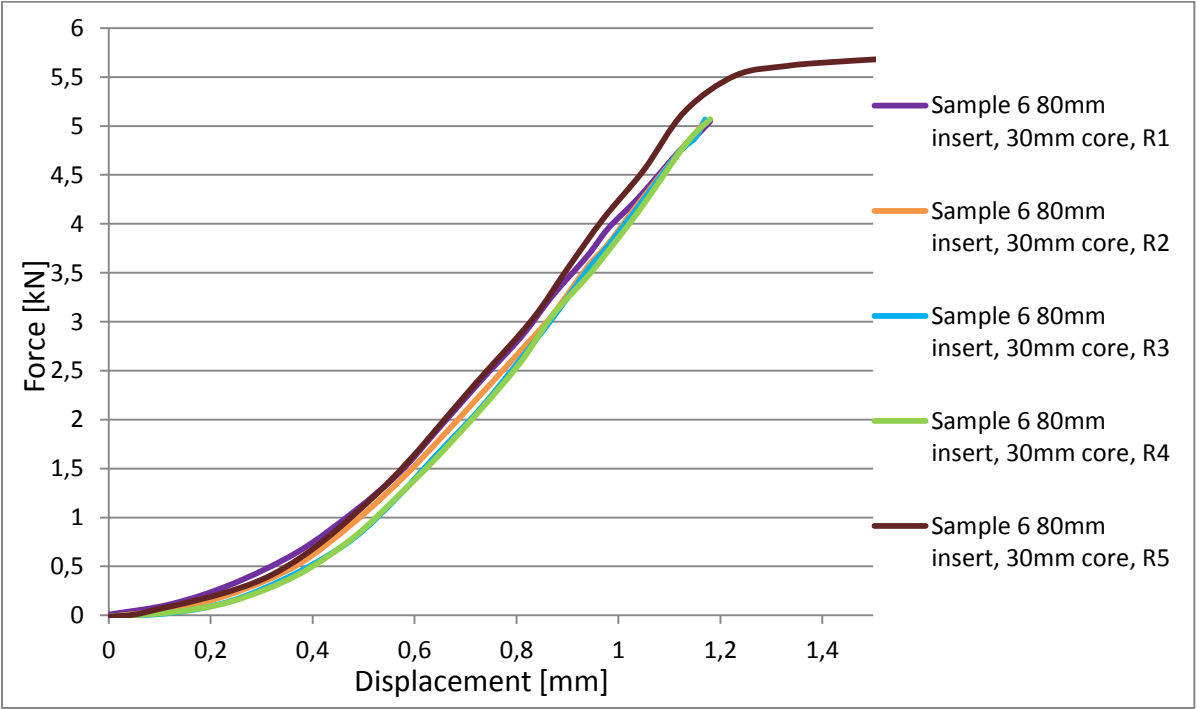


Figure 5.4: Repetitive testing of sample 6.

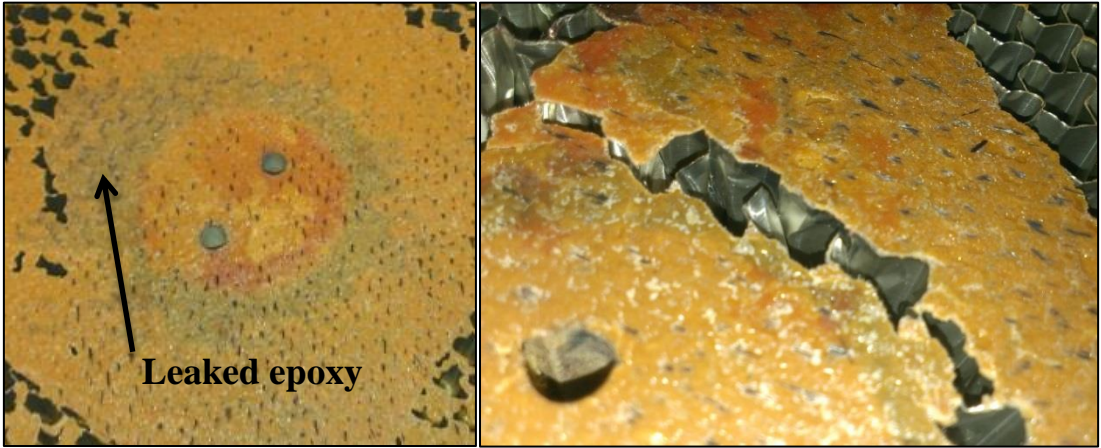


Figure 5.5: Evidence of leaked potting material (left) and core shear failure (right)

5.2.3.1 Foam-potted inserts

All samples produced in batch 2 and 3 are potted with adhesive foam. This is the same method that has been used on the monocoque. The facesheets are also cured directly on the core. This is less time consuming than the 2-step production method used for the samples in batch 1. As mentioned earlier, there are two types of foam-potted out of plane samples. Main focus will be the samples based on 20mm flexcore honeycomb, load-displacement curves for these samples are displayed in figure 5.6.

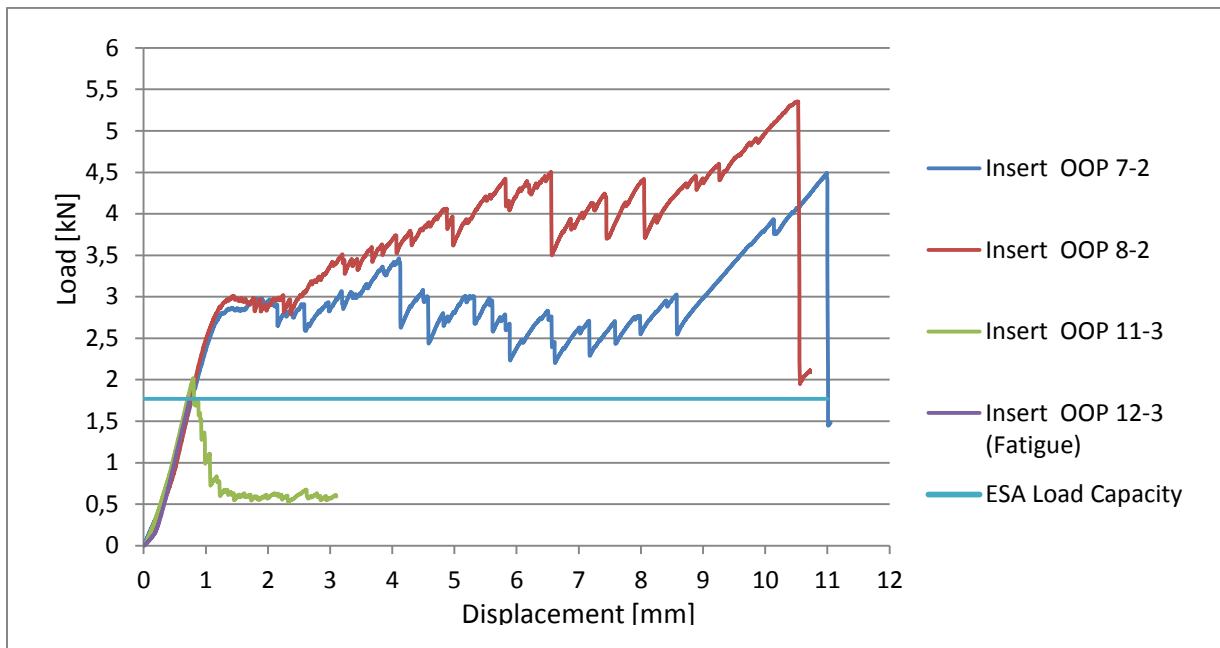


Figure 5.6: Load-displacement curve for foam-potted out of plane samples, flexcore

From figure 5.6, it can be seen that the failure load for sample 8-2 and 7-2 are close to each other in the range of 2.8kN to 2.9kN. The behavior of sample 11-3 differs dramatically from the other samples, with a failure load of only 2kN, which is about 70% of the failure load of the other samples. It should also be noted that the stiffness of sample 11-3 is identical to the others, but it fails earlier and more dramatically. While the other samples have an ultimate peak load at 4.5 and 5.3kN at high deformations, sample 11-3 immediately dropped to 0.6kN after the first peak. After investigation of the test samples, it was discovered that sample 8-2 and 7-2 failed as a result of core shear failure, while sample 11-3 failed as a result of face-core delamination. This explains the low failure load, and is also a reminder of the importance of production quality in sandwich structure. Non-visible defects may lead to dramatically reduced strength.

Load-displacement curves for samples with kevlar core are presented in figure 5.7. All three samples showed almost identical behavior, with a difference of only 3% between highest and

lowest failure load. The test for sample 13-3 was abandoned early due to problems with the data logging equipment. All these samples failed as a result of shear failure in the core, just as expected. Further discussion and evaluation of results are done in chapter 7, evaluation.

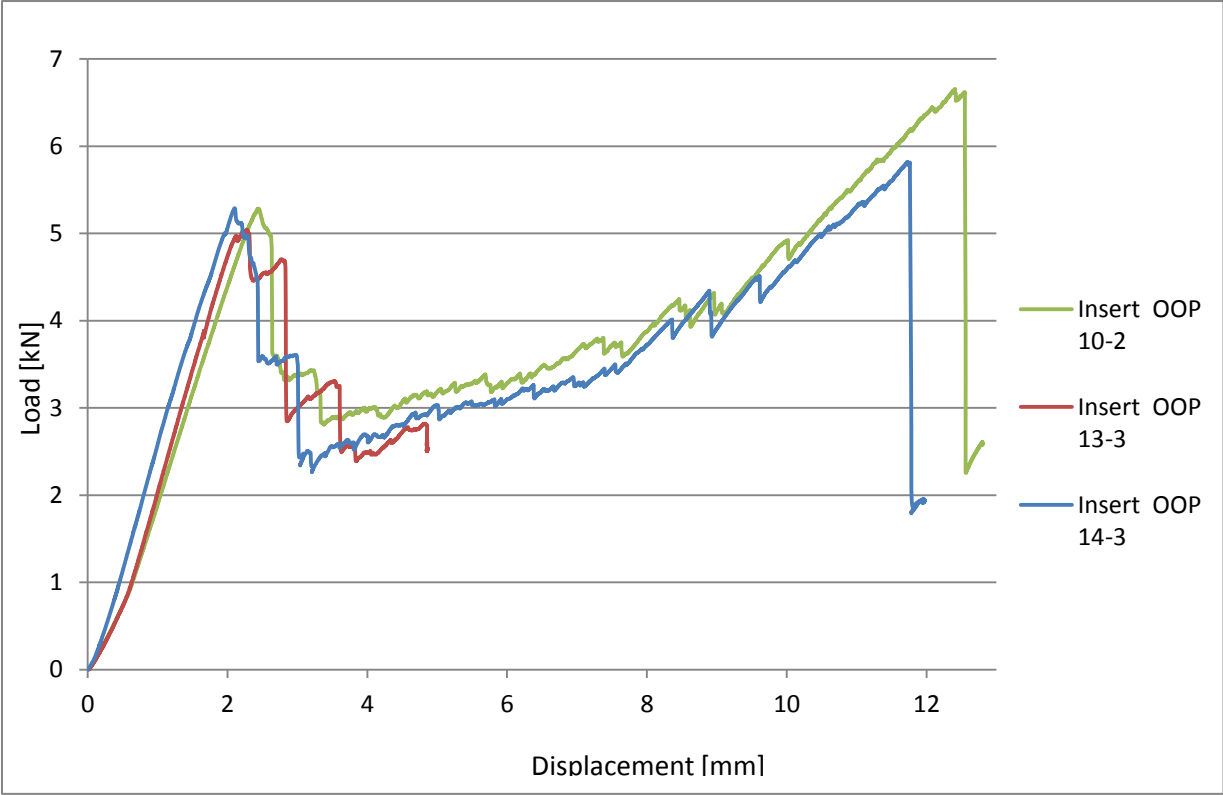


Figure 5.7: Load-displacement curves for 10-2, 13-3 and 14-3. Kevlar honeycomb core.

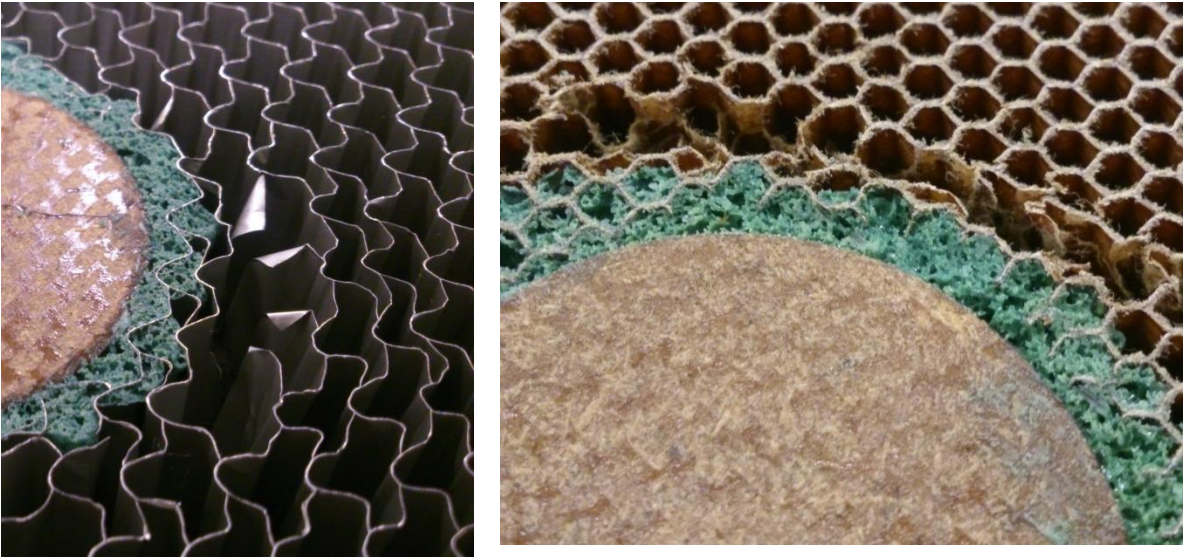


Figure 5.8: Shear failure of core in sample OOP 11-3 (left) and sample OOP 14-3 (right)

5.2.4 INSERT BENDING TEST RESULTS

There were produced five bending insert test samples, all with 20mm flexcore honeycomb as core material. The results from sample 1-2 and 2-2 showed that the insert itself failed as a result of the bending moment reacted into it. This problem was solved before the final samples were produced in batch 3. Load-displacement curves for all bending samples are plotted in figure 5.9 below. Sample 3-3 and 5-3 were tested to failure. The most noticeable is the difference in behavior of these two samples. While sample 5-3 had a failure load of just above 6kN and continues to an ultimate peak load at more than 9kN, sample 3-3 failed just before it reached 5kN. This was also the peak load of the sample. This behavior is comparable to sample 11-3 in the out of plane tests, and inspection of the sample revealed that face-core delamination was the cause of the failure. Sample 5-3 failed in core shear, just as expected.

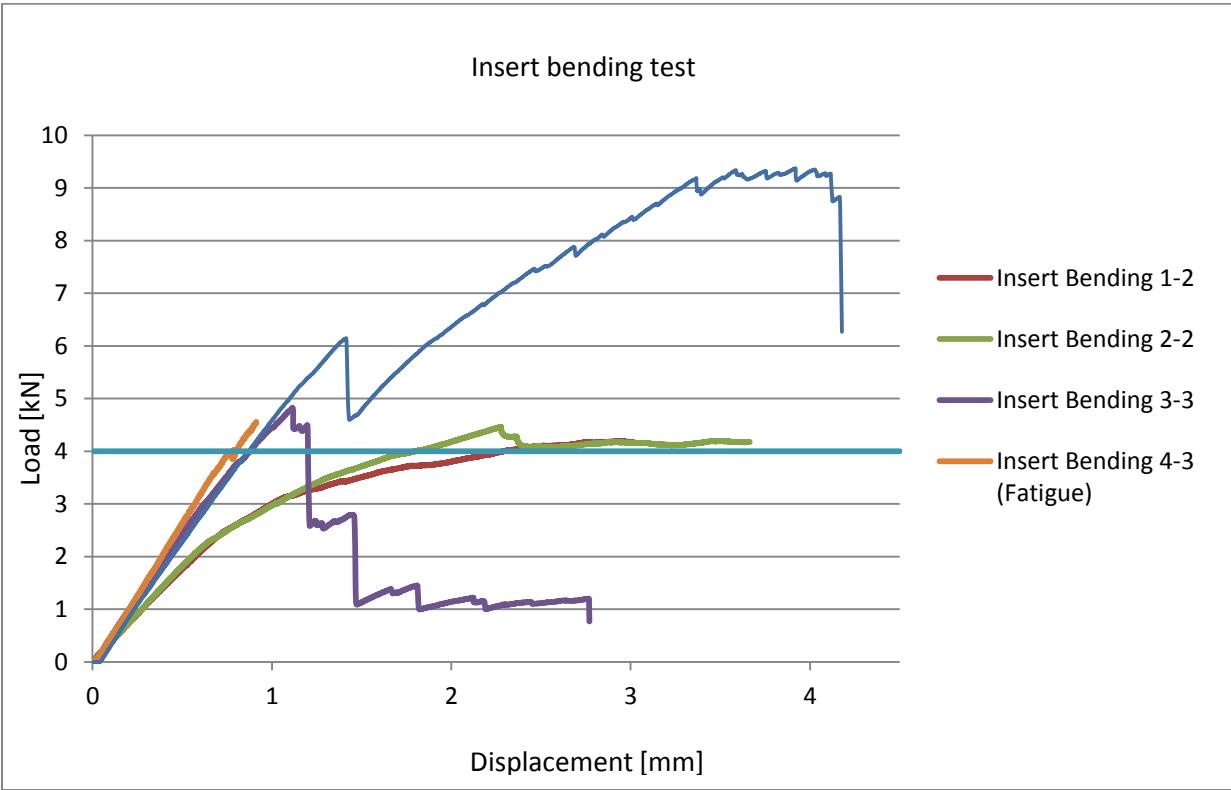


Figure 5.9: Load-displacement curves for insert bending tests.

5.2.5 FATIGUE TESTING

As mentioned in chapter 5.2.2, one bending sample and one out of plane sample have been low-cycle fatigue tested. From [21], assuming good production quality, composite sandwich structures are not prone to high cycle fatigue. It was therefore decided to do fatigue testing closer to the load limit of the panels. The purpose of these tests is to investigate the behavior when the insert panels are repeatedly loaded to, and beyond, their design loads. This is similar to what would happen in if the actual loads on the monocoque are higher than estimated, so that the monocoque is loaded beyond its designed capabilities.

5.2.5.1 Out of plane fatigue testing

Using ESA insert design handbook, the estimated load capacity of the insert test sample is 1.8kN. It was therefore decided run cyclic loading with 1kN as mid-load, and 0.8kN as load amplitude. Because of the test setup, reversed loading of the sample was not possible. The test was run with a frequency of 1Hz. No signs of defects or fatigue was visible after 2000 cycles. Initially, the peak deformation increased slightly, but it was stabilized after short time. It was therefore decided to increase the loading, with a mid-load of 1.2kN and a load amplitude of 1kN. Noise from initial defects and cracking in the core increased significantly, until the sample failed at 230 cycles with increased loading. The test procedure is shown in table 5.2.

| Sequence: | Load: | Cycles: | Comment: |
|-----------|----------------|---------|---------------------|
| 1 | 0N-1800N-1000N | 1 | Initial loading |
| 2 | 1000N±800N | 2000 | No signs of failure |
| 3 | 1200N±1000N | 230 | Failure |

Table 5.2: Out of plane fatigue testing, sample OOP 12-3

Figure 5.10 displays the load-displacement plot for the fatigue test as well as the three different phases described in table 5.2. When the load is increased, it is visible how degradation of the core starts to occur. The displacement increases significantly after only a few cycles, compared to the stage 2 loading where the deformation was more stable.

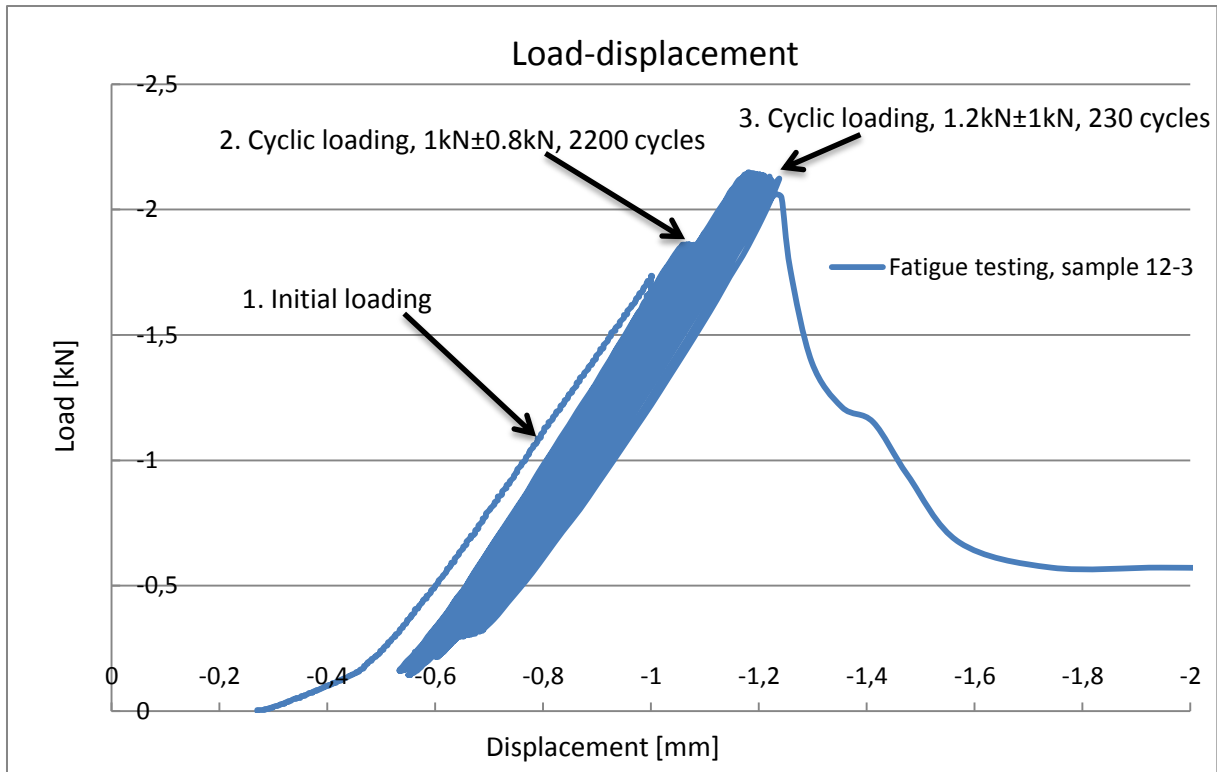


Figure 5.10: Out of plane fatigue testing

5.2.5.2 Bending fatigue testing

For the bending tests, the ESA estimated design load capacity was 4kN. From the destructive testing done earlier, there was not discovered any signs of initial core failure or defects before the failure loads, which was 4.85kN and 6.01kN for the two tests done. It was decided to run the fatigue test with a cyclic peak load at 4.5kN, which is 112.5% of the designed load capacity. The test was run with a frequency of 1Hz and load cycles 2500N+2000N. The sample failed at 1312 cycles. It can be seen from figure 5.11 that defects occurred regularly, as the peak displacement increased during the whole test.

| Sequence: | Load: | Cycles: | Comment: |
|-----------|----------------|---------|-----------------|
| 1 | 0N-4500N-2500N | 1 | Initial loading |
| 2 | 2500N±2000N | 1312 | Failure |

Table 5.3: Bending fatigue testing, sample insert bending 4-3

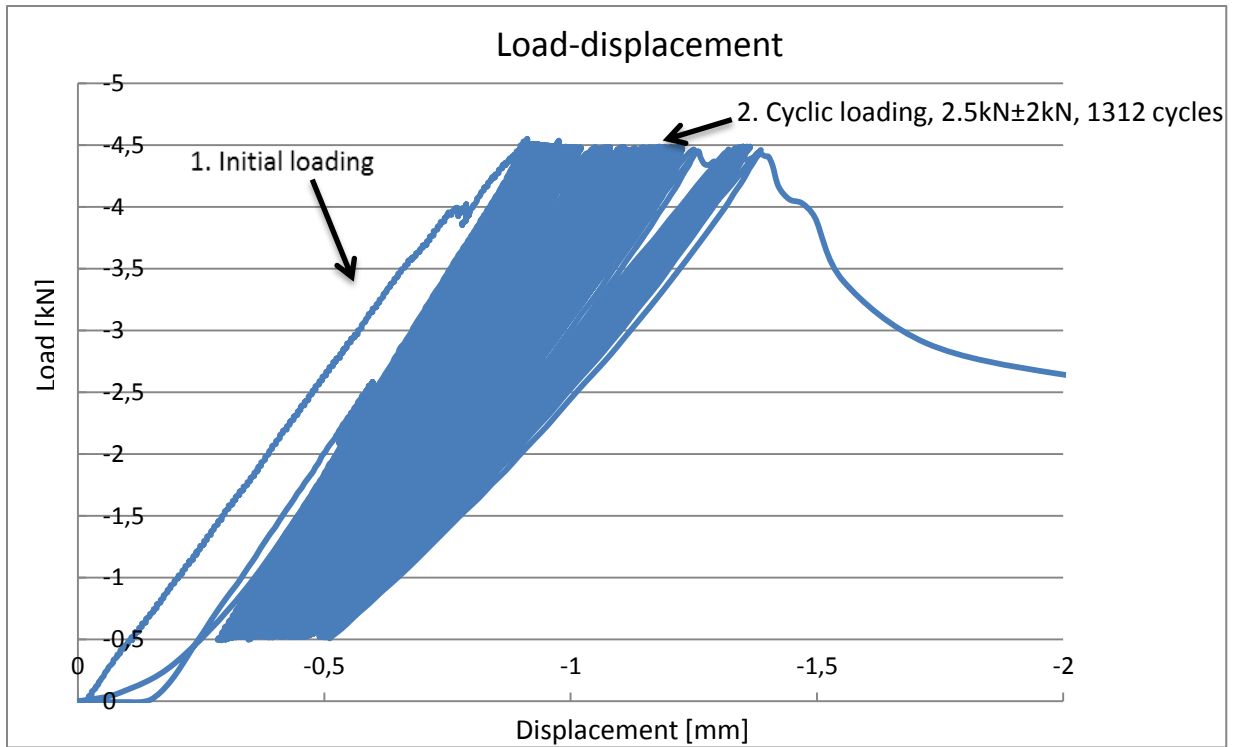


Figure 5.11: Load-displacement curve for fatigue testing, sample insert bending 4-3.



CHAPTER 6

EVALUATION

6.1 VALIDATION OF RESULTS

The information obtained in the experimental testing gives a fundament for evaluation and discussion around the analysis and theoretical work done earlier. Comparison between experimental results and the analysis is important in order to evaluate the accuracy and quality of the work that has been done, as well as identifying the most important sources of error. Focus will be the results from the foam potted insert test samples with flexcore honeycomb.

6.1.1 EVALUATION OF THEORETICAL AND EXPERIMENTAL STIFFNESS

To compare theoretical and experimental stiffness, the linear load-displacement curve from the finite element analysis is compared to the experimental curves. Looking at the results plotted in figure 6.1, the experimental curves are clearly offset compared to the linear FE-curve. This offset is caused by initial effects during loading of the sample. The FE-analysis does not include those non-linear effects, which means it is the linear area of the experimental curves that are will have to be evaluated. The average slope in this area is found to be 3.12kN/mm. When compared to the simulated stiffness of 3.26kN/mm, this gives a correlation of 95.7 % between finite element results and the experimental results.

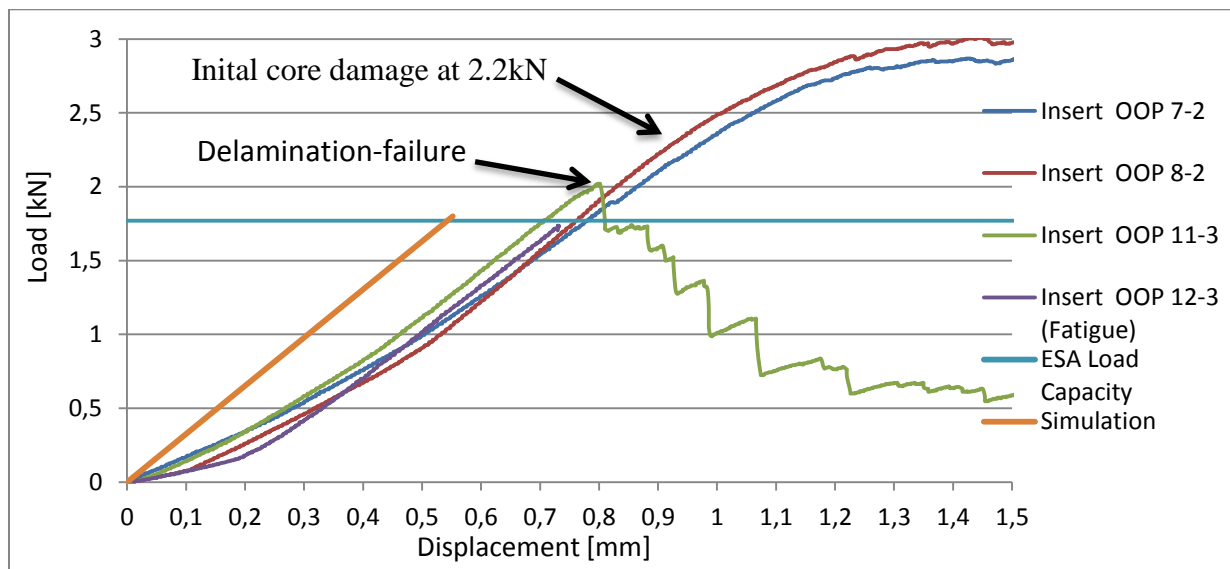


Figure 6.1: Experimental and theoretical load-displacement curves, out of plane test.

Looking at the results from the bending test samples in figure 6.2, there are large deviations between theoretical stiffness and tested stiffness, unlike what was the case for the out of plane tests. Another difference compared to the out of plane test samples is that there is no initial effect that delays the loading of the samples. The load-displacement curve is at its steepest when the displacement is low. It is likely that the difference between theoretical and actual stiffness is either caused by unknown compliance at one or more areas of the test setup rig, defects in the samples or incorrect finite element analysis. From what we have seen so far, production defects in the samples do not affect the stiffness noticeably, but it will lead to reduced load capacity.

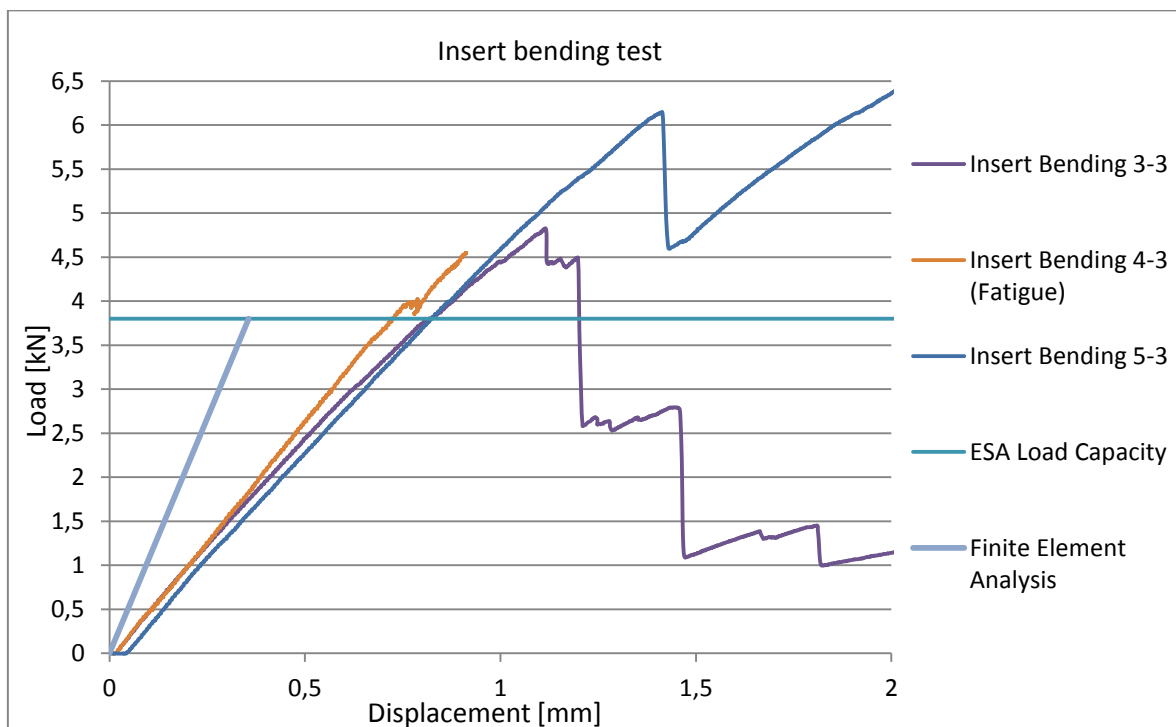


Figure 6.2: Experimental and theoretical load-displacement curve, bending insert test.

A compliance test of the test rig should have been carried out in order to get the exact stiffness of the rig, but this has not been done. Strain plots obtained from the experimental testing were compared to the strain from the FE-analysis, to further examine the correlation between testing and theory. Load-strain curves are plotted in figure 6.4, showing good correspondence at low displacements. As expected from the load curves, the strain curve for the test sample is degressive and separates from the linear FE-curve at higher loads. However, the accordance is much better than expected if the load-displacement curves are taken into account. It should also be mentioned that sample 3-3 was the only bending sample equipped with strain gauge. This sample had a more degressive curve than the other bending samples, which makes it a reasonable assumption that other one of the other samples would have showed better

correspondence with the FE-result. It is therefore reasonable to conclude that the main reason for the large deviation between the theoretical results and the test results is compliance in the test rig. Nevertheless, contribution from other samples cannot be completely ruled out without any compliance test of the rig.

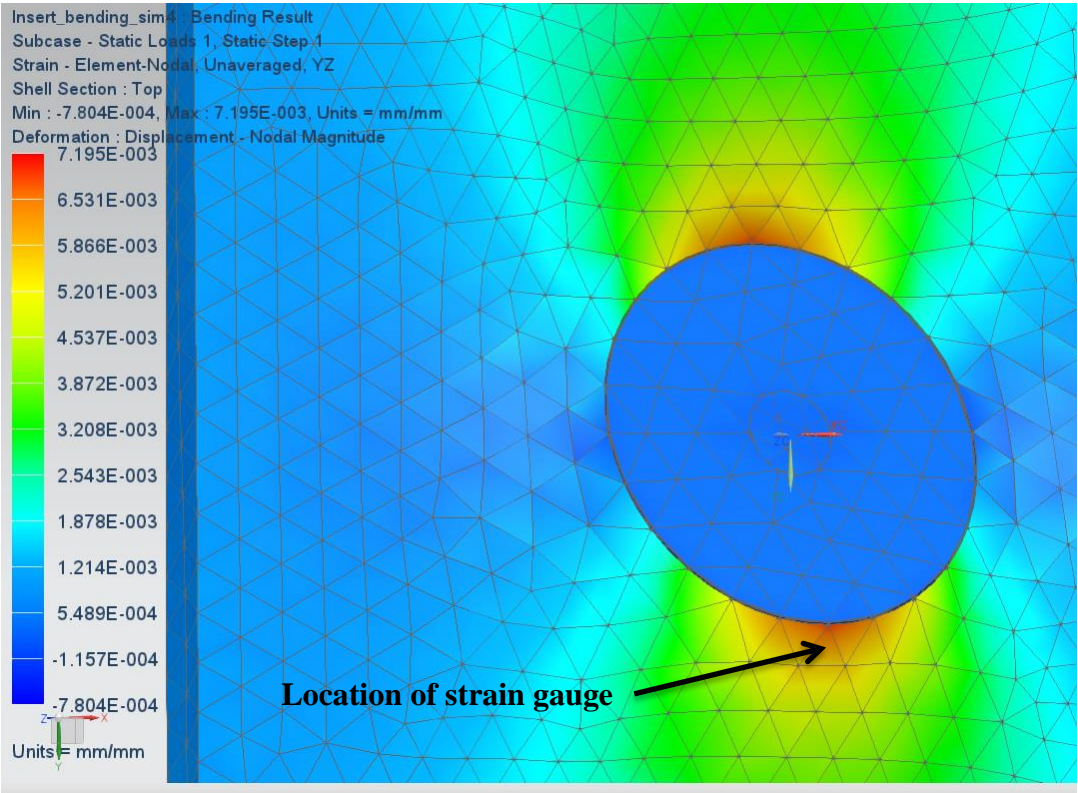


Figure 6.3: Strain plot of insert bending test at 3.8kN

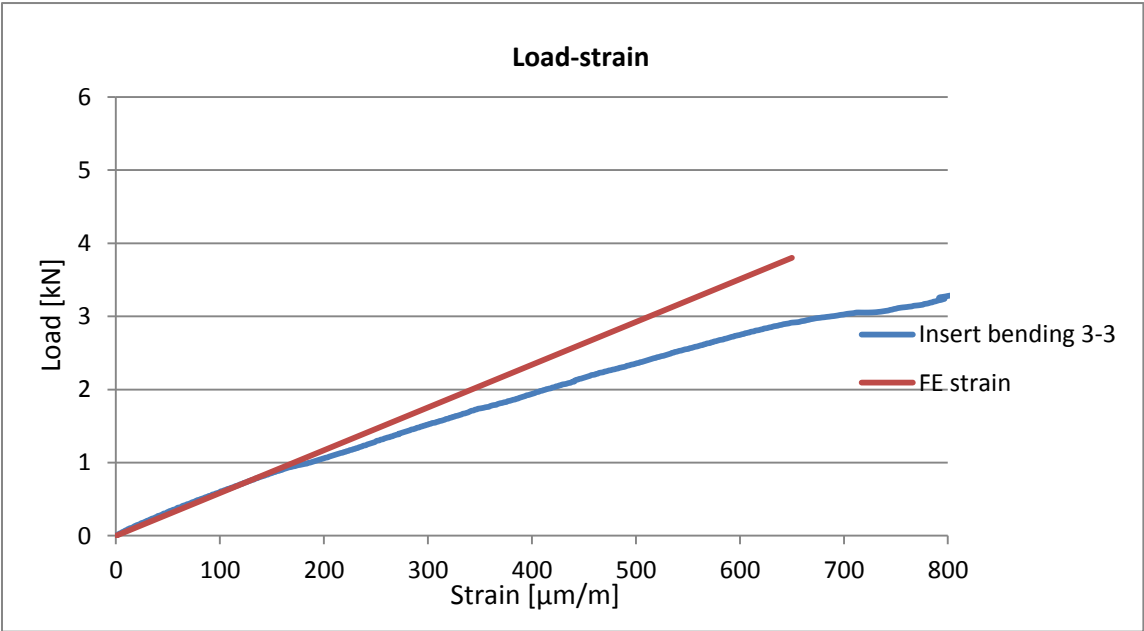


Figure 6.4: Load strain for insert bending test

6.1.2 EVALUATION OF FAILURE LOADS AND FAILURE BEHAVIOR

As mentioned in chapter 6 testing, the test samples of decent production quality failed as a result of core shear failure. Looking at sample 7-2 and 8-2 in figure 6.1, it can be seen that initial defects occur before the failure loads around 3kN. Local failure of core and debonding in these areas reduces the stiffness before the first peak load. The “plastic” zone of the curve is reached just above 2kN, which is where the panel starts to fail. This is where the core reaches its shear capacity. Figure 6.3 shows that the core shear stress around the insert when the sample is loaded to 1.8kN is around 0.6 Mpa. The shear capacity of the core is set by Hexcel to be 0.38 Mpa in W-direction and 0.72 Mpa in L-direction. It is then reasonable to assume that shear failure in the core starts to occur at this point. Using the weakest direction of the core in the equations given in the ESA insert design handbook [4], the load capacity of these insert panels should be 1.8kN.

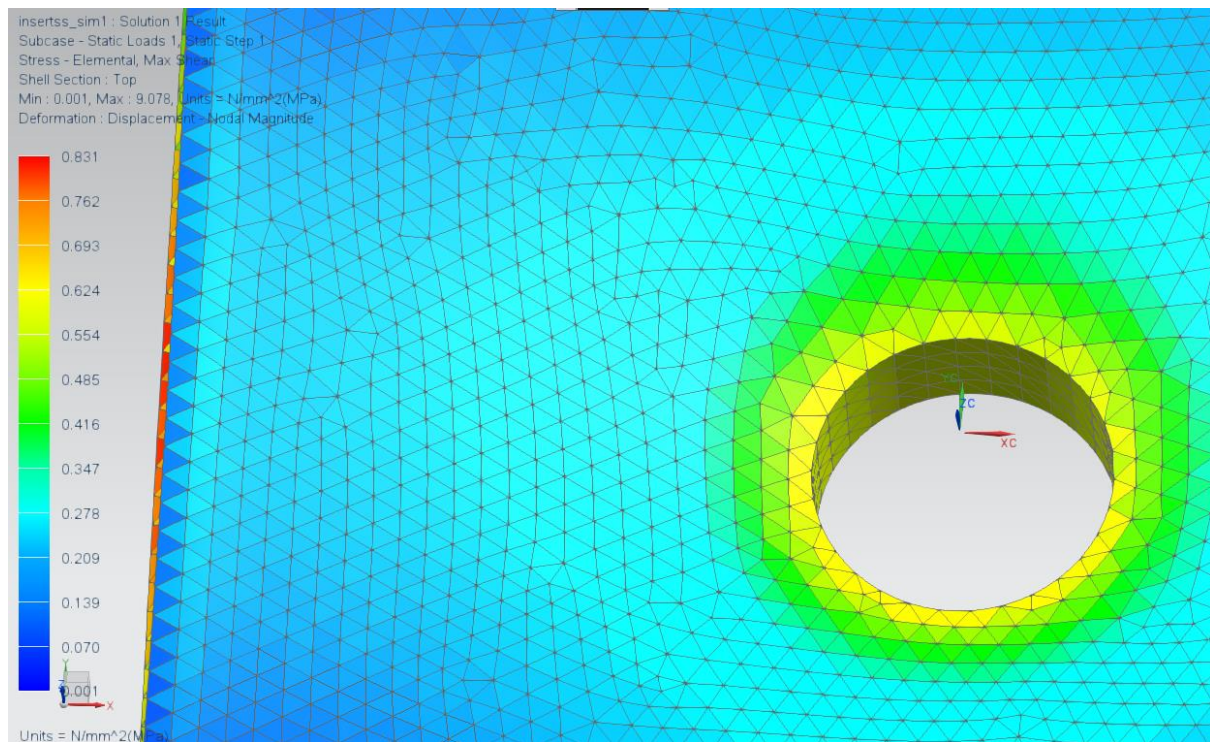


Figure 6.5: Shear-stress in core at 1.8kN.

The strains recorded by the strain gauges on the surface, has also decent correspondence with the results from the finite element analysis. The strain gauges measure the longitudinal strain of the fiber, and is placed in 0-degree direction, 5mm outside of the insert boundary. It should be mentioned that the strain values in the area around the strain gauge have large variations

over a small area, so any inaccuracy in the placement of the gauge may influence the results. After the initial response immediately after failure occurs, the strain values increases dramatically. As a result of the delamination between core and face sheet, the facesheet has to absorb more of the energy which results in higher fiber strain. At 0.5kN, the sample is almost completely debonded, and does not give any “resistance” to the load applied.

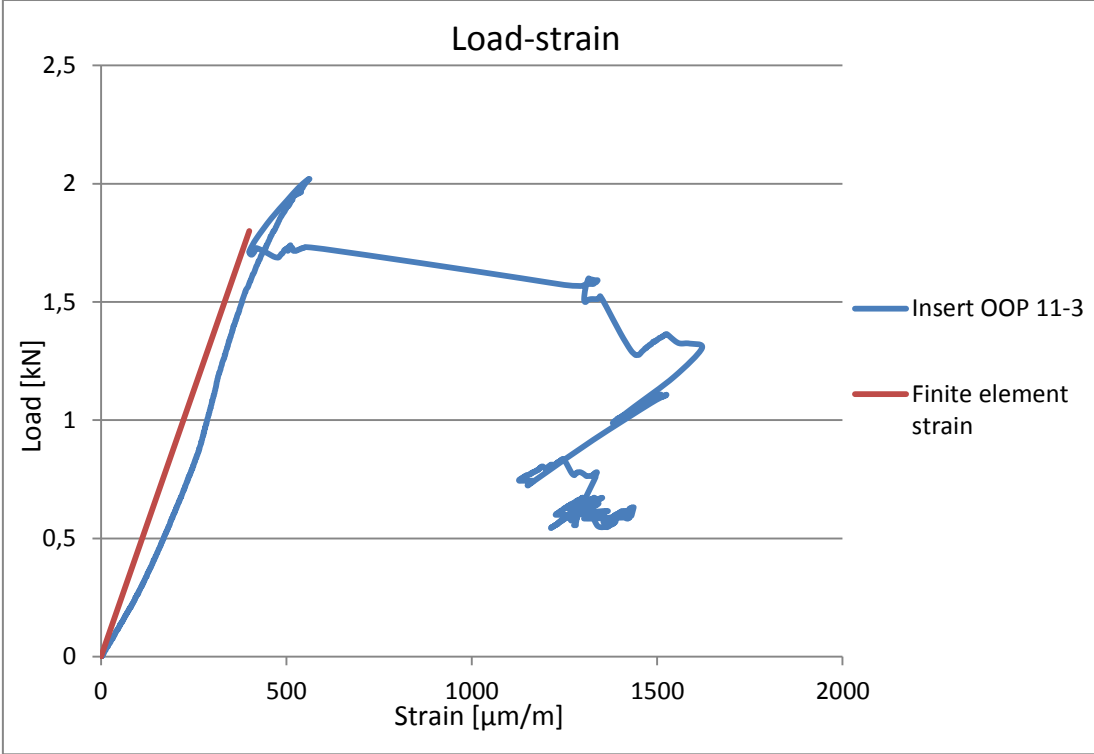


Figure 6.6: Load-strain curve for sample OOP 11-3.

6.1.3 FAILURE MODES

The failure modes observed are core shear and core-facesheet delamination. The results have shown that these two failure modes behave completely different. The samples that fail in core shear fail in a more predictable way. The load gradually increases as the core fails, and there are large deformations before complete failure occurs. The delamination failure happens more sudden, and at lower loads. This makes it more dangerous, as it is almost impossible to predict the failure. However, this failure mode should be seen as a consequence of manufacturing defects. Delamination should not be a problem if the production quality is decent, which means that core shear is the most relevant failure mode. When combining lightweight and relatively weak core material combined with stiff and high strength facesheet materials, the core will be the limiting factor.

6.1.4 SOURCES OF ERROR

During the testing, there have been unveiled a number of sources that may influence the results and lead to incorrect conclusions. Discussion of these sources is important to fully understand the results obtained. As already discussed, varying quality in the production of the samples caused some inconsistent results. It was later discovered that the out life for the prepreg used on some test samples was significantly exceeded. This results in partly pre-cured resin which leads to reduced bonding properties. This can explain some of the core-face delamination problems, and it is clear that the large celled aluminum honeycomb with thin cell walls makes good face-core bonding a challenge. Bonding problems did not occur with the denser kevlar honeycomb.

Compliance in the test rig is also a subject that should be discussed, especially for the bending tests. The load-displacement plots for these test samples had large difference from the curves obtained in the finite element analysis. When comparing the strain values obtained by the strain gauges on the sample and the FE-strain, the correspondence was reasonably good. This should indicate that the sandwich panel has the expected stiffness. Compliance in the test rig, in the shaft, in the insert itself, or a combination of these may cause 2.order effects resulting in measured deformations that are larger than expected. This should be further investigated; a compliance test of the rig should be carried out.

The load sensors in the test machine are another relevant source of error. Calibration using Intron's integrated calibration system was done, but a thoroughly calibration of the whole system is required to ensure correct results.

6.2 FURTHER DISCUSSION

The ESA insert design handbook has been used as design guide when designing inserts for the monocoque. It has also been used as a reference for the experimental testing of insert panels as well as the finite element analysis. For all test samples, failure occurred or started to occur at loads higher than the ESA load capacity of the sample. As found out earlier, the production quality was not satisfying for all samples. The weak samples failed at load just above their design loads, while the samples of decent quality failed at 125-160% of the ESA load capacity, depending on type of sample and definition of failure.



CHAPTER 7 PRODUCTION

7.1 INITIAL PROCESS

The manufacture of the monocoque is one of the largest and most complex challenges when building a first-time complex sandwich monocoque. The manufacturing process is demanding, both in time and complexity. A large amount of time has been used on research, tests and analysis of different production methods. There are many challenges that need to be overcome in order to successfully produce a high quality product. The first thing challenge that scratches surface is the general concept of the monocoque manufacture. One- or two stage moulding? One- or two part monocoque? What is our requirement for surface finish? These questions are basically the first things that is necessary to analyze and understand in order to get a great end result, as these choices may dictate other challenges at a later stage.

| | 1 stage, 2 moulds, 2 part cast | | 2 stage, 2 moulds, 1 part cast | |
|----------------------|---|--|---|--|
| Description | This method consist of a machined upper and lower negative mould. The sandwich is directly cast in each of the moulds, creating two halves of the monocoque to be bonded together after demoulding. | | This method consist of a machined upper and lower positive mould. Tooling CFRP prepreg is used to create two lightweight negative mould that are to be bolted together into a single negative mould. The sandwich is then made inside the mould. Slip conditions are met through disassembly of the two-part negative CFRP mould. | |
| Materials | MDF | Polyurethane | Aluminum | |
| Machinability | Good | Excellent | Excellent | |
| Machining tolerances | Fair | Good | Excellent | |
| Machine compability | Poor | Good | Excellent | |
| Laminate compability | Fair. Low temperature cure v | Fair. Low temperature cure v | Excellent | |
| Temperature comments | Good. Low CTE -> good tolerance. Can withstand high temperature with appropriate surface coating. | Poor. High CTE -> bigger deviations from original mould. Can only withstand <75 C before coming soft and unstable. | Fair. High CTE - > bigger deviations from original mould. Can withstand high temperaures | |
| End tolerance | Fair | Good | Excellent | |
| End finish | Good | Good | Excellent | |
| Estimated cost | Excellent. 1X | Fair. 3X | Poor. 10X | |

Table 7.1: Brief overview of the two most feasible tooling concepts

In order to overcome the slip condition and be able to produce the desired complex shape, a two pieced mould is required. This in combination

Precision, or end tolerances, eventually dictates where the most critical components are attached to the car. It is crucial to reduce deviations especially in suspension geometry as deviations here will not only change how the car behaves on the track, but it will also change both size and direction of the loads.

Based on this the 1-stage, 2-mould, 2 part cast manufacture concept was dismissed due to the fact that end tolerances was greatly compromised when bonding the two monocoque-halves together. Polyurethane boards has excellent machinability as well as good machining tolerances making and when combining this with the desired surface quality the polyurethane modeling boards make a suitable material for fulfilling Revolve NTNUs most important requirements. The PU boards are practically suited for prototyping, and the surface quality-to-cost ratio is also excellent.

The weight of the PU boards are however high, forcing Revolve NTNU to the tooling concept of a 2-stage,2-mould,1 part cast. The PU boards will first be machined to positive moulds, while using a low-temperature curing tooling prepreg to cast the final negative tools.

The tooling prepreg HX42 from Amber Composites was chosen due to its excellent surface quality as well as the low initial cure. The low temperature cure is indeed important as there is a large difference of coefficients of thermal expansion which would lead to an expansion of the mould proportional to the cure temperature. This would seem like a small uncertainty, but as the monocoque is rather large there will be significant change in the placement of the suspension geometry if the temperature is high.

A free-standing post cure at 190C will the tooling suitable for curing og resin systems up to ca185C, well within Revolve NTNUs resin system (135C).

7.2 PRECISION AND QUALITY

The downfall of using a composite negative two-part tooling will be the risk of springback or springing. Springback was originally a metalworking term to describe the action of sheet metal bent at an angle springing back after forming, caused by residual stress. By contrast, the majority of high-temperature curing composite prepregs spring-in during manufacture. Low-temperature curing prepregs may exhibit springin, springback, or even zero spring. The springback problem in tooling for composites occurs primarily on sharp angles and contours. Springin or springback can cause up to 4 ° of error on tools and parts. It poses more of a problem on thick parts than thin, mainly because thicker-section parts cannot be forced as easily into shape to conform to the rest of an assembly [26].

In order to reduce springback and/or other twist a layup specified form the manufacturer was selected. The layup of the tool is as of equal importance, thus Fibersim was used to simulate

draping of fibers for the correct fiber orientations. A balanced 1-8-1 layup, see table 7.2, consisting of 3k and 6k weaves was simulated and cut in accordance with FiberSim. Using a light weight fabric on the surface will aid surface finish, while the subsequent plies should be rotated 45 degrees each time to maximize strength and minimize the potential for twisting, the final ply should be the same weight as the first to give balance.

| Procedure | Ply number | Fiber orientation |
|---------------------------|------------|-------------------|
| Trim Strips PP1 | - | +45° |
| Laminate PP1 | 1 | 0° |
| Debulk | | |
| Laminate PP2 | 2 | 0° |
| Laminate PP2 | 3 | +45° |
| Laminate PP2 | 4 | -45° |
| Debulk | | |
| Laminate PP2 | 5 | 90° |
| Laminate PP2 | 6 | 90° |
| Laminate PP2 | 7 | -45° |
| Debulk | | |
| Laminate PP2 | 8 | +45° |
| Laminate PP2 | 9 | 0° |
| Laminate PP1 | 10 | 0° |
| Final debulk | | |
| Preparation for autoclave | | |
| Autoclave cure | | |
| Post cure | | |

Table 7.2: Tooling layup and procedure

As the tooling require a post cure to withstand the final cure of our 135C monocoque prepreg system care was taken in both the initial cure of the tools, as well as the post cure, in order to reduce twist and springback. For the initial cure a steady and uniform heat-up rate throughout the entire laminate is a key element. With our PU boards with a relatively high specific heat capacity the need for a slow temperature ramp is required to ensure that the inner plies of the laminate will have the same temperature as the outer plies. In order to ensure this multiple thermocouples was used in the cure, and the autoclave will regulate its temperature in accordance with the variance between the PU-thermocouple and the laminate couple.

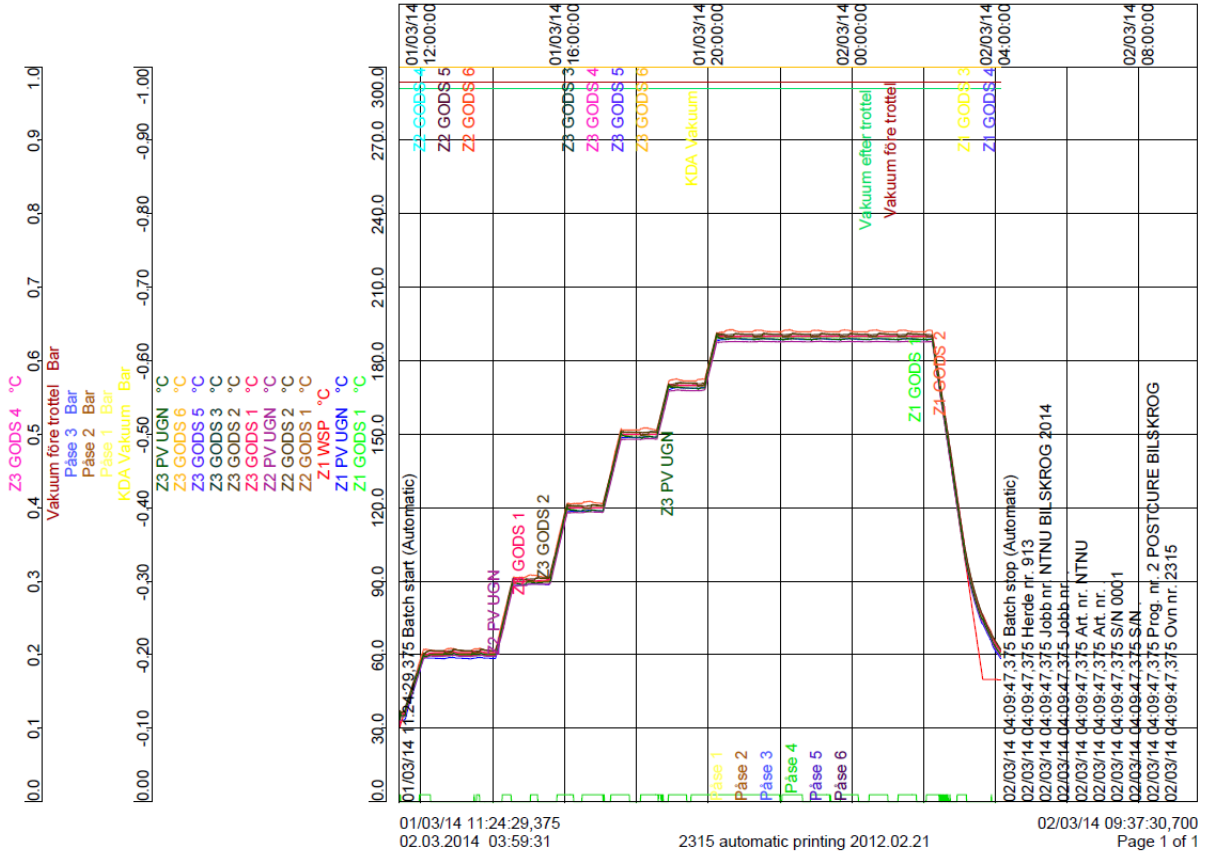


Figure 7.1: Thermocouple readings for monocoque tooling

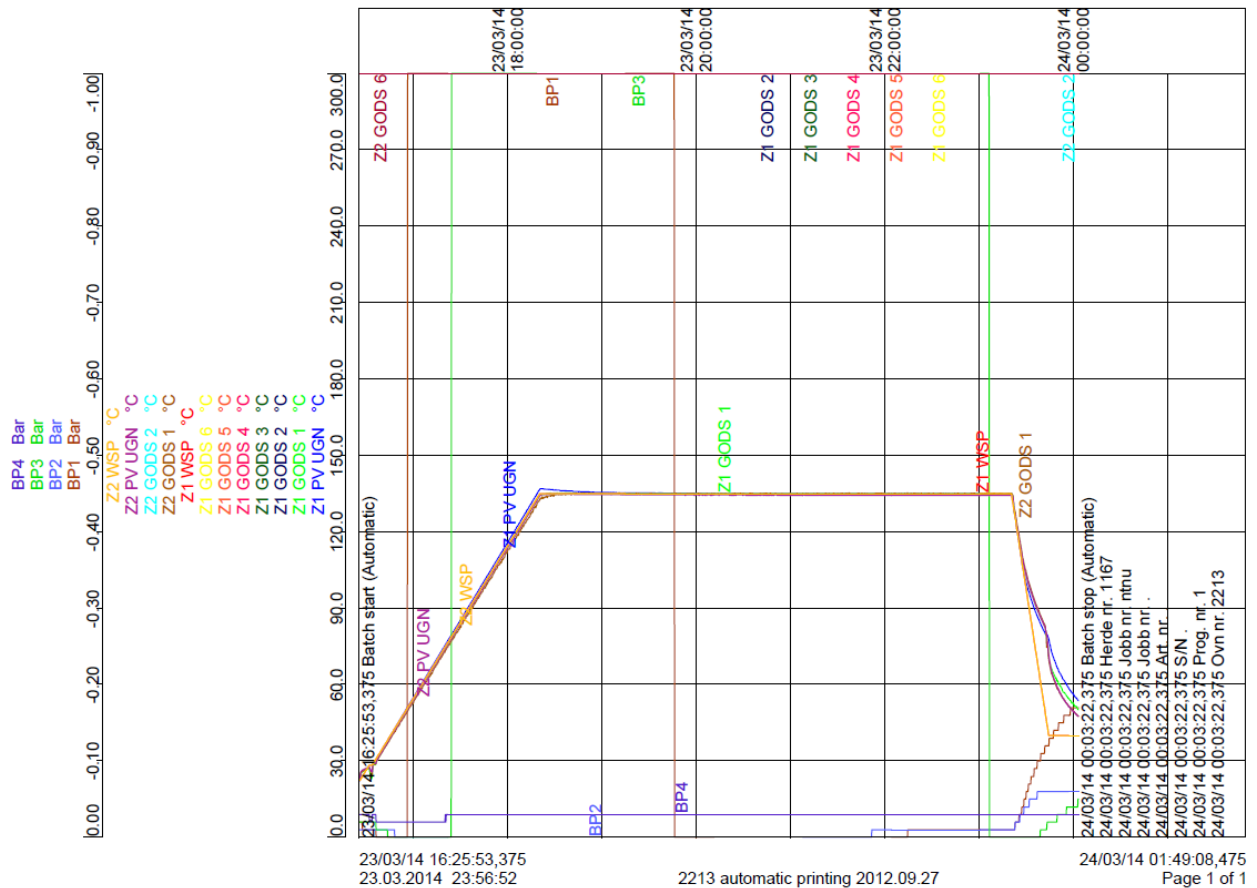


Figure 7.2: Thermocouple readings for monocoque outer facesheet.

Springback brings back the issue of precision and tolerances. As explained earlier deviations in attachment point are critical and must be reduced. The added manufacturing stage from 1 stage to 2-stage moulding increases the risk of deviations. In order to ensure that all attachment points and inserts will be placed on the exact right position a dowel pin system was designed to be integrated into the positive plugs. The moulds are machined with high precision, making the suspension mounts exactly at the right point in space. In order to benefit from this in the end, we designed a high precision dowel pin system to carry the precision through to the negative moulds, and finally the chassis. The system consists of machining an interference fit for the dowel pins for each of the inserts attachment points. Then dowel pins are assembled to the moulds, and the tooling moulds are created with the pins going through them. When the tooling mould is cured, it is demoulded with the dowel pins still inserted. Finally the outer skin of the monocoque can be placed in the tooling mould around the dowel pins, and then the inserts are placed onto the pins, in their correct position.

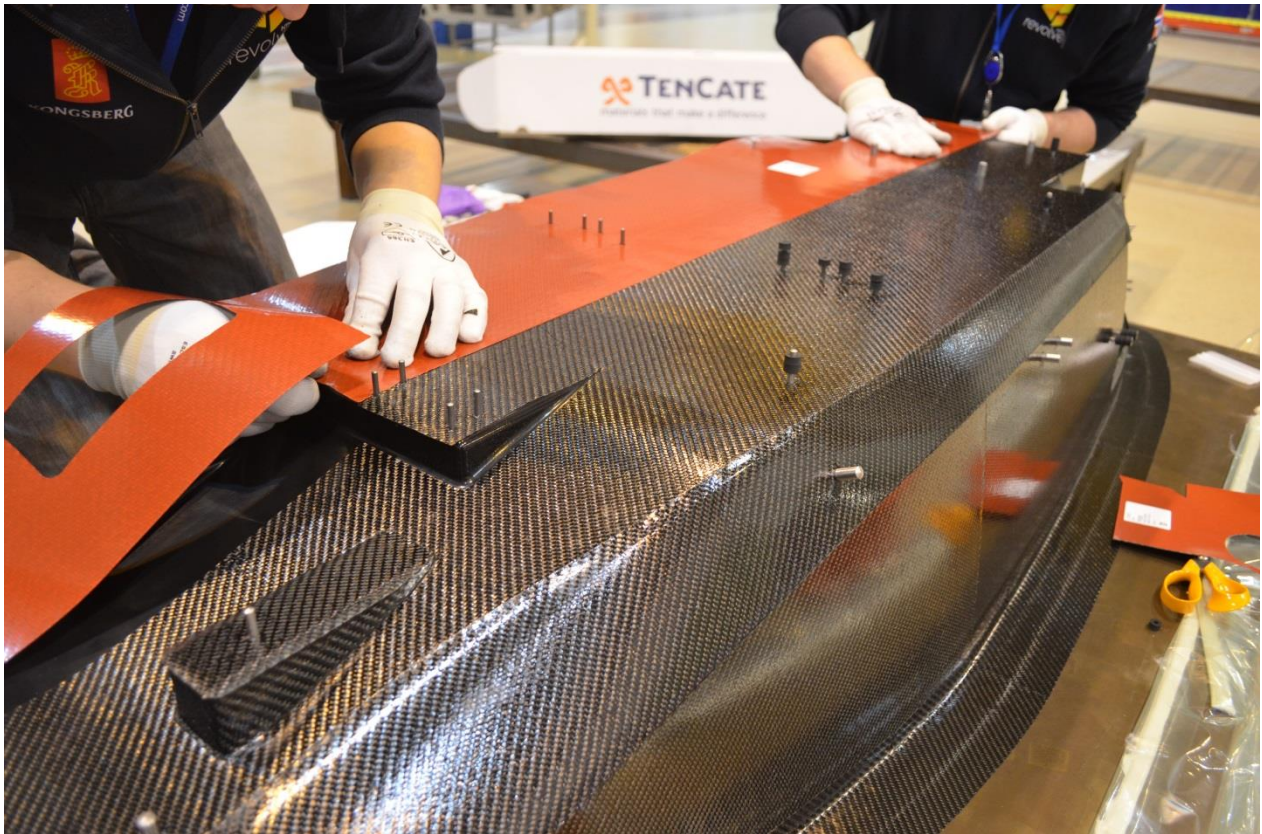


Figure 7.3: Layup of tooling prepreg for the composite tool.

In order to get the best surface finish on the outer skin, the best process would be to cure the outer skin separately. A separate cure of the outer skin will prevent the honeycomb and inserts from “denting” the outer skin. The prepreg resin systems provided by Amber Composites is designed for cure in an autoclave at a higher pressure. The dowel pins however induce a risk of bagburst, and total failure of the cure. A separate cure of the outer skin will eliminate this risk as it is then possible to disassemble the pins for the first cure, and assemble them again after the outer skin has been cured.

7.3 SANDWICH BONDING

In order to cure the outer skin separately and be able to bond the honeycomb core and inserts at a separate stage a film adhesive was needed. A lightweight film was chosen from our prepreg supplier, Amber Composites, as well as a 300g/m² adhesive film from Cytec. Testing of the different films proved that the lightest film was not suited to bond CFRP skin to the large-celled aluminum flexcore. Post inspection showed that 100g/m² adhesive film had at only about 0.1mm thickness failed to create sufficient fillets to the cell walls of the honeycomb, thus drastically reducing bonding area and therefore strength. To reduce complexity the 300g/m² was chosen for all the load critical areas of the chassis, regardless of core type.



Figure 7.4: Machining of moulds

The monocoque has, as mentioned before, a complex shape and there are practically no faces that do not have curvature. In order to make the inserts fit properly, we would in essence need to machine them to make them conform to the curvature of the monocoque. As our inserts are made of carbon they are ideally not machined as this is a both cost and time consuming process. The surface quality of machined CFRP could be substantially reduced and the laminate could experience delamination, fiber pullout, and uncut fibers. In addition it is expensive to machine due to rapid tool wear. To overcome this challenge we decided to use a water jet to cut out planar inserts. With a planar insert there will be a gap between the outer skin and the inserts, and the bonding between skin and insert would be practically non-existing. A thixotropic adhesive with the desirable cure and strength properties was found and will be used as a liquid shim between the insert and skin. The thixotropic nature of the two-component epoxy, Hysol EA9394, makes it suitable to gap filling, and will ensure contact and good bonding between the insert and face sheet. It will also be possible to work with the adhesive in ceiling mounts, working against gravity, due to the thixotropic nature of the adhesive.

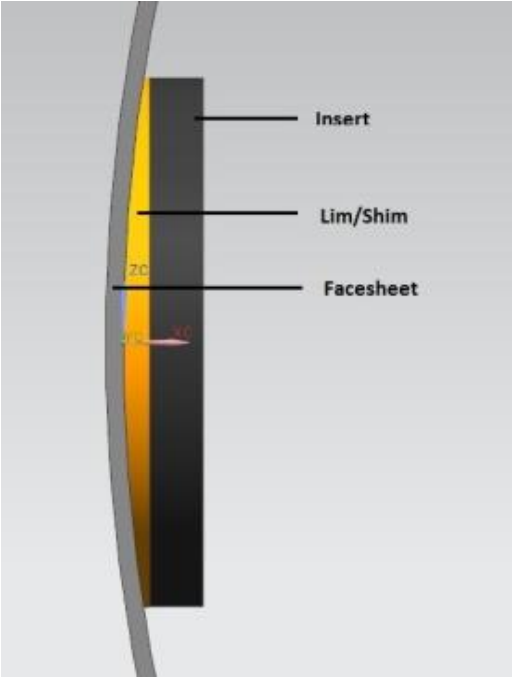


Figure 7.5: Liquid shim of insert.

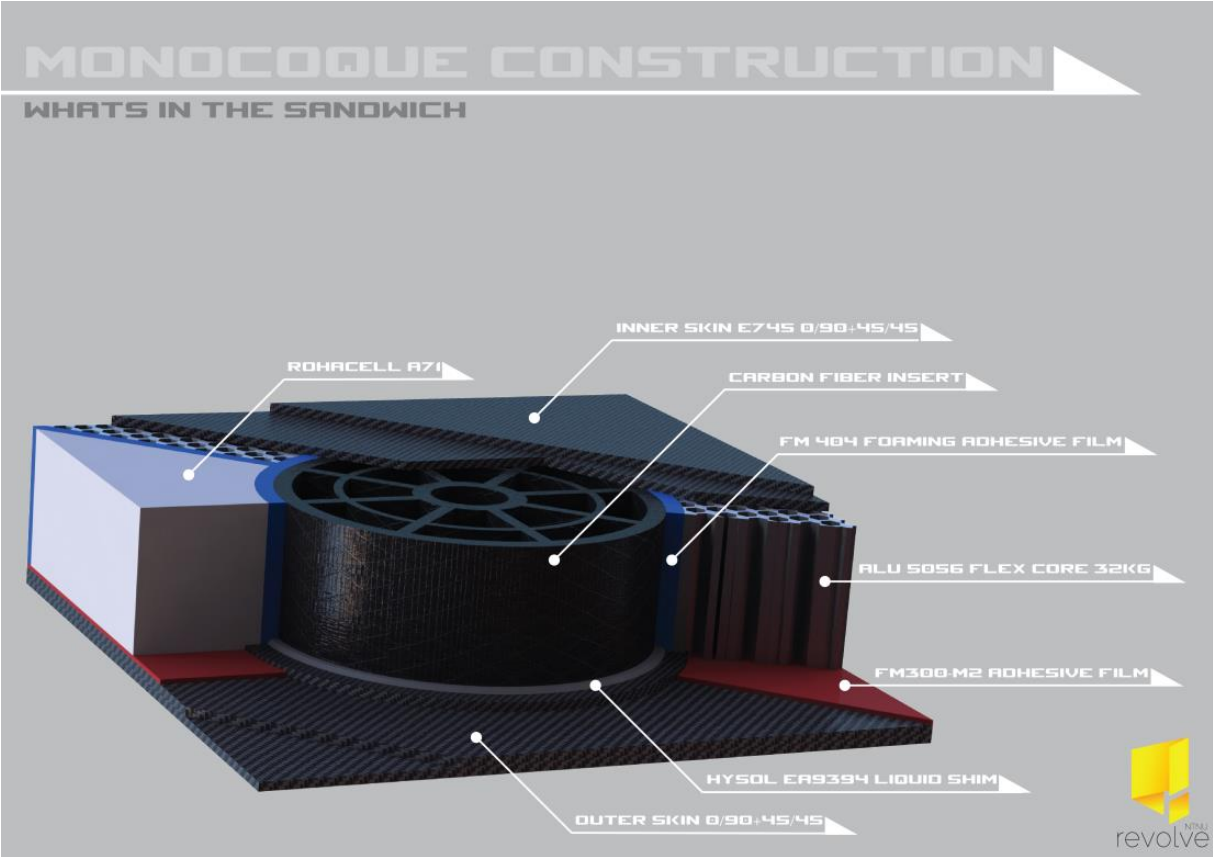


Figure 7.6: Cross section view of sandwich with insert

As described in chapter 4, the monocoque consists of several different layups with different core materials and core heights. This variety of different core combinations develops a need for a method to transfer the loads from one core configuration to another, acting as a single structure. Core splicing is the term used to bond separate core configurations to one another. Core splicing is usually done using some kind of adhesive, but it can also be done mechanically for instance by designating forms of attachment on each core piece. Adhesive bonding seems after careful evaluation like the best solution to the problem. Mechanically fastening will require different methods for each of the different core type (honeycomb/foam) inducing a time consuming design process, while adhesive bonding will work to regardless of core material or type.



Figure 7.7: Layup of inner facesheet onto the core material.

As a large-celled honeycomb was chosen, one of the challenges will be to bond our large-celled flexcore honeycomb to other substrates, i.e. other honeycombs as well as the rohacell core. An adhesive with expanding capabilities was the most suited solution. Several different adhesives, both in paste form as well as films were considered. The Cytec FM 410-1 adhesive film was mainly chosen for its accessibility, while still operating with higher strength than our different core materials, thus not weakening the sandwich structure. The Cytec FM 410-1 has shear strength in excess of 6MPa, while being able to expand up to 300 % of its original volume. This means that it is able to completely fill the gap between the honeycomb splices, improving the splices and insert bonding compared to early test panels.



Figure 7.8: Placing of rohacell foam core in the rear end of the monocoque.

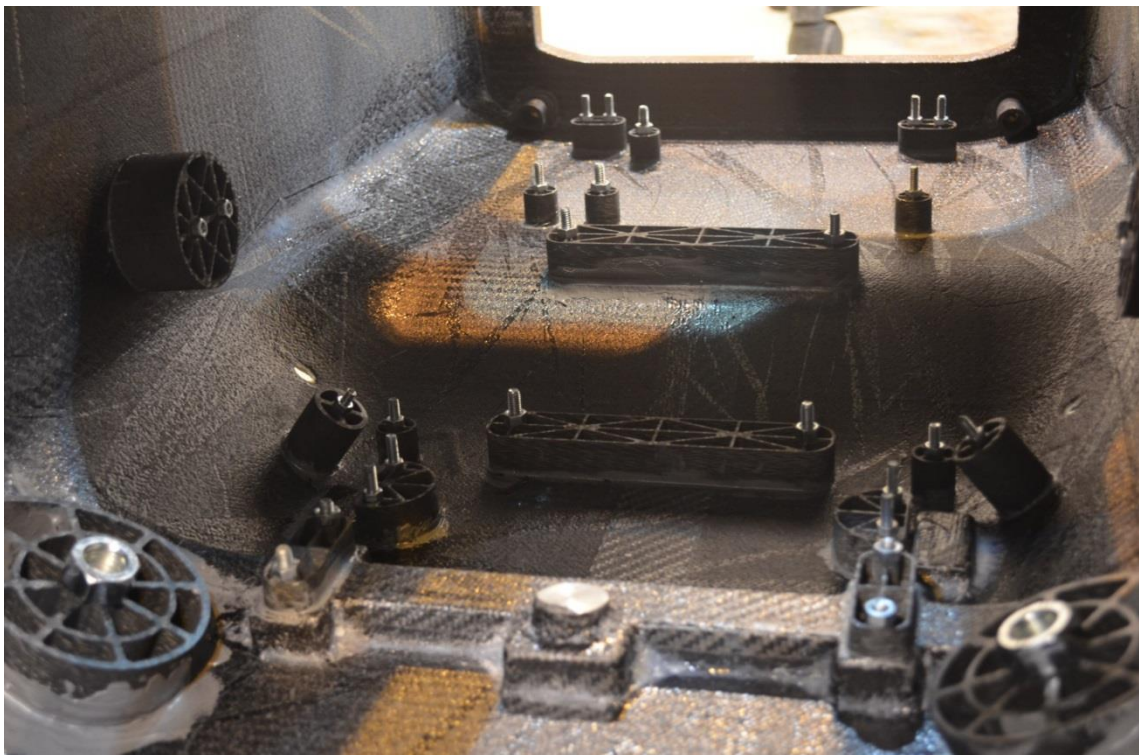


Figure 7.9: Bonding inserts to the outer facesheet in the front end of the monocoque

After the inserts and honeycomb is bonded to the outer skin and cured, the final face sheet is to be applied. This will be hot-bonded to the honeycomb, as opposed to the outer skin. This will ensure a solid bonding to the honeycomb. Several test regarding the need for adhesive films to bond the honeycomb to the inner skin has been performed. As the Amber E745 prepreg has excess resin, the test panels should no signs of being “dried out” when testing without adhesive film. The honeycomb-inner skin bonding was not noticeably better or worse, but with a lack of appropriate testing methods, we cannot conclude whether this result is valid or not. Our result is however supported by the manufacturer, advising us that the prepreg system was designed for honeycomb bonding.



Figure 7.10: Layup of outer face sheet.

The entire monocoque was produced in Kongsberg at Kongsberg Defense Systems as we have access to their autoclaves and cleanrooms. It follows that that we are able to produce high quality laminate and sandwich structures with minimal defects. To ensure the quality of the sandwich and eliminate foreign object damage the monocoque will be examined by ultrasound. A laser system will also measure each suspension mounting point to ensure that it is placed in the correct coordinate in space.

7.3 PRODUCTION EVALUATION

After a comprehensive manufacturing process there is several parts of the manufacture process that can be improved, while others was considered a good process.

The monocoque showed a maximum coordinate deviation of the attachment points of approximately 1mm, while the average deviation was less than 0.5mm, shown in appendix 1. This is well within our tolerances. The process of using machined holes and coherend dowel pins to place the attachment points were considered a success.

The monocoque and CFRP negative tooling showed little signs of springback or thermal expansion, proving our tooling concept as a process. The end-product finish was also very good, but the lower part of the monocoque was a bit rough due to some small issues making the bottom mould a bit rough.

The use of large celled honeycomb has proven to be a challenge when dealing with the core splices. Large cells leads to a large volume to be filled with adhesive in order to bond the different core parts together. A large amount, estimated at +1kg, was thus adding to the monocoque total weight. The large cells also contribute to difficulties concerning bonding of the facesheets to the honeycomb as the bonding area is reduced.



CHAPTER 8

CONCLUSION

Designing, testing and manufacturing of an advanced sandwich construction such as a carbon fiber monocoque chassis is a complex process composed of a lot of different challenges, both theoretical and practical. This makes it difficult to go in depth on only a few subjects.

Modeling and analysis of local areas on a honeycomb sandwich structure has proved to be a problematic task. Non-linear and unpredictable behavior of the core material made it necessary to simplify the problem. Linear finite element analysis combined with experimental testing of sandwich insert panels made it possible to study the behavior of loaded insert panels, and at the same time evaluate the quality on the analysis that have been done.

Assuming good production quality of the structure, the test samples behaves as expected and the practical results have good correspondence with the theoretical results. Defects in the test samples starts to occur at 125-155% of the ESA load capacity, depending on the load case and core material used. As ESA insert design handbook is commonly used as a design standard for composite structures with insert, it was expected that failure would occur with a certain margin above the ESA predicted load capacity. Cyclic tests shows that the insert panels are quickly weakened they are cyclic loaded above ESA load capacity. Unless appropriate safety factor is included in the load cases, a sandwich honeycomb insert structure should not be designed to withstand loads above its ESA load capacity



CHAPTER 9

FURTHER WORK

Further work on chassis design and analysis may be carried out in a number of areas, both as a continuation of the work presented in this thesis, but also on topics that has not been looked into. The following areas are a suggestion of what might be done as further work:

- The testing of insert panels gives a certain understanding and knowledge of the failure behavior of such panels. This may be used as a basis for a more complex non-linear finite element model of honeycomb sandwich structures with inserts.
- Further investigation of fatigue properties should be carried out. The fatigue testing presented in this thesis is somewhat incomplete. More testing over a wider range of loads is required to generate a decent base of results. A more theoretical approach should be used in order to achieve better understanding on the topic.
- Further analysis on torsional rigidity of the chassis may be done. Testing of the actual rigidity should be carried out in order to verify the results. Analysis of torsional damping and natural frequency may be included.
- Analysis and testing of core-joints. Improvement of the core-splicing method used for the honeycomb core may be included.
- The production methods used to produce the monocoque chassis for KOG Arctos R proved to work, but the methods are time consuming and expensive. Simplifying of the production methods is an area that should be looked into.



CHAPTER 10

REFERENCES

- 1 - Deakin, A., Crolla, D., Ramirez, J.P., Hanley, R. (2000) *The Effect of Chassis Stiffness on Race Car handling Balance*. SAE International
- 2 - Dowling NE. (2007) *Mechanical behavior of materials : engineering methods for deformation, fracture and fatigue*. 3rd edition. Upper Saddle River, N.J.: Pearson/Prentice Hall
- 3 - Eriksrud, S. (2012) *Aerodynamic Package for NTNUs Formula Student Car*. IPM, NTNU.
- 4 - European Cooperation For Space Standardization (2011) *Space engineering - insert design handbook*. ESA Requirements and Standards Division
- 5 - Hamilton L, Joyce P, Forero C, McDonald M. (2013) *Production of a Composite Monocoque Frame for a Formula SAE Racecar*. SAE International
- 6 - Heimbs, S., Pein, M. (2008) *Failure behaviour of honeycomb sandwich corner joints and inserts*. Hamburg University of Technology
- 7 - Henkel Corporation (2007) *Product Selector Guide for the Aerospace Industry*
- 8 - Hexcel Composites (2000) *HexWeb Honeycomb Sandwich Design Technology*.
- 9 - Hexcel Composites (2013) *HexPly Prepreg Technology*.
- 10 - Kim, J., Lee, D.G. (2008) *Characteristics of joining inserts for composite sandwich panels*. Department of Mechanical Engineering, Korea Advanced Institute of Science and Technology.
- 11 - Kollar LP, Springer GS. (2003) *Mechanics of composite structures*. Cambridge ; New York: Cambridge University Press
- 12 - Milliken WF, Milliken DL. (1995) *Race car vehicle dynamics*. SAE International
- 13 - SAE International (2013) *2014 Formula SAE Rules*. Available at: http://students.sae.org/cds/formulaseries/rules/2014_fsae_rules.pdf
- 14 - Sanchez, C.M. (2013) *Composite Sandwich Design for Formula SAE Monocoque*. IPM, NTNU.
- 15 - Savage G. (2010) *Development of penetration resistance in the survival cell of a Formula 1 racing car*. Engineering Failure Analysis.
- 16 - Savage, G. (2008) *Composite Materials Technology in Formula 1 Motor Racing*. Honda Racing F1 Team

- 17 - Song, K., Choi, J., Kweon, J., Choi, J., Kim, K. (2008) *An experimental study of the insert joint strength of composite sandwich structures*. School of Mechanical and Aerospace Engineering, Gyeongsang national university
- 18 - Thybo Thomsen, O. (1998) *Sandwich plates with 'through-the-thickness' and 'fully potted' inserts: evaluation of differences in structural performance*. Institute of Mechanical Engineering, Aalborg University.
- 19 - Van Straalen, I. J. *Comprehensive Overview of Theories for Sandwich Panels*. Delft University of Technology
- 20 - Vedvik, N. P. (2013) *Essential Mechanics of Composites*. Release R01. IPM, NTNU.
- 21 - Zenkert, D. (1997) *The Handbook of Sandwich Construction*. 1st edition.
- 22 – O.T Thomsen, W. M. Banks.(2013) *An improved model for the prediction of intra-cell buckling in CFRP sandwich panels under in-plane compressive loading*. Aalborg University
- 23 – Petras, A. Sutcliffe, M.P.F.(1999) *Failure mode maps for honeycomb sandwich panels*. Cambridge University
- 24 – Pokharel, N. (2003) *Behaviour and Design of Sandwich Panels Subjected to Local Buckling and Flexural Wrinkling Effects*. Queensland University of Technology
- 25 - Petras, A. Sutcliffe, M.P.F.(2000) *Indentation failure analysis of sandwich beams*. Cambridge University
- 26 – Benzie, M.A. (1997) *Investigation of Springback Associated With Composite Material Component Fabrication*. NASA.
- 27 – Allen, H.G. (1969) *Analysis and design of structural sandwich panels*. Oxford: Pergamon
- 28 – Frostig, Y. Baruch, M. (1996) *Localized load effects in high-order bending of sandwich panels with flexible core*. Journal of Engineering Mechanics, Vol. 122, No. 11.
- 29 – Formula 1 Dictionary. *Monocoque history*. Tilgjengelig fra: <http://www.formula1-dictionary.net/monocoque.html>
30. Thompson R.W., Matthews F.L., O'Rourke B.P. *Load attachment for honeycomb panels in racing cars*. London: Imperial College, Center for Composite Materials; 2005.

Appendices:

A1: Leica Lazer Tracker Report, Revolve NTNU monocoque

A2: X –Ray report, Revolve NTNU monocoque

A3: Thermocouple readings for monocoque curing

A4: Datasheet, FM 410 Adhesive foam

A5: Insert documentation testing

A6: Experimental Results 3pt. bending and penetration testing

A7: Insert Testing Results

A8: Hexweb honeycomb attributes and properties

A9: Datasheet, Tencate E745

A10: Datasheet, ECK Kevlar honeycomb

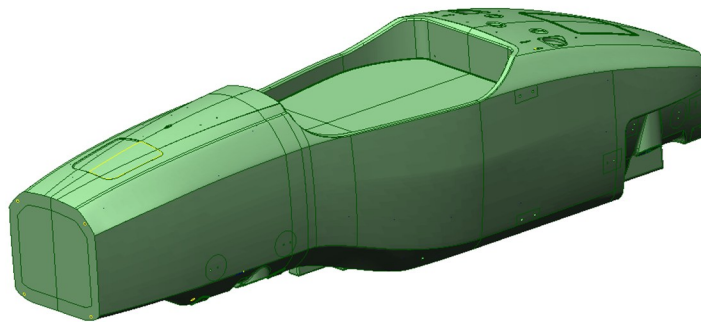
A11: Insert Calculations

A12: Failure modes

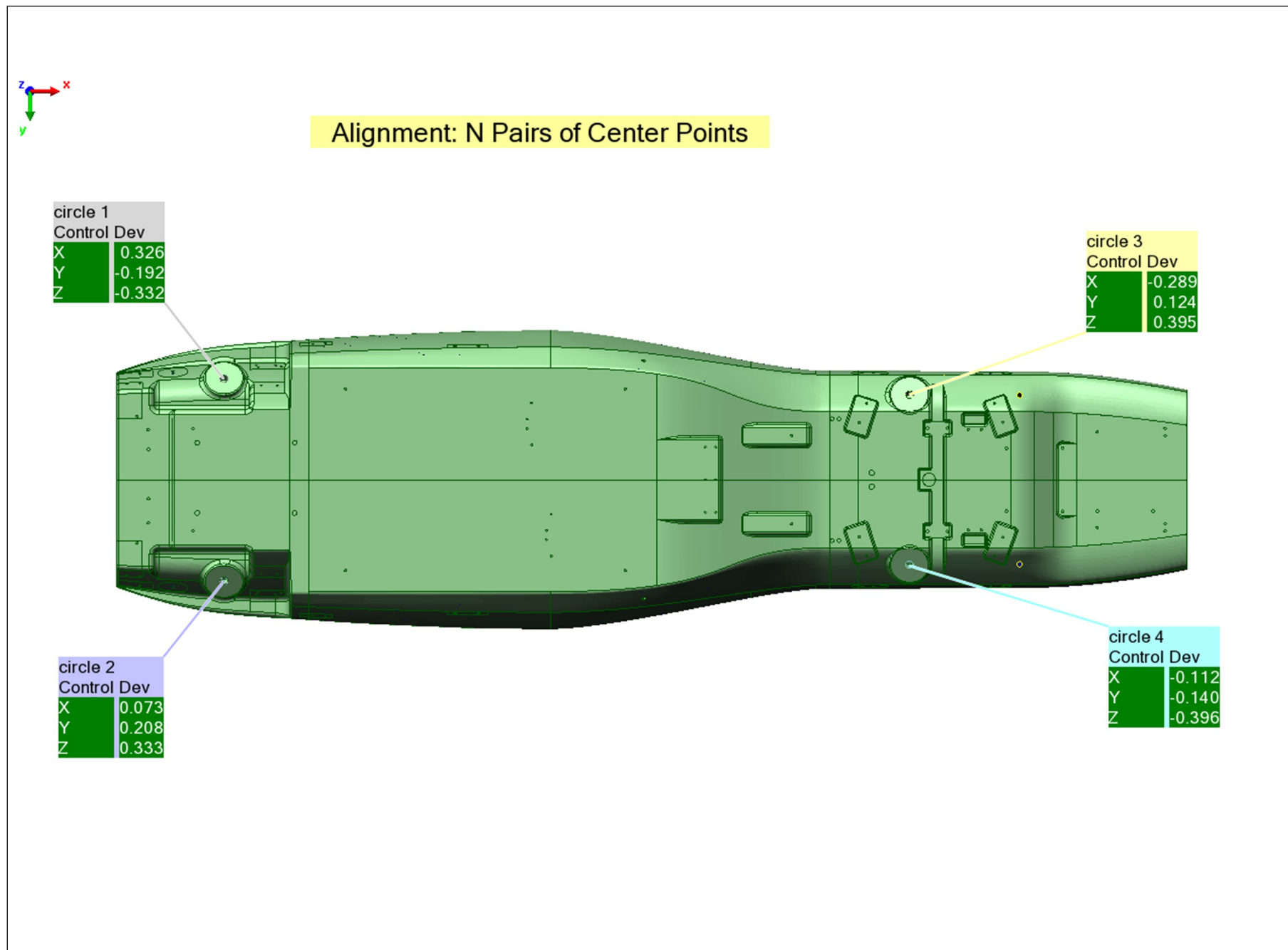
A13: Chassis Reaction Forces

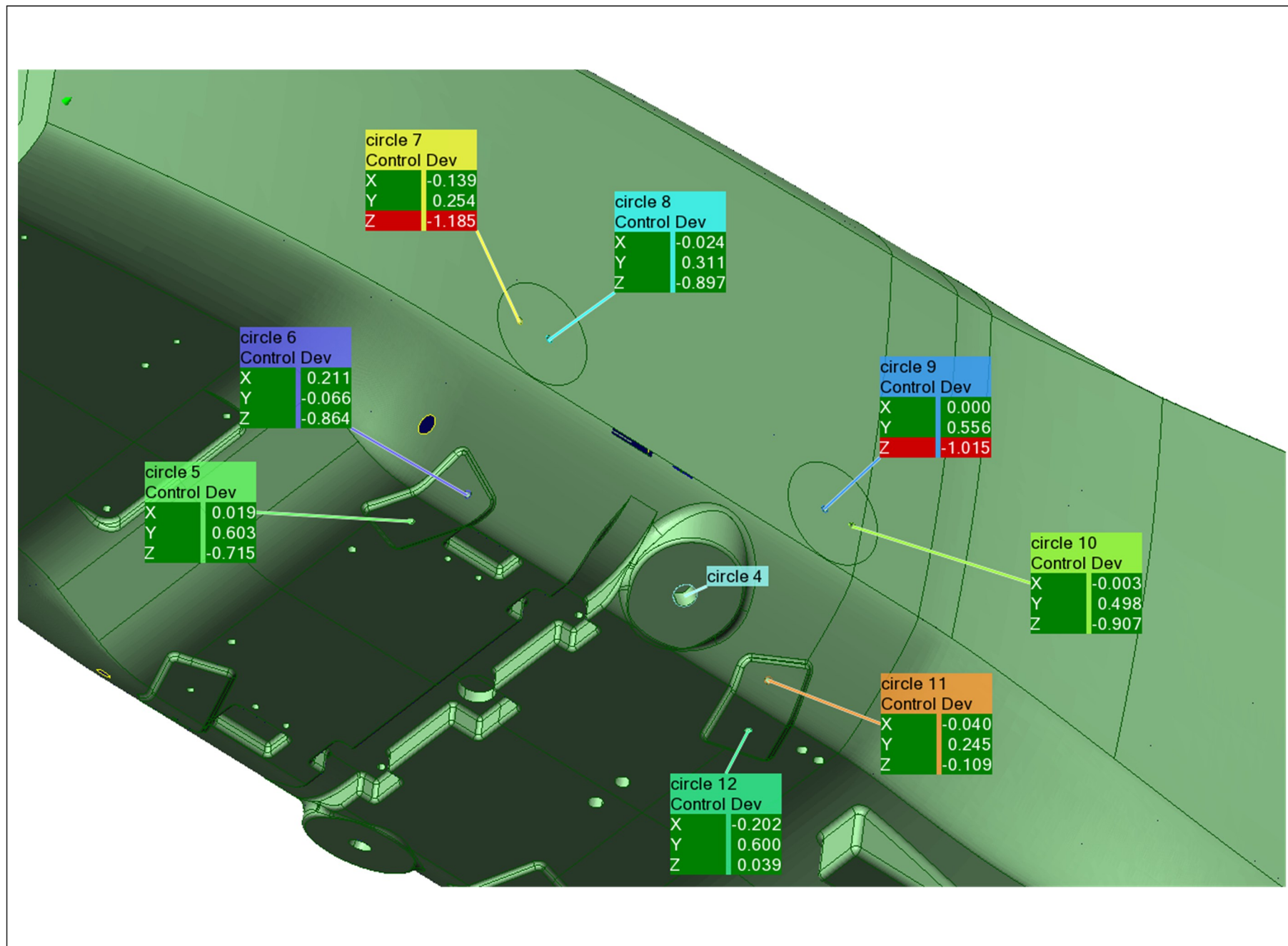
A14 Datasheet, Hexply prepreg

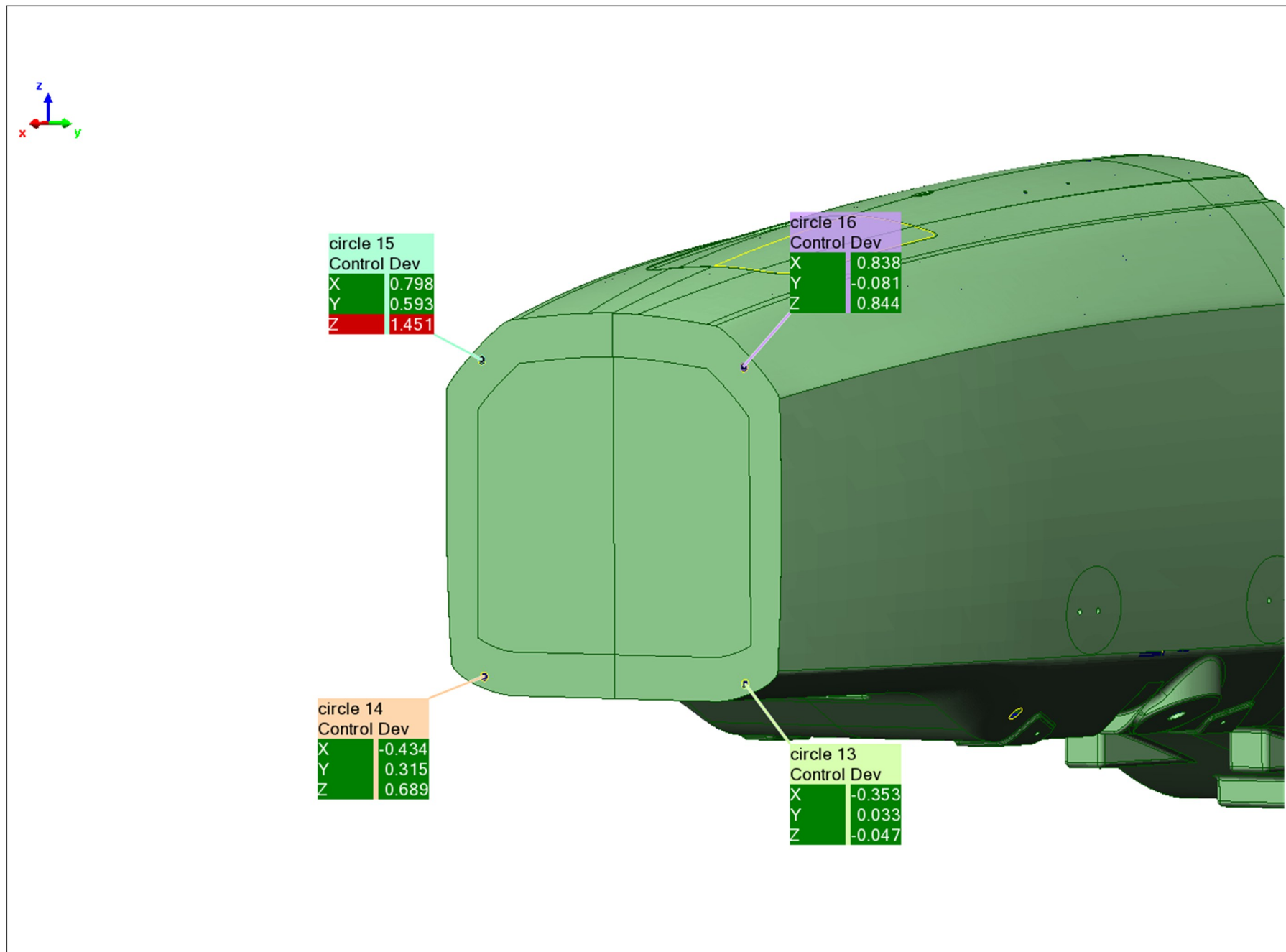
Revolve NTNU Monocoque 2014

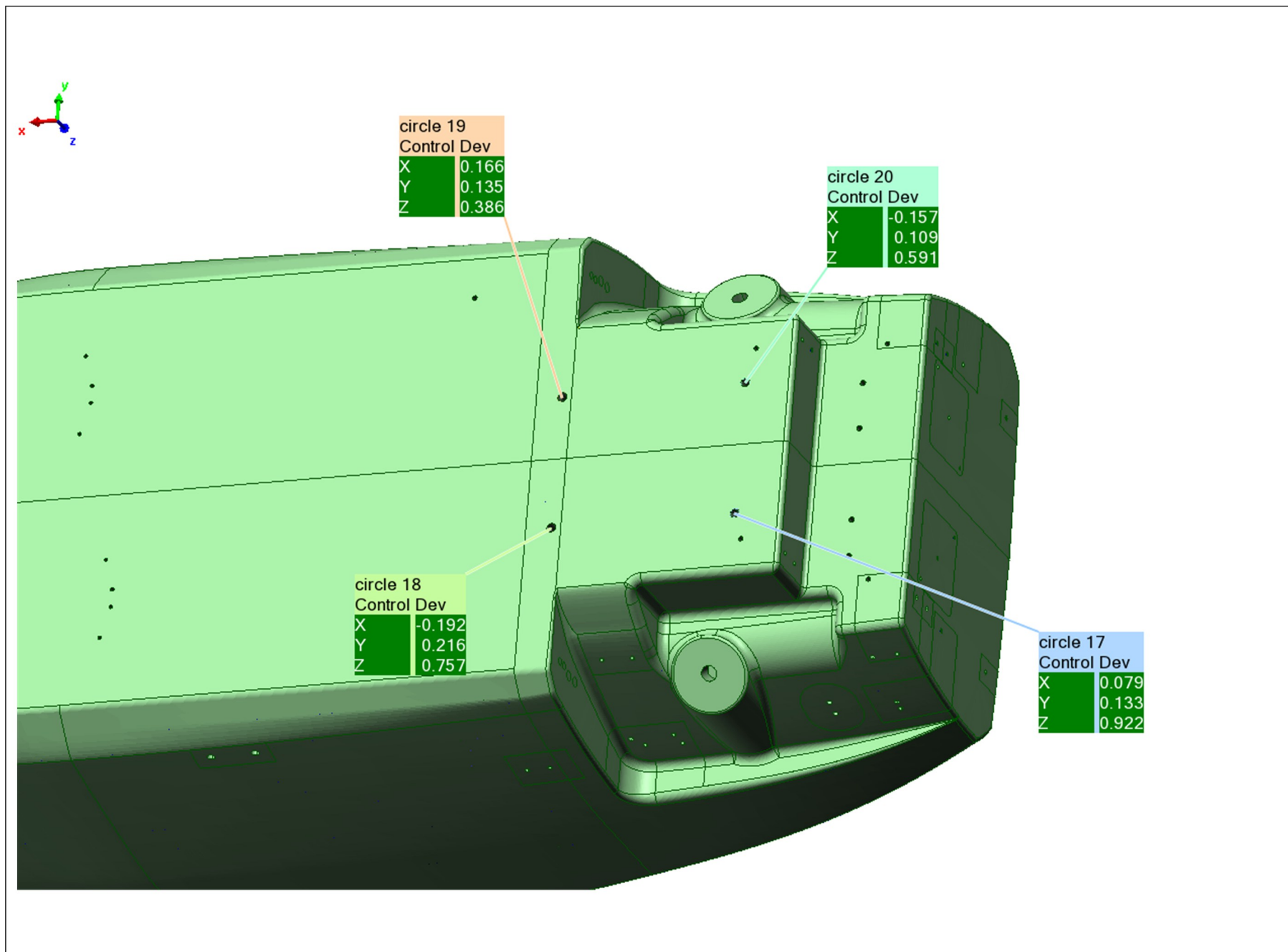


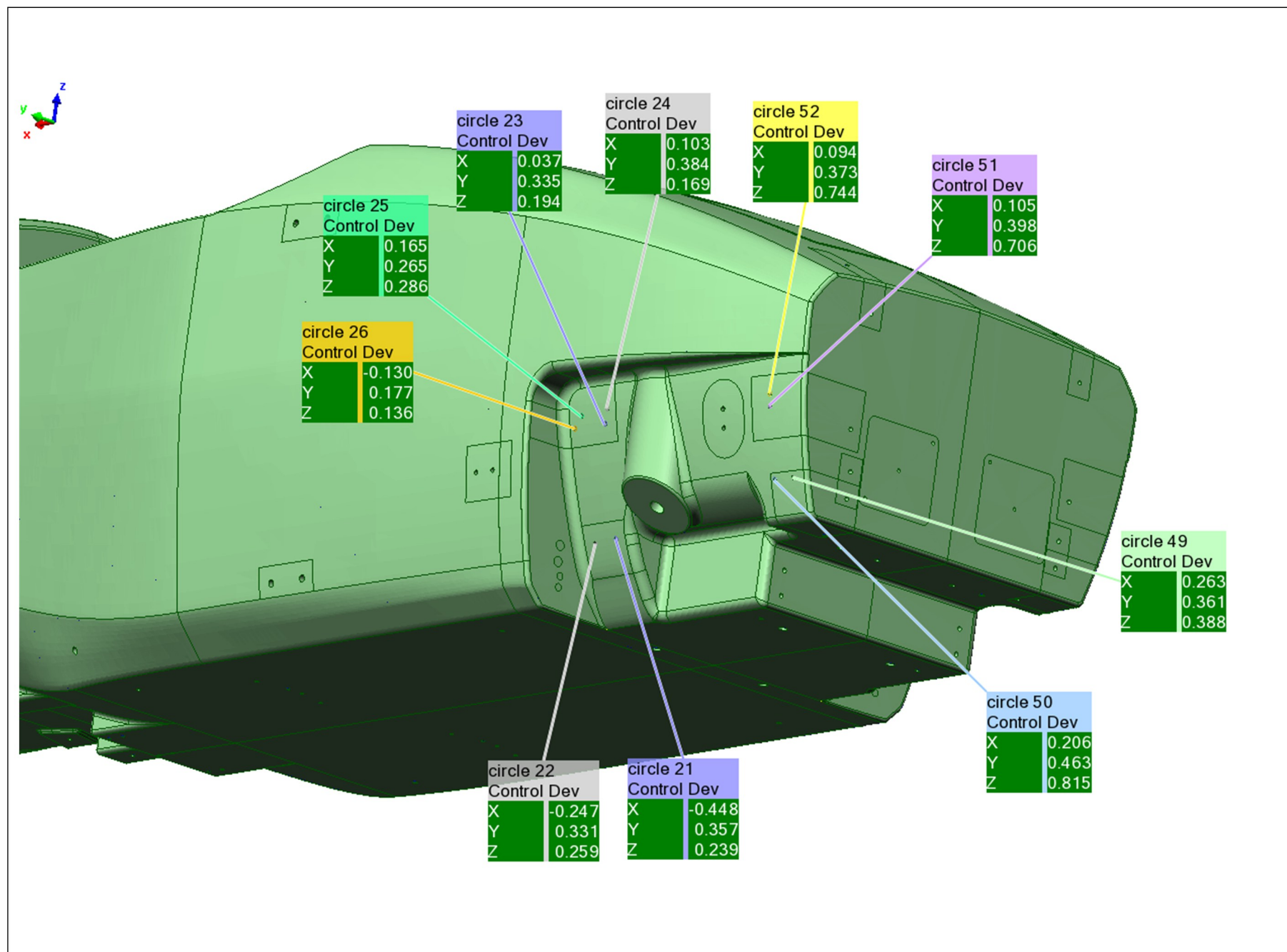
| | |
|----------------|---|
| Organization | Kongsberg Defence & Aerospace AS |
| Report author | mk |
| e-mail address | |
| Part name | Revolve NTNU Monocoque 2014 |
| Part number | |
| Device | Leica Laser Tracker |
| Date | 26/03/2014 |

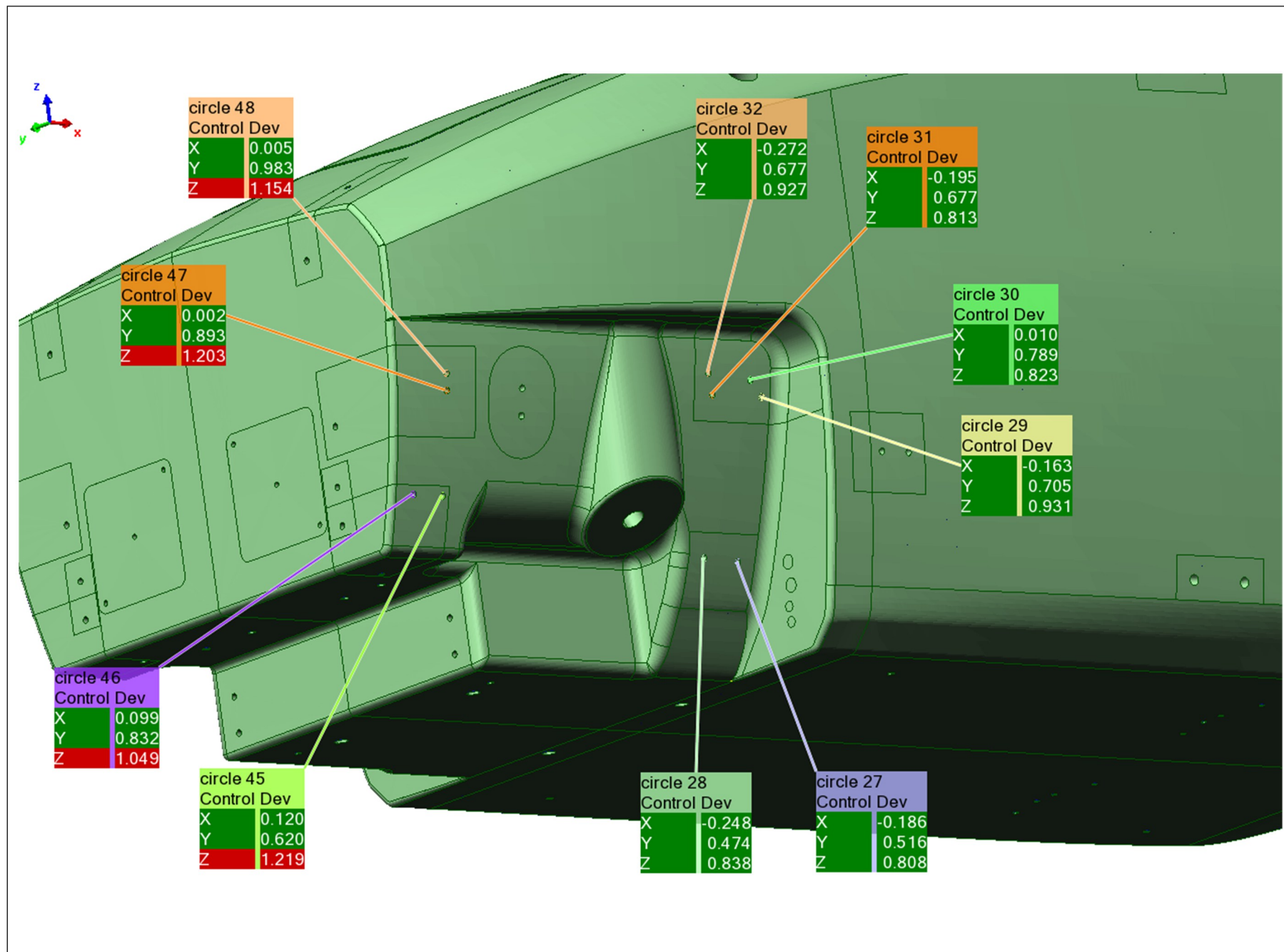


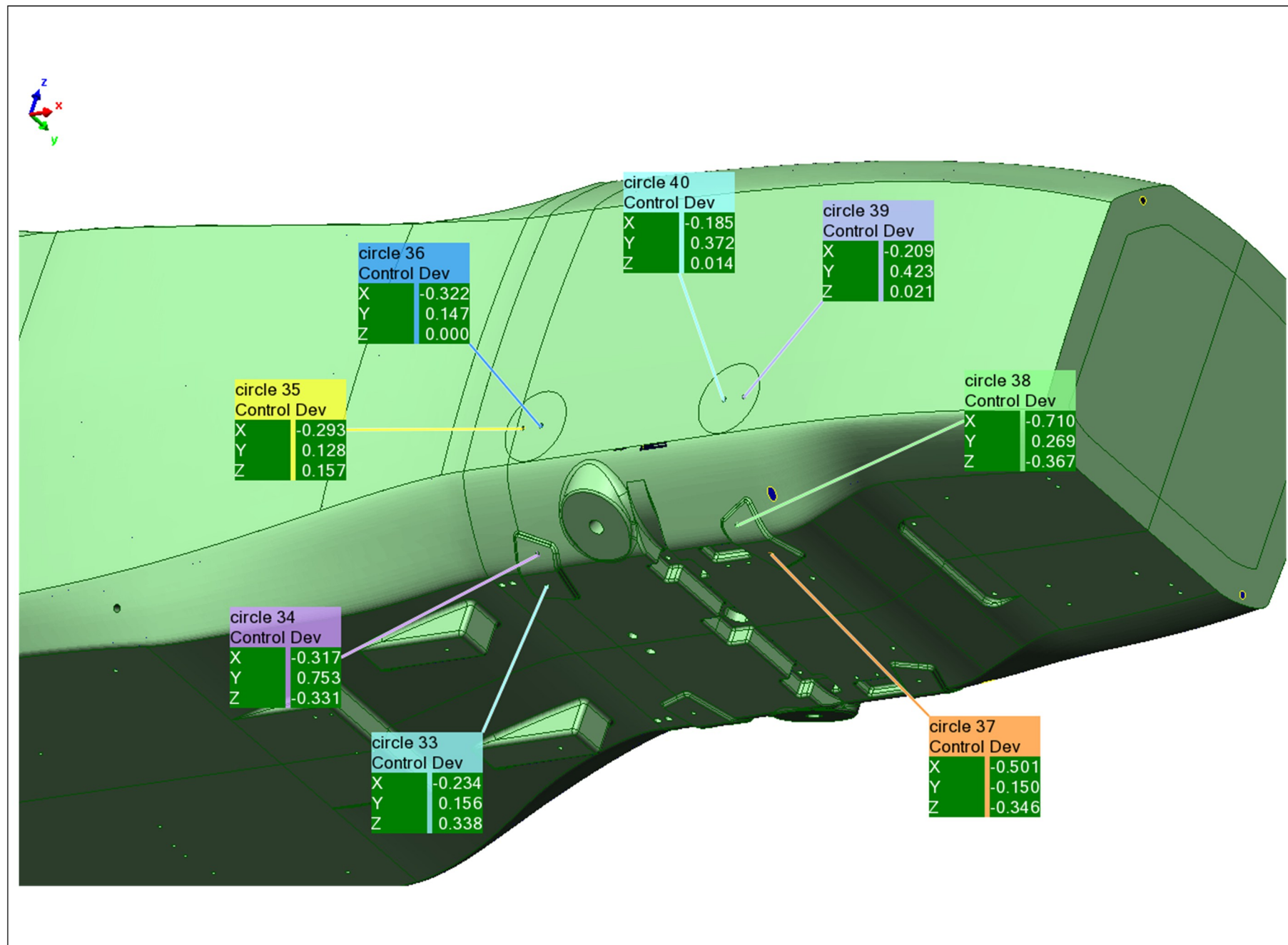


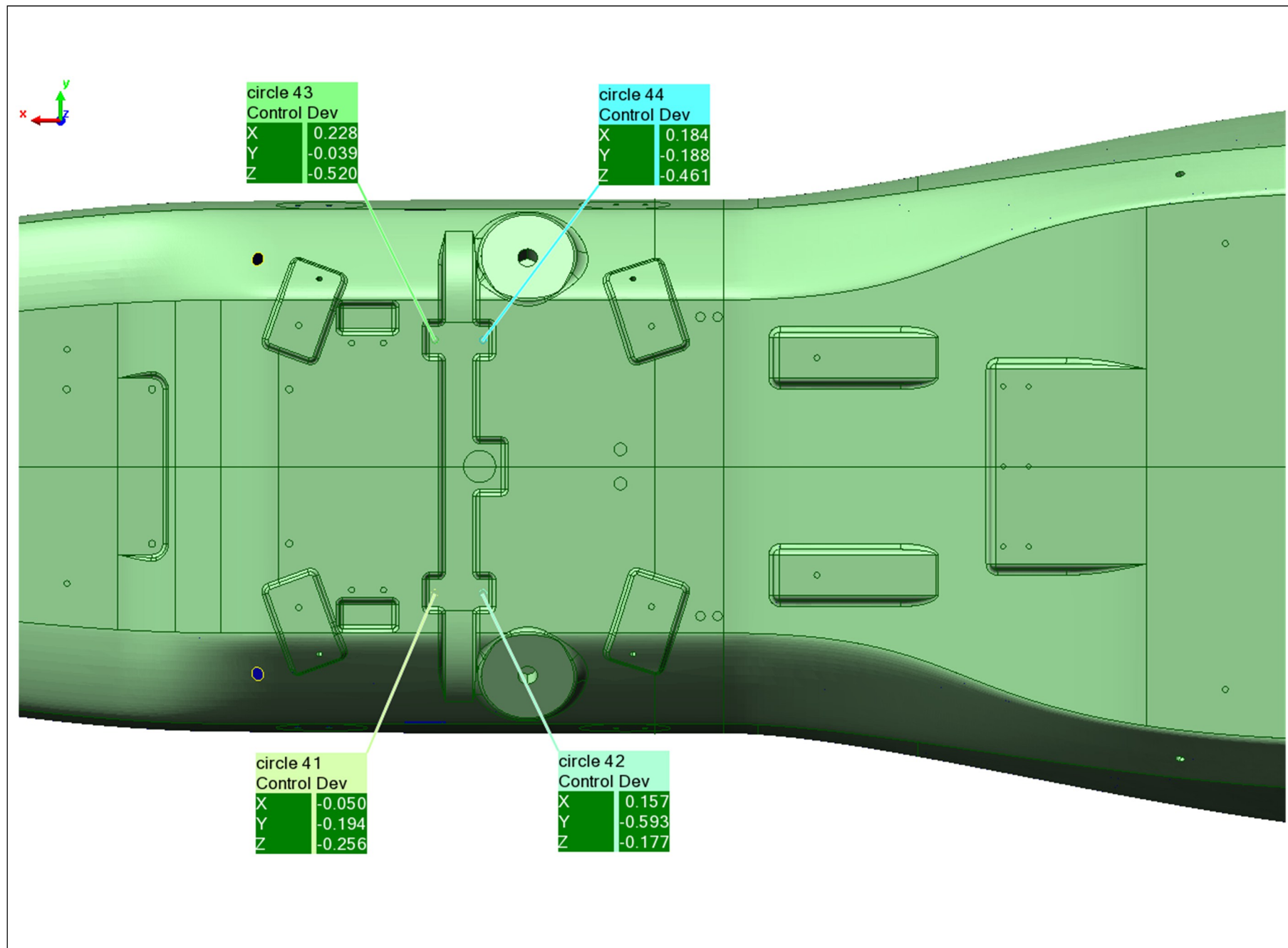












Kongsberg Defence & Aerospace



KONGSBERG

Inspection Report Radiographic Testing

| | | | | | |
|---|--|-------------------------------------|--|-------------------------------------|--|
| Supplier: Kongsberg Defence & Aerospace AS | | Part name: Formula NTNU-Bil | | Part number: | |
| Method Standard and Issue: KVS-8008 Rev.03 | | Acceptance Specification and Issue: | | Order no: | |
| RT No: | | Operator RT: Elisabeth Storhaug | | Inspector RT: Elisabeth Storhaug | |
| | | Lot size: 1 | | Date: 24 March - 2014 | |

Test Results:

| RT No: | Remarks: | Accept , Reject: |
|-------------------------------|--|------------------|
| Exponering 1 +exponering 6 | Karboninsert har bra limdekke. Noen luftlommer, hovedsaklig øvre kvadrant, høyre side. Over 95% limdekke. Honeycomb i øvre kvadranter ser i hovedsak fine ut, noe distorted cells. Aluminiumsbøyle har en lengre luftlomme og noen middels store. Tilsvarende ca 80 % limdekke. | Accept |
| Exponering 2+ exponering 5 | Karboninsert har bra limdekke. Noen små luftlommer, og noe limutflyt. Over 95% limdekke. Honeycombceller i øvre kvadranter er hele og velformede. Aluminiumsbøyle har et lengre område med luft, og noen middels store. Tilsvarende ca. 80% limdekke | Accept |
| Exponering 3 | Karboninsert har bra limdekke. Noen spredte, mindre luftlommer og noe limutflyt. Limdekke ca. 95% Fin Rohacellkjerne. | Accept |
| Exponering 4 | Karboninsert har bra limdekke. Noen små luftlommer. Endel limutflyt inni insert. Limdekke over 95%. Fin Rohacellkjerne. | Accept |
| | | |
| | | |
| | | |
| | | |

Corrective Actions:

Kongsberg Defence & Aerospace AS NDT RT Signature/ Stamp and Date:

Elisabeth Storhaug

24 March - 2014

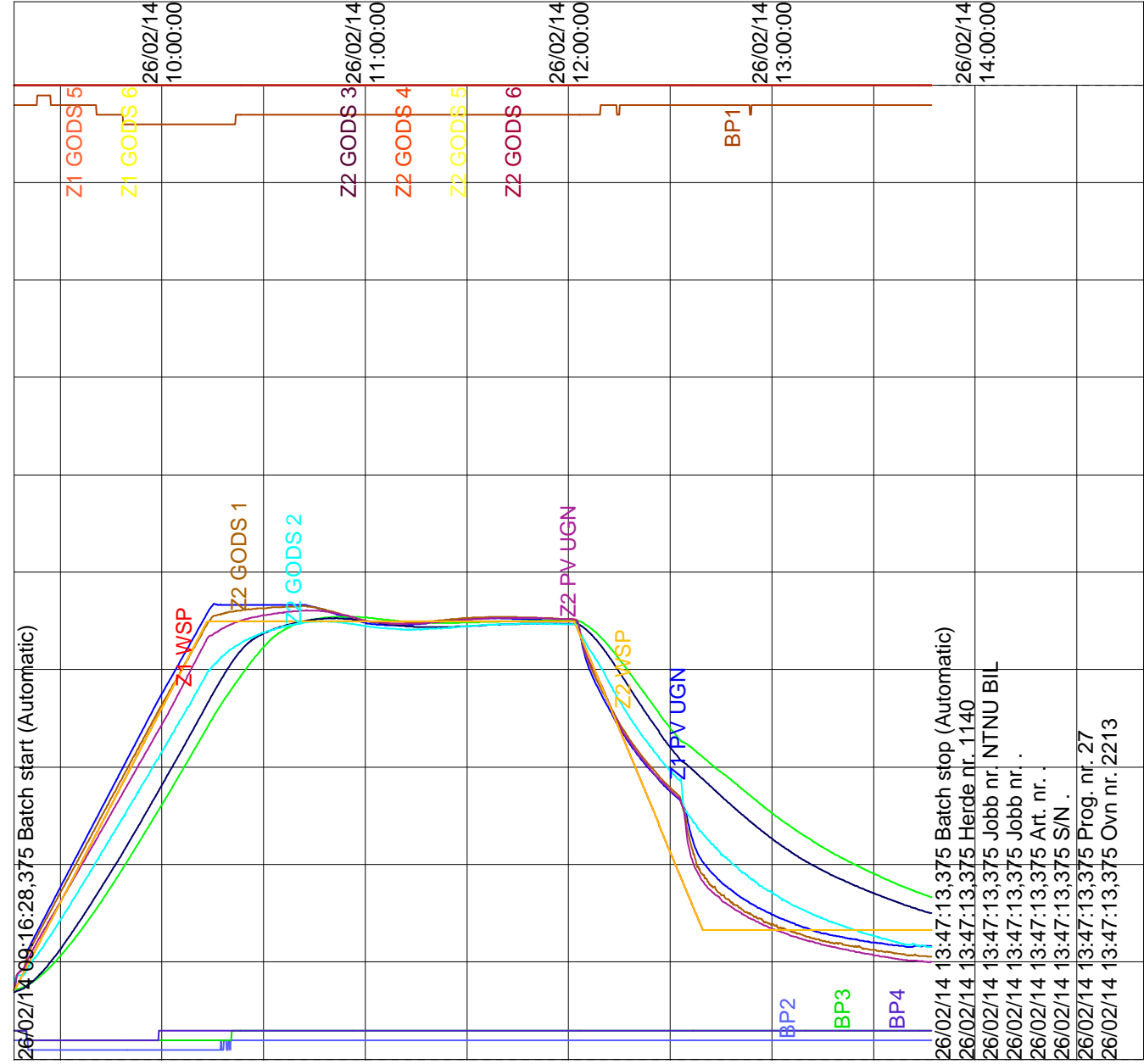
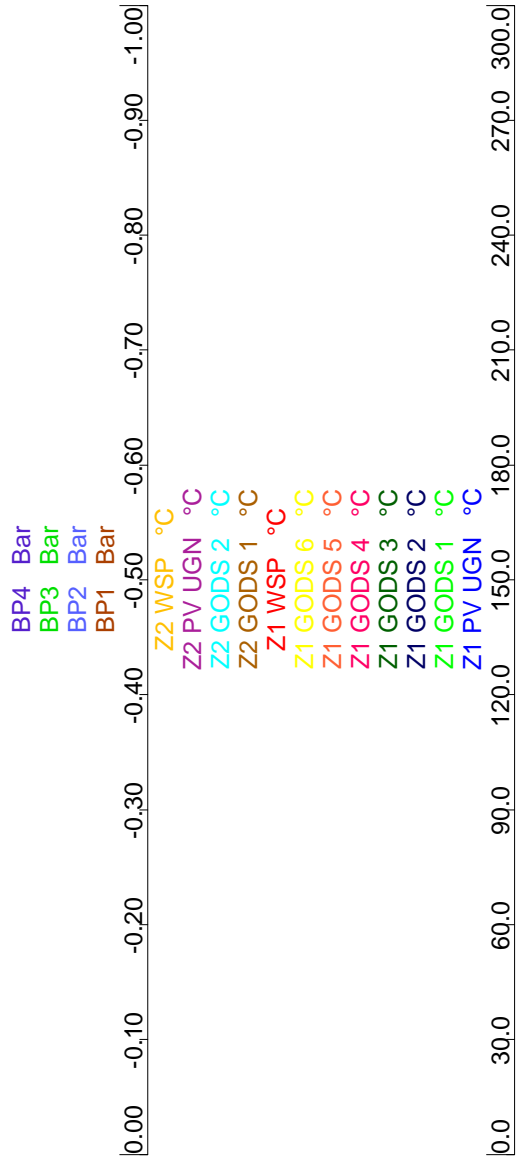


Name (printed) Elisabeth Storhaug

The lot is:

Approved

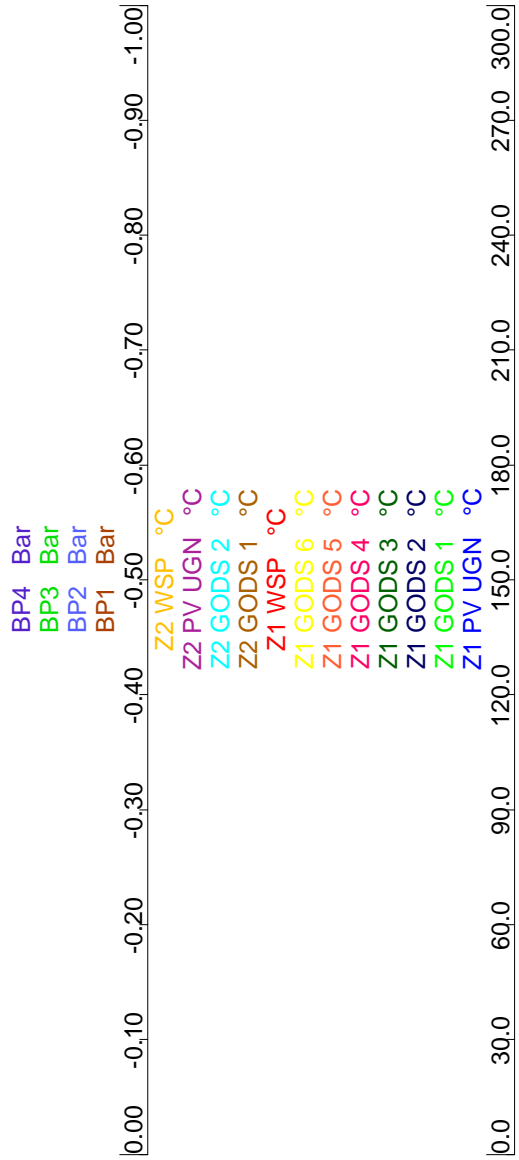
Rejected



26/02/14 09:16:28,375
26.02.2014 13:43:32

2213 automatic printing 2012.09.27

26/02/14 14:49:49,155
Page 1 of 1



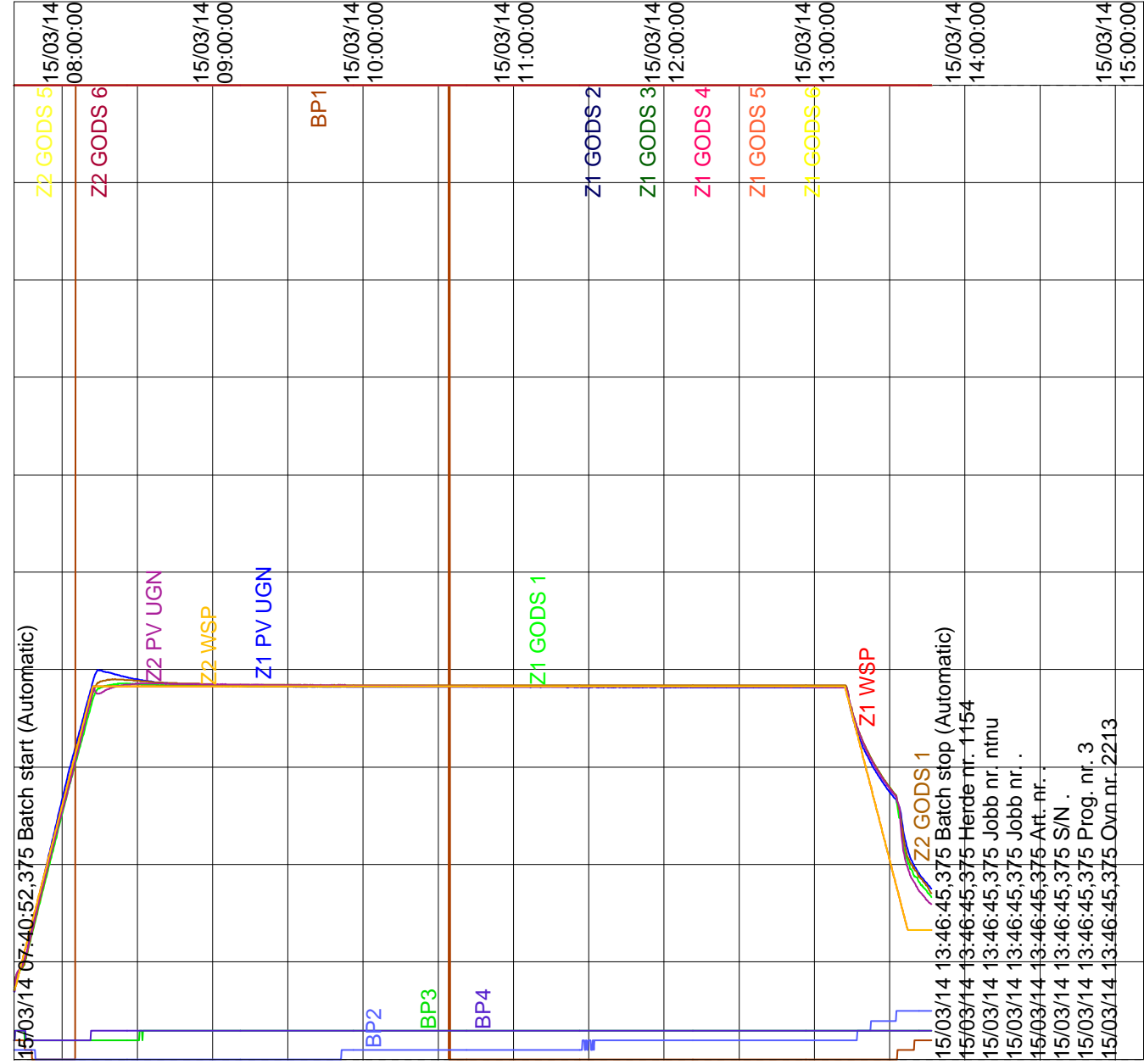
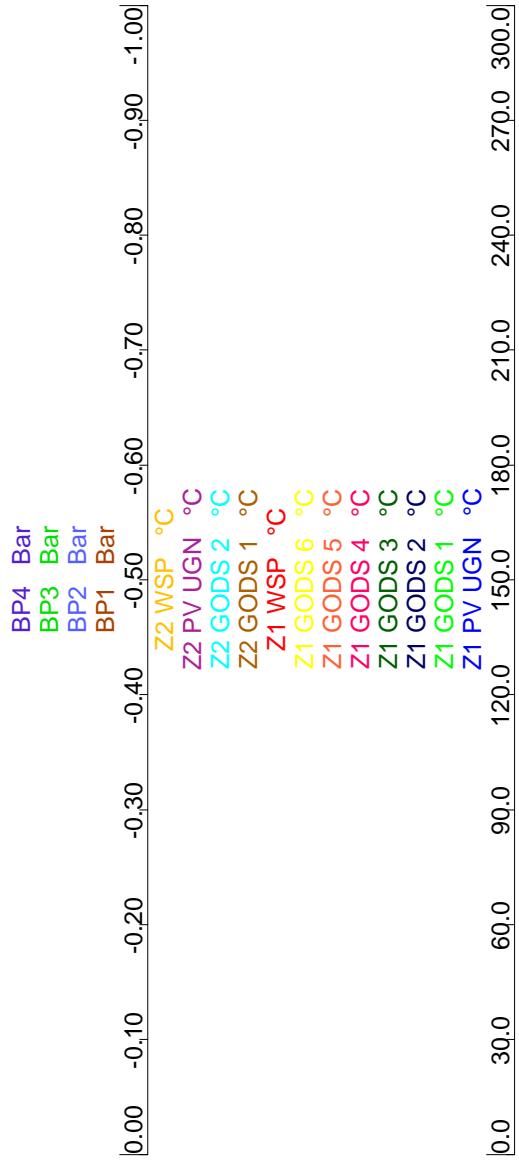
BP4 Bar
 BP3 Bar
 BP2 Bar
 BP1 Bar
 Z2 WSP °C
 Z2 PV UGN °C
 Z2 GODS 2 °C
 Z2 GODS 1 °C
 Z1 WSP °C
 Z1 GODS 6 °C
 Z1 GODS 5 °C
 Z1 GODS 4 °C
 Z1 GODS 3 °C
 Z1 GODS 2 °C
 Z1 GODS 1 °C
 Z1 PV UGN °C

07/03/14 08:36:14,375
 08.03.2014 02:11:40

2213 automatic printing 2012.09.27

08/03/14 06:22:36,010
 Page 1 of 1

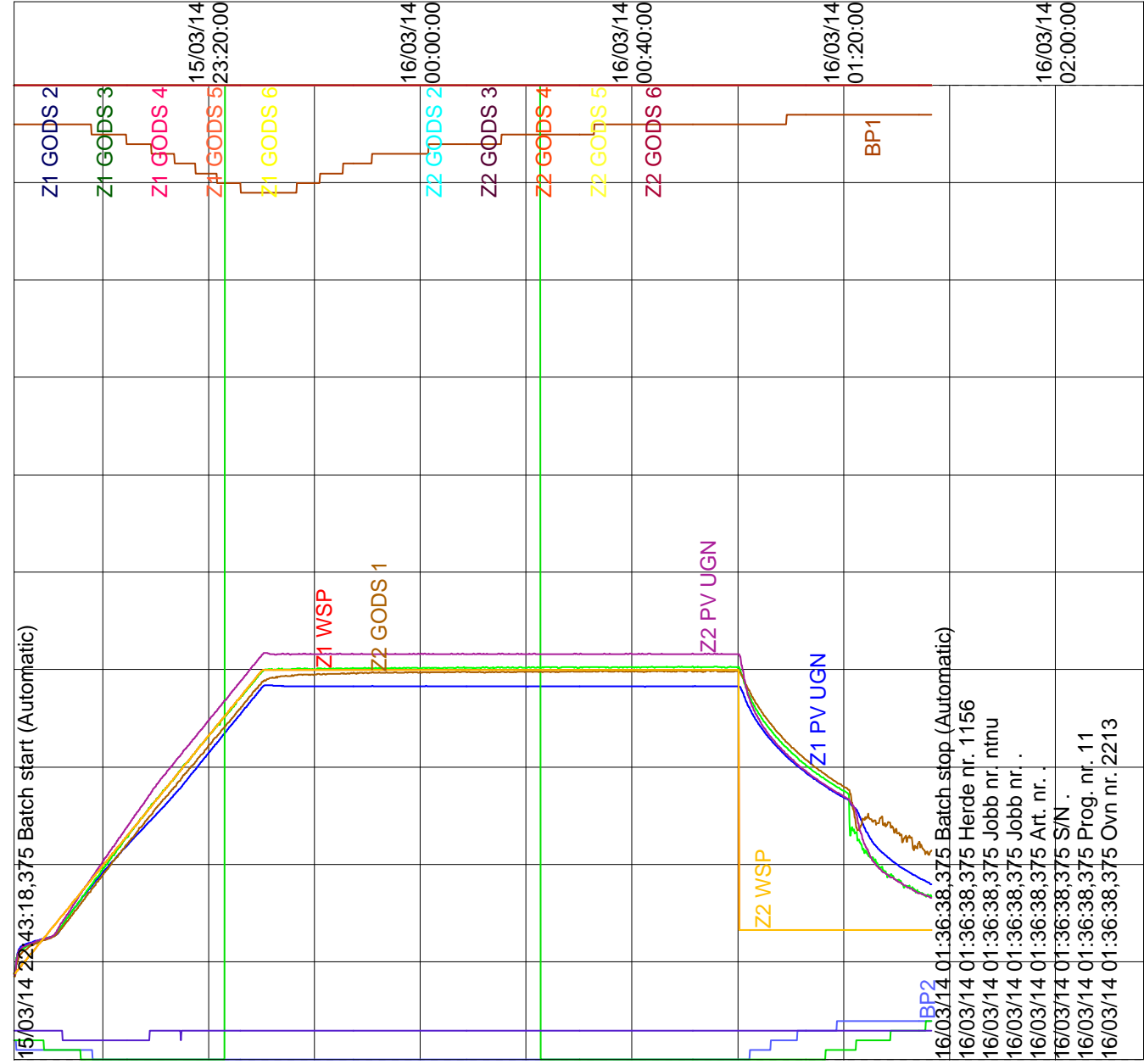
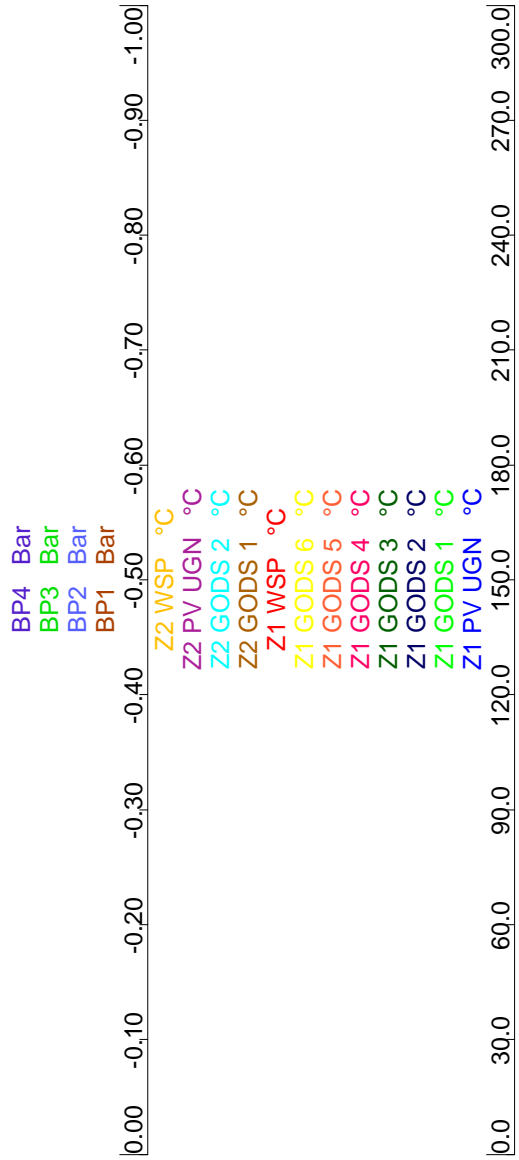
| | |
|-----------------------|-------------------------|
| 07/03/14 08:36:14,375 | Batch start (Automatic) |
| 08/03/14 02:17:17,375 | Batch stop (Automatic) |
| 08/03/14 02:17:17,375 | Herde nr. 1147 |
| 08/03/14 02:17:17,375 | Jobb nr. NTNU DELER |
| 08/03/14 02:17:17,375 | Jobb nr. |
| 08/03/14 02:17:17,375 | Art. nr. |
| 08/03/14 02:17:17,375 | S/N . |
| 08/03/14 02:17:17,375 | Prog. nr. 42 |
| 08/03/14 02:17:17,375 | Ovn nr. 2213 |



15/03/14 07:40:52,375
15.03.2014 13:40:46

2213 automatic printing 2012.09.27

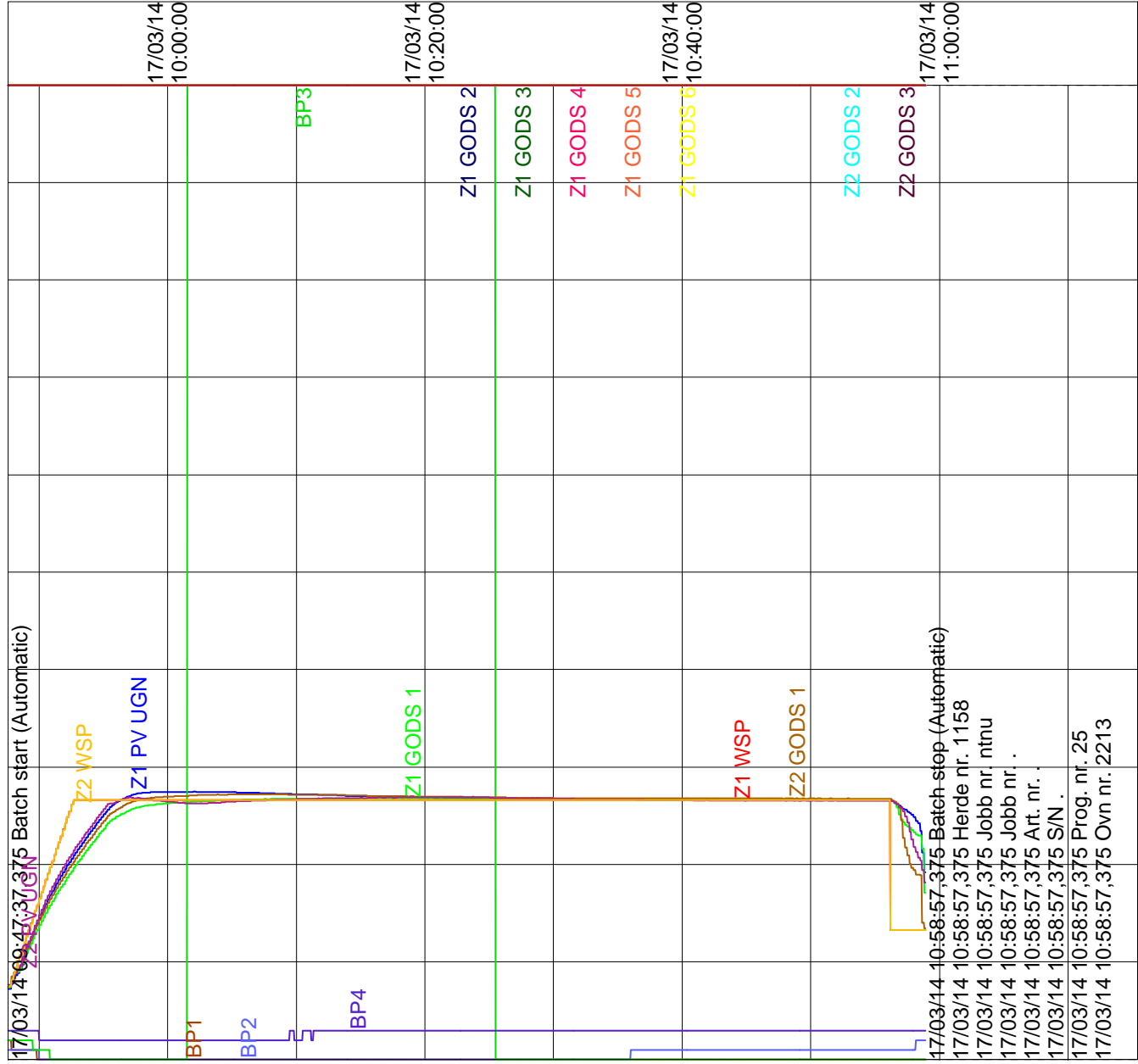
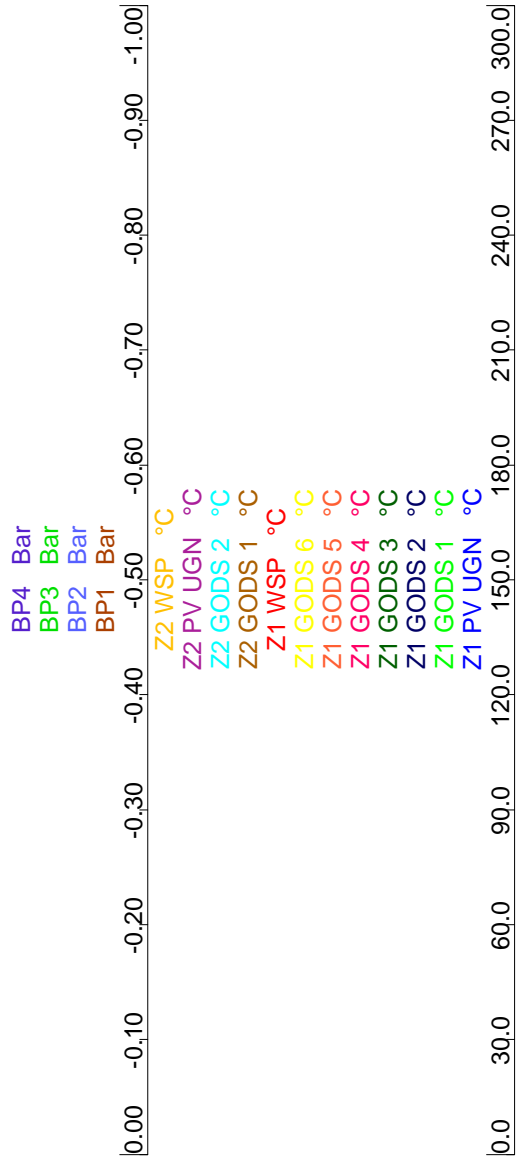
15/03/14 15:11:20,820
Page 1 of 1



15/03/14 22:43:18,375
16.03.2014 01:30:45

2213 automatic printing 2012.09.27

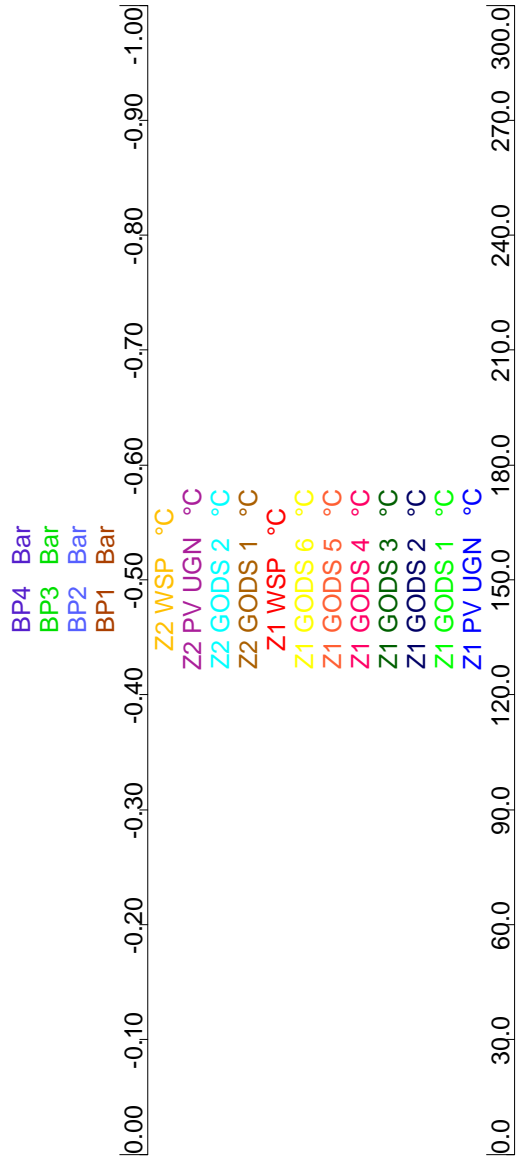
16/03/14 02:16:42,815
Page 1 of 1



17/03/14 09:47:37,375
17.03.2014 10:54:32

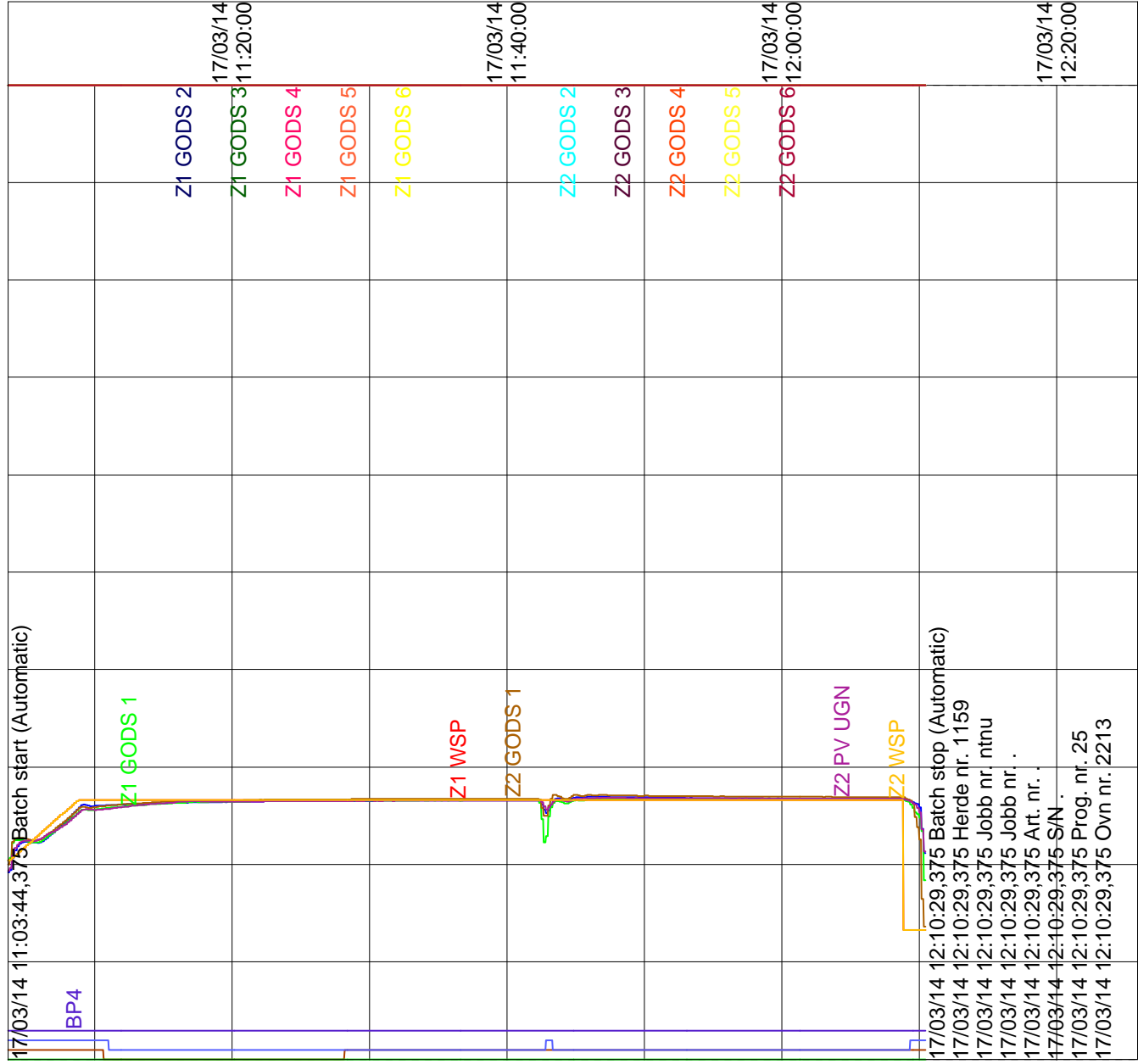
2213 automatic printing 2012.09.27

17/03/14 11:15:26,895
Page 1 of 1

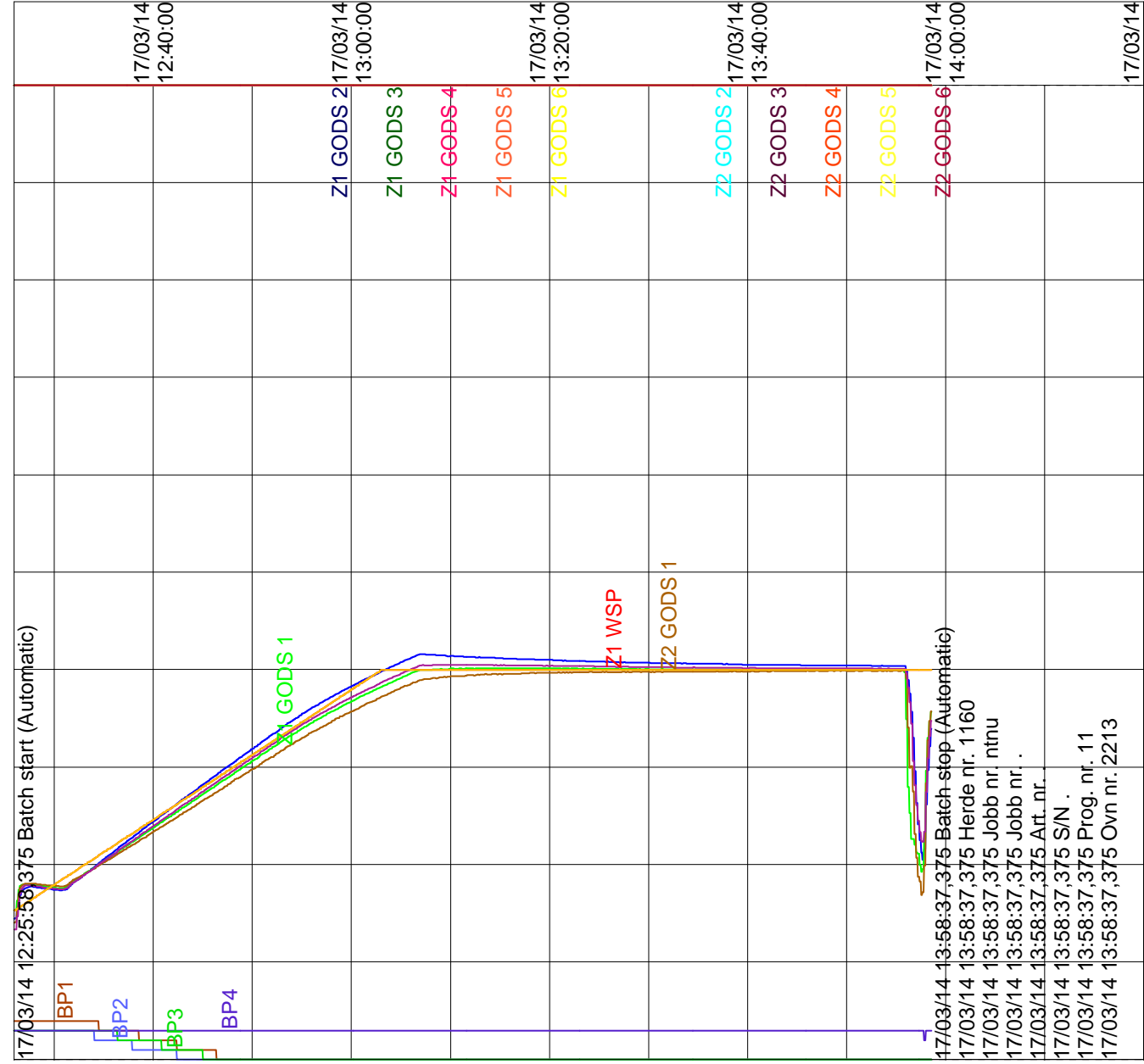
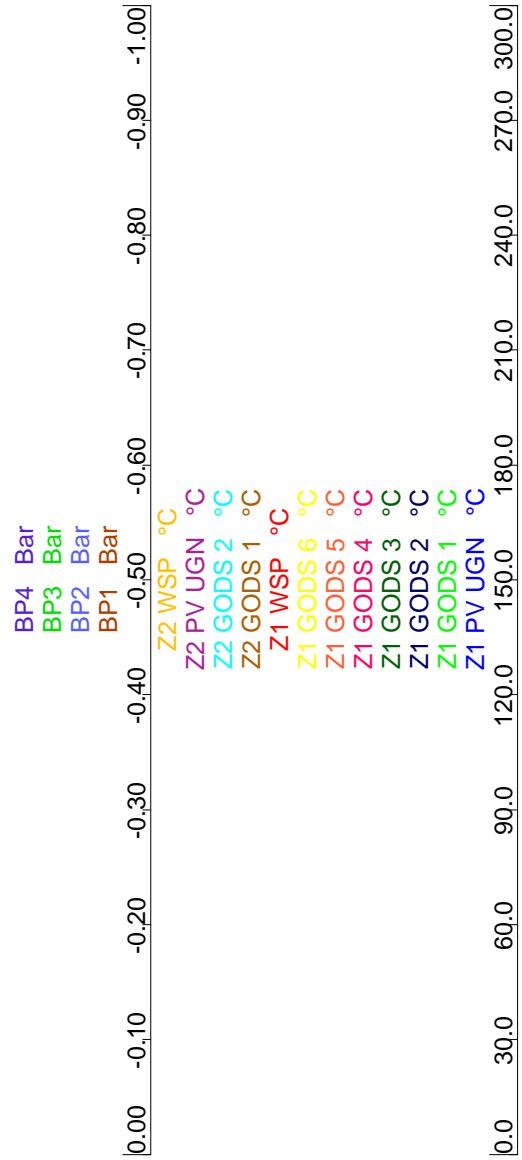


17/03/14 11:03:44,375
17.03.2014 12:04:32

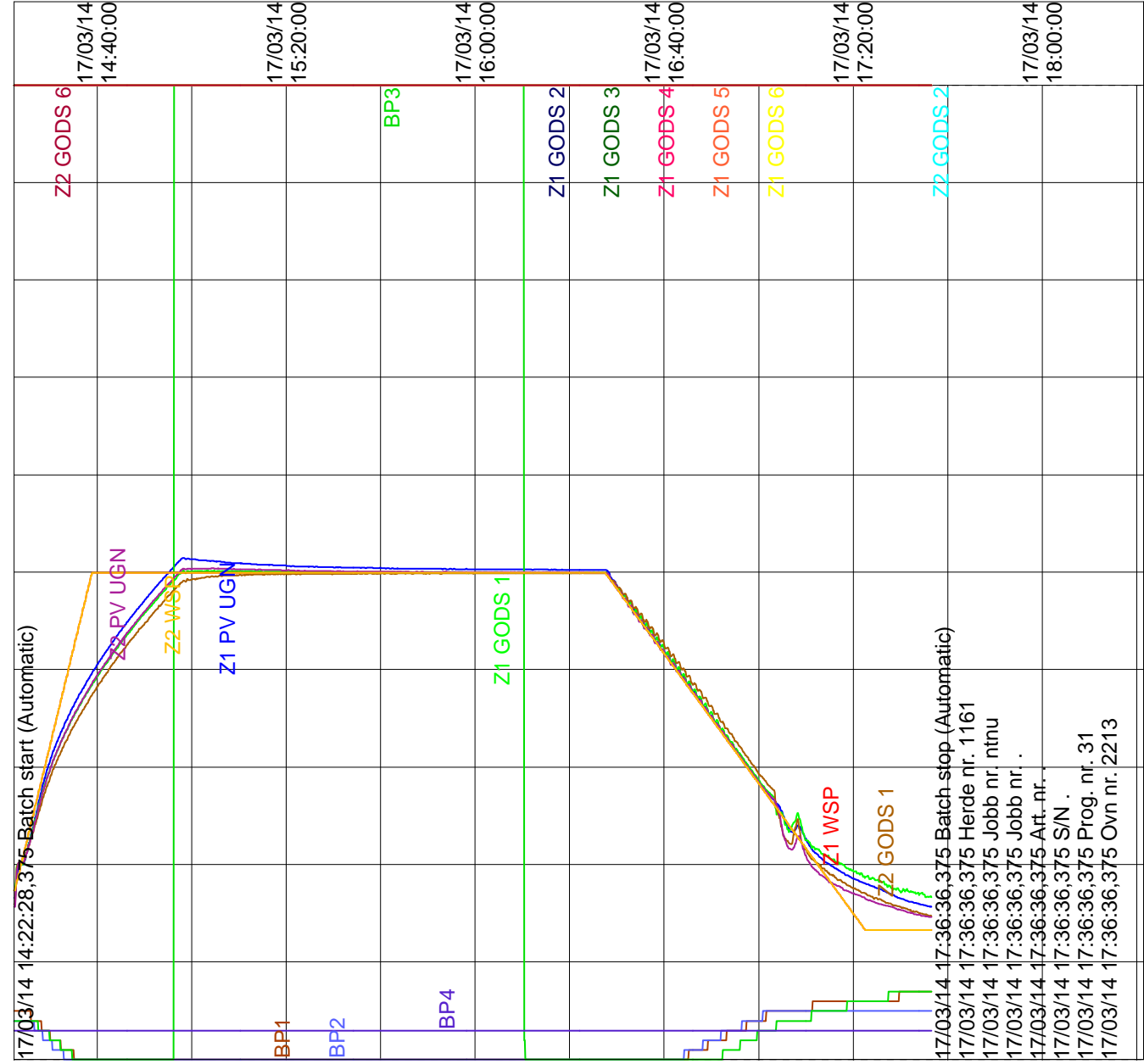
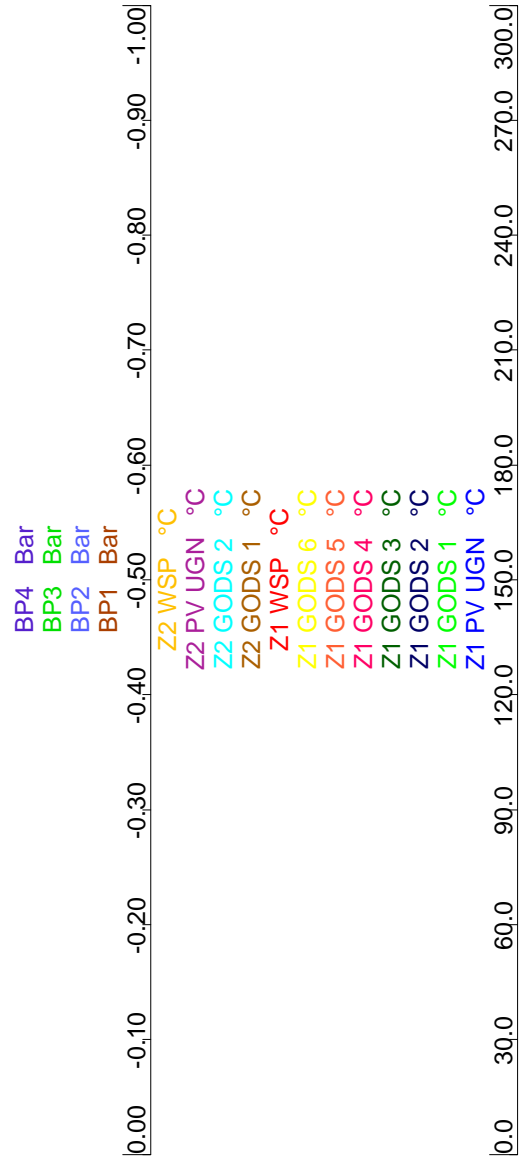
2213 automatic printing 2012.09.27



17/03/14 12:25:55,315
Page 1 of 1



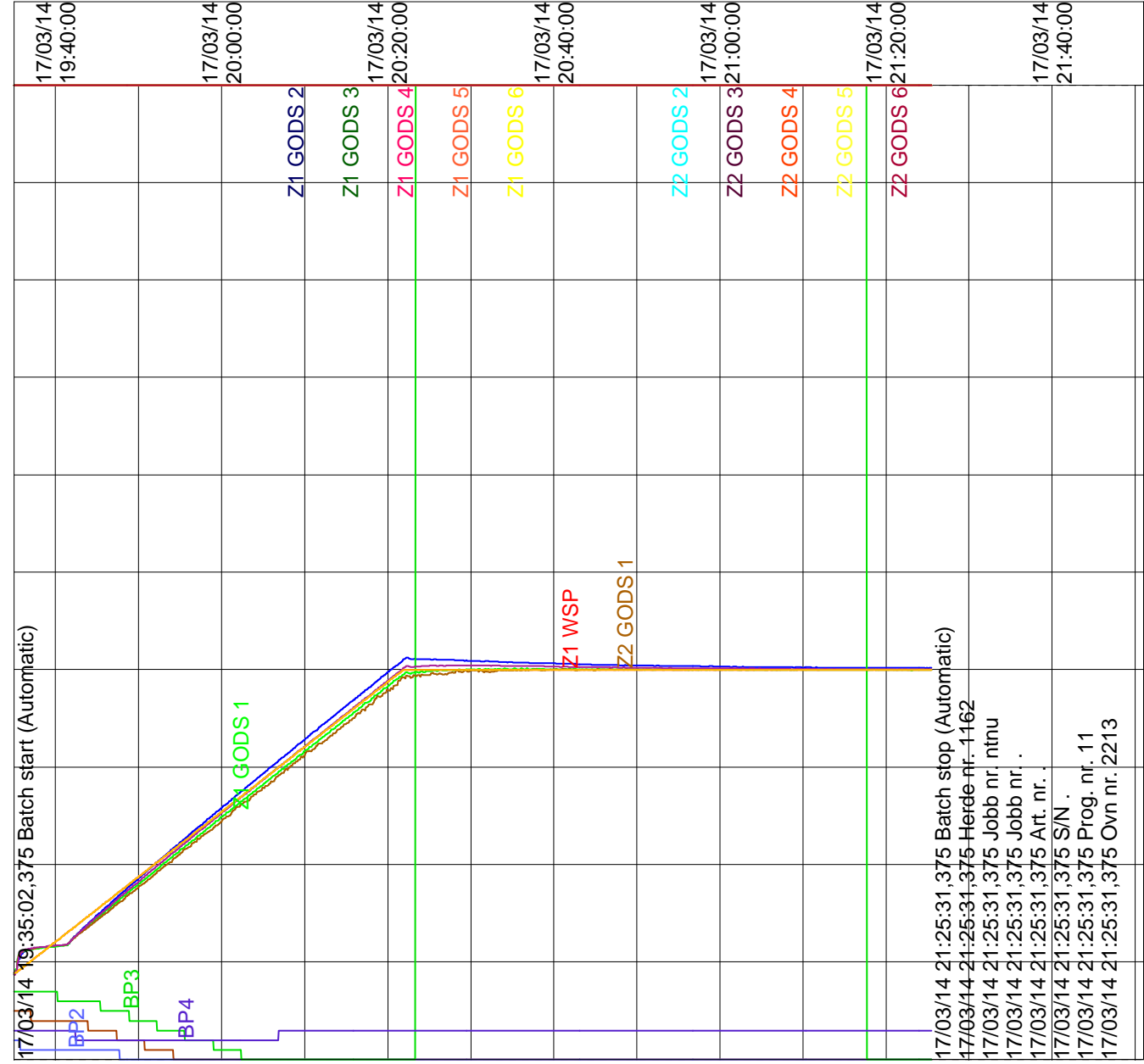
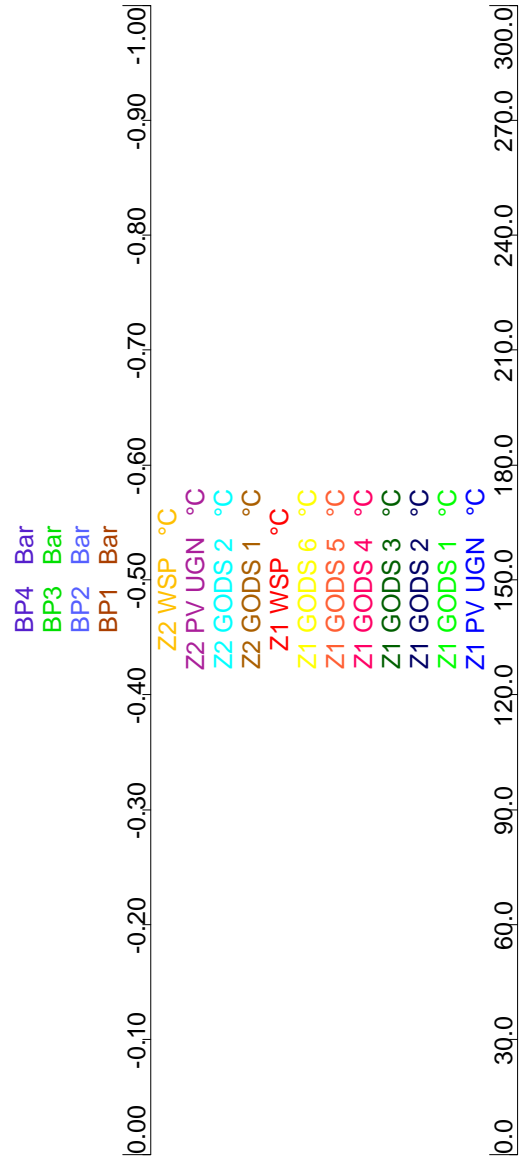
17/03/14 12:25:58,375
17.03.2014 13:52:31

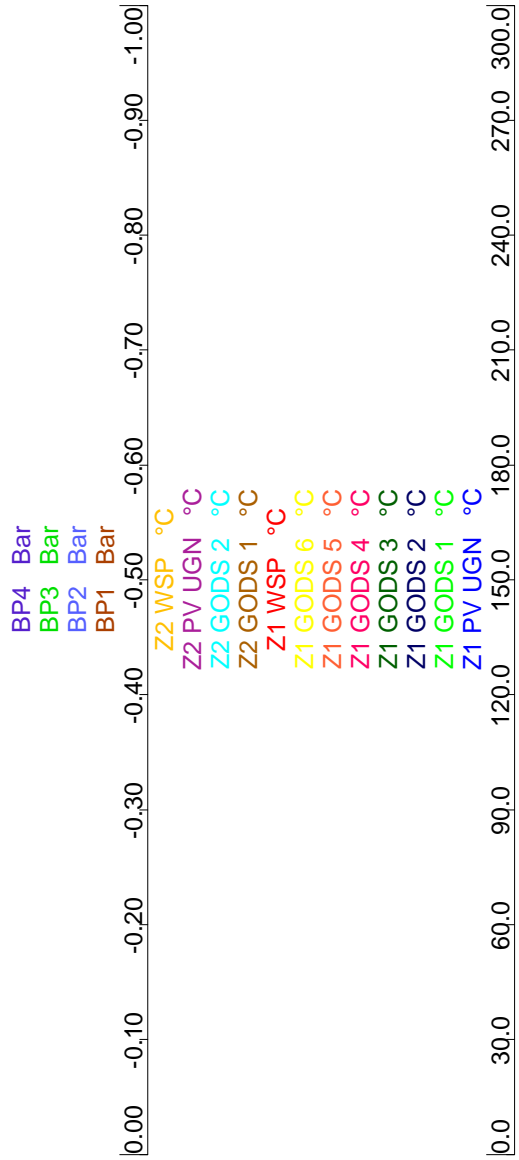


17/03/14 14:22:28,375
17.03.2014 17:30:43

2213 automatic printing 2012.09.27

17/03/14 18:21:29,345
Page 1 of 1

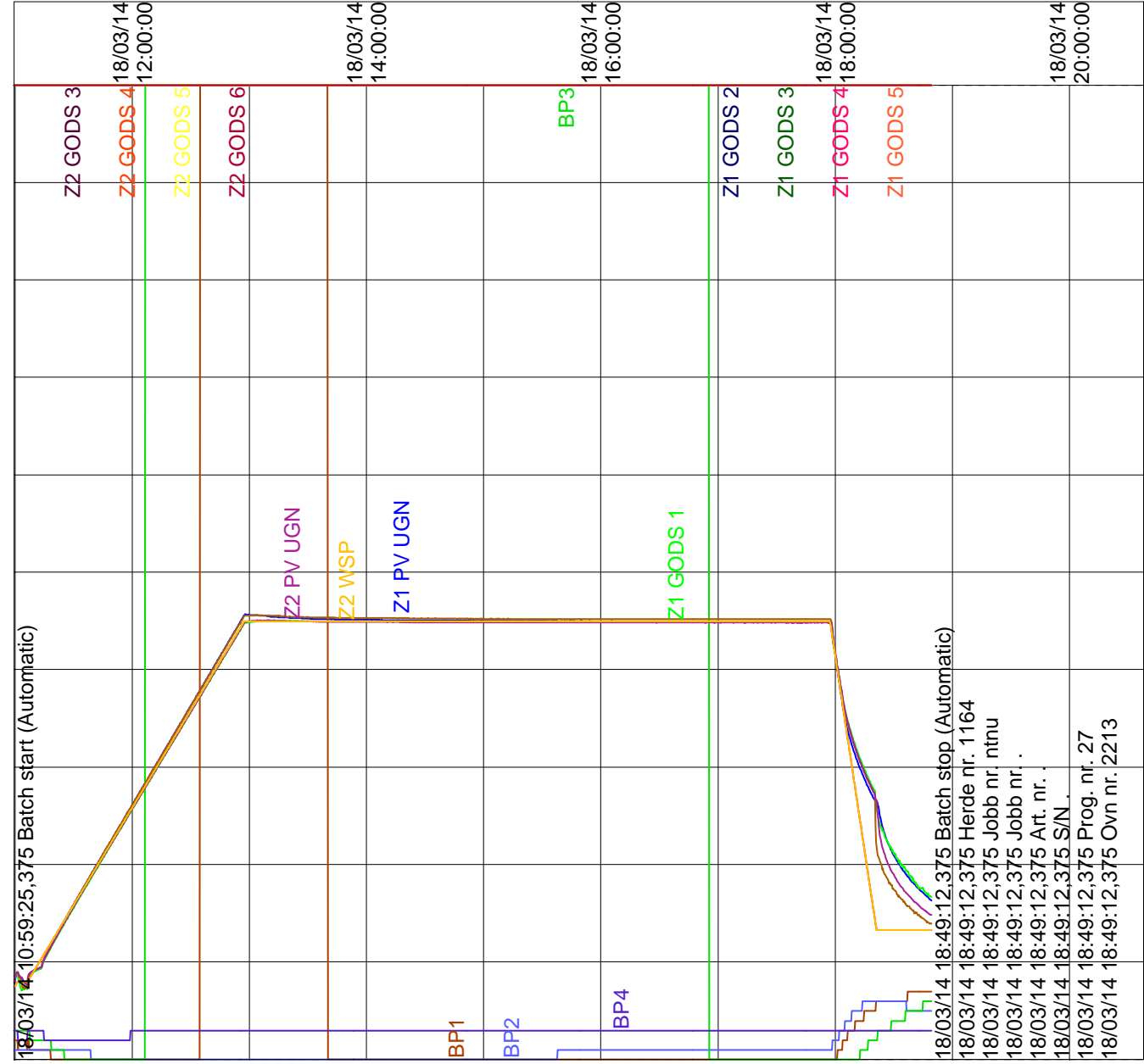
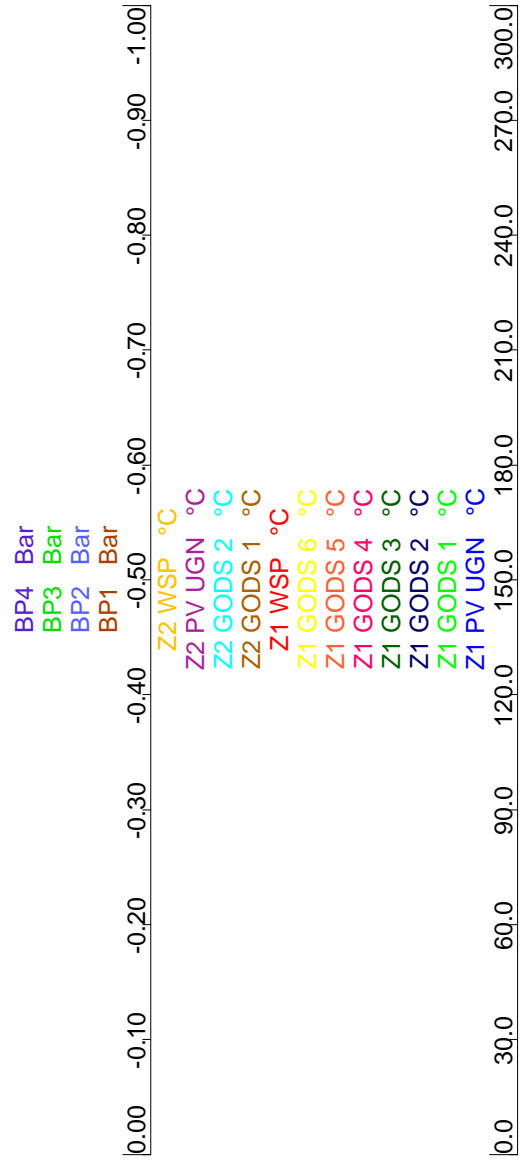


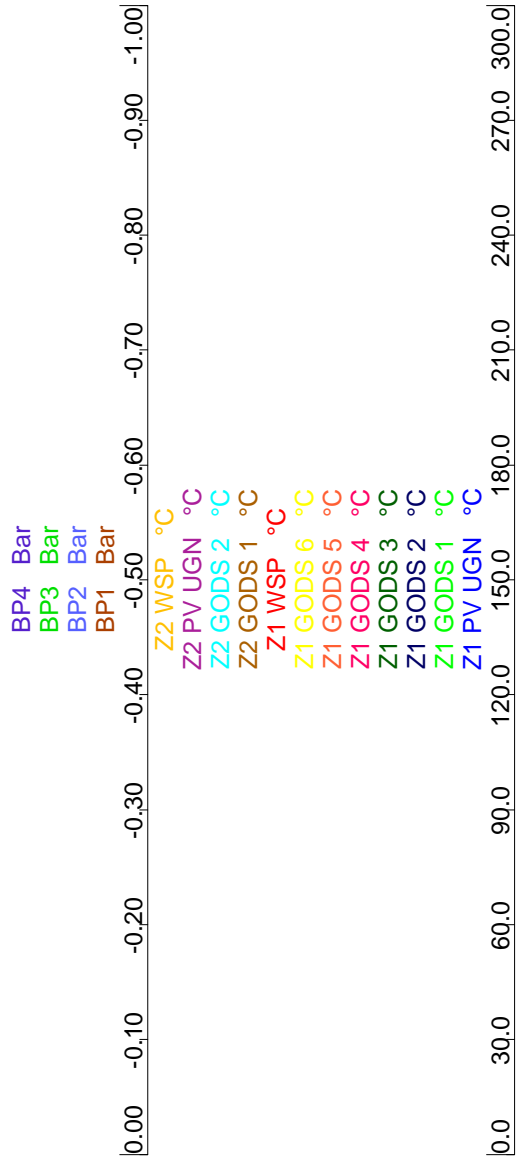


18/03/14 01:18:00,375 Batch start (Automatic)
 18.03.2014 04:26:39

2213 automatic printing 2012.09.27

18/03/14 04:31:15,375 Batch stop (Automatic)
 18/03/14 05:15:56,095
 Page 1 of 1





BP4 Bar
 BP3 Bar
 BP2 Bar
 BP1 Bar
 Z2 WSP °C
 Z2 PV UGN °C
 Z2 GODS 2 °C
 Z2 GODS 1 °C
 Z1 WSP °C
 Z1 GODS 6 °C
 Z1 GODS 5 °C
 Z1 GODS 4 °C
 Z1 GODS 3 °C
 Z1 GODS 2 °C
 Z1 GODS 1 °C
 Z1 PV UGN °C

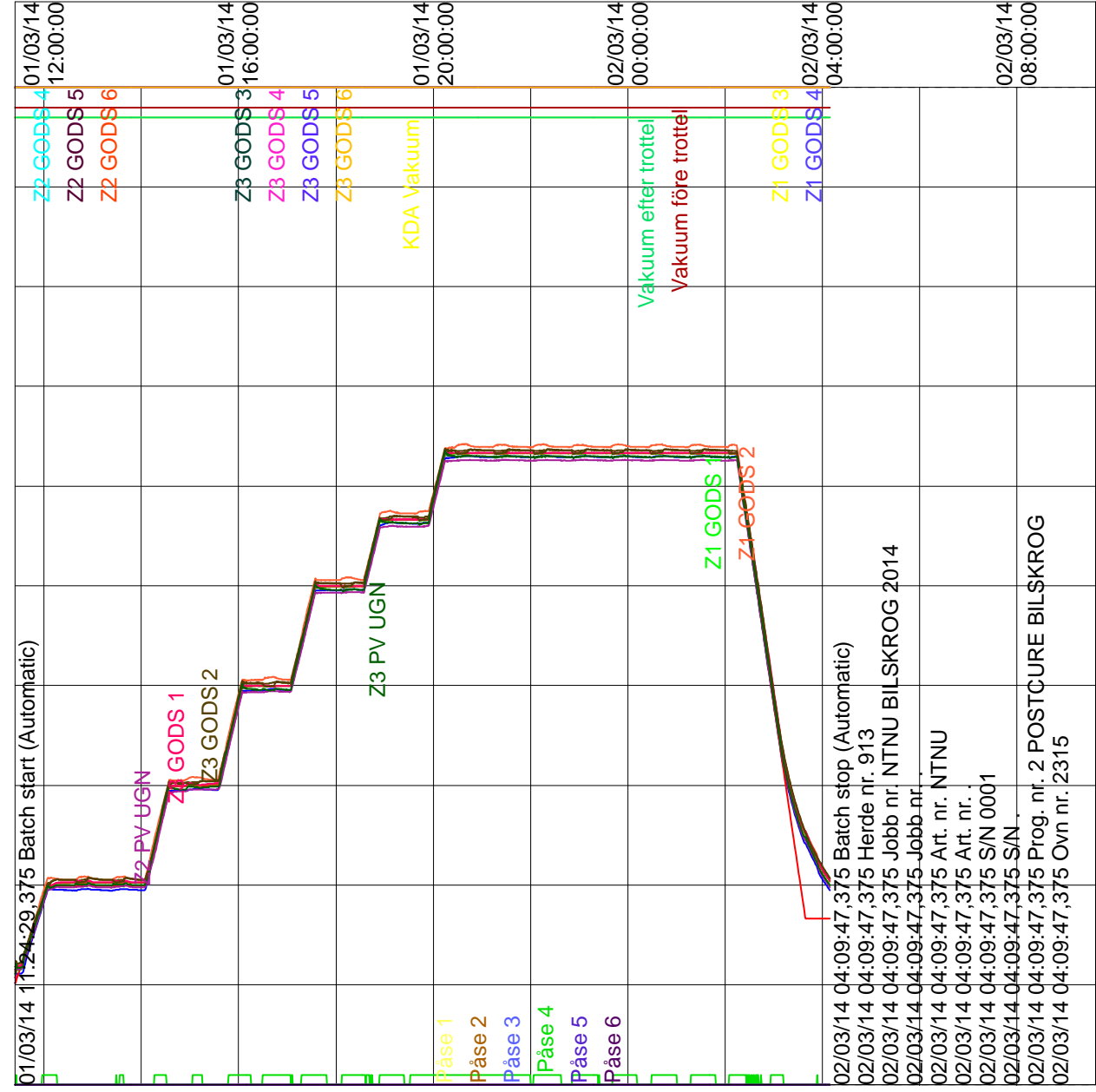
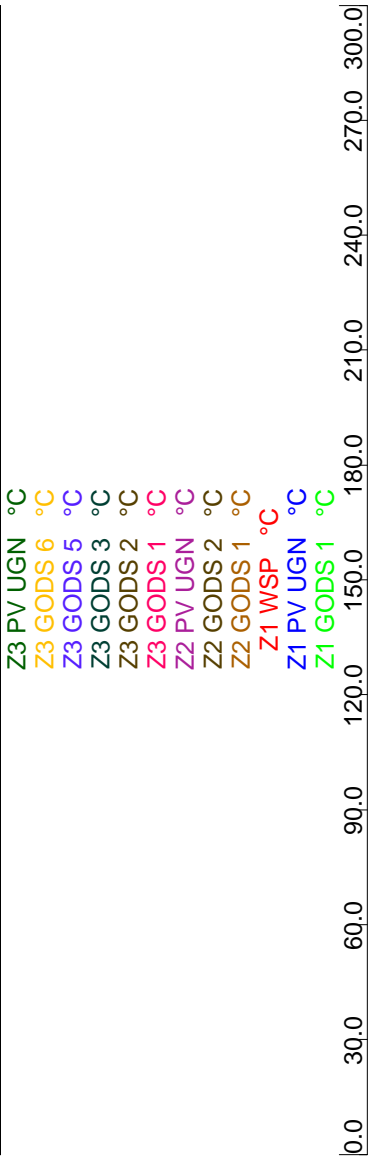
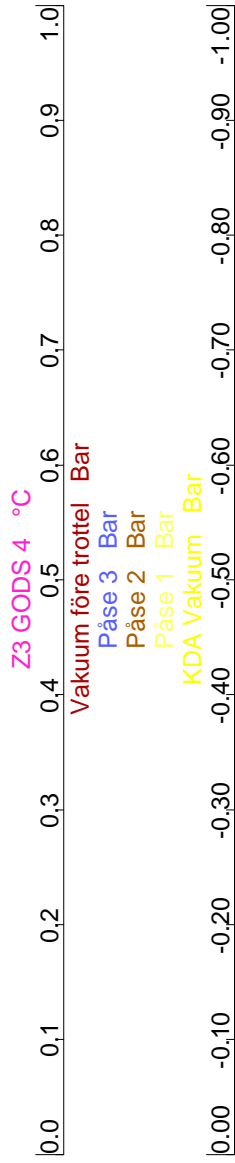
23/03/14 16:25:53,375
 23.03.2014 23:56:52

2213 automatic printing 2012.09.27

24/03/14 01:49:08,475
 Page 1 of 1

23/03/14 16:25:53,375 Batch start (Automatic)

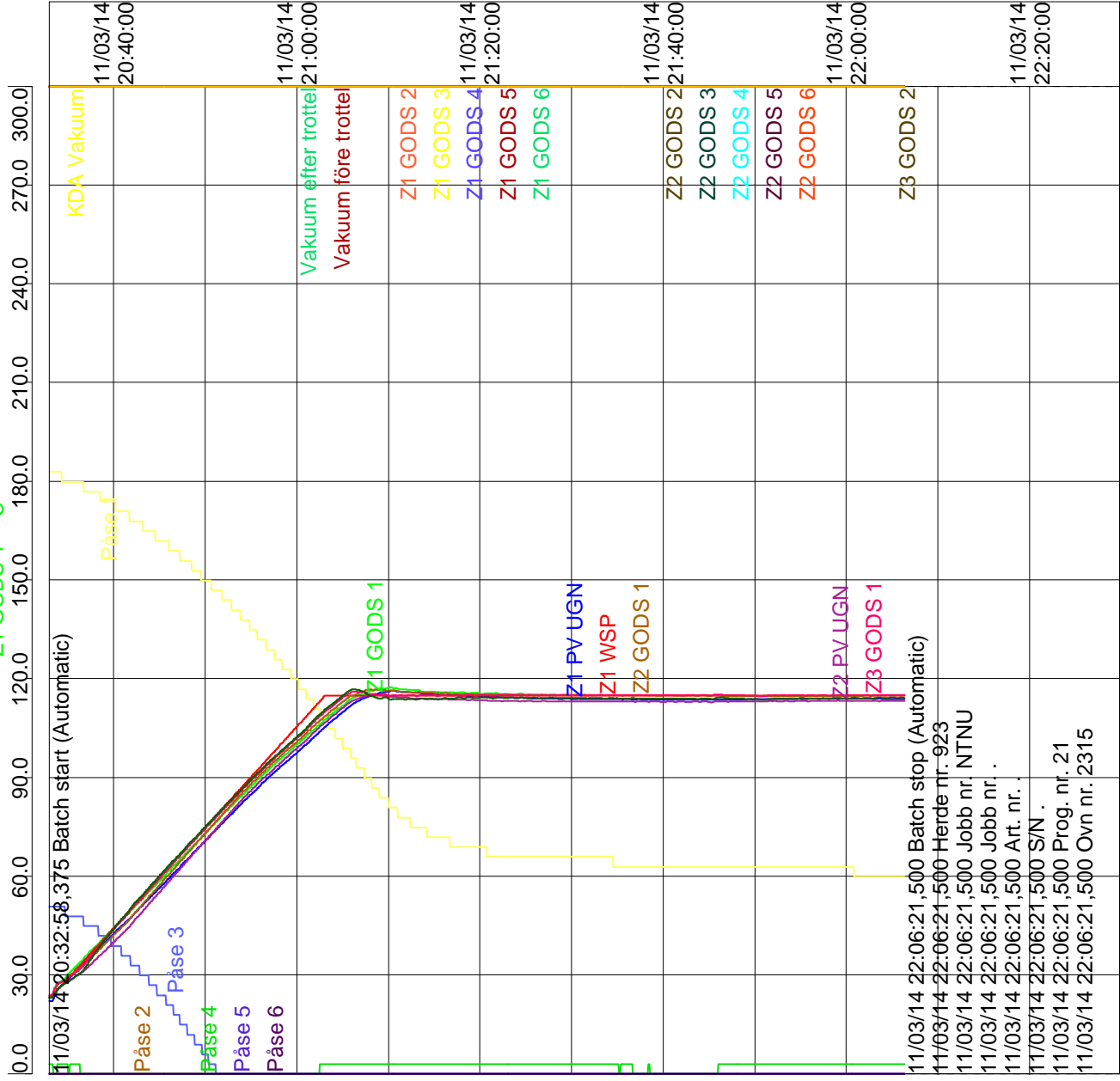
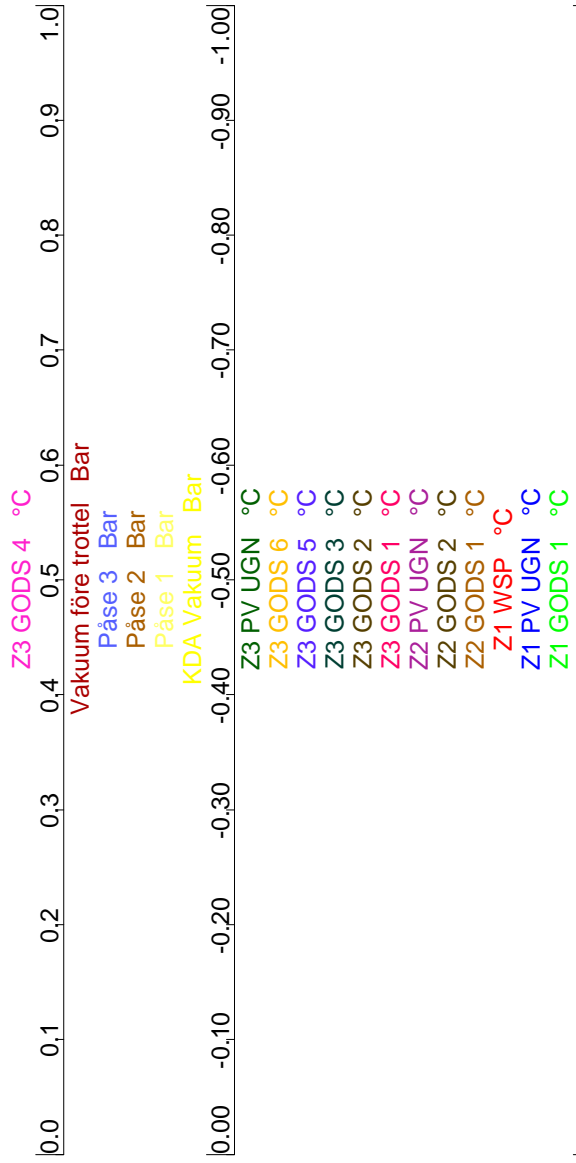
24/03/14 00:03:22,375 Batch stop (Automatic)
 24/03/14 00:03:22,375 Herde nr. 1167
 24/03/14 00:03:22,375 Jobb nr. ntnu
 24/03/14 00:03:22,375 Jobb nr. .
 24/03/14 00:03:22,375 Art. nr.
 24/03/14 00:03:22,375 S/N .
 24/03/14 00:03:22,375 Prog. nr. 1
 24/03/14 00:03:22,375 Ovn nr. 2213



01/03/14 11:24:29,375
02.03.2014 03:59:31

2315 automatic printing 2012.02.21

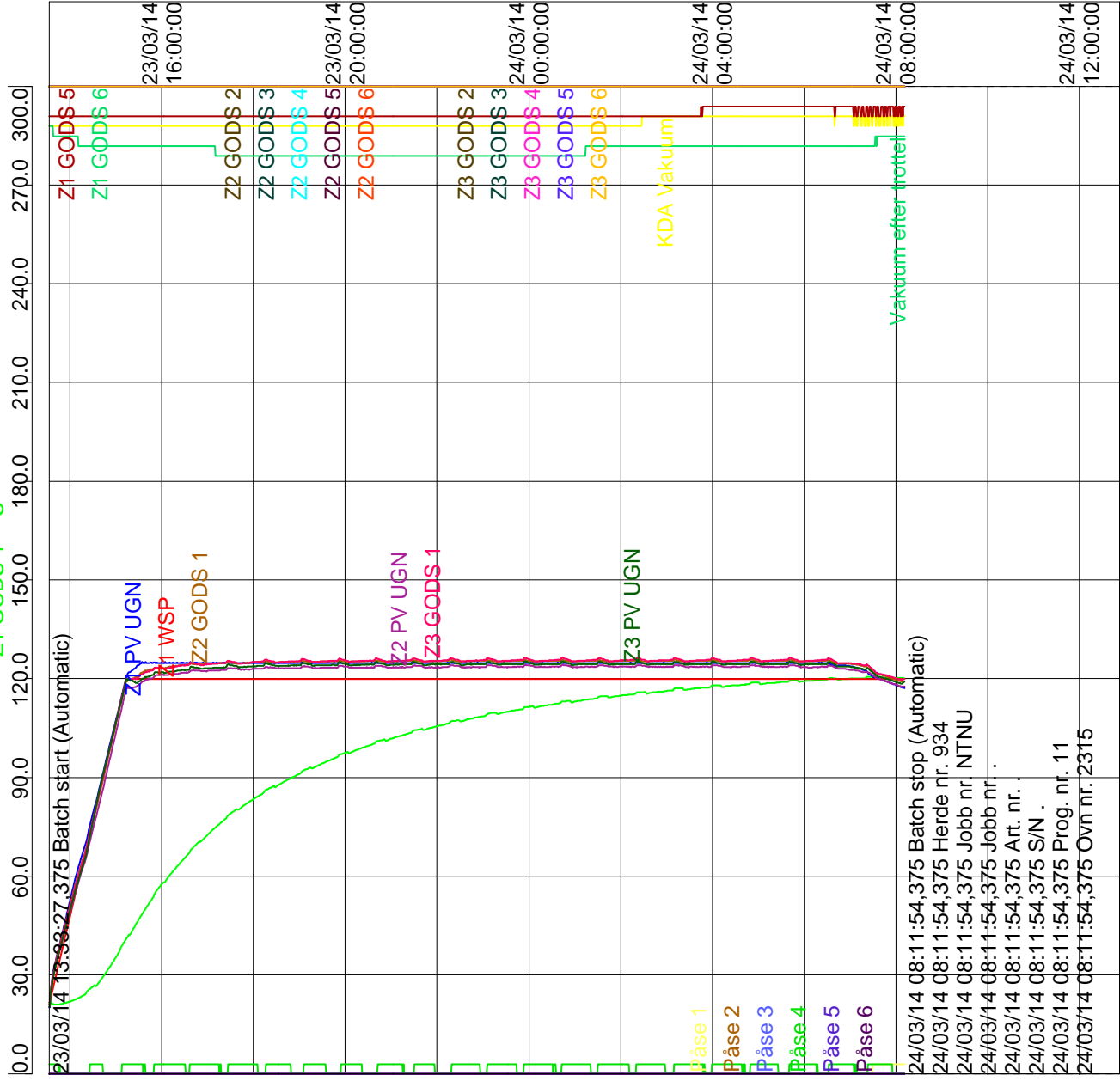
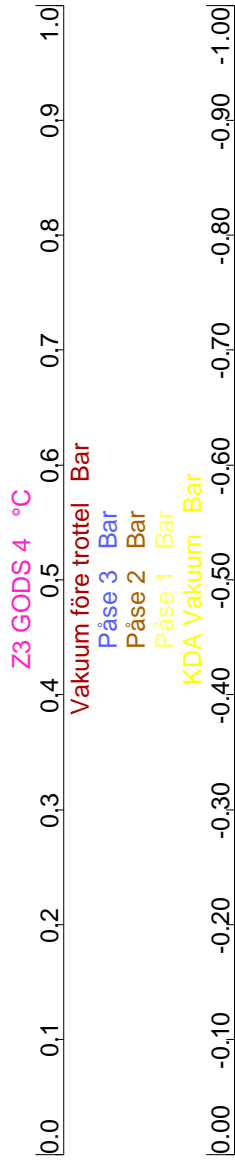
02/03/14 09:37:30,700
Page 1 of 1



11/03/14 20:32:58,375
12.03.2014 06:36:45

2315 automatic printing 2012.02.21

11/03/14 22:29:49,795
Page 1 of 1



23/03/14 13:33:27,375
24.03.2014 07:59:31

2315 automatic printing 2012.02.21

24/03/14 12:53:01,080
Page 1 of 1

> FM[®] 410-1 CORE SPLICE FOAM

TECHNICAL DATA SHEET



DESCRIPTION

FM[®] 410-1 adhesive foam is a modified epoxy adhesive foam designed for splicing honeycomb core under zero pressure, bonding of inserts or edge members to core and local honeycomb core reinforcement where increased shear strength is required. FM 410-1 adhesive foam contains no aluminum powder and has good radar transparency.

FM 410-1 adhesive foam is supplied in sheet or roll form and may be cured in place with either free foaming or restrained foaming processes. The operating temperature is -67°F to 350°F (-55°C to 177°C).

FEATURES & BENEFITS

- Improved handling characteristics
- No metallic powders or asbestos
- Splices honeycomb using ambient pressure
- Bonds inserts or edge members to honeycomb core
- Provides local honeycomb core reinforcement where increased shear is required
- Cures in 60 minutes at 250°F to 350°F (121° to 177°C)

SUGGESTED APPLICATIONS

- Splicing honeycomb core
- Bonding inserts or edge members to core
- Localized reinforcement of honeycomb where increased shear strength is required

> FM[®] 410-1 CORE SPLICE FOAM

TECHNICAL DATA SHEET

CHARACTERISTICS

Table 1 | Product Description

| | |
|----------------------------|---|
| Material Form | Unsupported 1 x 2 ft (0.3 x 0.6 m) sheets protected by an easily removed release paper and in rolls slit to customer specified widths |
| Thickness | 0.025 ± 0.005 inch (0.64 ± 0.13mm) 0.050 ± 0.005 inch (1.27 ± 0.13mm) 0.100 ± 0.005 inch (2.54 ± 0.13mm) |
| Color | Blue turning to green during cure |
| Volatile | Less than 1% |
| Expansion | 1.7 – 3.5 times original thickness |
| Density | 15 to 35 lbs/ft ³ (240 to 560 kg/m ³) |
| Shop Life | 10 days at 90°F (32°C) |
| Shelf Life | 6 months from date of shipment when stored at recommended storage temperature |
| Recommended Storage | Store at or below 0°F (-18°C) |

PROPERTIES

Table 2 | Typical Average Mechanical Properties

| Test Condition | Average Results | |
|------------------------------|------------------|------------------|
| | 250°F (121°C) | 350°F (177°C) |
| | Cure Temperature | Cure Temperature |
| Tube Shear, psi (MPa) | | |
| Tested at -67°F (-55°C) | 1000 (6.9) | 1400 (9.7) |
| Tested at 75°F (24°C) | 900 (6.2) | 1100 (7.6) |
| Tested at 180°F (82°C) | 1000 (6.9) | 1000 (6.9) |
| Tested at 300°F (149°C) | - | 850 (5.9) |

CURE CYCLES

FM 410-1 adhesive foam may be cured using one of the following cure cycles:

- **Cure Cycle A:** Heat to 225°F (107°C) in 45 minutes, hold at 225°F (107°C) for 90 minutes
- **Cure Cycle B:** Heat to 250°F (121°C) in 30 minutes, hold at 250°F (121°C) for 60 minutes
- **Cure Cycle C:** Heat to 350°F (177°C) in 60 minutes, hold at 350°F (177°C) for 60 minutes

> FM[®] 410-1 CORE SPLICE FOAM

TECHNICAL DATA SHEET

PRODUCT HANDLING AND SAFETY

Cytec Engineered Materials recommends wearing clean, impervious gloves when working with adhesives to reduce skin contact and to avoid contamination of the product.

Materials Safety Data Sheets (MSDS) and product labels are available upon request and can be obtained from any Cytec Engineered Materials Office.

DISPOSAL OF SCRAP MATERIAL

Disposal of scrap material should be in accordance with local, state, and federal regulations.

CONTACT INFORMATION

GLOBAL HEADQUARTERS

Tempe, Arizona
tel 480.730.2000
fax 480.730.2088

NORTH AMERICA

Olean, New York
tel 716.372.9650
fax 716.372.1594

Winona, Minnesota
tel 507.454.3611
fax 507.452.8195

Greenville, Texas
tel 903.457.8500
fax 903.457.8598

Springfield, Massachusetts
tel 1.800.253.4078
fax 716.372.1594

Anaheim, California
tel 714.630.9400
fax 714.666.4345

Cytec Carbon Fibers LLC
Piedmont, South Carolina
tel 864.277.5720
fax 864.299.9373

Havre de Grace, Maryland
tel 410.939.1910
fax 410.939.8100

Orange, California
tel 714.639.2050
fax 714.532.4096

D Aircraft Products, Inc.
Anaheim, California
tel 714.632.8444
fax 714.632.7164

EUROPE AND ASIA

Wrexham, United Kingdom
tel +44.1978.665200
fax +44.1978.665222

Östringen, Germany
tel +49.7253.934111
fax +49.7253.934102

Shanghai, China
tel +86.21.5746.8018
fax +86.21.5746.8038

DISCLAIMER: The data and information provided in this document have been obtained from carefully controlled samples and are considered to be representative of the product described. Cytec Engineered Materials (CEM) does not express or imply any guarantee or warranty of any kind including, but not limited to, the accuracy, the completeness or the relevance of the data and information set out herein. Because the properties of this product can be significantly affected by the fabrication and testing techniques employed, and since CEM does not control the conditions under which its products are tested and used, CEM cannot guarantee that the properties provided will be obtained with other processes and equipment. No guarantee or warranty is provided that the product is adapted for a specific use or purpose and CEM declines any liability with respect to the use made by any third party of the data and information contained herein. CEM has the right to change any data or information when deemed appropriate.

All trademarks are the property of their respective owners.

The primary goal of this testing was to learn more about local deformation of a small panel and load capacity of the inserts. It is also important to verify the insert calculations.

There were produced three different insert test samples, two of each sample, as shown in table xx. The samples were produced by first curing the face sheets separately, then bonding them to the core with FM 300-2M adhesive film while potting cells around the insert with epoxy. This manufacturing process will coincide well with actual manufacture of the monocoque.

Testing was done by putting the samples on top of a 170x170mm steel frame to test the out of plane load capacity of the test panels. Sample 1, 3 and 5 were run to destruction, test 2 and 4 were tested to their expected load limits. This gave the possibility to see how the sample failed when peeling of the face sheets after testing and identify any sign of core failure on the samples loaded to their limits.

Table 1 – Insert test specimens

| Sample | Layup | Core thickness | Panel size | Insert diameter |
|--------|-----------------------|----------------|-------------|-----------------|
| 1 | 90/45/ C /45/90 | 20mm | 200mmx200mm | 50mm |
| 2 | 90/45/ C /45/90 | 20mm | 200mmx200mm | 50mm |
| 3 | 90/45/ C /45/90 | 30mm | 200mmx200mm | 50mm |
| 4 | 90/45/ C /45/90 | 30mm | 200mmx200mm | 50mm |
| 5 | 90/45/ C /45/90 | 30mm | 200mmx200mm | 80mm |
| 6 | 90/45/ C /45/90 | 30mm | 200mmx200mm | 80mm |

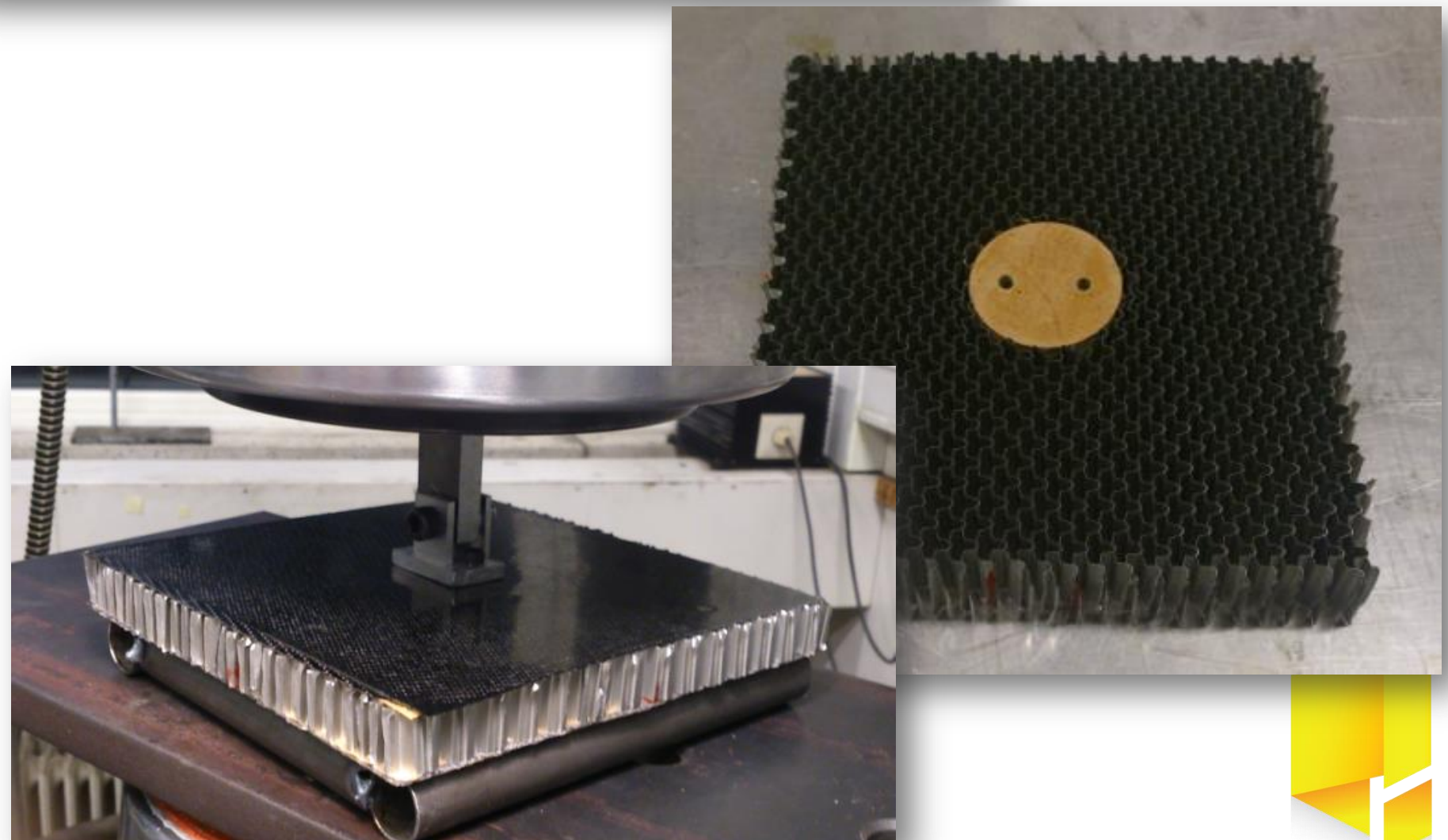
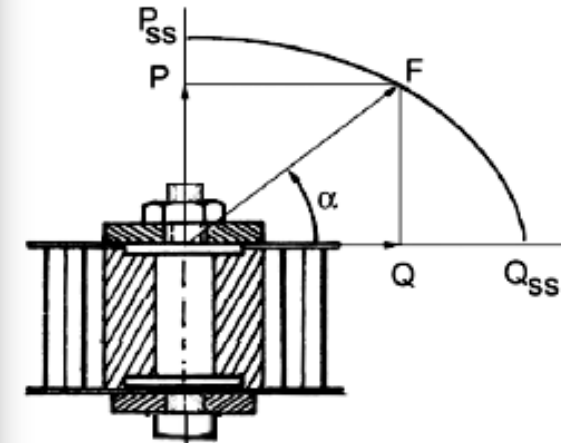
| Input | | Load case | | Force | |
|-------|----|-----------|----|-------|----|
| 1 | 2 | 3 | 4 | 5 | 6 |
| 7 | 8 | 9 | 10 | 11 | 12 |
| 13 | 14 | 15 | 16 | 17 | 18 |
| 19 | 20 | 21 | 22 | 23 | 24 |
| 25 | 26 | 27 | 28 | 29 | 30 |
| 31 | 32 | 33 | 34 | 35 | 36 |

| Core data | |
|------------------------------|--------------------|
| Modell | HX-FC-5056/F40-2.1 |
| Compressive strength [MPa] | 1,65 |
| Compressive modulus [MPa] | 448,18 |
| Plate shear strength [MPa] | 0,72 |
| Plate shear L modulus [GPa] | 0,12 |
| Plate shear W strength [MPa] | 0,38 |
| Plate shear W modulus [GPa] | 0,07 |
| Height [mm] | 30 |
| Weight [kg/m3] | 33,642 |
| Cell size [mm] | 7,62 |

| Skin data | |
|--------------------|--------|
| Modell | Hexply |
| E1 [Mpa] | 62500 |
| E2 [Mpa] | 62500 |
| G12 [Mpa] | 2840 |
| v12 | 0,08 |
| v21 | 0,08 |
| Ply thickness [mm] | 0,3 |
| Weight [g/m²] | 45 |

| Insert calculations | |
|----------------------------|----------------------------|
| Bearing coefficient | $K_b = 2,2$ |
| Dimpling coefficient | $K_d = 2$ |
| Shear strength, cell walls | $\tau_c = 200$ MPa |
| Foil thickness, core | $t_c = 0,036$ mm |
| Effective Shear Modulus | $G_s^* = 22,983$ MPa |
| Effective Shear Strength | $\tau_{c,eff} = 0,516$ MPa |
| Minimum potting radius | $b_{p,min} = 27,834$ mm |
| Typical potting radius | $b_{p,typ} = 31,096$ mm |
| Real potting radius, min | $b_{r,min} = 27,667$ mm |
| Real potting radius, typ | $b_{r,typ} = 28,81$ mm |
| Dist. between facesheets | $d = 30,6$ mm |
| $E^* = \sqrt{E1 \cdot E2}$ | $E^* = 62500,0$ MPa |

| Used capacity | |
|---------------------------|------------------------------|
| Out of plane capacity | $P_{crit} = 2760,0$ N |
| Shear capacity | $Q_{crit,unsym} = 30728,7$ N |
| Dimpling capacity | $Q_d = 8292,7$ N |
| In-plane bearing capacity | $Q_b = 19327,8$ N |
| Bending capacity | $M_{crit} = 69,0$ Nm |
| Torsional capacity | $T_{crit} = 69,3$ Nm |

$$\left(\frac{P}{P_{crit}}\right)^2 + \left(\frac{Q}{Q_{crit,unsym}}\right)^2 + \left(\frac{M}{M_{crit}}\right)^2 + \left(\frac{T}{T_{crit}}\right)^2 \leq 1$$


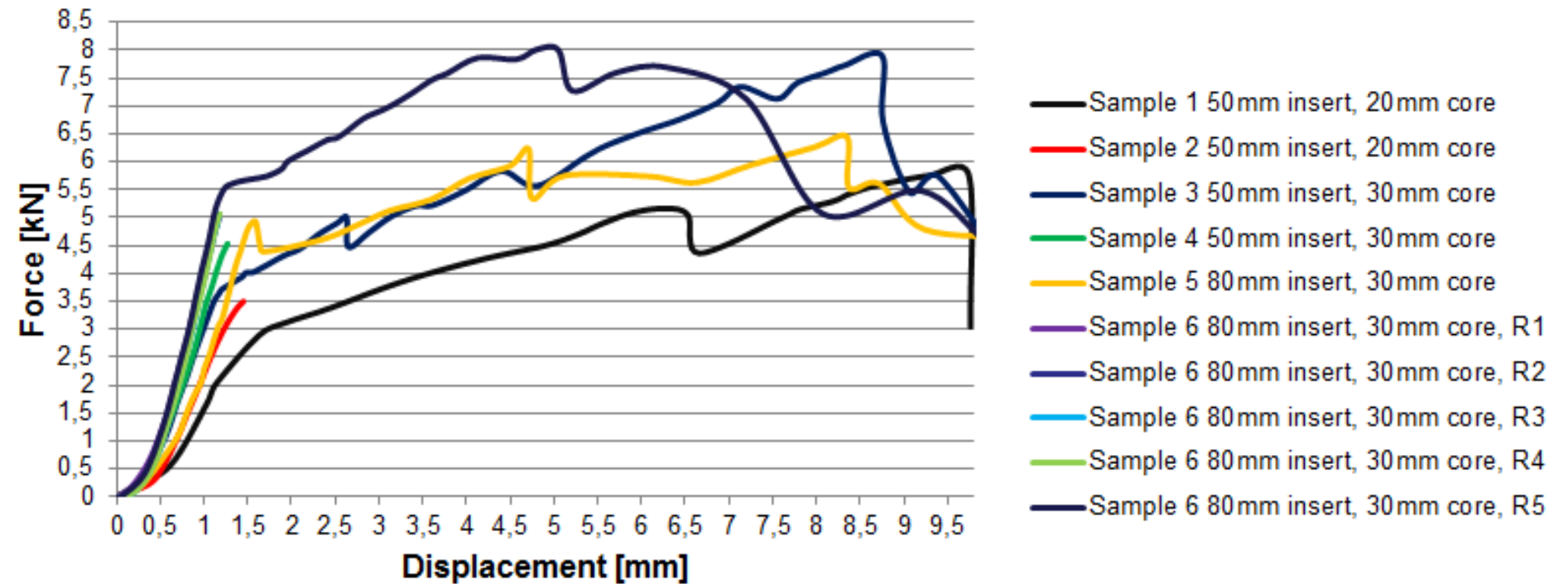
All insert samples managed to withstand loads higher than their analytical design-loads before being permanently damaged. Compared to the results obtained in the analysis, the insert panels had some deformation, about 0,3mm, under low loads before the force-displacement curve reached the linear zone. This is believed to be caused by the bracket not tightened enough to the panel as small compliances in the connection between face sheet and insert. Once the linear zone is reached, most insert panels achieved their expected stiffness.

Disassembling the panels after testing revealed that some epoxy-potting on sample 1 and 5 had leaked between the core and bottom face sheet, so that the inserts no longer were fully potted. This did not seem to affect the results noticeably, but it should be noted that some of the identically samples had a certain deviation in stiffness. This is believed to be due to variances in the production quality, as it is difficult to pot and bond an insert completely the same way every time.

Table 1 – Insert test specimens

| Sample | Layup | Core thickness | Panel size | Insert diameter |
|--------|-----------------------|----------------|-------------|-----------------|
| 1 | 90/45/ C /45/90 | 20mm | 200mmx200mm | 50mm |
| 2 | 90/45/ C /45/90 | 20mm | 200mmx200mm | 50mm |
| 3 | 90/45/ C /45/90 | 30mm | 200mmx200mm | 50mm |
| 4 | 90/45/ C /45/90 | 30mm | 200mmx200mm | 50mm |
| 5 | 90/45/ C /45/90 | 30mm | 200mmx200mm | 80mm |
| 6 | 90/45/ C /45/90 | 30mm | 200mmx200mm | 80mm |

Insert testing S1-S6



One can observe the bonding between face sheet and aluminum honeycomb. On close look one can see that fibers remaining in the adhesive film surrounding the insert, a clear sign of good bonding. On inspection the adhesive film is both located on the honeycomb and the face sheet. On certain parts of the bond it seemed to be adhesive on both sides of the same section, giving the possibility that it is the adhesive itself that as failed, not the bonding.

Inspection showed us that all of the insert test failed at the potting-core interface by shear failure of the surrounding cells. This is in accordance with the assumptions made in the insert theory, and validates the empirical formulae. Evaluation of results show a higher maximum capacity than calculated from the ESA formulae, but the panels started crackling at about half way through the linear region. This was assumed to be local buckling of the core, and that plastic deformation was starting.



Appendix: Experimental results of 3pt bending, insert and penetration test.

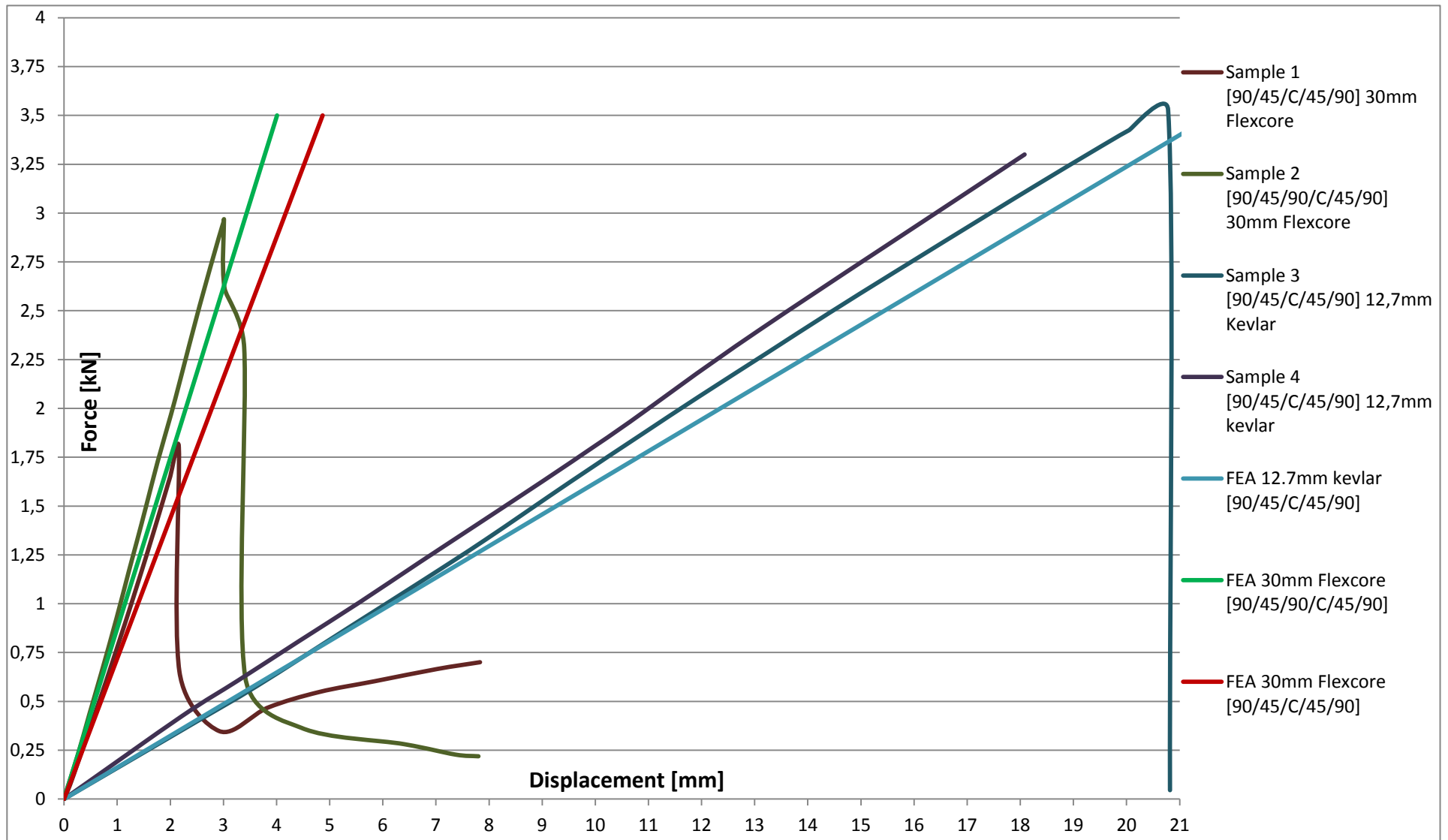


Figure 28 - 3pt bending testing.

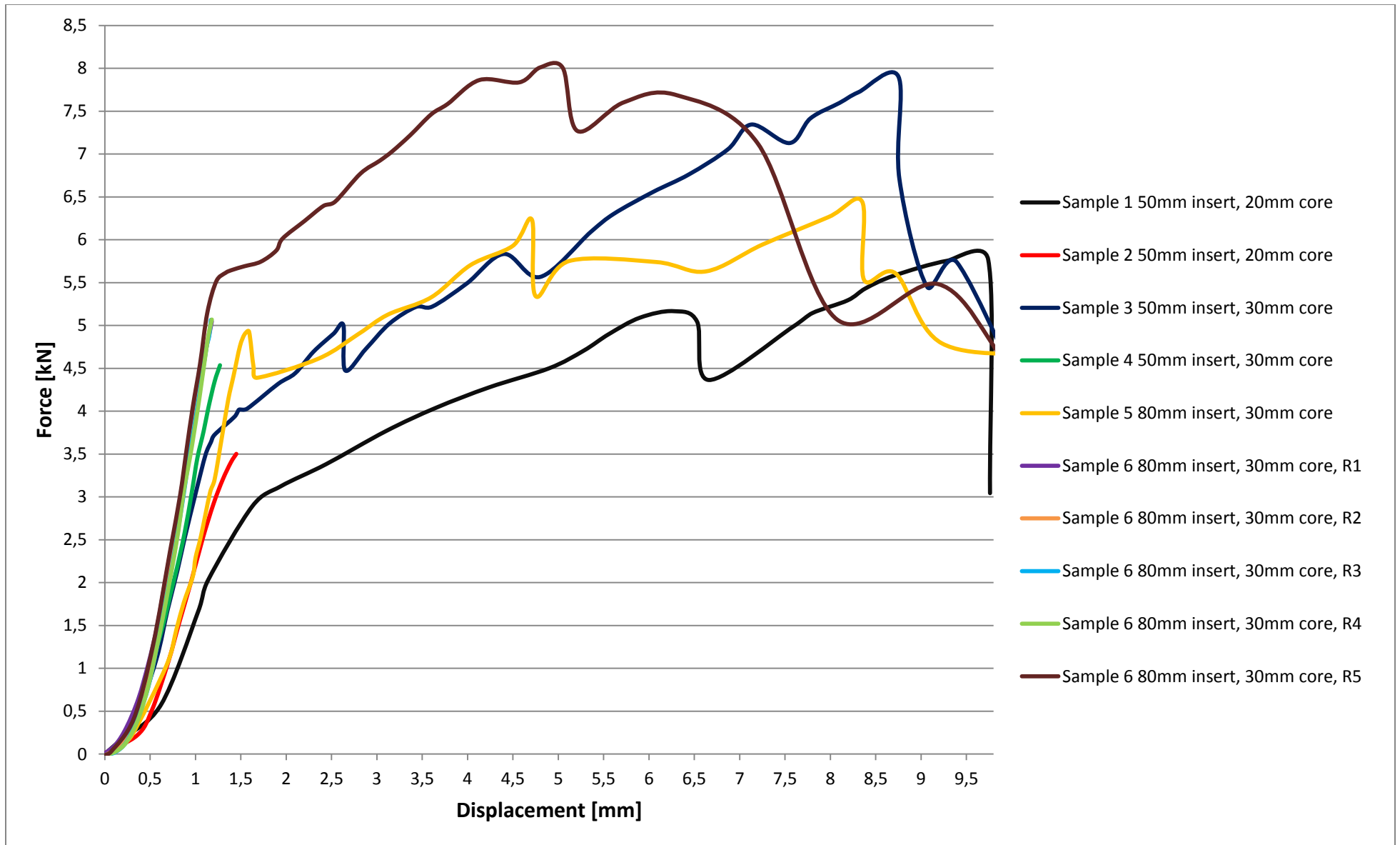


Figure 29 – Insert testing

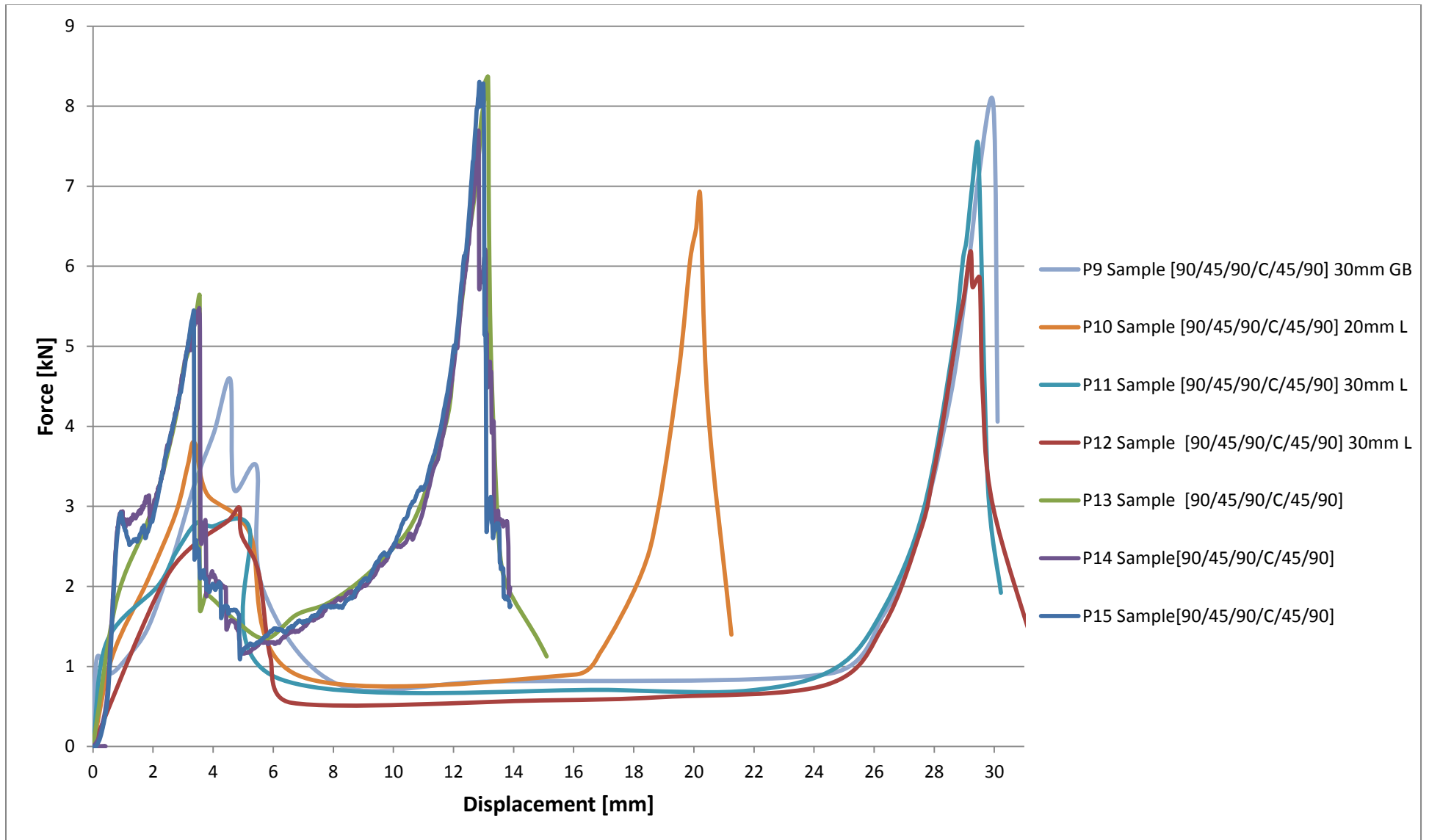
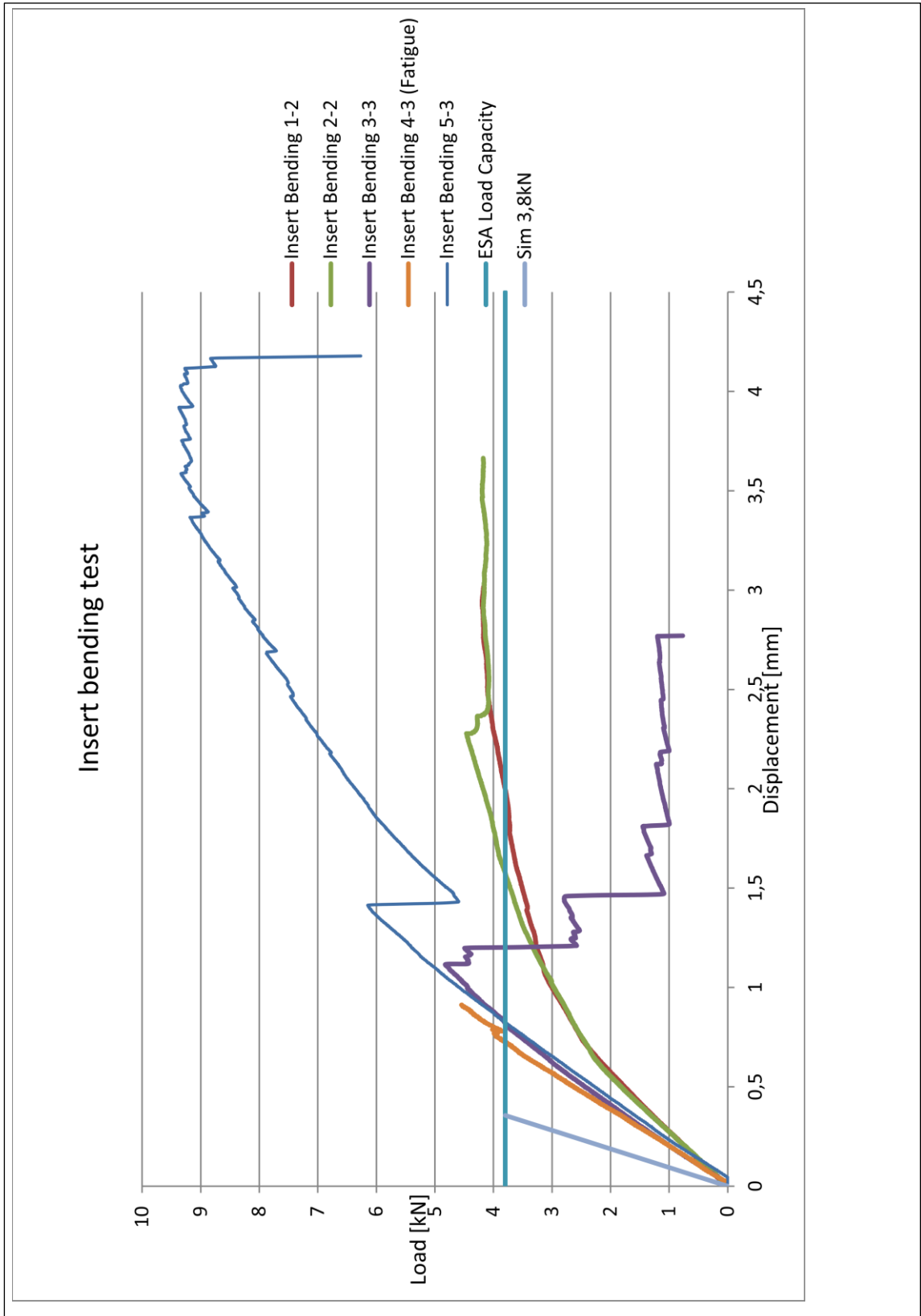
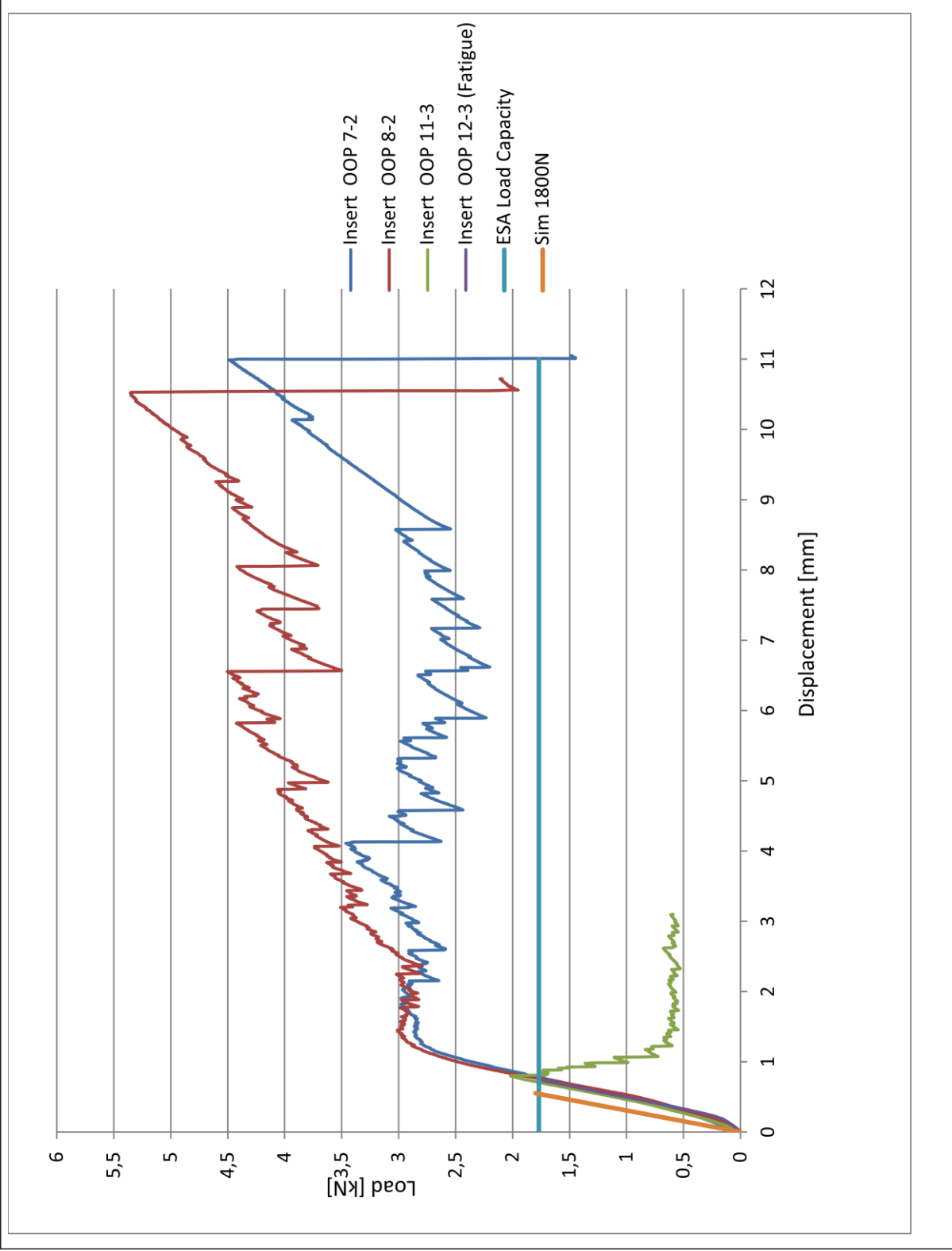


Figure 23 – Graph of penetration results 1

A7: Insert testing results

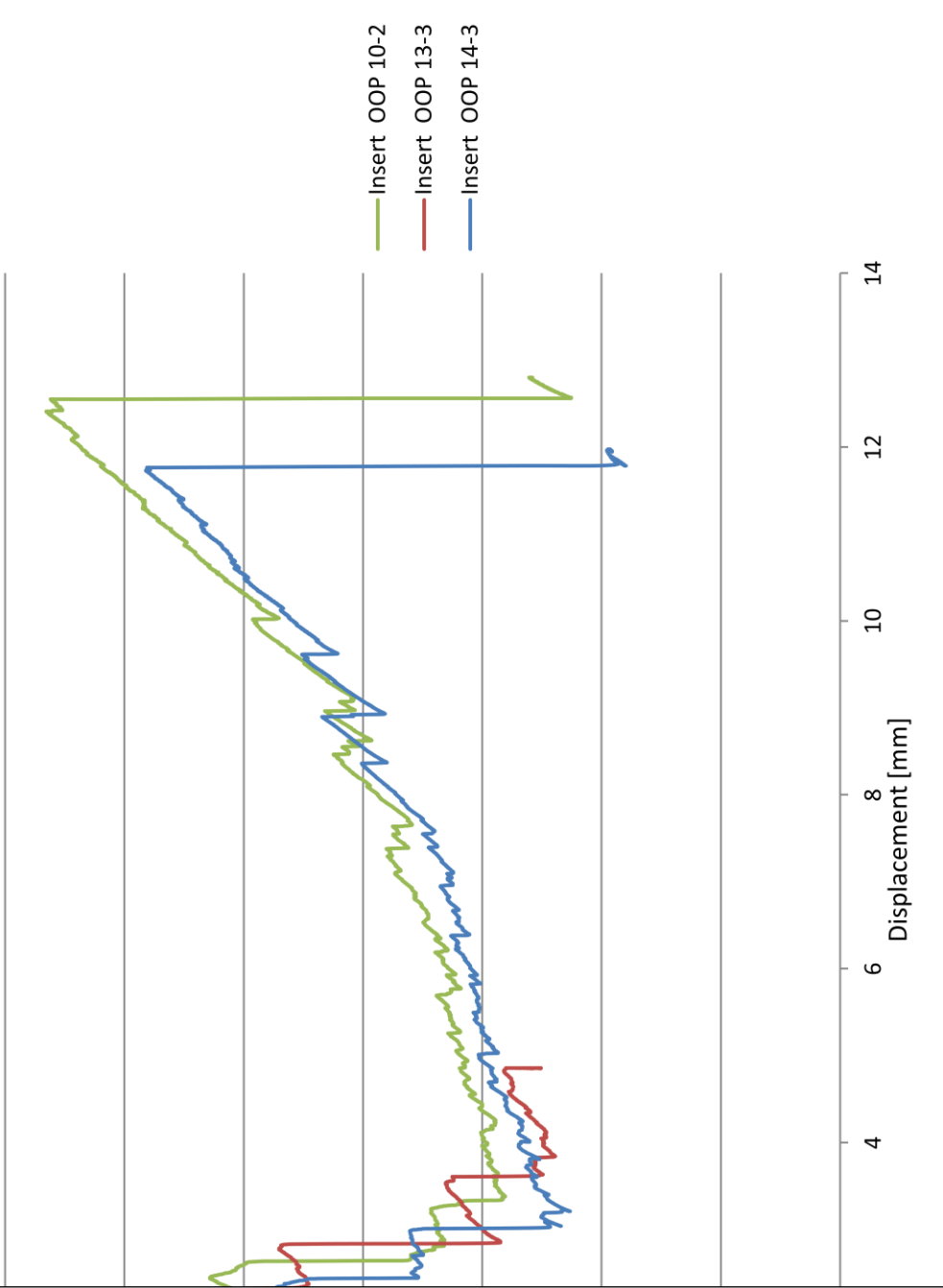




IP8
IP7
IP4

12000

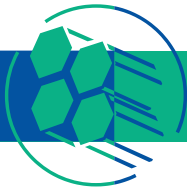
00





HexWeb™ Honeycomb Attributes and Properties

*A comprehensive
guide to standard
Hexcel honeycomb
materials,
configurations,
and mechanical
properties*



Contents

| | |
|--|----|
| Introduction | 2 |
| How Honeycomb Is Manufactured | 3 |
| Honeycomb Cell Configurations | 4 |
| Honeycomb Materials | 6 |
| Aluminum | 6 |
| Fiberglass | 7 |
| Aramid Fiber | 7 |
| Nomex® | 7 |
| Kevlar® | 7 |
| KOREX® | 8 |
| Special Honeycomb | 8 |
| Carbon | 8 |
| Polyurethane | 8 |
| Specifying Honeycomb | 9 |
| Guide to Determining Which Type of Honeycomb to Specify | 9 |
| Most Important Attributes of Each Honeycomb Material | 9 |
| Mechanical Properties and Test Methods | 10 |
| Density and Thickness Measurements | 10 |
| Compressive Properties | 10 |
| Crush Strength | 10 |
| L and W Shear Properties | 11 |
| Additional Mechanical Properties | 12 |
| Classification of Mechanical Properties | 12 |
| Correlation of Shear Strength Data | 13 |
| Effect of Core Thickness on Plate Shear Strength | 13 |
| Correlation of Flexural Shear Strength Data | 14 |
| Mechanical Property Tables | 15 |
| 5052 Alloy Hexagonal Aluminum Honeycomb – Specification Grade | 16 |
| 5056 Alloy Hexagonal Aluminum Honeycomb – Specification Grade | 17 |
| Aluminum Commercial Grade (ACG®) | 17 |
| 5052 Alloy Rigidcell™ Aluminum Corrugated Honeycomb | 18 |
| 5052 and 5056 Alloy Aluminum Flex-Core® – Specification Grade | 18 |
| HRP® Fiberglass Reinforced Phenolic Honeycomb | 19 |
| HFT® Fiberglass Reinforced Phenolic Honeycomb | 19 |
| HRH®-327 Fiberglass Reinforced Polyimide Honeycomb | 20 |
| HRH®-10 Aramid Fiber/Phenolic Resin Honeycomb | 21 |
| HRH®-310 Aramid Fiber/Polyimide Resin Honeycomb | 21 |
| HRH®-78 Nomex Commercial Grade Aramid Fiber/Phenolic Resin Honeycomb | 22 |
| HRH®-49 Kevlar 49 Honeycomb | 22 |
| KOREX® Aramid Fiber/Phenolic Resin Honeycomb | 22 |
| TPU™ Thermoplastic Polyurethane Honeycomb | 22 |

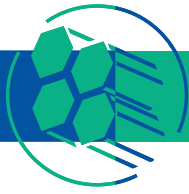
Contents cont.

| | |
|--|----|
| Comparison of Typical Mechanical Properties and Other Design Considerations | 23 |
| Additional Properties of Honeycomb | 28 |
| Acoustical | 28 |
| Air/Fluid Directionalization | 28 |
| Pressure Drop Across Honeycomb | 28 |
| Bending of Honeycomb | 29 |
| Coefficient of Thermal Expansion | 29 |
| Dielectric | 30 |
| Energy Absorption | 31 |
| Moisture Absorption | 32 |
| Radio Frequency Shielding | 32 |
| Thermal Conductivity | 32 |
| Comparison and Benefits of Honeycomb Versus Alternative Core Materials | 34 |
| Applications | 35 |
| Hexcel Honeycomb Technical Literature Index | 36 |

TM CFC, CR-PAA, Double-Flex, HexWeb, Micro-Cell, OX-Core, Rigidcell, and TPU are trademarks of Hexcel Corporation, Pleasanton, California.

® ACG, Acousti-Core, CECORE, CR III, CROSS-CORE, Fibertruss, Flex-Core, HFT, HOBE, HRH, HRP, Tube-Core, Hexcel, and the Hexcel logo are registered trademarks of Hexcel Corporation, Pleasanton, California.

® Kevlar, KOREX, and Nomex and are registered trademarks of E.I. DuPont de Nemours, Wilmington, Delaware.



HexWeb Honeycomb Attributes and Properties

Introduction

Hexcel has produced more than 700 varieties of honeycomb over the past 50 years. Today, HexWeb honeycomb is available in a wide range of materials and cell configurations, and additional products are continually developed in response to new uses for honeycomb sandwich construction.

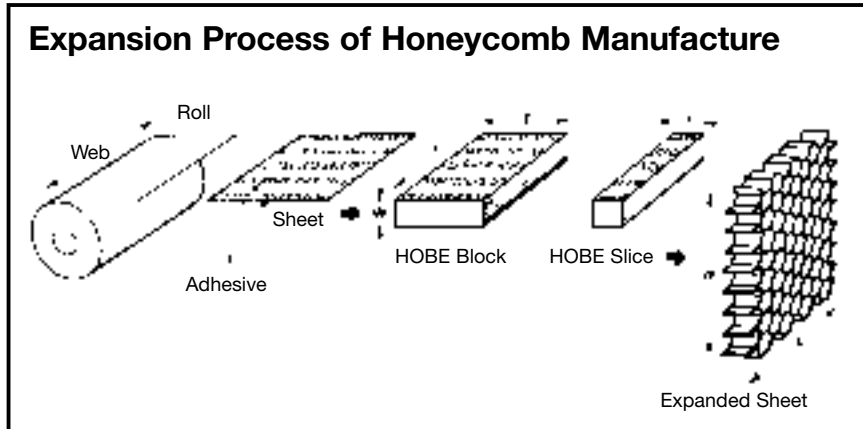
This brochure lists the materials, configurations, and mechanical properties of Hexcel's standard honeycomb as a guide to selecting honeycomb core best suited for particular applications.

| | Solid Metal Sheet | Sandwich Construction | Thicker Sandwich |
|--------------------|-------------------|------------------------------|------------------------------|
| | | | |
| Relative Stiffness | 100 | 700 7 times more rigid | 3700 37 times more rigid! |
| Relative Strength | 100 | 350 3.5 times as strong | 925 9.25 times as strong! |
| Relative Weight | 100 | 103 3% increase in weight | 106 6% increase in weight |

A striking example of how honeycomb stiffens a structure without materially increasing its weight.

How Honeycomb Is Manufactured

Honeycomb is made primarily by the expansion method. The corrugated process is most common for high density honeycomb materials.

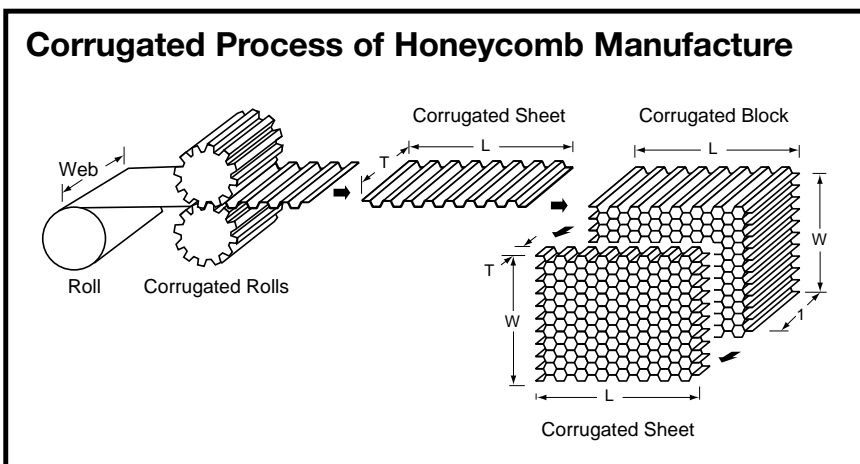


Expansion Process

The honeycomb fabrication process by the expansion method begins with the stacking of sheets of the substrate material on which adhesive node lines have been printed. The adhesive lines are then cured to form a HOBE[®] (Honeycomb Before Expansion) block.

The HOBE block itself may be expanded after curing to give an expanded block. Slices of the expanded block may then be cut to the desired T dimension. Alternately, HOBE slices can be cut from the HOBE block to the appropriate T dimension and subsequently expanded. Slices can be expanded to regular hexagons, underexpanded to 6-sided diamonds, and overexpanded to nearly rectangular cells.

The expanded sheets are trimmed to the desired L dimension (ribbon direction) and W dimension (transverse to the ribbon).



Corrugated Process

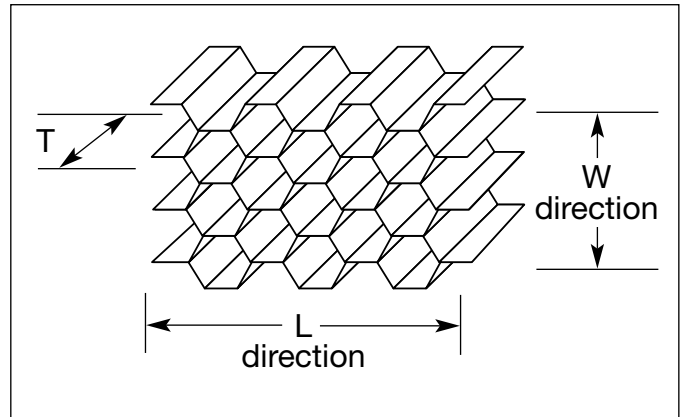
The corrugated process of honeycomb manufacture is normally used to produce products in the higher density range. In this process adhesive is applied to the corrugated nodes, the corrugated sheets are stacked into blocks, the node adhesive cured, and sheets are cut from these blocks to the required core thickness.



Honeycomb Cell Configurations

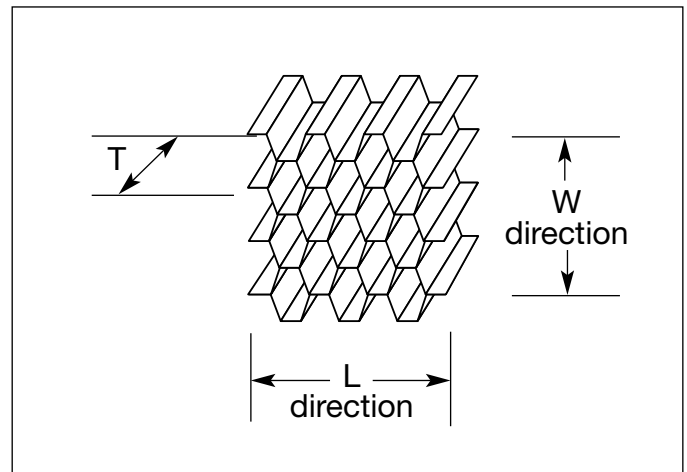
Hexagonal Core

The standard hexagonal honeycomb is the basic and most common cellular honeycomb configuration, and is currently available in all metallic and nonmetallic materials.



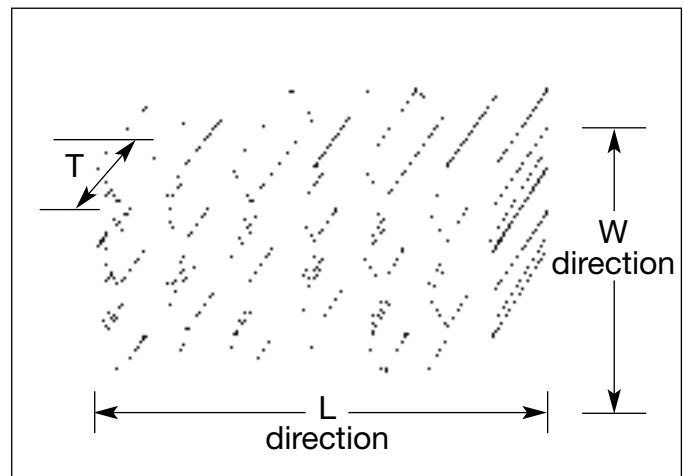
OX-Core™

The OX configuration is a hexagonal honeycomb that has been overexpanded in the W direction, providing a rectangular cell configuration that facilitates curving or forming in the L direction. The OX process increases W shear properties and decreases L shear properties when compared to hexagonal honeycomb.



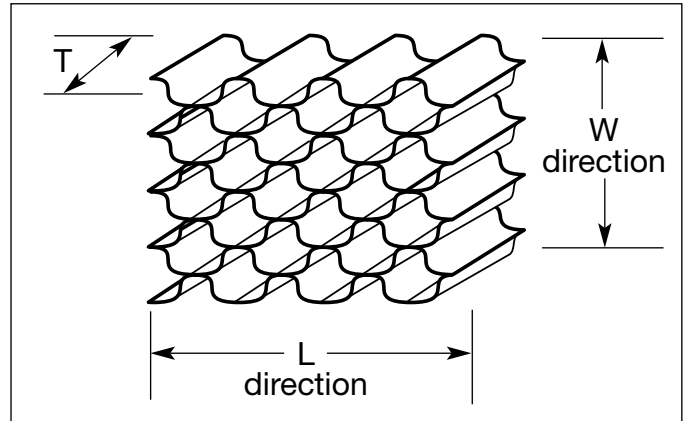
Reinforced Hexagonal Core

Reinforced honeycomb has a sheet of substrate material placed along the nodes in the ribbon direction to increase the mechanical properties.



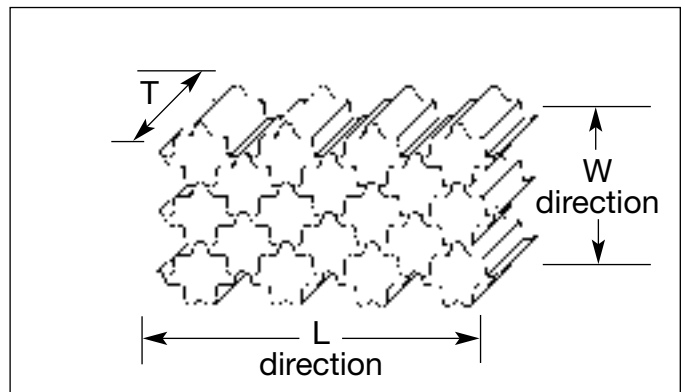
Flex-Core®

The Flex-Core cell configuration provides for exceptional formability in compound curvatures with reduced anticlastic curvature and without buckling the cell walls. Curvatures of very tight radii are easily formed. When formed into tight radii, Flex-Core provides higher shear strengths than comparable hexagonal core of equivalent density. Flex-Core is manufactured from aluminum, Nomex®, and fiberglass substrates.



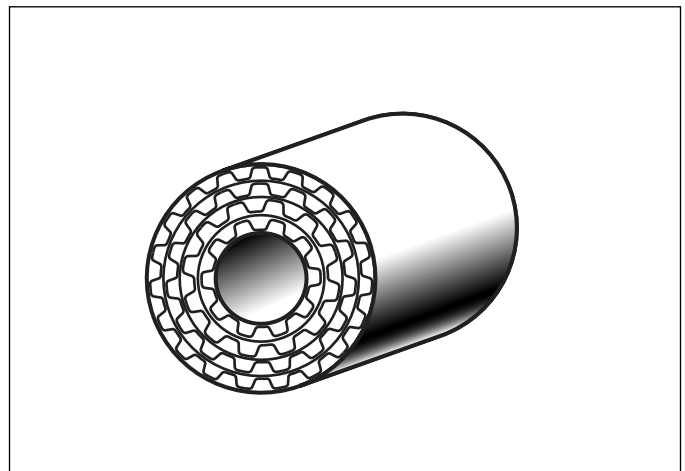
Double-Flex™

Double-Flex is a unique large cell Flex-Core for excellent formability and high specific compression properties. Double-Flex is the most formable cell configuration.



Tube-Core®

Tube-Core configuration provides a uniquely designed energy absorption system when the space envelope requires a column or small diameter cylinder. The design eliminates the loss of crush strength that occurs at the unsupported edges of conventional honeycomb. Tube-Core is constructed of alternate sheets of flat aluminum foil and corrugated aluminum foil wrapped around a mandrel and adhesively bonded. Outside diameters can range from 1/2 inch to 30 inches and lengths from 1/2 inch to 36 inches.



Other Configurations

Hexcel can design and fabricate special geometrics in response to specific needs.



Honeycomb Materials

Aluminum Honeycomb

Hexcel aluminum honeycombs are designated as follows:

Material – Cell Size – Alloy – Foil Thickness – Density

Example:

CR III - 1/4 - 5052 - .002N - 4.3

Where:

CR III® – signifies the honeycomb is treated with a corrosion-resistant coating

1/4 – is the cell size in fractions of an inch

5052 – is the aluminum alloy used

.002 – is the nominal reference foil thickness in inches

N – indicates the cell walls are nonperforated (P indicates perforated)

4.3 – is the density in pounds per cubic foot

Corrosion-Resistant Coatings

Corrosion-resistant coatings consist of a base layer underlying a primer layer. Aluminum honeycomb is available with two different corrosion-resistant coating options. These are CR III chromate-based and CR-PAA™ phosphoric acid anodized. The corrosion resistant coating is applied to the foil before the node adhesive is placed on the foil, thereby ensuring corrosion protection over the full foil surface.

CR III

CR III corrosion-resistant coating consists of a chromate-based protective layer and an organo-metallic polymer. CR III corrosion-resistant coating has been specified by the U.S. military for almost 30 years.

CR-PAA™

CR-PAA phosphoric acid anodized coating provides superior performance in certain instances. CR-PAA is superior with regards to:

- bond strength to aluminum facings in sandwich panel applications
- salt spray environments
- resistance to crack propagation
- hot/wet environments

Aluminum honeycomb is available in four different alloys, aerospace grades 5052 and 5056, and commercial grades 3104 and 3003.

5052 Alloy

Specification grade honeycomb in the 5052 H39 aluminum alloy is available for general purpose applications, in a very wide range of cell size/density combinations in the hexagonal and Flex-Core configurations. OX-Core and underexpanded cell configuration can also be provided.

5056 Alloy

Specification grade honeycomb in the 5056 H39 aluminum alloy offers superior strength over 5052 alloy honeycomb. It is also available in a broad range of cell size/density combinations in the hexagonal and Flex-Core configurations. The strength properties of 5056 alloy honeycomb are approximately 20% greater than the comparable properties of 5052 alloy honeycomb of similar cell size, foil gauge, and density.

ACG®

Aluminum Commercial Grade (ACG) honeycomb provides a low-cost aluminum honeycomb product for industrial applications. All ACG materials are provided with CR III coating. Hexcel produces ACG from 3000 series aluminum alloys. 3003 aluminum alloy is used for energy absorption applications where previous qualification studies specified this particular alloy. Hexcel also uses 3104 alloy for the manufacture of honeycomb with the flexibility to provide either 3104 or 3003 ACG, whichever is more appropriate for the application.

* Perforated honeycomb is used when the curing of the core-to-skin adhesive results in volatiles that must be vented, and in space applications where the atmosphere must be evacuated. The honeycomb may be slotted, if necessary.

Fiberglass Reinforced Honeycomb

Hexcel fiberglass reinforced honeycombs are designated as follows:

Material – Cell Size – Density

Example:

HRP – 3/16 – 4.0

Where:

HRP® – refers to the type of material

3/16 – is the cell size in fractions of an inch

4.0 – is the nominal density in pounds per cubic foot

HRP

HRP is a fiberglass fabric reinforced honeycomb dipped in a heat-resistant phenolic resin to achieve the final density. This product was developed for use at service temperatures up to 350°F. However, it is also well suited for short exposures at higher temperatures. The HRP-series honeycomb is available in the standard hexagonal configuration, as well as in the two formable configurations—OX-Core and Flex-Core.

HFT®

HFT is a fiberglass fabric reinforced honeycomb that incorporates a ±45° Fibertruss® bias weave dipped in a heat-resistant phenolic resin to achieve the final density. This material is recommended for use at service temperatures up to 350°F but is well suited for short exposures at higher temperatures. The Fibertruss configuration greatly enhances the shear properties. HFT has a much higher shear modulus than HRP or HRH®-10.

HRH®-327

HRH-327 is a fiberglass fabric, polyimide node adhesive, bias weave reinforced honeycomb dipped in a polyimide resin to achieve the final density. This material has been developed for extended service temperatures up to 500°F with short range capabilities up to 700°F.

HDC-F

HDC-F is a heavy density core fiberglass honeycomb that offers enhanced compressive properties.

Aramid Fiber Reinforced Honeycomb

Hexcel aramid-fiber reinforced honeycomb is designated as follows:

Material – Cell Size – Density

Example:

HRH-10 – 3/16 – 3.0

Where:

HRH-10 – refers to the type of material

3/16 – is the cell size in fractions of an inch

3.0 – is the nominal density in pounds per cubic foot

Hexcel manufactures aramid-fiber reinforced honeycomb from three types of para-aramid substrates.

These para-aramid substrates are Nomex® (HRH-10, HRH-78, HRH-310), Kevlar® (HRH-49), and KOREX®.

HRH®-10

This product consists of Dupont's Nomex aramid-fiber paper dipped in a heat-resistant phenolic resin to achieve the final density. It features high strength and toughness in a small cell size, low density nonmetallic core. It is available in hexagonal, OX-Core, and Flex-Core configurations. It is fire-resistant and recommended for service up to 350°F.

HRH®-310

HRH-310 is made from the same aramid-fiber paper described above, except dipped in a polyimide resin to achieve the final density. It is produced in both hexagonal and overexpanded cell configurations. Outstanding features are its relatively low dielectric and loss tangent properties.

HRH®-78

HRH-78 is DuPont's non-aerospace specification grade Nomex aramid-fiber paper dipped in a heat-resistant phenolic resin to achieve the final density. HRH-78 is used in marine, rail, and other non-aerospace applications.

HRH®-49

HRH-49 is made from Kevlar 49 fabric impregnated with an epoxy resin. Significant advantages of HRH-49 honeycomb are its excellent thermal stability and relatively low coefficient of thermal expansion.



KOREX®

KOREX honeycomb is made from KOREX aramid paper dipped in a heat-resistant phenolic resin to achieve the final density. KOREX honeycomb offers improved strength-to-weight ratios and/or lower moisture absorption than Nomex honeycomb of a similar configuration.

Special Honeycomb

HFT®-G

HFT-G is a bias weave carbon fabric reinforced honeycomb dipped in either a heat-resistant phenolic resin or a polyimide resin to achieve the final density. This product was developed for use at service temperatures up to 500°F. However, it is well suited for short exposures at higher temperatures. HFT-G has a very low coefficient of thermal expansion and a high shear modulus value.

TPU®

TPU is thermoplastic polyurethane honeycomb. TPU honeycomb has unique properties of energy redirection, fatigue resistance, and flexibility.

Micro-Cell™

Micro-Cell is 1/16 inch cell size. Micro-Cell is available in 5052 and 5056 aluminum alloys and HRH-10 Nomex aramid honeycomb. Micro-Cell was developed for air directionalizing systems and for use in structural panels where minimized dimpling and distortion of the facings are required.

Acousti-Core®

Acousti-Core consists of honeycomb filled with sound absorbing fiberglass batting. Any honeycomb material may be used, with HRH-10 and aluminum the most common. The cell size must be 3/16 inch or greater. See page 29 for the noise reduction coefficient of honeycomb filled with fiberglass batting. In addition to Acousti-Core's sound absorption characteristics, two side benefits also result from the addition of the batting to the honeycomb core. The smoke generated in the N.B.S. smoke chamber is greatly reduced with the aramid Acousti-Core materials, and the thermal conductivity is reduced due to the batting.

Specifying Honeycomb

When honeycomb is specified, the following information needs to be provided:

- Material
- Cell configuration (hexagonal, OX-Core, Flex-Core, etc.)
- Cell size
- Alloy and foil gauge (aluminum honeycomb only)
- Density

Cell sizes range from 1/16" to 1", with 1/8", 3/16", 1/4", and 3/8" being the most common. Honeycomb densities range from 1.0 lb/ft³ to 55 lb/ft³.

Guide to Determining Which Type of Honeycomb to Specify

Determining which type of honeycomb to specify requires that the relevant possible attributes be defined for the application. The attributes that help determine the most appropriate honeycomb type can include the following:

- Cost vs. value/performance
- Piece size
- Density
- Strength
 - Compressive
 - Impact
 - Shear
 - Fatigue
 - Flatwise tensile
- Cell wall thickness
- Moisture
- Color
- Ultraviolet light exposure
- Environmental chemicals
- Processing and operating temperature range
- Flammability/fire retardance
- Thermal conductivity/insulation/heat transfer
- Electrical conductivity
- Wall surface smoothness
- Abrasion resistance
- Cushioning
- Machinability/Formability
- Facings
 - Material
 - Bonding process, adhesive, conditions
 - Thickness

Most Important Attributes of Each Honeycomb Material

Each of the honeycomb materials profiled above has specific benefits that are key to its specification. In general terms, some of the most beneficial properties of each honeycomb material are as follows:

Aluminum Honeycomb

- relatively low cost
- best for energy absorption
- greatest strength/weight
- thinnest cell walls
- smooth cell walls
- conductive heat transfer
- electrical shielding
- machinability

Aramid Fiber Honeycomb

- flammability/fire retardance
- large selection of cell sizes, densities, and strengths
- formability and parts-making experience
- insulative
- low dielectric properties

Fiberglass

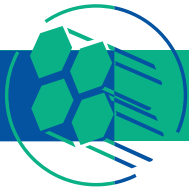
- multidimensional strength of a woven structure
- heat formability
- insulative
- low dielectric properties

Carbon

- dimensional stability and retention
- strength retention and performance at high temperatures
- very low coefficient of thermal expansion
- tailorable thermal conductivity
- relatively high shear modulus

Polyurethane

- cushioning
- unaffected by moisture
- energy redirection
- fatigue-resistant
- color choices



Mechanical Properties and Test Methods

The test methods used for the honeycomb properties listed in this brochure are based on MIL-STD-401 and the applicable ASTM Standards. The properties and the test methods employed are outlined below. Unless specifically stated, the test properties listed have been performed at room temperature.

Density and Thickness Measurements

The density of honeycomb is expressed in pounds per cubic foot. Hexcel certifies that aerospace grade core will not vary in density by more than $\pm 10\%$ from list nominal values. The density tolerance for commercial grade aluminum core is $\pm 17\%$. The density of production honeycomb is normally measured on full-size expanded sheets.

Physical dimensions and weight measurements are taken to within 0.5%. The thickness is measured to the nearest 0.001 inch in accordance with ASTM C366, Method B.

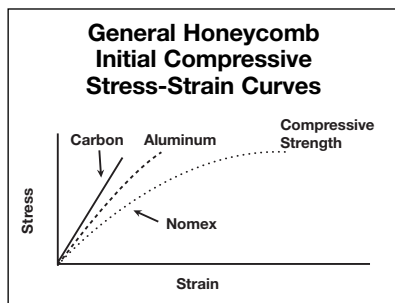
Compressive Properties

The stabilized compressive strength (also called flat-wise compressive strength) represents the ultimate compressive strength of the honeycomb in pounds per square inch when loaded in the T direction. Normally for this test, facings are adhesively bonded to the honeycomb material (stabilized compressive).

The stabilized compressive modulus, also expressed in pounds per square inch, is determined from the slope of the initial straight-line

portion of the stress-strain curve. Some honeycomb materials exhibit a linear initial stress-strain relationship, while other honeycomb materials exhibit a nonlinear curved initial stress-strain relationship.

The bare compressive strength is the ultimate compressive strength of the core in pounds per square inch when loaded in the T direction without stabilization of the cell edges. The value is normally used for an acceptance criteria since this test is easier and faster to perform.



Test Methods

The standard specimen size for bare and stabilized compressive tests is 3" L x 3" W x 0.625" T for aluminum honeycomb and 3" L x 3" W x 0.500" T for nonmetallic cores. For cell sizes 1/2 inch or larger, a 4" x 4" or even a 6" x 6" specimen size is used to reduce the error developed by edge effect on small samples. Stabilized compressive specimens are normally prepared by bonding .032" AL 5052 thick facings to each side.

Both bare and stabilized compressive tests are conducted with self-aligning loading heads. Unless otherwise specified, the loading rate used is 0.020 inches per minute. Deflection recordings are made with a displacement transducer that measures the relative movement of the loading and bearing surfaces through the center of the specimen.

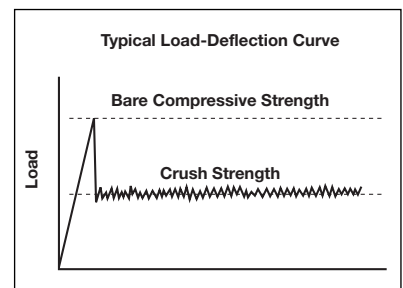
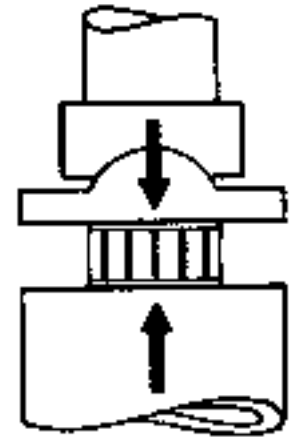
Crush Strength

After honeycomb has exceeded its ultimate compressive strength, it will continue to deform plastically and crush uniformly. The load-deflection curve shows such a typical response.

The average crush load per unit cross-sectional area is defined as the crush strength, expressed in pounds per square inch. Honeycomb will crush at virtually a constant stress level

(dependent on the core material and density), hence its absorption capacity is predictable, making it ideal for energy absorption applications. When used in this manner, the core is often precrushed slightly to remove the compressive peak in the load-deflection curve. The crush strength of honeycomb decreases with increasing angle loading from the thickness.

Compressive Test



Test Methods

Fixed loading and bearing plates are used for crush strength tests and a deflectometer is employed to measure the travel of the crosshead of the test machine. In order to obtain a meaningful crush load-deflection curve, a minimum core thickness of 0.625 inches should be used.

It should be noted that the crush strength values presented in this brochure are typical static test results. It has been found that under dynamic loading, these values increase nonlinearly with impact velocity, and numbers as much as 30% higher have been reported.

L and W Shear Properties

The shear strength of honeycomb as presented in this brochure refers to the ultimate stress in pounds per square inch when a shear load is applied parallel to the L-W plane. The shear modulus is the slope of the initial straight-line portion of the stress-strain curve. The values so obtained are dependent upon the orientation of the applied loading with respect to the L and W dimensions, being highest in the L direction and lowest in the W direction for hexagonal honeycomb.

Test Methods

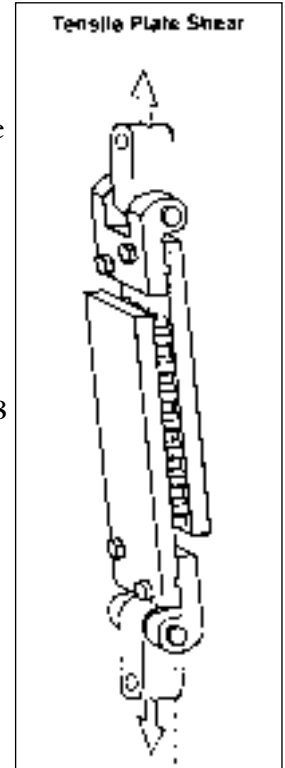
Plate Shear Test Method

The shear strength and modulus values presented in this brochure were obtained using the compressive and/or tensile plate shear method. The specimen size for aluminum honeycomb is normally 7.5" x 2" x 0.625" T. Nonmetallic honeycombs test sample size is 6" x 2" x 0.500" T.

Thicknesses conform to MIL-C-7438 and MIL-C-8073, respectively. The specimens are bonded to 1/2-inch thick steel loading plates and then tested as shown.

The loading rate is normally 0.020 inches per minute. Shear deflections are measured with a displacement transducer that senses the relative movement of the two plates. Since some non-metallic materials will not always have a truly linear stress-strain curve (particularly at elevated temperatures), the shear modulus is normally calculated from the slope of the initial straight-line portion of the load-deflection curve.

Honeycomb with densities of 8.0 pcf and higher are sometimes difficult to fail in shear by the plate shear method because of the high shear loads introduced to the adhesive bond between the core and the steel plates. In some cases, shear data from beam-flexure testing will be more applicable. This is true for thicker and also heavier density cores.



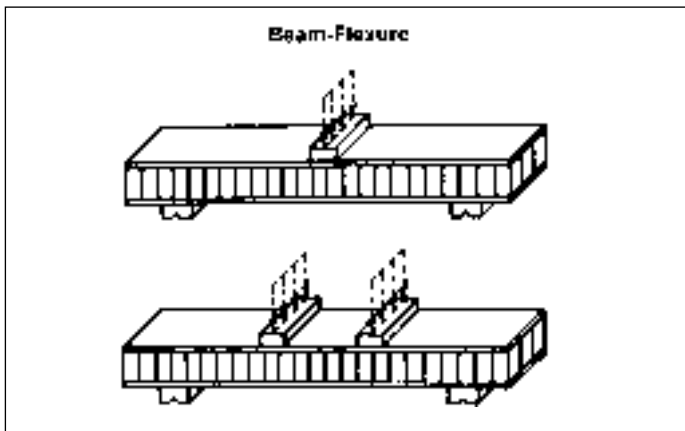


Beam-Flexure Test Method

Although the plate shear method is preferred for obtaining actual honeycomb shear strength and modulus results, the beam-flexure test is often used to evaluate overall sandwich panel performance. Experience indicates that since these values are very much dependent on the facing thickness, facing material, and loading conditions, the calculated honeycomb properties may vary considerably from one test series to the next. Many types of beam-flexure tests have been used. The two most common techniques are shown schematically below.

The specimen size is 8" x 3". The span between supports is 6" and either one or two point loading can be used. The distance between the load pads for two point loading is normally 1/3 the span. For additional details refer to MIL-C-7438 and ASTM C393.

Again, it should be stressed that the resulting beam-flexure data should only be considered a test of the facings, adhesives, and core acting as a composite sandwich structure. Core shear values obtained by flexure tests are often higher than those obtained from plate shear tests (see page 14 for correlation factors between plate shear and beam-flexure data).



Flatwise Tensile

Flatwise tensile is used to measure bond strength of adhesives and/or the tensile strength of the honeycomb core. Most structural adhesives will be stronger than aluminum core up to about 6 pcf. This test is most useful in determining skin preparation, bonding conditions, and prepreg adhesions. See MIL-STD-401 and ASTM C297.

Additional Mechanical Properties

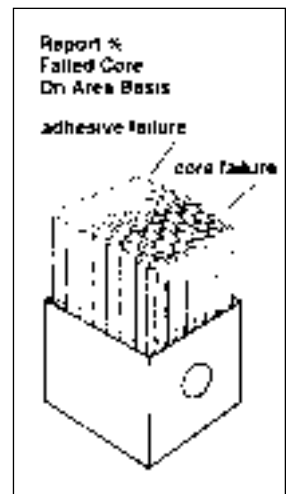
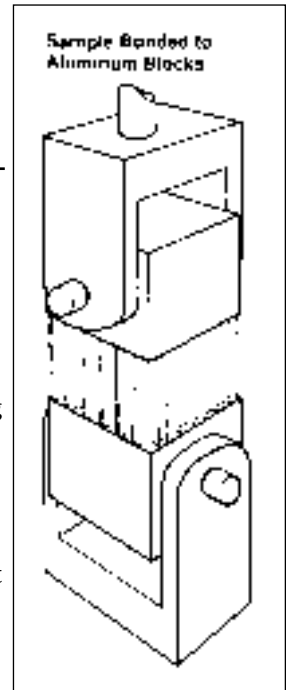
Numerous tests on both core materials and bonded sandwich panels have been run by Hexcel laboratory personnel for qualification to military specifications, or for internal R&D purposes.

Classification of Mechanical Properties

Hexcel classifies its mechanical properties data into three categories dependent upon the extent of the testing being reported. These classifications are as follows:

- 1. Preliminary** – Data resulting from a very limited amount of testing are indicative of the properties expected, but do not necessarily represent the mean values of a normal scatter of test data. Generally, preliminary values are obtained from testing one or two blocks of a honeycomb type. Numbers followed by the letter P indicate preliminary data.
- 2. Typical** – Data representing extensive testing of many blocks of a particular honeycomb material. A typical value is the mean average of a relatively large number of test values.
- 3. Minimum** – Hexcel guarantees the minimum individual properties listed on standard honeycomb types.

Predicted values based upon Hexcel's educated best guess are provided in the mechanical property tables for core types when data do not exist.



Correlation of Shear Strength Data

Effect of Core Thickness on Plate Shear Strength

Honeycomb shear strength will vary with core thickness.

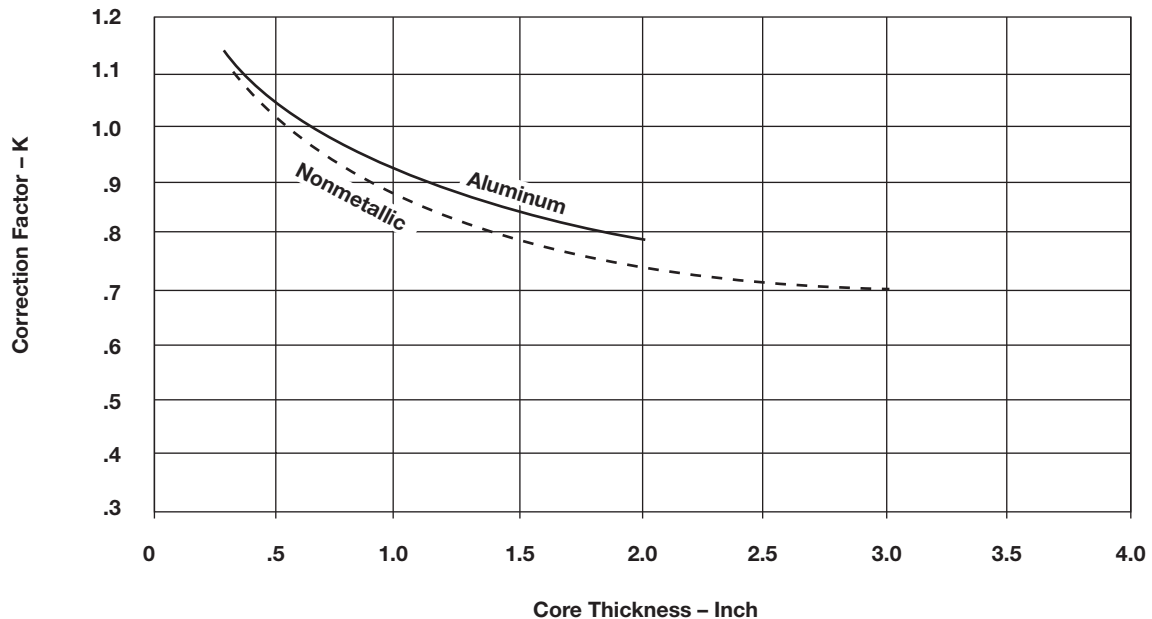
Referring to the tensile plate shear shown on page 11, it can be shown that the shear load induces a minor component parallel to the cell axis that stretches the honeycomb. The honeycomb, therefore, is not being subjected to pure shear but to a combination of shear and tension. Thicker cores will have a lower usable shear strength than thinner ones.

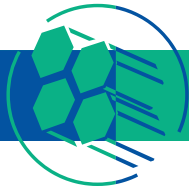
In view of the above, one might conclude that a plot of usable shear strength vs. core thickness would show the “true” core shear strength approached asymptotically with vanishing core thickness. However, for very thin cores the filleting of the core-to-skin adhesives has a strengthening effect on the shear data. Normally, the filleting depth is but a fraction of the core thickness,

but for very thin cores this depth is a substantial fraction of the thickness and possibly the entire cell wall may be filleted. Such a phenomenon would affect the “apparent” core shear strength considerably. Also, since the filleting depth depends on the adhesive used, test results on thin cores vary from one adhesive to another.

For the above reasons and in view of typical core thickness values in actual usage, as well as several aircraft company and military specifications, aluminum honeycomb is generally tested at 0.625" T while nonmetallic honeycomb is tested at 0.500" T. However, Hexcel is often asked to qualify core materials to other thickness values. The graph below, generated from actual Hexcel data, gives correction factors for both aluminum and nonmetallic honeycomb for values other than 0.625" T and 0.500" T, respectively. The graph shows average correction factors.

Correction Factors





Correlation of Flexural Shear Strength Data

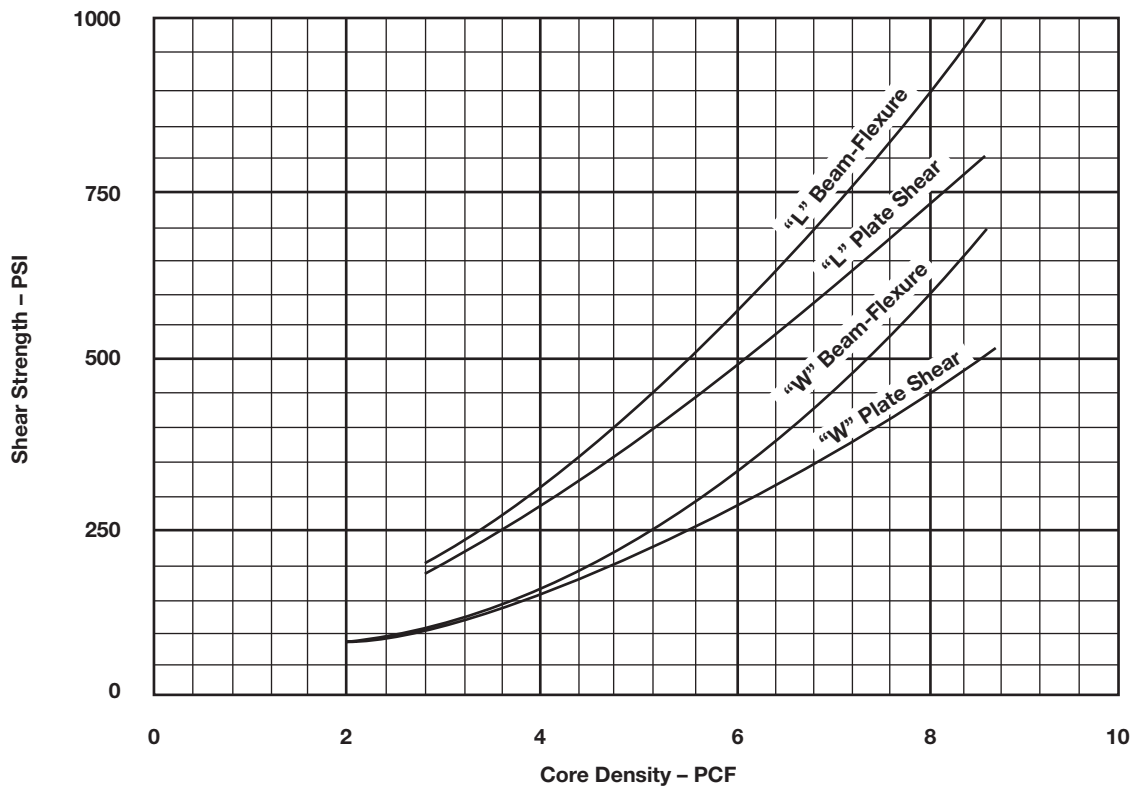
As previously indicated, the plate shear test method is regarded as the most desirable way of obtaining actual honeycomb shear properties. The results from the beam-flexure method have been found to be influenced by several parameters, such as facing thickness, facing material, core thickness, and loading conditions. The facing thickness alone will cause large variations because the skins are able to carry shear loads in addition to what the core carries and, furthermore, are able

to take on additional shear loads after the core has yielded. Several specifications, such as MIL-C-7438, still call for beam-flexure tests for heavy density cores. We have therefore provided the graph below, which shows the results of beam-flexures on 5052 aluminum honeycomb when tested per the military specifications, and compares the L and W curves to the plate shear data for the same core type. It should be noted that the military specification calls for facing thicknesses that are different for L and W tests at a given density.

5052 Shear Strength Comparison

Plate Shear vs. Beam-Flexures
Typical Values

Beam-Flexures per MIL-C-7438E with facing thickness as specified



Mechanical Property Tables

The most commonly measured honeycomb properties are bare compressive strength, stabilized compressive strength and modulus, crush strength, and L direction and W direction plate shear strength and moduli.

The following tables contain the mechanical properties of the various honeycomb core types for which Hexcel has data. It should be noted that some of the core types listed are not always readily available.

Hexcel has produced additional core types not listed, and in some cases larger or smaller cell sizes, intermediate or higher densities, and special materials can be provided.

For detailed information on standard or special sheet sizes, refer to the appropriate data sheets.

Crush strength values presented in this brochure are to be used for preliminary designs. For core densities below 3 pcf, these values vary as much as $\pm 20\%$. For all other densities, crush strength values vary by $\pm 15\%$.

The honeycomb properties that follow are for the compressive strength and modulus in the T direction, and the shear strength and moduli in the LT and WT directions. The honeycomb properties in other secondary directions are extremely low compared to the properties provided for the primary designed orientation of honeycomb. The L and W direction compressive properties are typically less than 5% of the compressive properties in the T direction. The plate shear strength is substantially less in the LW plane than in either the LT or WT plane, while the plate shear modulus in the LW plane is typically less than 5% of the plate shear modulus in either the LT plane or WT plane.

In addition to compressive strength and plate shear properties, sometimes other honeycomb properties are important for particular applications. These include fatigue for repeated loads, creep from constant stress over a long period of time (especially at elevated temperatures or when combined with other materials), and flatwise tensile strength.

Note: See page 12 for definitions of “preliminary,” “typical,” and “minimum.”



HexWeb Honeycomb Attributes and Properties

5052 Alloy Hexagonal Aluminum Honeycomb – Specification Grade

Both CR-PAA and CR III corrosion-resistant coating

| Hexcel Honeycomb Designation Cell Size – Alloy – Foil Gauge | Nominal Density pcf | Compressive | | | | | Crush Strength psi | Plate Shear | | | | | |
|--|------------------------|-----------------|-------|-----------------|-------|----------------|-----------------------|-----------------|-------|----------------|-----------------|-------|----------------|
| | | Bare | | Stabilized | | | | L Direction | | | W Direction | | |
| | | Strength psi | | Strength psi | | Modulus ksi | | Strength psi | | Modulus ksi | Strength psi | | Modulus ksi |
| | | typ | min | typ | min | typ | typ | typ | min | typ | typ | min | typ |
| 1/16 – 5052 – .0007 | 6.5 | 950 | 740 | 1000 | 780 | 275 | 505x | 560 | 440 | 90.0 | 350 | 270 | 40.0 |
| 1/16 – 5052 – .001 | 9.2 | 1500 | 1170 | 1550 | 1200 | 420 | 750x | 850 | 660 | 150.0 | 520 | 400 | 53.0 |
| 1/16 – 5052 – .0015 | 12.4 | 2430 | 1900 | 2650 | 2000 | 650 | 1200x | 1150 | 900 | 210.0 | 715 | 560 | 65.0 |
| 1/8 – 5052 – .0007 | 3.1 | 285 | 200 | 300 | 215 | 75 | 130 | 210 | 155 | 45.0 | 130 | 90 | 22.0 |
| 1/8 – 5052 – .001 | 4.5 | 550 | 375 | 570 | 405 | 150 | 260 | 340 | 285 | 70.0 | 220 | 168 | 31.0 |
| 1/8 – 5052 – .0015 | 6.1 | 980 | 650 | 1020 | 680 | 240 | 450 | 560 | 455 | 98.0 | 340 | 272 | 41.0 |
| 1/8 – 5052 – .002 | 8.1 | 1500 | 1000 | 1560 | 1100 | 350 | 750 | 800 | 670 | 135.0 | 470 | 400 | 54.0 |
| 1/8 – 5052 – .0025 | 10.0 | 2100p | 1575p | 2250p | 1685p | 500x | 1050x | 980p | 735p | 175.0p | 550p | 415p | 65.0p |
| 1/8 – 5052 – .003 | 12.0 | 2700 | 2100 | 2900 | 2200 | 900 | 1350x | 1940I | 1250I | 210.0x | 1430I | 1000I | 78.0x |
| 5/32 – 5052 – .0007 | 2.6 | 220 | 150 | 240 | 160 | 55 | 90 | 165 | 120 | 37.0 | 100 | 70 | 19.0 |
| 5/32 – 5052 – .001 | 3.8 | 395 | 285 | 410 | 300 | 110 | 185 | 270 | 215 | 56.0 | 165 | 125 | 26.4 |
| 5/32 – 5052 – .0015 | 5.3 | 690 | 490 | 720 | 535 | 195 | 340 | 420 | 370 | 84.0 | 270 | 215 | 36.0 |
| 5/32 – 5052 – .002 | 6.9 | 1080 | 770 | 1130 | 800 | 285 | 575 | 590 | 540 | 114.0 | 375 | 328 | 46.4 |
| 5/32 – 5052 – .0025 | 8.4 | 1530 | 1070 | 1600 | 1180 | 370 | 800 | 760 | 690 | 140.0 | 475 | 420 | 56.0 |
| 3/16 – 5052 – .0007 | 2.0 | 160 | 90 | 175 | 100 | 34 | 60 | 120 | 80 | 27.0 | 70 | 46 | 14.3 |
| 3/16 – 5052 – .001 | 3.1 | 290 | 200 | 335 | 215 | 75 | 130 | 210 | 155 | 45.0 | 125 | 90 | 22.0 |
| 3/16 – 5052 – .0015 | 4.4 | 520 | 360 | 550 | 385 | 145 | 250 | 330 | 280 | 68.0 | 215 | 160 | 30.0 |
| 3/16 – 5052 – .002 | 5.7 | 820 | 560 | 860 | 600 | 220 | 390 | 460 | 410 | 90.0 | 300 | 244 | 38.5 |
| 3/16 – 5052 – .0025 | 6.9 | 1120 | 770 | 1175 | 800 | 285 | 575 | 590 | 540 | 114.0 | 375 | 328 | 46.4 |
| 3/16 – 5052 – .003 | 8.1 | 1600 | 1000 | 1720 | 1100 | 350 | 750 | 725 | 670 | 135.0 | 480 | 400 | 54.0 |
| 1/4 – 5052 – .0007 | 1.6 | 90 | 60 | 100 | 70 | 20 | 40 | 85 | 60 | 21.0 | 50 | 32 | 11.0 |
| 1/4 – 5052 – .001 | 2.3 | 190 | 120 | 210 | 130 | 45 | 75 | 140 | 100 | 32.0 | 85 | 57 | 16.2 |
| 1/4 – 5052 – .0015 | 3.4 | 340 | 240 | 370 | 250 | 90 | 150 | 230 | 180 | 50.0 | 140 | 105 | 24.0 |
| 1/4 – 5052 – .002 | 4.3 | 500 | 350 | 540 | 370 | 140 | 230 | 320 | 265 | 66.0 | 200 | 155 | 29.8 |
| 1/4 – 5052 – .0025 | 5.2 | 690 | 500 | 760 | 510 | 190 | 335 | 410 | 360 | 82.0 | 265 | 200 | 35.4 |
| 1/4 – 5052 – .003 | 6.0 | 990 | 630 | 1100 | 660 | 235 | 430 | 530 | 445 | 96.0 | 340 | 265 | 40.5 |
| 1/4 – 5052 – .004 | 7.9 | 1420 | 970 | 1490 | 1050 | 340 | 725 | 700 | 650 | 130.0 | 440 | 390 | 52.8 |
| 3/8 – 5052 – .0007 | 1.0 | 50 | 20 | 55 | 20 | 10 | 25 | 45 | 32 | 12.0 | 30 | 20 | 7.0 |
| 3/8 – 5052 – .001 | 1.6 | 90 | 60 | 95 | 70 | 20 | 40 | 85 | 60 | 21.0 | 50 | 32 | 11.0 |
| 3/8 – 5052 – .0015 | 2.3 | 190 | 120 | 200 | 130 | 45 | 75 | 135 | 100 | 32.0 | 80 | 57 | 16.2 |
| 3/8 – 5052 – .002 | 3.0 | 285 | 190 | 310 | 200 | 70 | 120 | 200 | 145 | 43.0 | 125 | 85 | 21.2 |
| 3/8 – 5052 – .0025 | 3.7 | 370 | 270 | 410 | 285 | 105 | 180 | 250 | 200 | 55.0 | 160 | 115 | 26.0 |
| 3/8 – 5052 – .003 | 4.2 | 520 | 335 | 560 | 355 | 135 | 220 | 310 | 255 | 65.0 | 200 | 150 | 29.0 |
| 3/8 – 5052 – .004 | 5.4 | 740 | 500 | 800 | 535 | 200 | 360 | 430 | 380 | 86.0 | 280 | 228 | 36.8 |
| 3/8 – 5052 – .005 | 6.5 | 950 | 700 | 1000 | 750 | 265 | 505 | 545 | 500 | 105.0 | 350 | 300 | 43.5 |

Notes:

Test data obtained at 0.625" thickness.

I = Beam shear for 1/8 12.0 pcf product.

p = Preliminary (see page 12).

x = Predicted value.

5056 Alloy Hexagonal Aluminum Honeycomb – Specification Grade

Both CR-PAA and CR III corrosion-resistant coating

| Hexcel Honeycomb Designation Cell Size – Alloy – Foil Gauge | Nominal Density pcf | Compressive | | | | Crush Strength psi | Plate Shear | | | | | | |
|--|------------------------|-----------------|-----------------|----------------|----------------|-----------------------|-----------------|----------------|-----------------|----------------|-----------------|----------------|--------------|
| | | Bare | | Stabilized | | | L Direction | | | W Direction | | | |
| | | Strength psi | Strength psi | Modulus ksi | Modulus ksi | | Strength psi | Modulus ksi | Strength psi | Modulus ksi | Strength psi | Modulus ksi | |
| 1/16 – 5056 – .001 | 9.2 | typ 1700p | min 1300p | typ 1800p | min 1400p | typ 500p | typ 850x | typ 980p | min 760p | typ 155.0p | typ 600p | min 460p | typ 50.0p |
| 1/8 – 5056 – .0007 | 3.1 | 320 | 250 | 350 | 260 | 97 | 170 | 250 | 200 | 45.0 | 155 | 110 | 20.0 |
| 1/8 – 5056 – .001 | 4.5 | 630 | 475 | 690 | 500 | 185 | 320 | 440 | 350 | 70.0 | 255 | 205 | 28.0 |
| 1/8 – 5056 – .0015 | 6.1 | 1120 | 760 | 1200 | 825 | 295 | 535 | 690 | 525 | 102.0 | 400 | 305 | 38.0 |
| 1/8 – 5056 – .002 | 8.1 | 1750 | 1200 | 1900 | 1300 | 435 | 810 | 945 | 740 | 143.0 | 560 | 440 | 51.0 |
| 5/32 – 5056 – .0007 | 2.6 | 250 | 180 | 265 | 185 | 70 | 120 | 200 | 152 | 37.0 | 115 | 80 | 17.0 |
| 5/32 – 5056 – .001 | 3.8 | 450 | 360 | 500 | 375 | 140 | 235 | 335 | 272 | 57.0 | 195 | 155 | 24.0 |
| 5/32 – 5056 – .0015 | 5.3 | 820 | 615 | 865 | 650 | 240 | 420 | 550 | 435 | 85.0 | 325 | 250 | 33.0 |
| 5/32 – 5056 – .002 | 6.9 | 1220 | 920 | 1340 | 1000 | 350 | 650 | 760 | 610 | 118.0 | 430 | 360 | 43.0 |
| 3/16 – 5056 – .0007 | 2.0 | 190 | 110 | 200 | 120 | 45 | 75 | 140 | 105 | 27.0 | 85 | 50 | 13.0 |
| 3/16 – 5056 – .001 | 3.1 | 380 | 250 | 410 | 260 | 97 | 170 | 265 | 200 | 45.0 | 150 | 110 | 20.0 |
| 3/16 – 5056 – .0015 | 4.4 | 620 | 460 | 670 | 490 | 180 | 310 | 425 | 340 | 68.0 | 245 | 198 | 27.0 |
| 3/16 – 5056 – .002 | 5.7 | 920 | 685 | 1000 | 735 | 270 | 480 | 565 | 480 | 94.0 | 330 | 280 | 36.0 |
| 1/4 – 5056 – .0007 | 1.6 | 100 | 75 | 110 | 80 | 30 | 50 | 90 | 78 | 20.0 | 60 | 38 | 10.5 |
| 1/4 – 5056 – .001 | 2.3 | 240 | 145 | 265 | 155 | 58 | 100 | 180 | 130 | 32.0 | 100 | 62 | 15.0 |
| 1/4 – 5056 – .0015 | 3.4 | 400 | 300 | 480 | 315 | 115 | 200 | 290 | 230 | 50.0 | 175 | 130 | 22.0 |
| 1/4 – 5056 – .002 | 4.3 | 580 | 440 | 620 | 465 | 172 | 300 | 400 | 325 | 67.0 | 230 | 190 | 27.0 |
| 1/4 – 5056 – .0025 | 5.2 | 790 | 600 | 820 | 645 | 230 | 410 | 490 | 425 | 84.0 | 300 | 245 | 32.0 |
| 3/8 – 5056 – .0007 | 1.0 | 55 | 25 | 60 | 35 | 15 | 35 | 55 | 45 | 15.0 | 35 | 25 | 6.8 |
| 3/8 – 5056 – .001 | 1.6 | 100 | 75 | 110 | 80 | 30 | 50 | 90 | 78 | 20.0 | 60 | 38 | 10.5 |
| 3/8 – 5056 – .0015 | 2.3 | 215 | 155 | 225 | 155 | 58 | 100 | 170 | 130 | 32.0 | 95 | 62 | 15.0 |
| 3/8 – 5056 – .002 | 3.0 | 320 | 240 | 340 | 260 | 92 | 160 | 245 | 190 | 43.0 | 145 | 100 | 19.0 |

Notes:

p = Preliminary (see page 12).

x = Predicted value.

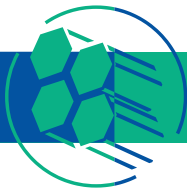
Aluminum Commercial Grade (ACG) for 3000 Series Alloy

| Hexcel Honeycomb Designation Material – Cell Size | Nominal Density pcf | Compressive | | | Crush Strength psi | Plate Shear | | | |
|--|------------------------|-----------------|-----------------|----------------|-----------------------|-----------------|----------------|-----------------|----------------|
| | | Bare | Stabilized | | | L Direction | | W Direction | |
| | | Strength psi | Strength psi | Modulus ksi | | Strength psi | Modulus ksi | Strength psi | Modulus ksi |
| ACG – 1/4 | 4.8 | typ 630 | typ 660 | typ 148 | typ 245 | typ 365 | typ 70 | typ 215 | typ 38 |
| ACG – 3/8 | 3.3 | 340 | 370 | 92 | 120 | 230 | 45 | 130 | 22 |
| ACG – 1/2 | 2.3 | 190 | 205 | 40 | 60 | 140 | 28 | 80 | 14 |
| ACG – 3/4 | 1.8 | 120 | 130 | 24 | 45 | 100 | 20 | 65 | 11 |
| ACG – 1 | 1.3 | 80 | 85 | 16p | 25 | 65 | 14 | 45 | 7 |

Notes:

Test data obtained at 0.625" thickness.

p = Preliminary (see page 12).



HexWeb Honeycomb Attributes and Properties

5052 Alloy RigidCell™ Aluminum Corrugated Honeycomb

Both CR-PAA and CR III corrosion-resistant coating

| Hexcel Honeycomb Designation Cell Size – Alloy Foil Gauge – Configuration | Nominal Density pcf | Crush Strength psi | Compressive Strength | | | Beam Shear Strength | | | |
|---|------------------------|-----------------------|----------------------|-------------------|----------------|-----------------------|----------------|-----------------------|----------------|
| | | | Bare psi | Stabilized psi | Modulus ksi | L Direction psi | Modulus ksi | W Direction psi | Modulus ksi |
| 1/8 – 2 – .003-STD | 12.0 | typ 1600 | typ 2300 | typ 2400 | 560x | typ 1950 | 210x | typ 1500 | 75x |
| 1/8 – 2 – .0038-STD | 14.5 | 2150 | 2900 | 3050 | 650x | 2200 | 260x | 1600 | 80x |
| 1/8 – 2 – .006-STD | 22.1 | 4000 | 5100 | 5200 | 970x | 3000 | 440x | 2050 | 100x |
| 1/8 – 2 – .006-R2 | 38.0 | 6500 | 8500 | 8700 | 1650x | 4300p | 950x | 2200p | 140x |
| 1/8 – 2 – .006-2R2 | 55.0 | – | 12500x | 13000p | 2400x | 4900p | 1370x | 2610p | 180x |
| 3/16 – 2 – .006-STD | 15.7 | 2400 | 3200 | 3300 | 700x | 2400x | 280x | 1500x | 85x |
| 3/16 – 2 – .006-R2S | 25.0 | 4400p | 5700 | 5800p | 1100x | 3350p | 670x | 1700p | 105x |
| 1/4 – 2 – .006-STD | 10.5 | 1350 | 2100 | 2200 | 980x | 1300x | 180x | 800x | 70x |

Notes:

Test data obtained at 0.625" thickness.

p = Preliminary (see page 12).

R2 = Reinforced (inter leaf) every ribbon, non-staggered.

2R2 = Corrugation double lap, reinforced

x = Predicted value.

R2S = Reinforced (inter leaf) every ribbon, staggered.

(inter leaf) every ribbon, non-staggered

Aluminum Flex-Core

Both CR-PAA and CR III corrosion-resistant coating

5052 Alloy Aluminum Flex-Core – Specification Grade

| Hexcel Honeycomb Designation Alloy/Cell Count – Foil Gauge | Nominal Density pcf | Compressive | | | | | Crush Strength psi | Plate Shear | | | | | |
|---|------------------------|-----------------|------|-----------------|------|----------------|-----------------------|-----------------|-----|----------------|-----------------|-----|----------------|
| | | Bare | | Stabilized | | | | L Direction | | | W Direction | | |
| | | Strength psi | | Strength psi | | Modulus ksi | | Strength psi | | Modulus ksi | Strength psi | | Modulus ksi |
| 5052/F40 – .0013 | 2.1 | typ | min | typ | min | typ | typ | min | typ | min | typ | min | typ |
| 5052/F40 – .0016 | 2.5 | 200 | 126 | 225 | 157 | 65 | 80 | 90 | 63 | 18.0 | 50 | 37 | 10.0 |
| 5052/F40 – .0019 | 3.1 | 260 | 200 | 285 | 215 | 90x | 120x | 120x | 95x | 24.0x | 70x | 55x | 11.0x |
| 5052/F40 – .0025 | 4.1 | 350 | 238 | 380 | 280 | 125 | 165 | 165 | 126 | 32.0 | 95 | 75 | 13.0 |
| 5052/F40 – .0037 | 5.7 | 525 | 378 | 560 | 420 | 185 | 250 | 260 | 182 | 45.0 | 165 | 115 | 17.0 |
| 5052/F40 – .0037 | 5.7 | 935 | 630 | 1050 | 700 | 290 | 380 | 430 | 280 | 68.0 | 260 | 170 | 23.0 |
| 5052/F80 – .0013 | 4.3 | 615 | 402 | 650 | 455 | 195 | 275x | 300 | 196 | 45.0 | 190 | 120 | 20.0 |
| 5052/F80 – .0019 | 6.5 | 1140 | 700 | 1250 | 735 | 310 | 510x | 500 | 308 | 72.0 | 310 | 180 | 24.0 |
| 5052/F80 – .0025 | 8.0 | 1600 | 1100 | 1750 | 1120 | 400 | 720x | 645 | 434 | 98.0 | 440 | 260 | 31.0 |

5052 Alloy Aluminum Double-Flex – Specification Grade

| | | | | | | | | | | | | | |
|-------------------|-----|------|------|------|------|------|------|------|------|-------|------|------|-------|
| 5052/DF25 – .0025 | 2.7 | 360 | 270 | 390 | 290 | 120p | 145p | 185 | 140 | 29.0p | 100 | 80 | 13.0p |
| 5052/DF25 – .0047 | 4.8 | 850 | 680 | 960 | 720 | 220x | 430p | 370 | 290 | 50.0p | 240 | 180 | 22.0p |
| 5052/DF40 – .0025 | 4.2 | 760p | 600p | 850p | 680p | 190x | 350p | 280p | 220p | 30.0p | 190p | 150p | 17.0p |

5056 Alloy Aluminum Flex-Core – Specification Grade

| | | | | | | | | | | | | | |
|------------------|-----|------|------|------|------|-----|------|-----|-----|-------|-----|-----|------|
| 5056/F40 – .0014 | 2.1 | 240 | 150 | 260 | 182 | 65 | 105x | 105 | 74 | 18.0 | 55 | 42 | 10.0 |
| 5056/F40 – .0020 | 3.1 | 460 | 284 | 510 | 329 | 125 | 205x | 200 | 150 | 32.0 | 120 | 90 | 13.0 |
| 5056/F40 – .0026 | 4.1 | 680 | 440 | 740 | 483 | 185 | 305x | 310 | 217 | 45.0 | 200 | 132 | 17.0 |
| 5056/F80 – .0014 | 4.3 | 780 | 475 | 860 | 518 | 195 | 350x | 375 | 235 | 47.0 | 240 | 138 | 20.0 |
| 5056/F80 – .0020 | 6.5 | 1400 | 805 | 1500 | 910 | 310 | 630x | 650 | 364 | 73.0 | 420 | 213 | 24.0 |
| 5056/F80 – .0026 | 8.0 | 1800 | 1210 | 1950 | 1260 | 410 | 810x | 770 | 518 | 100.0 | 475 | 307 | 32.0 |

Notes: Test data obtained at 0.625" thickness.

p = Preliminary (see page 12).

x = Predicted values.

HRP Fiberglass Reinforced Phenolic Honeycomb

| Hexcel Honeycomb Designation Material – Cell Size – Density | Compressive | | | | | Plate Shear | | | | | |
|--|--------------|------|--------------|------|-------------|--------------|-----|-------------|--------------|-----|-------------|
| | Bare | | Stabilized | | | L Direction | | | W Direction | | |
| | Strength psi | | Strength psi | | Modulus ksi | Strength psi | | Modulus ksi | Strength psi | | Modulus ksi |
| Hexagonal | typ | min | typ | min | typ | typ | min | typ | typ | min | typ |
| HRP – 3/16 – 4.0 | 480 | 400 | 590 | 480 | 57 | 310 | 210 | 13.0 | 160 | 130 | 6.5 |
| HRP – 3/16 – 5.5 | 800 | 620 | 900 | 750 | 95 | 490 | 390 | 19.0 | 265 | 200 | 11.0 |
| HRP – 3/16 – 7.0 | 1150 | 900 | 1300 | 1040 | 136 | 650 | 510 | 30.0 | 370 | 290 | 14.0 |
| HRP – 3/16 – 8.0 | 1350 | 1100 | 1530 | 1280 | 164 | 750 | TBD | TBD | 460 | 370 | 19.0 |
| HRP – 3/16 – 12.0 | 2300 | 1800 | 2520 | 1960 | 260 | 985 | 815 | 48.0 | 675 | 525 | 28.0 |
| HRP – 1/4 – 3.5 | 390 | 280 | 455 | 400 | 46 | 250 | 180 | 10.0 | 125 | 100 | 5.0 |
| HRP – 1/4 – 4.5 | 585 | 480 | 640 | 560 | 70 | 355 | 280 | 15.0 | 200 | 155 | 8.0 |
| HRP – 1/4 – 5.0 | 680 | 530 | 820 | 660 | 84 | 400 | 305 | 20.0 | 230 | 180 | 10.0 |
| HRP – 1/4 – 6.5 | 1025 | 850 | 1180 | 920 | 120 | 580 | 450 | 25.0 | 330 | 260 | 13.0 |
| HRP – 3/8 – 2.2 | 165 | 125 | 180 | 145 | 13 | 120 | 90 | 6.0 | 60 | 45 | 3.0 |
| HRP – 3/8 – 3.2 | 315 | 260 | 390 | 350 | 38 | 205 | 160 | 12.0 | 110 | 85 | 5.0 |
| HRP – 3/8 – 4.5 | 610 | 450 | 690 | 550 | 65 | 325 | 260 | 14.0 | 190 | 150 | 8.0 |
| HRP – 3/8 – 6.0 | 900 | 750 | 1000 | 800 | 100 | 520 | 400 | 25.0 | 300 | 210 | 12.0 |
| HRP – 3/8 – 8.0 | 1400 | 1000 | 1540 | 1180 | 150 | 700 | 540 | 27.0 | 450 | 350 | 18.0 |
| OX-Core | | | | | | | | | | | |
| HRP/OX – 1/4 – 4.5 | 560 | 480 | 675 | 540 | 43 | 250 | 200 | 7.0 | 260 | 210 | 15.0 |
| HRP/OX – 1/4 – 5.5 | 775 | 580 | 890 | 670 | 65 | 300 | 230 | 10.0 | 330 | 255 | 18.0 |
| HRP/OX – 1/4 – 7.0 | 1150 | 850 | 1230 | 990 | 84 | 395 | 310 | 14.0 | 450 | 350 | 20.0 |
| HRP/OX – 3/8 – 3.2 | 340 | 260 | 390 | 300 | 32 | 140 | 110 | 4.5 | 150 | 120 | 9.0 |
| HRP/OX – 3/8 – 5.5 | 700 | 580 | 820 | 615 | 60 | 270 | 210 | 10.0 | 355 | 275 | 17.0 |
| Flex-Core | | | | | | | | | | | |
| HRP/F35 – 2.5 | 180 | 135 | 240 | 185 | 25 | 125 | 95 | 12.0 | 70 | 55 | 7.0 |
| HRP/F35 – 3.5 | 320 | 245 | 400 | 300 | 37 | 200 | 140 | 15.0 | 105 | 75 | 10.0 |
| HRP/F35 – 4.5 | 440 | 340 | 600 | 470 | 49 | 280 | 220 | 22.0 | 140 | 110 | 12.0 |
| HRP/F50 – 3.5 | 315 | 225 | 395 | 255 | 37 | 170 | 130 | 16.0 | 90 | 65 | 8.0 |
| HRP/F50 – 4.5 | 420 | 340 | 600 | 500 | 49 | 265 | 200 | 25.0 | 140 | 100 | 13.0 |
| HRP/F50 – 5.5 | 700 | 540 | 800 | 680 | 61 | 440 | 330 | 40.0 | 235 | 180 | 18.0 |

Note: Test data obtained at 0.500" thickness.

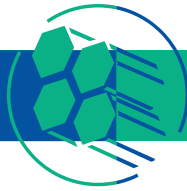
HFT Fiberglass Reinforced Phenolic Honeycomb (Fibertruss Bias Weave)

| Hexcel Honeycomb Designation Material – Cell Size – Density | Compressive | | | Plate Shear | | | | | |
|--|--------------|------|-------------|--------------|-----|-------------|--------------|-----|-------------|
| | Stabilized | | | L Direction | | | W Direction | | |
| | Strength psi | | Modulus ksi | Strength psi | | Modulus ksi | Strength psi | | Modulus ksi |
| | typ | min | typ | typ | min | typ | typ | min | typ |
| HFT – 1/8 – 3.0 | 350 | 270 | 23.0 | 195 | 150 | 19.0 | 95 | 75 | 7.5 |
| HFT – 1/8 – 4.0 | 560 | 420 | 46.0 | 315 | 240 | 25.0 | 150 | 120 | 12.0 |
| HFT – 1/8 – 5.5 | 900 | 700 | 69.0 | 525 | 410 | 40.0 | 250 | 190 | 16.0 |
| HFT – 1/8 – 8.0 | 1750 | 1500 | 100.0 | 675 | 525 | 45.0 | 480 | 400 | 21.5 |
| HFT – 3/16 – 2.0 | 170 | 130 | 17.0 | 115 | 90 | 15.0 | 60 | 50 | 5.0 |
| HFT – 3/16 – 3.0 | 365 | 275 | 34.0 | 200 | 155 | 19.0 | 100 | 80 | 9.0 |
| HFT – 3/16 – 4.0 | 550 | 460 | 44.0 | 340 | 270 | 25.0 | 190 | 140 | 12.0 |
| HFT – 3/8 – 4.0 | 500 | 400 | | 380 | 290 | 27.0 | 195 | 140 | 13.0 |
| HFT/OX – 3/16 – 6.0 | 1200 | 1020 | 63.0 | 320 | 240 | 18.0 | 260 | 190 | 19.0 |

Notes:

Test data obtained at 0.500" thickness.

HFT Fiberglass Reinforced Phenolic Honeycomb normally is not tested for bare compressive strength.



HexWeb Honeycomb Attributes and Properties

HRH-327 Fiberglass Reinforced Polyimide Honeycomb

| Hexcel Honeycomb Designation Material – Cell Size – Density | Compressive | | | Plate Shear | | | | | |
|--|-----------------|------|----------------|-----------------|------|----------------|-----------------|------|----------------|
| | Stabilized | | | L Direction | | | W Direction | | |
| | Strength psi | | Modulus ksi | Strength psi | | Modulus ksi | Strength psi | | Modulus ksi |
| | typ | min | typ | typ | min | typ | typ | min | typ |
| HRH-327 – 1/8 – 3.2 | 310 | 220 | 27 | 195 | 140 | 19 | 95 | 70 | 7.5 |
| HRH-327 – 1/8 – 5.5 | 790p | 600p | 80p | 465p | 300p | 30p | 245p | 175p | 14.5p |
| HRH-327 – 3/16 – 4.0 | 440p | 340p | 40p | 280p | 200p | 24p | 130p | 90p | 10.0p |
| HRH-327 – 3/16 – 4.5 | 520 | 400 | 45 | 320 | 220 | 33 | 150 | 110 | 11.0 |
| HRH-327 – 3/16 – 5.0 | 600p | 480p | 68p | 370p | 280p | 37p | 180p | 135p | 12.0p |
| HRH-327 – 3/16 – 6.0 | 780 | 625 | 87 | 460 | 345 | 45 | 230 | 170 | 15.0 |
| HRH-327 – 3/16 – 8.0 | 1210 | 1000 | 100 | 700 | 490 | 55 | 420 | 300 | 22.0 |
| HRH-327 – 3/8 – 4.0 | 440 | 325 | 50 | 280 | 195 | 29 | 150 | 100 | 12.0 |
| HRH-327 – 3/8 – 5.5 | 680 | 540 | 78 | 420 | 300 | 41 | 210 | 160 | 13.0 |
| HRH-327 – 3/8 – 7.0 | 1000p | 875p | 106p | 575p | 480p | 53p | 340p | 280p | 18.0p |

Notes:

Test data obtained at 0.500" thickness.

p = Preliminary (see page 12).

HRH-327 Fiberglass Reinforced Polyimide Honeycomb normally is not tested for bare compressive strength.

HRH-10 Aramid Fiber/Phenolic Resin Honeycomb

| Hexcel Honeycomb Designation Material – Cell Size – Density | Compressive | | | | | Plate Shear | | | | | |
|---|--------------|------|--------------|------|-------------|--------------|-----|-------------|--------------|-----|-------------|
| | Bare | | Stabilized | | | L Direction | | | W Direction | | |
| | Strength psi | | Strength psi | | Modulus ksi | Strength psi | | Modulus ksi | Strength psi | | Modulus ksi |
| Hexagonal | typ | min | typ | min | typ | typ | min | typ | typ | min | typ |
| HRH-10 – 1/16 – 3.4 | 195 | 160 | 205 | 170 | 20 | 155 | 125 | 6.0 | 85 | 65 | 2.9 |
| HRH-10 – 1/8 – 1.8 | 105 | 85 | 115 | 95 | 8 | 90 | 75 | 3.8 | 50 | 40 | 1.5 |
| HRH-10 – 1/8 – 3.0 | 290 | 235 | 325 | 270 | 20 | 175 | 155 | 6.5 | 100 | 85 | 3.5 |
| HRH-10 – 1/8 – 4.0 | 520 | 400 | 575 | 470 | 28 | 255 | 225 | 8.6 | 140 | 115 | 4.7 |
| HRH-10 – 1/8 – 5.0 | 700 | 560 | 770 | 620 | 37 | 325 | 275 | 10.2 | 175 | 150 | 5.4 |
| HRH-10 – 1/8 – 6.0 | 1050 | 850 | 1125 | 925 | 60 | 385 | 330 | 13.0 | 200 | 170 | 6.5 |
| HRH-10 – 1/8 – 8.0 | 1675 | 1370 | 1830 | 1450 | 78 | 480 | 400 | 16.0 | 260 | 210 | 9.5 |
| HRH-10 – 1/8 – 9.0 | 2000 | 1525 | 2100 | 1600 | 90 | 515 | 425 | 17.5 | 300 | 250 | 11.0 |
| HRH-10 – 3/16 – 1.5 | 85 | 70 | 95 | 80 | 6 | 65 | 50 | 3.0 | 35 | 28 | 1.6 |
| HRH-10 – 3/16 – 1.8 | 120 | 95 | 130 | 105 | 8 | 90 | 75 | 3.8 | 50 | 40 | 1.9 |
| HRH-10 – 3/16 – 2.0 | 135 | 110 | 150 | 130 | 11 | 95 | 80 | 4.3 | 55 | 45 | 2.1 |
| HRH-10 – 3/16 – 3.0 | 275 | 235 | 325 | 270 | 20 | 175 | 140 | 6.5 | 100 | 85 | 3.4 |
| HRH-10 – 3/16 – 4.0 | 500 | 430 | 540 | 470 | 28 | 245 | 215 | 7.8 | 140 | 110 | 4.7 |
| HRH-10 – 3/16 – 6.0 | 935 | 780 | 1020 | 865 | 60 | 420 | 370 | 13.0 | 225 | 200 | 6.5 |
| HRH-10 – 1/4 – 1.5 | 80 | 65 | 90 | 75 | 6 | 70 | 55 | 3.0 | 35 | 25 | 1.3 |
| HRH-10 – 1/4 – 2.0 | 120 | 100 | 130 | 105 | 11 | 95 | 80 | 4.2 | 45 | 36 | 2.0 |
| HRH-10 – 1/4 – 3.1 | 285 | 240 | 310 | 265 | 21 | 185 | 160 | 6.5 | 90 | 75 | 3.0 |
| HRH-10 – 1/4 – 4.0 | 440 | 360 | 480 | 390 | 28 | 250 | 205 | 8.0 | 125 | 100 | 3.5 |
| HRH-10 – 3/8 – 1.5 | 95 | 75 | 105 | 80 | 6 | 70 | 55 | 3.0 | 35 | 25 | 1.5 |
| HRH-10 – 3/8 – 2.0 | 140 | 115 | 155 | 125 | 11 | 90 | 72 | 3.7 | 55 | 36 | 2.4 |
| HRH-10 – 3/8 – 3.0 | 255 | 210 | 270 | 225 | 17 | 200 | 160 | 6.5 | 100 | 80 | 3.0 |
| HRH-10 – 3/4 – 1.5 | 70p | 50p | 80p | 55p | 7p | 70p | 55p | 3.4p | 35p | 25p | 1.7p |
| OX-Core | | | | | | | | | | | |
| HRH-10/OX – 3/16 – 1.8 | 100 | 80 | 110 | 90 | 7 | 50 | 40 | 2.0 | 60 | 50 | 3.0 |
| HRH-10/OX – 3/16 – 3.0 | 320 | 260 | 350 | 285 | 17 | 105 | 95 | 2.5 | 120 | 100 | 6.0 |
| HRH-10/OX – 3/16 – 4.0 | 600 | 500 | 650 | 550 | 26 | 130 | 105 | 4.6 | 150 | 130 | 8.4 |
| HRH-10/OX – 1/4 – 3.0 | 350 | 280 | 385 | 310 | 17 | 110 | 90 | 3.0 | 135 | 110 | 6.0 |
| Flex-Core | | | | | | | | | | | |
| HRH-10/F35 – 2.5 | 200 | 150 | 235 | 175 | 12 | 110 | 90 | 4.0 | 65 | 50 | 2.5 |
| HRH-10/F35 – 3.5 | 410 | 320 | 430 | 330 | 24 | 220 | 170 | 6.0 | 120 | 90 | 3.7 |
| HRH-10/F35 – 4.5 | 580 | 440 | 620 | 480 | 33 | 300 | 230 | 9.0 | 190 | 150 | 4.3 |
| HRH-10/F50 – 3.5 | 380 | 300 | 400 | 310 | 24 | 175 | 130 | 5.5 | 100 | 75 | 3.6 |
| HRH-10/F50 – 4.5 | 565 | 450 | 585 | 470 | 33 | 330 | 250 | 9.5 | 175 | 140 | 4.7 |
| HRH-10/F50 – 5.0 | 670 | 520 | 690 | 540 | 37 | 380 | 300 | 10.0 | 215 | 170 | 5.2 |
| HRH-10/F50 – 5.5 | 800 | 620 | 850 | 660 | 42 | 400 | 320 | 10.5 | 230 | 180 | 5.7 |

Notes: Test data obtained at 0.500" thickness.
p = Preliminary (see page 12).

HRH-310 Aramid Fiber/Polyimide Resin Honeycomb

| Hexcel Honeycomb Designation Material – Cell Size – Density | Compressive | | | Plate Shear | | | |
|---|--------------|--------------|-------------|--------------|-------------|--------------|-------------|
| | Bare | Stabilized | | L Direction | | W Direction | |
| | Strength psi | Strength psi | Modulus ksi | Strength psi | Modulus ksi | Strength psi | Modulus ksi |
| | typ | typ | typ | typ | typ | typ | typ |
| HRH-310 – 1/8 – 1.8 | 60 | 70 | – | 57 | 3.4 | 30 | 1.0 |
| HRH-310 – 1/8 – 5.0 | 660 | 730 | 40 | 325 | 10.0 | 175 | 5.0 |

Notes: Test data obtained at 0.500" thickness.
Data are from a very limited amount of testing.



HexWeb Honeycomb Attributes and Properties

HRH-78 Nomex Commercial Grade Aramid Fiber/Phenolic Resin Honeycomb

| Hexcel Honeycomb Designation Material – Cell Size – Density | Compressive | | | Plate Shear | | | |
|---|-----------------|-----------------|----------------|-----------------|----------------|-----------------|----------------|
| | Bare | Stabilized | | L Direction | | W Direction | |
| | Strength psi | Strength psi | Modulus ksi | Strength psi | Modulus ksi | Strength psi | Modulus ksi |
| HRH-78 – 1/8 – 3.0 | typ 280 | typ 315 | typ 18.5p | typ 160 | typ 5.3p | typ 90 | typ 3.1p |
| HRH-78 – 1/8 – 8.0 | 1600 | 1750 | 60.0p | 470 | 15.0p | 250 | 7.8p |
| HRH-78 – 3/16 – 3.0 | 270 | 330 | 18.2p | 124 | 4.6p | 81 | 3.5p |
| HRH-78 – 3/16 – 6.0 | 1125 | 1200 | – | 450 | 13.0p | 235 | 5.5p |
| HRH-78 – 1/4 – 3.0 | 265 | 285 | 19.0p | 120 | 4.6p | 80 | 3.0p |
| HRH-78 – 3/8 – 1.5 | 85 | 95 | 6.0p | 60 | 2.5p | 33 | 1.5p |

Notes: Test data obtained at 0.500" thickness. p = Preliminary value obtained from limited testing (see page 12).

HRH-49 Kevlar 49 Honeycomb

| Hexcel Honeycomb Designation Material – Cell Size – Density | Compressive | | | Plate Shear | | | | | |
|--|-----------------|-----|----------------|-----------------|-----|----------------|-----------------|-----|----------------|
| | Stabilized | | | L Direction | | | W Direction | | |
| | Strength psi | | Modulus ksi | Strength psi | | Modulus ksi | Strength psi | | Modulus ksi |
| HRH-49 – 1/4 – 2.1 | typ | min | typ | typ | min | typ | typ | min | typ |
| | 130 | 100 | 25 | 85 | 50 | 2.7 | 40 | 30 | 1.3 |

Note: Test data obtained at 0.500" thickness.

KOREX Aramid Fiber/Phenolic Resin Honeycomb

| Hexcel Honeycomb Designation Material – Cell Size – Density | Compressive | | Plate Shear | | | |
|--|-----------------|-----------------|-----------------|----------------|-----------------|----------------|
| | Bare | Stabilized | L Direction | | W Direction | |
| | Strength psi | Strength psi | Strength psi | Modulus ksi | Strength psi | Modulus ksi |
| KOREX – 1/8 – 3.0 | typ 260 | typ 280 | typ 178 | typ 14.4 | typ 105 | typ 7.0 |
| KOREX – 1/8 – 4.5 | 530 | 590 | 360 | 29.5 | 220 | 12.0 |
| KOREX – 1/8 – 6.0 | 980 | 1000 | 520 | 34.5 | 310 | 16.0 |
| KOREX – 5/32 – 2.4 | 230 | 260 | 168 | 11.7 | 101 | 6.6 |
| KOREX – 3/16 – 2.0 | 150 | 160 | 85 | 12.0 | 70 | 5.0 |
| KOREX – 3/16 – 3.0 | 280 | 280 | 220 | 20.0 | 115 | 9.0 |
| KOREX – 3/16 – 4.5 | 580 | 660 | 370 | 31.0 | 220 | 11.4 |
| KOREX – 1/4 – 1.5 | 100 | 110 | 85 | 7.4 | 47 | 3.1 |
| KOREX – 3/8 – 4.5 | 520 | 560 | 343 | 22.4 | 189 | 8.3 |
| KOREX – 3/8OX – 1.5 | 90 | 100 | 65 | 4.2 | 49 | 4.2 |

Notes: Test data obtained at 0.500" thickness. Data are from a very limited amount of testing.

TPU Thermoplastic Polyurethane Honeycomb

| Hexcel Honeycomb Designation Material – Cell Size – Film Gauge – Density |
|---|
| TPU – 7/32 – .008 – 7.2 |
| TPU – 9/32 – .012 – 8.0 |
| TPU – 7/16 – .0015 – 7.4 |

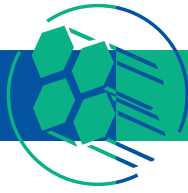
Comparison of Typical Mechanical Properties and Other Design Considerations

The curves on the following pages compare the typical mechanical properties of several honeycomb types. They are intended to show relative strength and shear moduli at ambient temperature. Included also are two graphs showing the effect of elevated temperatures on honeycomb strength after 30 minutes and 100 hours of exposure.

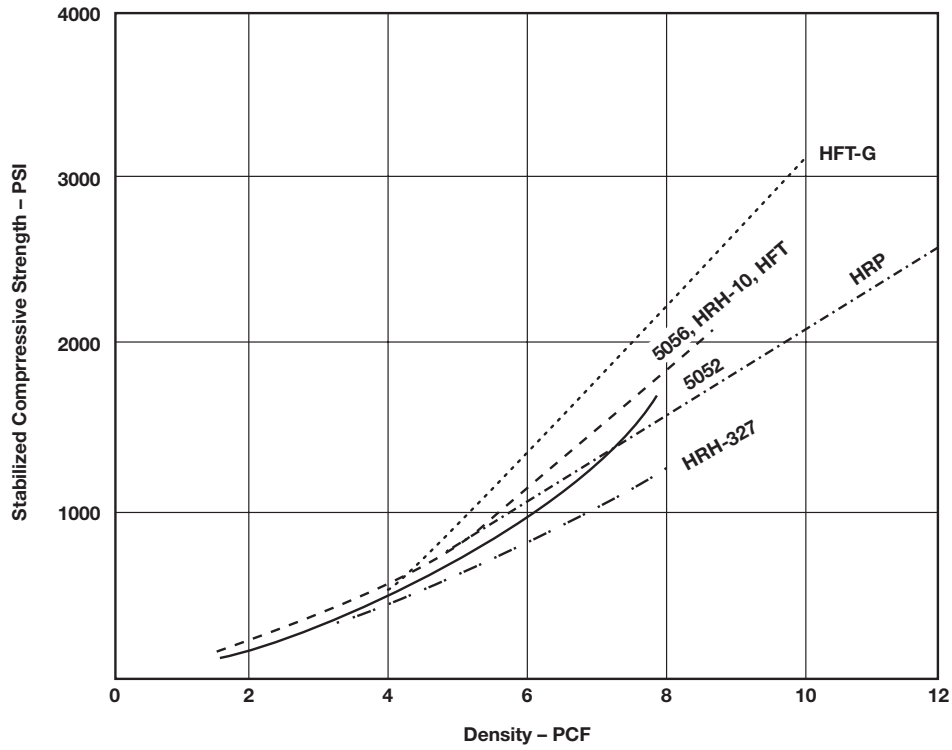
The selection of a particular honeycomb type is, of course, not only dependent on the mechanical properties. Many other factors have to be considered. A few of these considerations and the relative ratings of several honeycomb materials are presented in the table below. In overall economics or value analysis, one should also keep in mind such factors as tooling requirements, shop losses, previous experience, and, of course, the optimization of structural properties at minimum weight for the overall structure. Hexcel can assist with honeycomb material selection and trade-off analysis.

| Attributes | 5052 5056 CR III | 5052 5056 CR-PAA | ACG CR III | HRP | HFT | HRH- 327 | HRH- 10 | KOREX | HFT- G-327 |
|-------------------------------|------------------------|------------------------|---------------|----------|-------|-------------|------------|-------|---------------|
| Relative Cost | Mod Low | Med | Very Low | Mod High | High | Very High | Med | High | Very High |
| Maximum Long-Term Temperature | 350°F | 350°F | 350°F | 350°F | 350°F | 500°F | 350°F | 350°F | 500°F |
| Flammability Resistance | E | E | E | E | E | E | E | E | E |
| Impact Resistance | G | G | G | F | G | F | E | E | F |
| Moisture Resistance | E | E | E | E | E | E | G | E | E |
| Fatigue Strength | G | G | G | G | G | G | E | E | E |
| Heat Transfer | High | High | High | Low | Low | Low | Low | Low | Med |
| Corrosion Resistance | G | E | G | E | E | E | E | E | E |

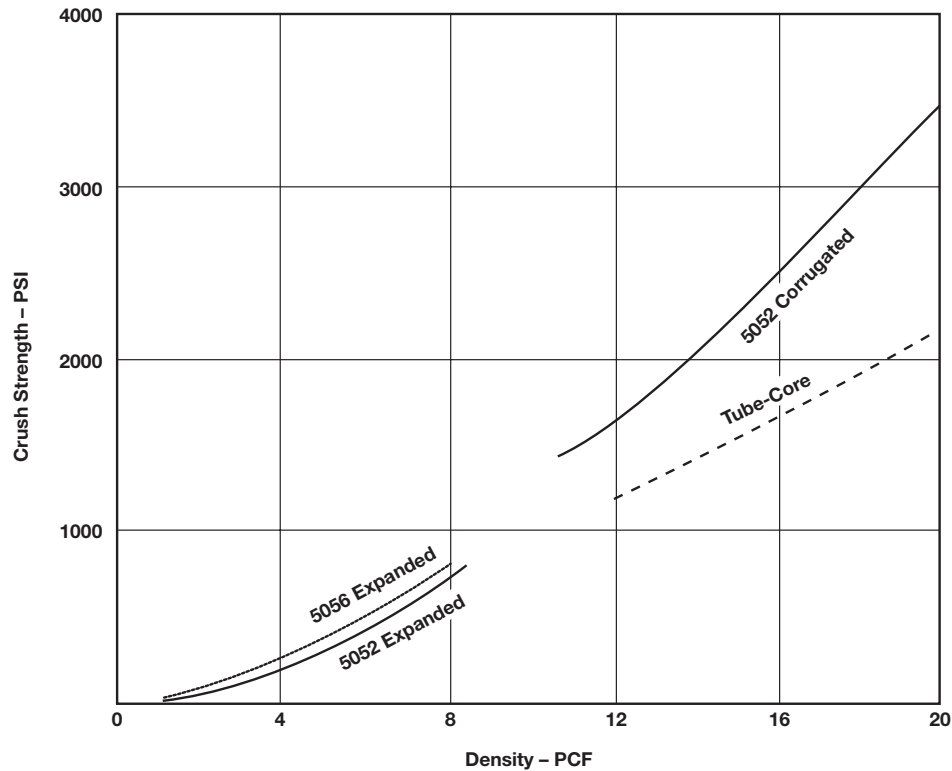
E = Excellent.
 G = Good.
 F = Fair.
 P = Poor.
 Mod = Moderately.
 Med = Medium.



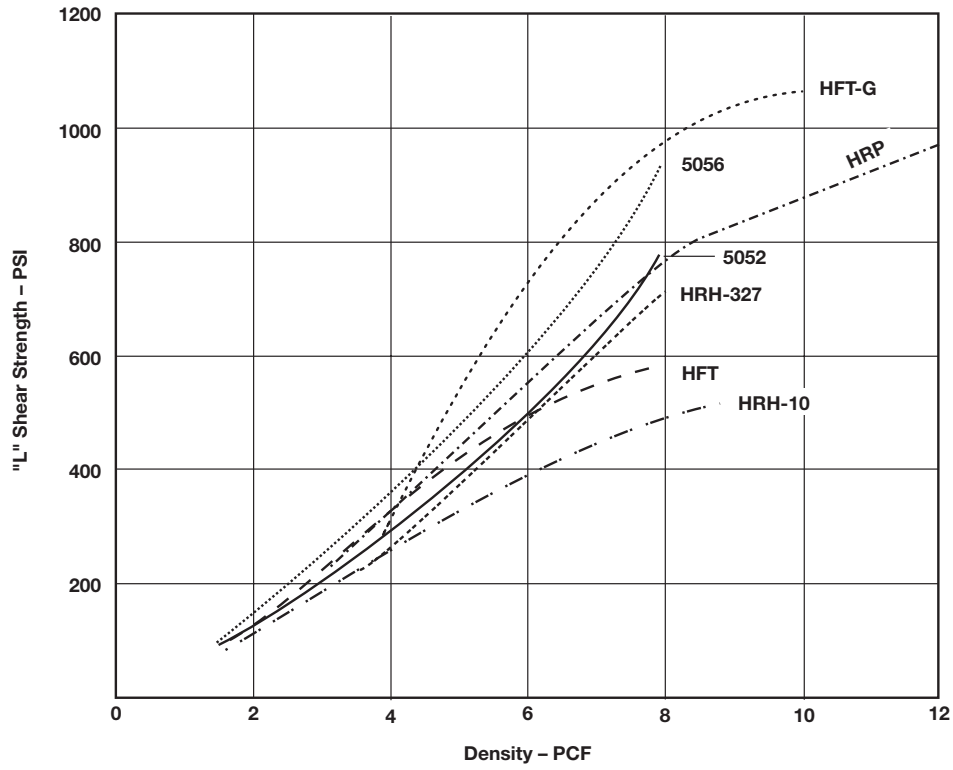
Typical Stabilized Compressive Strength



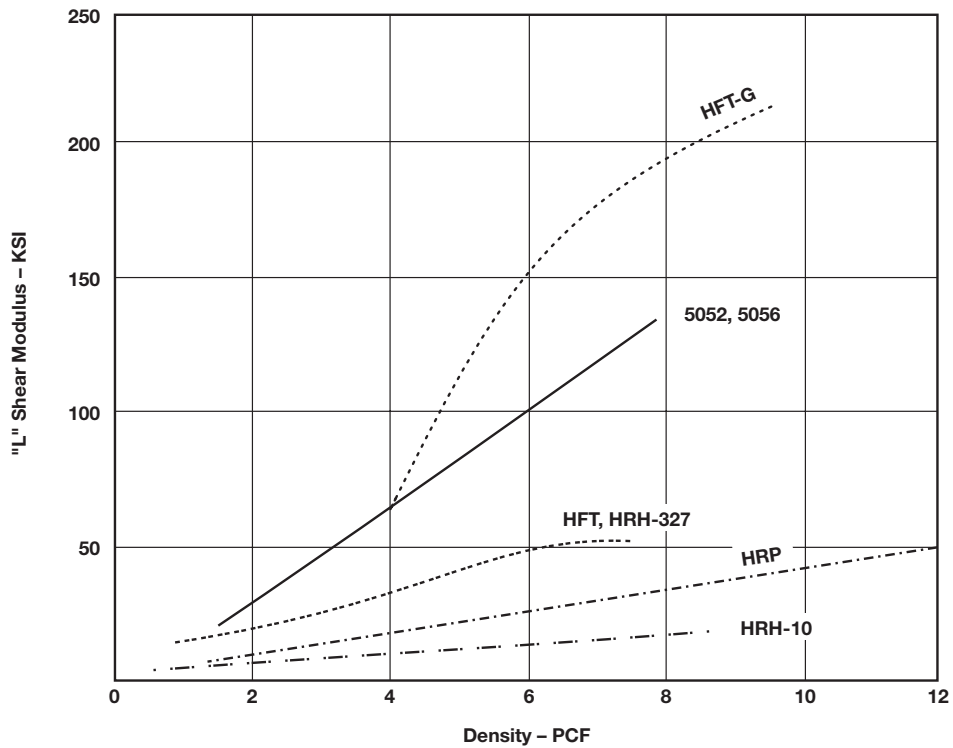
Typical Static Crush Strength

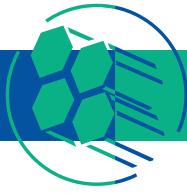


Typical L Shear Strength



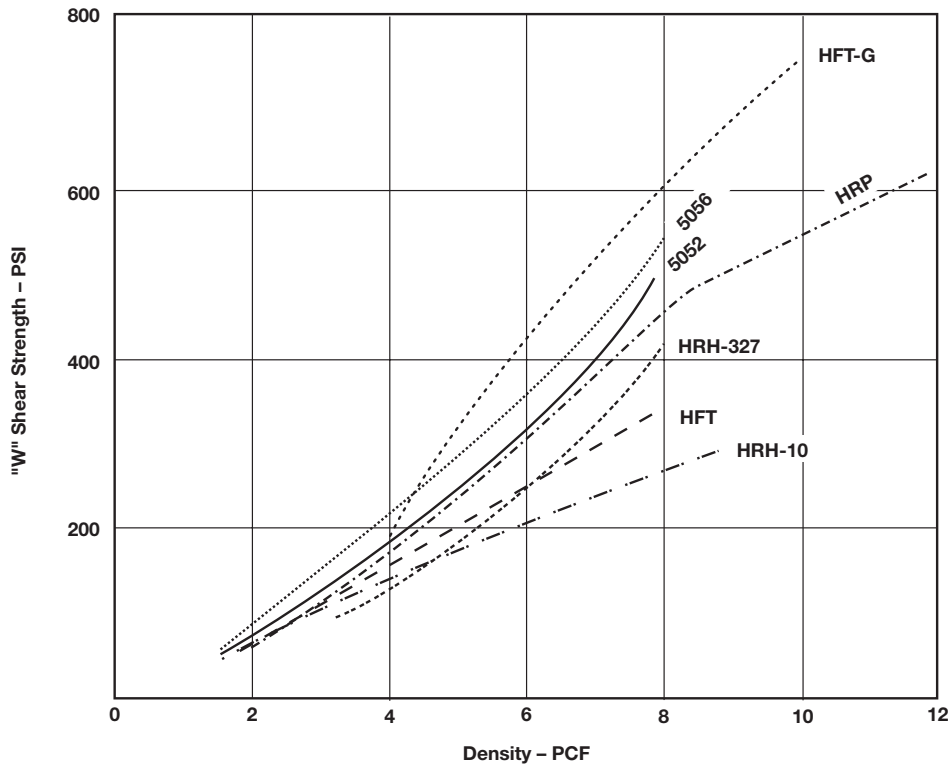
Typical L Shear Modulus



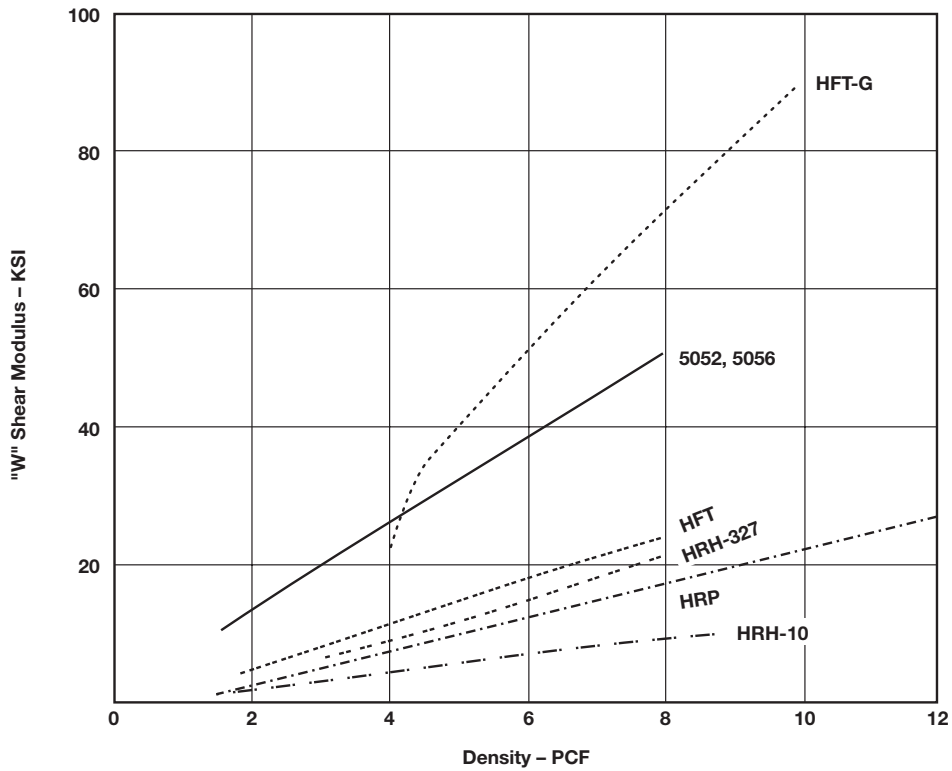


HexWeb Honeycomb Attributes and Properties

Typical W Shear Strength

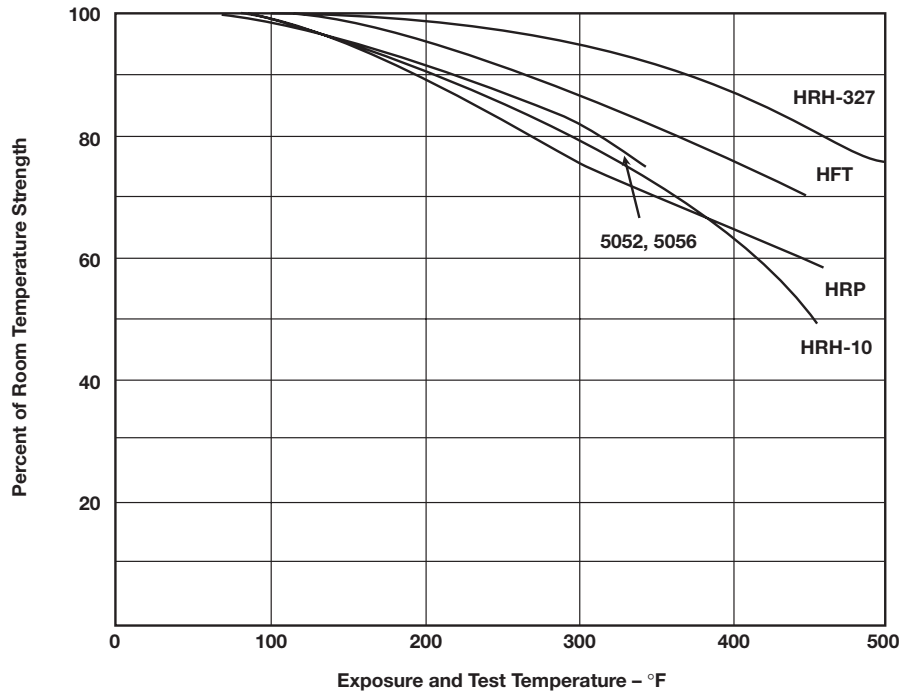


Typical W Shear Modulus

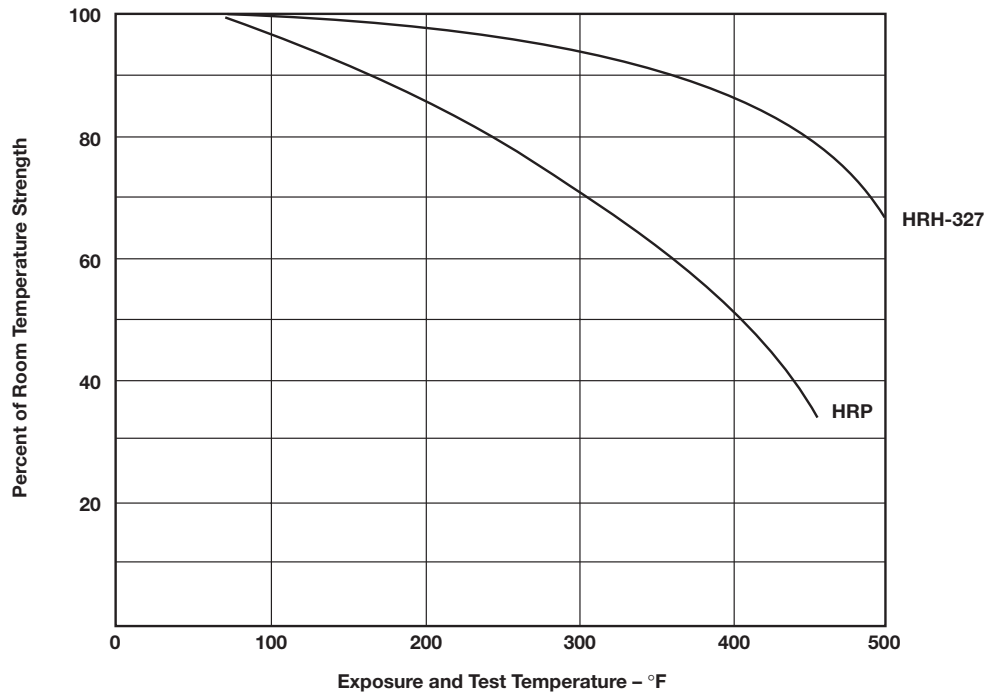


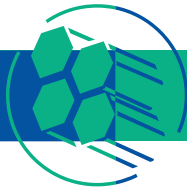
Temperature Effects

30-Minute Exposure (tested at temperature)



100-Hour Exposure (tested at temperature)



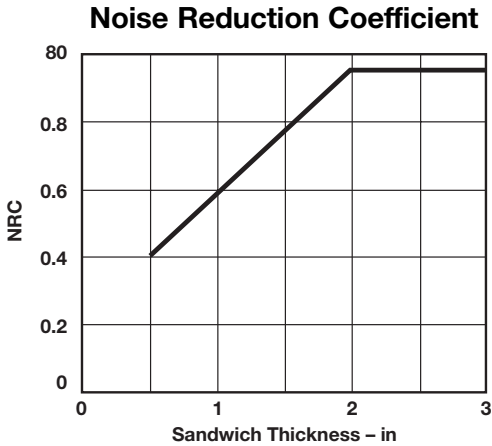


Additional Properties of Honeycomb

Acoustical

Honeycomb, to which a perforated facing skin has been applied, is often used for sound attenuation applications.

Hexcel's Acousti-Core honeycomb is filled with fiberglass batting. Available in many of the standard core types of 3/16" and larger cell size, this honeycomb with porous or perforated facings can be used for lightweight sound absorption panels that have considerable structural integrity.



The noise reduction coefficient (NRC) of Acousti-Core is shown on the graph to the left. The NRC value is the average of sound absorption coefficients at 250, 500, 1000, and 2000 cycles per second. The higher the NRC value, the more efficient the absorber.

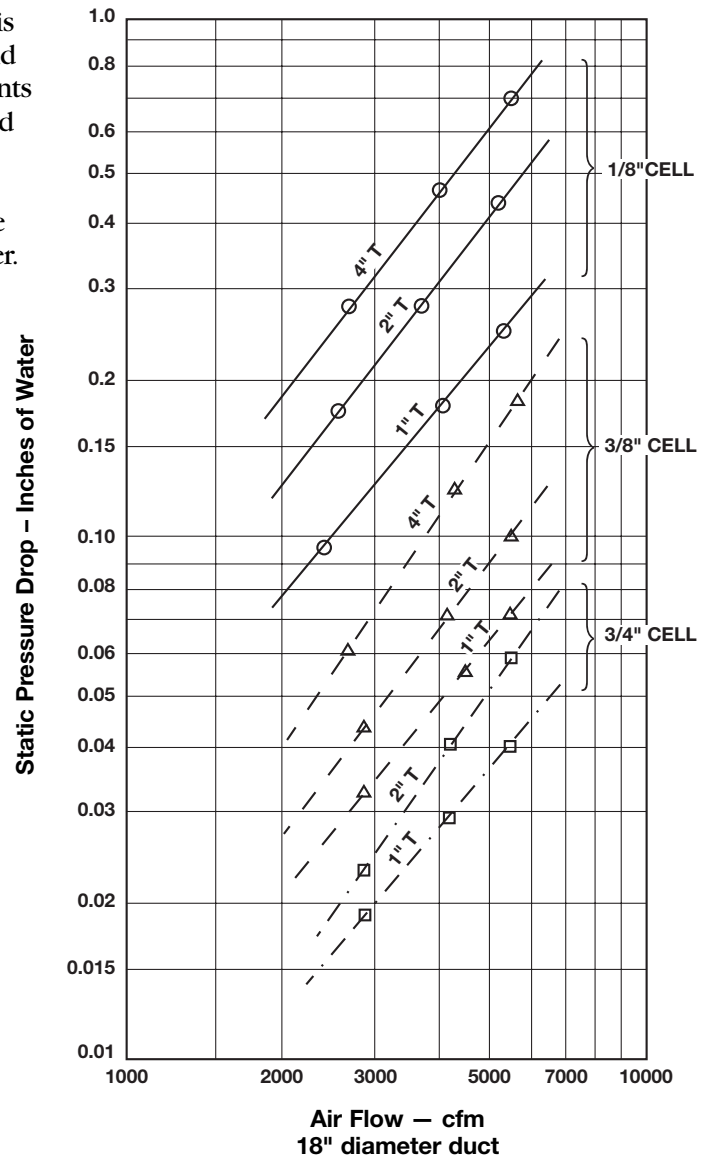
Air/Fluid Directionalization

Over the years, honeycomb has been used very successfully for directionalizing air, water, and fluid flow in a wide variety of ducts and channels. The open, straight honeycomb cells are an efficient means of controlling the flow of air with a minimum pressure drop. Laminar flow can typically be attained by using a honeycomb thickness to cell size ratio of 6-8 for most flow rates. Aluminum honeycomb with CR III corrosion-resistant coating is used for air directionalization applications.

Pressure Drop Across Honeycomb

The pressure drop across honeycomb placed in a fluid stream has been found to be extremely small compared with alternate devices such as wire screens and perforated metal panels. The large open frontal area of honeycomb is the dominant reason for this. All honeycomb types considered for air directional applications have 95-99% open area. The major flow resistance is related to friction drag on the cell walls. As would be expected, smaller cell sizes and thicker honeycomb cores have higher pressure drops. The cell wall foil gauge has a negligible effect on the pressure drop. The figure at right shows the pressure drop measured across three aluminum honeycomb types at 1-, 2-, and 4-inch thickness. These measurements were made in a straight 18-inch diameter duct.

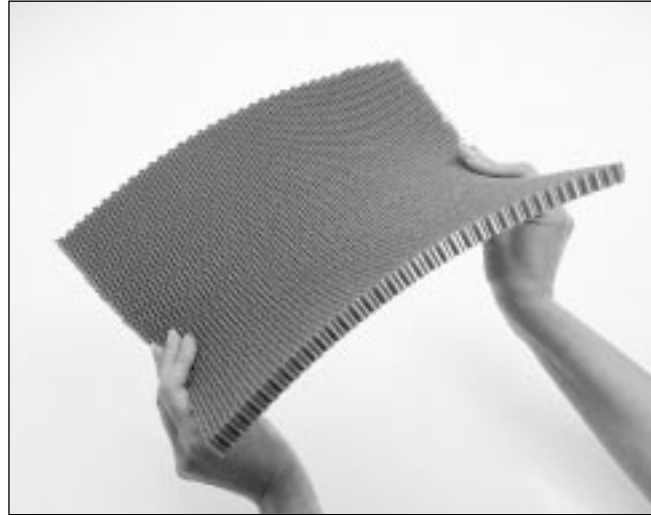
Pressure Drop Across Aluminum Honeycomb



Bending of Honeycomb

When hexagonal honeycomb is bent, it exhibits a phenomenon where the honeycomb is forcibly curved around one axis and the core reacts by bending in a reversed curvature along an axis oriented 90°. This phenomenon is called anticlastic curvature.

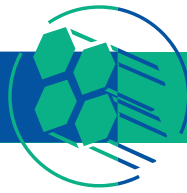
Poisson's ratio μ is the ratio of the lateral strain to the axial strain when the resulting strains are caused by a uniaxial stress. Poisson's ratios for different types of honeycomb have been determined to vary between 0.1 and 0.5. As would be expected, Poisson's ratio for Flex-Core cell configuration is less than Poisson's ratio for hexagonal cell configuration.



Coefficient of Thermal Expansion

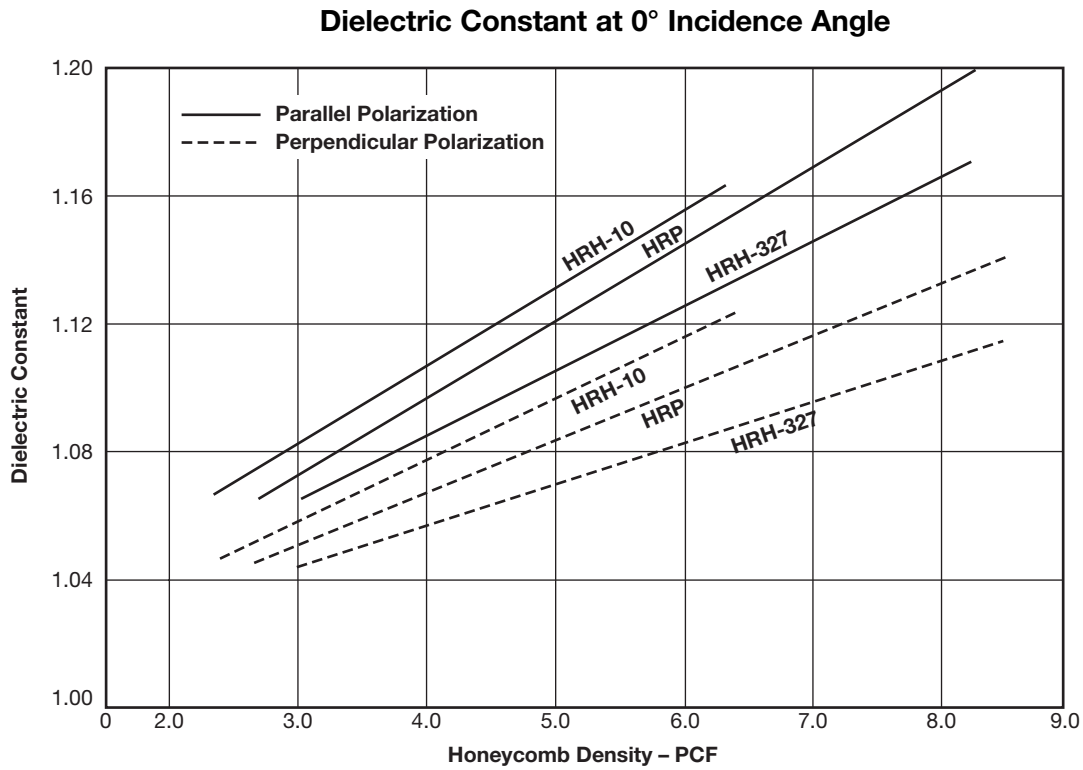
Honeycomb will change its dimensions slightly when subject to a change in temperature. The change in dimensions as a function of temperature is determined by the substrate material. Coefficients of thermal expansion in the thickness direction for various honeycomb materials are as follows:

| Honeycomb Core | Coefficient of Thermal Expansion (inch/inch – °F) |
|--|--|
| CR III, CR-PAA, 5052, 5056, ACG Aluminum | 13.2×10^{-6} |
| HRP, HFT, HRH-327 Fiberglass | 8.2×10^{-6} |
| HRH-10, HRH-310, HRH-78 Nomex | 19.4×10^{-6} |
| HRH-49 Kevlar | 2.7×10^{-6} |
| HFT-G Carbon | 2.0×10^{-6} |



Dielectric

Nonmetallic honeycomb is used extensively in radomes, both airborne and stationary, because of its very low dielectric constant and loss tangent. Thus nonmetallic honeycomb allows the wave energy to be transmitted with only negligible reflection and absorption. The figure below shows the dielectric constant as a function of core density for several honeycomb types. The values were obtained for both polarizations and with the electric field vector E perpendicular and parallel to the ribbon direction. Testing was conducted at 9375 Megahertz. In addition to the electric field polarization, the dielectric constant is a function of the incidence angle and the thickness of the honeycomb.

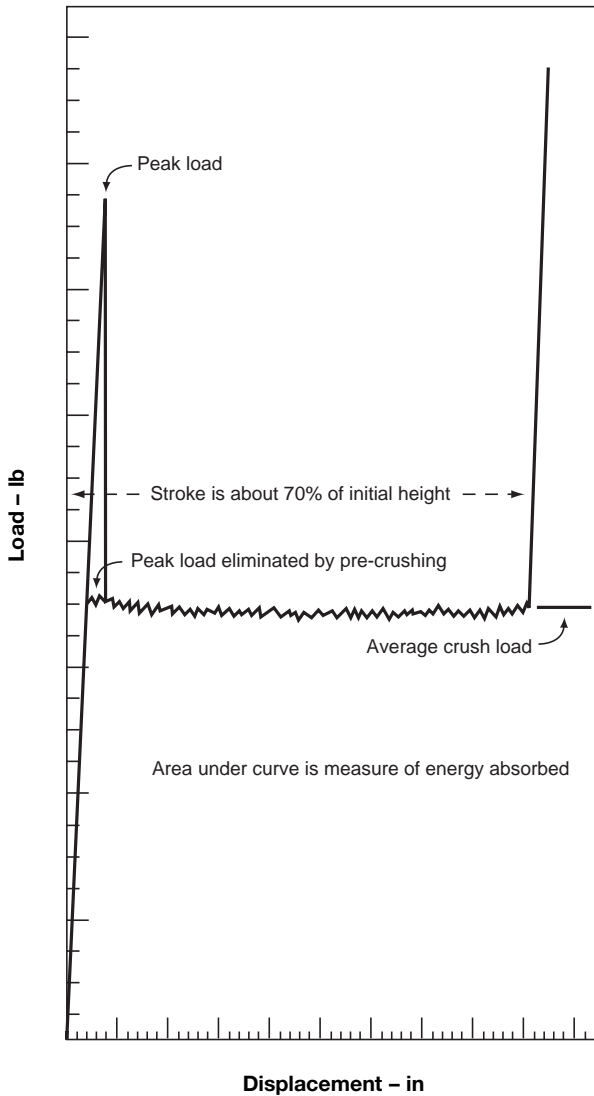


Energy Absorption

As mentioned under the Crush Strength property description (page 10), honeycomb loaded axially beyond its ultimate compressive peak will absorb energy at constant stress. The figure below shows the crush curve of aluminum honeycomb. Hexagonal honeycomb or Tube-Core used in this manner can be designed to crush uniformly at a predetermined level, thereby providing a highly reliable absorber at low weight.

See Hexcel technical brochure TSB 122, *Design Data for the Preliminary Selection of Honeycomb Energy Absorption Systems*, and the data sheet *Tube-Core Energy Absorption Cylinder* for further information on honeycomb for energy absorption applications.

Aluminum Honeycomb Crush Curve



Aluminum honeycomb absorbs energy by crushing under load.



Moisture Absorption

Samples of HFT, HRP, and HRH-10 were exposed to 95% relative humidity at 120°F for 120 hours to determine the moisture pickup. The following percent moisture pickups were measured.

| | |
|---------------------|------|
| HRP – 3/16 – 4.0 | 1.7% |
| HFT – 1/8 – 4.0 | 1.3% |
| HFT – 3/16 – 4.0 | 1.6% |
| HRH-10 – 3/16 – 4.0 | 4.4% |
| HFT-G – 3/16 – 6.0 | 2.0% |
| KOREX – 3/16 – 4.5 | 3.4% |

Radio Frequency Shielding

Aluminum honeycomb has been used for RF shielding because the cellular structure can be compared to a myriad of wave guides. When properly designed as to cell size and cell depth, honeycomb will attenuate a required Db level through a wide frequency range.

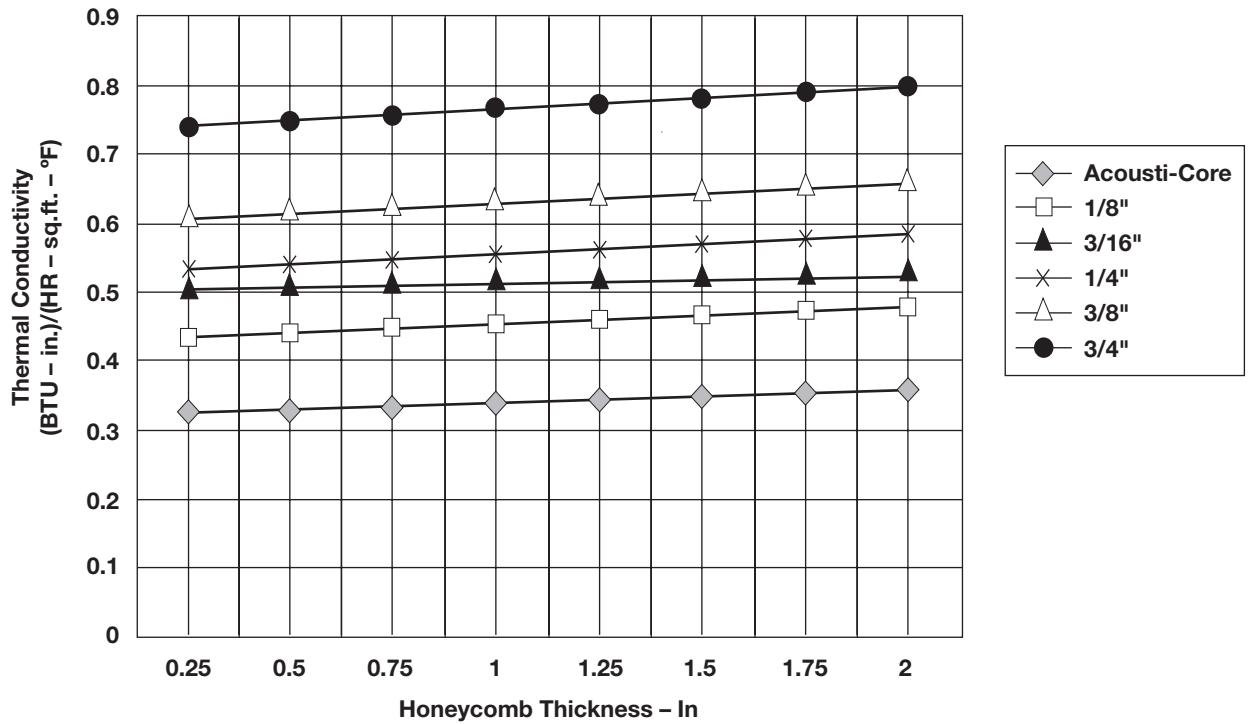
Thermal Conductivity

Thermal conductivity through sandwich panels can be isolated into the contribution of each component: facings, core, and adhesive. The resistances ($R = \frac{t}{k}$ or reciprocal of conductivity) can simply be added—including the effect of boundary layer conditions. The thermal properties of typical facing materials may be found in handbooks. Thermal resistance values for typical core-to-facing adhesives are 0.03 for film adhesives with a scrim cloth support and 0.01 for unsupported adhesives. The thermal conductivity of aluminum and nonmetallic honeycomb at a mean temperature of 75°F is shown below. For nonmetallic honeycomb, cell size is much more important than core density. For aluminum honeycomb, density is the variable that determines the thermal conductivity. The thermal conductivity of aluminum honeycomb is nearly independent of the core thickness, for thicknesses between 0.375–4.0". To adjust for mean temperature, multiply the thermal conductivity at 75°F by Q using the bottom figure. Thermal conductivity of honeycomb may be decreased by filling the cells with insulating materials.)

Thermal Conductivity of Aluminum Honeycomb

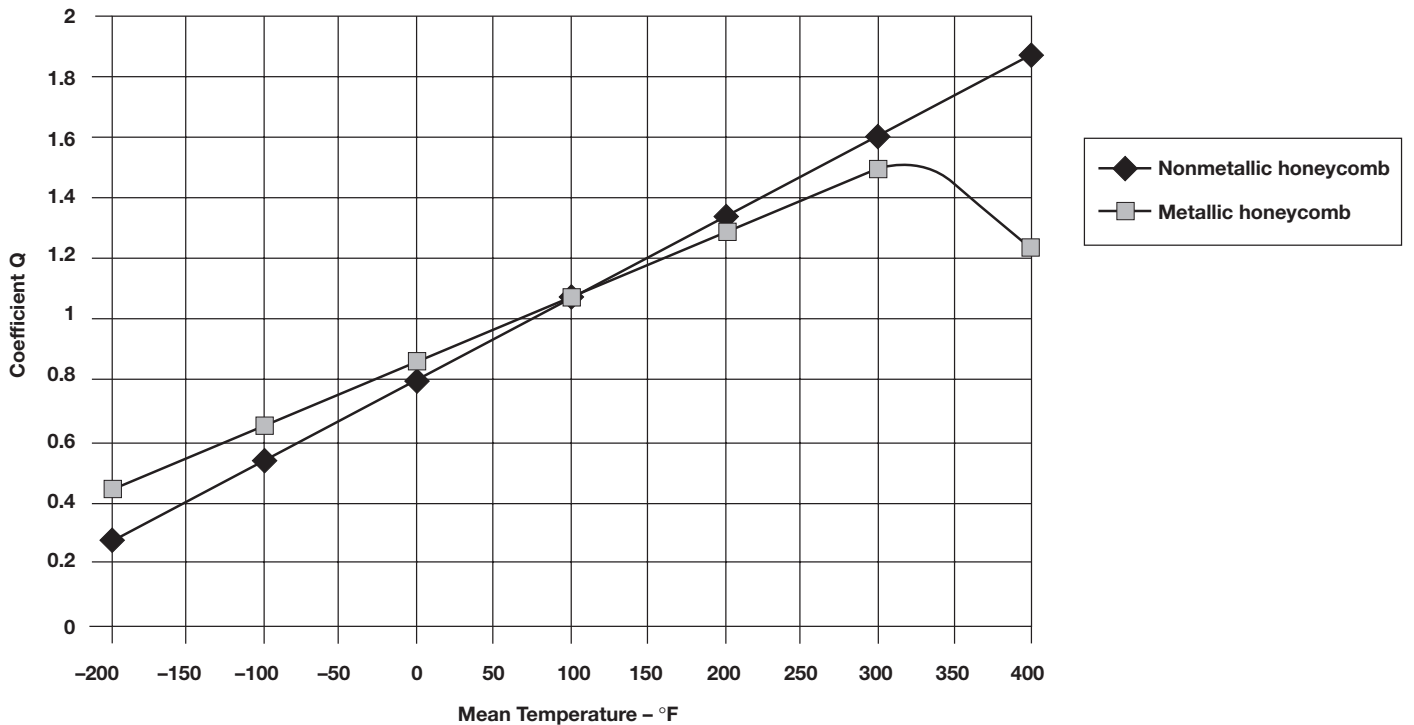
| | Units | | | | |
|--------------------------|-----------------------------------|------------|------------|------------|------------|
| Density | (lb/ft ³) | 2.0 | 4.0 | 6.0 | 8.0 |
| Thermal conductivity (k) | (BTU-in)/(hr-ft ² -°F) | 27 | 38 | 61 | 103 |

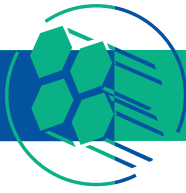
Thermal Conductivity – Nonmetallic Honeycomb



Effect of Mean Temperature on Thermal Conductivity

$$k_T = k_{(75^\circ\text{F})} * Q$$





Comparison and Benefits of Honeycomb Versus Alternative Core Materials

Materials other than honeycomb are used as core materials. These are primarily foams and wood-based products. The advantages of honeycomb compared to these alternative core materials are as follows.

| Material | Property | Honeycomb Advantages |
|--|---|--|
| Foam includes – polyvinyl chloride (PVC) – polymethacrylimide – polyurethane – polystyrene – phenolic – polyethersulfone (PES) | Relatively low crush strength and stiffness Increasing stress with increasing strain Friable Limited strength Fatigue Cannot be formed around curvatures | Excellent crush strength and stiffness Constant crush strength Structural integrity Exceptionally high strengths available High fatigue resistance OX-Core and Flex-Core cell configurations for curvatures |
| Wood-based includes – plywood – balsa – particleboard | Very heavy density Subject to moisture degradation Flammable | Excellent strength-to-weight ratio Excellent moisture resistance Self-extinguishing, low smoke versions available |

Sub-Panel Structure Comparison

The comparison at the right shows the relative strength and weight attributes of the most common types of sandwich panels.

| | Relative Strength | Relative Stiffness | Relative Weight |
|----------------------|-------------------|--------------------|-----------------|
| Honeycomb | 100% | 100% | 3% |
| Foam Sandwich | 26% | 68% | |
| Structural Extrusion | 62% | 99% | |
| Sheet & Stringer | 64% | 86% | |
| Plywood | 3% | 17% | 100% |

Applications

The major usage of honeycomb is for structural applications. Honeycomb's beneficial strength-to-weight and stiffness-to-weight ratios (see diagram on bottom of page 1) compared to other materials and configurations are unmatched.

Honeycomb's long-standing traditional application is in aircraft. Some of the aircraft parts that are made from honeycomb include:

- ailerons
- elevators
- flaps
- nacelles
- slats
- struts
- trailing edges
- cowls
- empennages
- flooring
- radomes
- spoilers
- tabs
- doors
- fairings
- leading edges
- rudders
- stabilizers
- thrust reversers

Other aerospace vehicles that use honeycomb include:

- helicopters
- satellites
- missiles
- space shuttle
- satellite launch vehicles

After aircraft and other airborne aerospace vehicles, the next most prominent uses for honeycomb occur in various land and water transportation vehicles. The different types of vehicles and most common applications are:

Automobiles

- energy absorption protective structures in Formula I race cars
- air directionalization for engine fuel injection system
- energy absorption in pillars and along roof line for passenger protection
- crash testing barriers

Rail

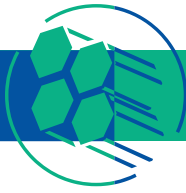
- doors
- floors
- energy absorbers/bumpers
- ceilings
- partitions

Marine

- commercial vessel and naval vessel bulkheads
- America's Cup sailing yachts
- wall, ceiling, and partition panels

Other applications for honeycomb that are not transportation related include:

- clean room panels
- exterior architectural curtain wall panels
- air, water, fluid, and light directionalization
- heating, ventilation, air conditioning (HVAC) equipment and devices
- skis and snowboards
- energy absorption protective structures
- electronic shielding enclosures
- acoustic attenuation



Hexcel Honeycomb Technical Literature Index

Brochures

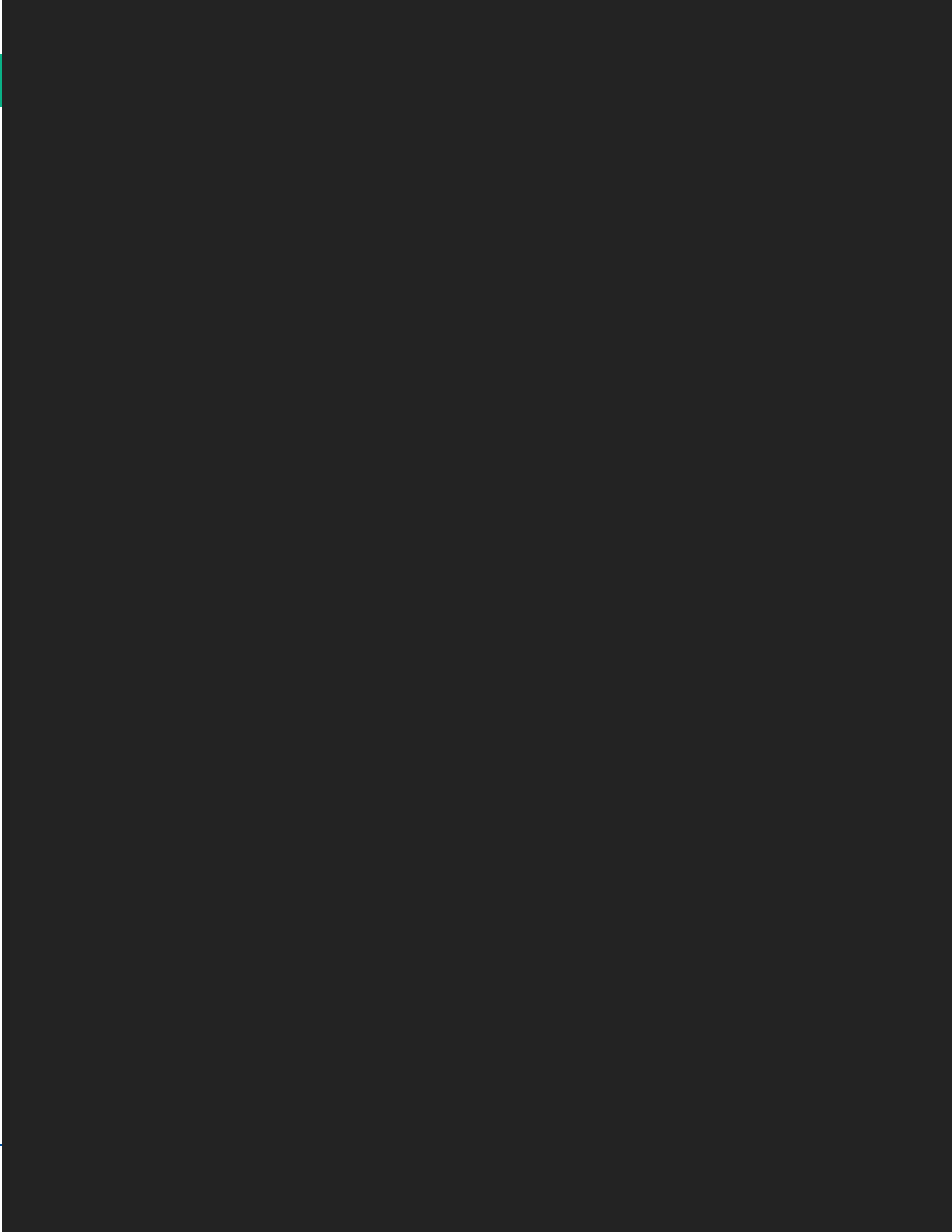
- Design Data for the Preliminary Selection of Honeycomb Energy Absorption Systems – TSB 122
- Hexcel CR-PAA™
- Hexcel Honeycomb FMVSS 201U Safety Standards
- Hexcel Special Process
- HexWeb™ Honeycomb Attributes and Properties
- Honeycomb Sandwich Design Technology
- Honeycomb Selector Guide

Data Sheets

- A1 and A10. High Strength Aramid Honeycomb [U.K. manufactured equivalents to HRH®-10 and HRH®-78 respectively]
- ACG® Honeycomb. Aluminum Commercial Grade
- Acousti-Core® Acoustical Absorption Honeycomb
- Aluminum Flex-Core® Formable Aluminum Honeycomb
- CFC™-20. Composite Flooring Honeycomb Core
- CR III® Corrosion Resistant Specification Grade Aluminum Honeycomb
- CR III® Micro-Cell™ Aluminum Honeycomb
- CR-PAA™ Phosphoric Acid Anodized Aluminum Honeycomb
- CROSS-CORE® Bi-directional Aluminum Corrugated Honeycomb
- Fibertruss® HFT® Fiberglass/Phenolic Honeycomb
- Nonmetallic Flex-Core® Formable Nonmetallic/Phenolic Honeycomb
- Hexcel Honeycomb in Air Directionalizing Applications
- HRH®-10. Aramid Fiber/Phenolic Honeycomb
- HRH®-49. Honeycomb of Kevlar® 49
- HRH®-78. Nomex® Commercial Grade Honeycomb
- HRH®-310. Aramid Fiber/Polyimide Resin Honeycomb
- HRH®-327. Fiberglass Reinforced Polyimide Honeycomb
- HRP® Fiberglass/Phenolic Honeycomb
- KOREX® Para-Aramid/Phenolic Core
- Rigicell™ Corrosion Resistant Aluminum Corrugated Honeycomb
- TPU™ Thermoplastic Polyurethane Honeycomb
- Tube-Core® Energy Absorption Cylinder
- 3003. [U.K. manufactured equivalent to ACG®]
- 5052. High Strength Aluminum Honeycomb [U.K. manufactured equivalent to CR III®]

Guide

- Aluminum and Nomex® Honeycombs Cross Reference Guide





HexWeb Honeycomb Attributes and Properties

Hexcel Composite Materials

For further information, please contact your nearest Hexcel Sales Office, or visit our web site at www.hexcel.com

Suite 2, 86 Grimshaw Street
Greensborough, Victoria 3088,
Australia
Tel **61** 3 9432 7100
Fax **61** 3 9432 7200

Industriestrasse 1, A-4061
Pasching, **Austria**
Tel **43** (0) 7229 7720
Fax **43** (0) 7229 772299

Rue Trois Bourdons, 54
B-4840 Welkenraedt, **Belgium**
Tel **32** 87 307 411
Fax **32** 87 882 895

Suite 2105, Hong Kong Plaza
283 Huai Hai Zhong Road
Shanghai 200021, **China**
Tel **8621** 6390 6668
Fax **8621** 6390 7180

ZI La Plaine, B.P. 27 Dagneux
01121 Montluel, **France**
Tel **33** (0) 4 72 25 26 27
Fax **33** (0) 4 72 25 27 30

Am Westpark 1-3
81373 München, **Germany**
Tel **49** 89 743 5250
Fax **49** 89 743 52520

Via San Cristoforo, 44
21047 Saronno (VA), **Italy**
Tel **39** 02 96709082
Fax **39** 02 9600809

27-06 Suntec Tower Four
6 Temasek Boulevard
Singapore 038986
Tel **65** 332 2430
Fax **65** 332 2431

Bruselas, 10-16
Polig. Ind. "Ciudad de Parla"
28980 Parla, Madrid, **Spain**
Tel **34** 91 664 4900
Fax **34** 91 698 4914

Duxford, Cambridge
CB2 4QD, **UK**
Tel **44** (0) 1223 833141
Fax **44** (0) 1223 838808

5794 West Las Positas Boulevard
PO Box 8181
Pleasanton, CA 94588-8781, **USA**
Tel 1 (925) 847-9500
Fax 1 (925) 734-9676

N.B. Telephone/fax numbers include country codes (**in bold**) that should be omitted for national dialing. For international dialing, use international code but omit number in parentheses.

Important

Hexcel Corporation makes no warranty, whether expressed or implied, including warranties of merchantability or of fitness for a particular purpose. Under no circumstances shall Hexcel Corporation be liable for incidental, consequential, or other damages arising out of a claim from alleged negligence, breach of warranty, strict liability or any other theory, through the use or handling of this product or the inability to use the product. The sole liability of Hexcel Corporation for any claims arising out of the manufacture, use, or sale of its products shall be for the replacement of the quantity of this product which has proven to not substantially comply with the data presented in this bulletin. Users should make their own assessment of the suitability of any product for the purposes required. The above supercedes any provision in your company's forms, letters, or other documents.

PRODUCT DATASHEET



TENCATE ADVANCED COMPOSITES

TenCate E745 Mid temperature curing toughened epoxy component prepreg

PRODUCT TYPE

275°F (135°C) cure

Mid temperature curing toughened epoxy component prepreg

TYPICAL APPLICATIONS

- Side impact structures
- F1 nose boxes
- Mechanically demanding structural applications

SHELF LIFE

Out life

60 days at @ 20°C (68°F)

Storage life

12 months @ -18°C (0°F)

Out life is the maximum time allowed at room temperature before cure.

To avoid moisture condensation:

Following removal from cold storage, allow the prepreg to reach room temperature before opening the polythene bag. Typically the thaw time for a full roll of material will be 4 to 6 hours.

PRODUCT DESCRIPTION

TenCate E745 is a toughened epoxy resin system developed for impact structures and other mechanically demanding structural applications. The resin system cures at 135°C (275°F) and can be impregnated into a range of fibre and fabric types.

TENCATE E745 PREPREG BENEFITS/FEATURES

- Excellent tack and drape
- 1 hour at 135°C (275°F) cure
- High toughness and impact properties
- 60 days shelf life at ambient temperature
- Excellent surface finish
- Low volatile content - no solvents used during processing

TYPICAL NEAT RESIN PROPERTIES

Density 1.24 g/cm³ (77.4 lbs/ft³) at 23°C (73°F)

Tg (DMTA) after 1 hr at 135°C (275°F)..... Onset: 118°C (244.4°F);
Peak tan δ: 131°C (267.8°F)

TYPICAL LAMINATE PROPERTIES

GIC (J/m²) 1,137 J/m²

SEA (Dynamic crush test)(J/g) 84.0 J/g

IM0223 - CARBON 200 GSM 2x2 TWILL IM7 GP 6K 42% R.W. CURED 1 HR AT 135°C (275°F)

| Property | Condition | Method | Results | |
|------------------------------|-----------|-----------|----------|----------|
| Tensile Strength (Warp)* | RTD | ISO 527-4 | 1072 MPa | 156 ksi |
| Tensile Modulus (Warp)* | RTD | ISO 527-4 | 75.9 GPa | 11.0 Msi |
| Poisson's Ratio | RTD | ISO 527-4 | 0.04 | |
| Tensile Strength (Weft)* | RTD | ISO 527-4 | 1130 MPa | 164 ksi |
| Tensile Modulus (Weft)* | RTD | ISO 527-4 | 78.9 GPa | 11.4 Msi |
| Poisson's Ratio | RTD | ISO 527-4 | 0.81 | |
| Compression Strength (Warp)* | RTD | EN2580 | 717 MPa | 104 ksi |
| Compression Modulus (Warp)* | RTD | EN2580 | 70.6 GPa | 10.2 Msi |
| Compression Strength (Warp)* | RTD | EN2580 | 707 MPa | 103 ksi |
| Compression Modulus (Weft)* | RTD | EN2580 | 71.4 GPa | 10.4 Msi |
| In-Plane Shear Strength | RTD | ISO 14129 | 124 MPa | 18 ksi |
| In-Plane Shear Modulus | RTD | ISO 14129 | 3.9 GPa | 0.6 Msi |
| ILSS Warp | RTD | ISO 14130 | 70 MPa | 10 ksi |
| ILSS Weft | RTD | ISO 14130 | 69 MPa | 10 ksi |

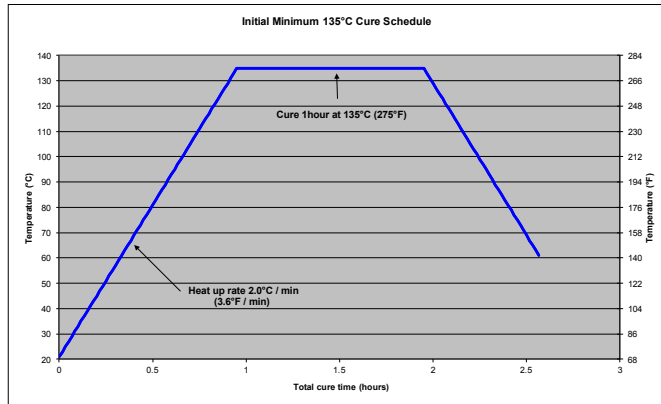
PRODUCT DATASHEET



TENCATE ADVANCED COMPOSITES

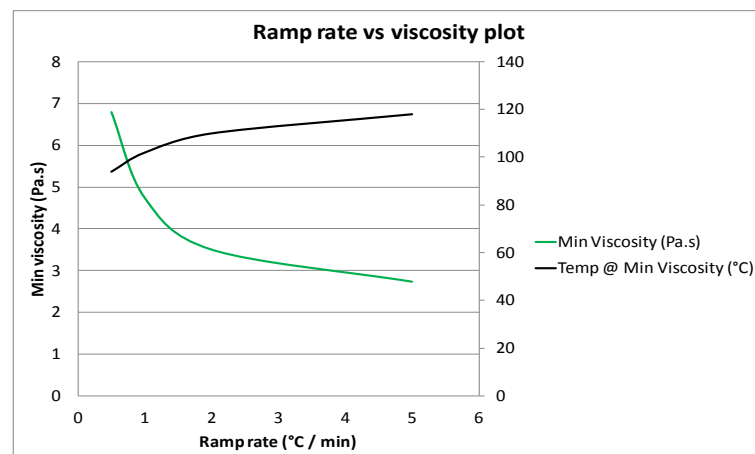
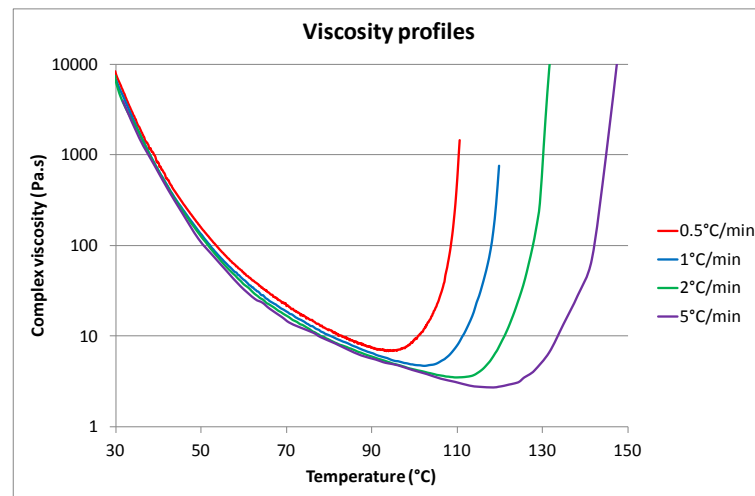
TenCate E745

Mid temperature curing modified epoxy resin component prepreg



RECOMMENDED CURE CYCLE

- TenCate E745 can be successfully moulded by vacuum bag, autoclave, or matched die moulding techniques.
- Increase autoclave pressure to 1.4 bar (20 psi) with vacuum applied.
- Vent to atmosphere and raise pressure to 6.2 bar (90 psi) (or max allowed by the core material).
- Increase air temperature at 2°C (3.6°F) /min and hold for 1 hour at 135°C (275°F).
- Allow to cool to 60°C (140°F) before removal of pressure.



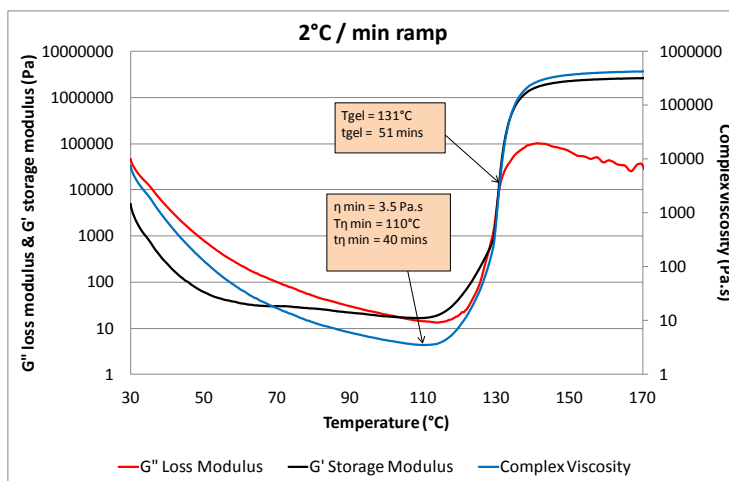
PRODUCT DATASHEET



TENCATE ADVANCED COMPOSITES

TenCate E745

Mid temperature curing modified epoxy resin component prepreg



CURE PROPERTIES: VISCOSITY PROFILE (30°C TO 170°C OR 86°F TO 338°F)

| Ramp rate [°C (°F)/min] | Min viscosity (Pa.s) | Temp @ min viscosity °C (°F) |
|-------------------------|----------------------|------------------------------|
| 0.5 (1) | 6.8 | 94 (201) |
| 1 (1.8) | 4.74 | 102 (216) |
| 2 (3.6) | 3.5 | 110 (230) |
| 5 (9) | 2.73 | 118 (244) |

PROCESSING

Following removal from refrigerated storage, allow the prepreg to reach room temperature before opening the polythene bag, to avoid moisture condensation. Typically the thaw time for a full roll of material will be 4 to 6 hours.

Cut patterns to size and lay up the laminate in line with design instructions taking care not to distort the prepreg. If necessary, the tack of the prepreg may be increased by gentle warming with hot air. The lay-up should be vacuum debulked at regular intervals using a P3 (pin pricked) release film on the prepreg surface, vacuum of 980 mbar (29 in Hg) is applied for 20 minutes.

For autoclave cures, use of a non-perforated release film on the prepreg surface trimmed to within 25-30mm of prepreg edge is recommended for the cure cycle, a vacuum bag should be installed using standard techniques.

EXOTHERM

In certain circumstances, such as the production of thick section laminates rapid heat up rates or highly insulating masters. TenCate E745 can undergo exothermic heating leading to rapid temperature rise and component degradation in extreme cases.

Where this is likely, a cure incorporating an intermediate dwell is recommended in order to minimize the risk.

Revised 08/2013

All data given is based on representative samples of the materials in question. Since the method and circumstances under which these materials are processed and tested are key to their performance, and TenCate Advanced Composites has no assurance of how its customers will use the material, the corporation cannot guarantee these properties.

Page 3 of 3

TENCATE_E745_V4_DS_082313

TENCATE ADVANCED COMPOSITES

Amber Drive, Langley Mill
Nottingham, NG16 4BE UK
Tel: +44 (0)1773 530899
Fax: +44 (0)1773 768687

Campbellweg 30
7443 PV Nijverdal NL
Tel: +31 548 633 933
Fax: +31 548 633 299

18410 Butterfield Blvd.
Morgan Hill, CA 95037 USA
Tel: +1 408 776 0700
Fax: +1 408 776 0107

www.tencate.com

www.tencateadvancedcomposites.com
www.tencateindustrialcomposites.com
E-mail: tcac-us@tencate.com (USA)
E-mail: ambersales@tencate.com (Europe)

ISO 9001
ISO 14001
Registered
AS 9100

| Product designation | | | | Compression | | Plate Shear | | | | | | | | |
|--|-----|------|-----|-----------------|-------|-----------------|------|----------------|-----|-----------------|------|----------------|-----|-----|
| | | | | | | L-direction | | | | W-direction | | | | |
| cell size-density mm kg/m ³ | | (µm) | | strength MPa | | strength MPa | | modulus MPa | | strength MPa | | modulus MPa | | |
| | | | | min | typ | min | typ | min | typ | min | typ | min | typ | |
| ECK | 3.2 | - | 40 | (36) | 1.40 | 1.83 | 1.25 | 1.41 | 80 | 121 | 0.70 | 0.86 | 40 | 62 |
| ECK | 3.2 | - | 48 | (36) | 2.20 | 2.75 | 1.50 | 1.74 | 90 | 119 | 0.90 | 1.08 | 55 | 66 |
| ECK | 3.2 | - | 48 | (46) | 1.90 | 2.41 | 1.70 | 1.95 | 110 | 172 | 0.95 | 1.18 | 65 | 73 |
| ECK | 3.2 | - | 64 | (36) | 4.30 | 5.17 | 2.15 | 2.52 | 115 | 128 | 1.10 | 1.83 | 60 | 70 |
| ECK | 3.2 | - | 72 | (46) | 4.55 | 5.59 | 2.45 | 2.92 | 135 | 183 | 1.46 | 1.79 | 90 | 108 |
| ECK | 3.2 | - | 96 | (46) | 6.50 | 9.39 | 3.00 | 3.55 | 150 | 188 | 1.90 | 2.24 | 95 | 118 |
| ECK | 4.0 | - | 72 | (46) | 5.25 | 6.53 | 2.50 | 2.91 | 140 | 172 | 1.35 | 1.58 | 70 | 96 |
| ECK | 4.0 | - | 96 | (71) | 7.60 | 9.17 | 3.45 | 4.11 | 195 | 264 | 1.95 | 2.28 | 90 | 120 |
| ECK | 4.8 | - | 28 | (36) | 0.80 | 1.03 | 0.70 | 0.82 | 50 | 69 | 0.40 | 0.52 | 25 | 36 |
| ECK | 4.8 | - | 32 | (36) | 0.95 | 1.43 | 0.80 | 0.99 | 60 | 71 | 0.52 | 0.60 | 25 | 40 |
| ECK | 4.8 | - | 37 | (36) | 1.55 | 1.99 | 0.90 | 1.10 | 60 | 67 | 0.62 | 0.78 | 35 | 44 |
| ECK | 4.8 | - | 48 | (46) | 2.45 | 3.02 | 1.50 | 1.75 | 90 | 112 | 0.87 | 1.06 | 50 | 69 |
| ECK | 4.8 | - | 144 | (99) | 13.40 | 17.50 | 4.35 | 5.60 | 210 | 330 | 2.50 | 3.70 | 135 | 195 |
| ECK-R | 4.8 | - | 32 | (36) | 0.87 | 1.27 | 0.40 | 0.51 | 25 | 36 | 0.52 | 0.68 | 46 | 56 |
| ECK-R | 4.8 | - | 32 | (46) | 0.47 | 1.17 | 0.37 | 0.68 | 36 | 59 | 0.45 | 0.67 | 41 | 70 |
| ECK-R | 4.8 | - | 48 | (46) | 1.84 | 2.69 | 0.87 | 1.23 | 41 | 64 | 0.95 | 1.22 | 59 | 90 |
| ECK-R | 4.8 | - | 64 | (46) | 3.21 | 4.21 | 1.37 | 1.79 | 46 | 70 | 1.44 | 1.77 | 77 | 110 |
| ECK-R | 4.8 | - | 80 | (46) | 5.00 | 7.00 | 1.50 | 1.80 | 55 | 75 | 2.1 | 2.2 | 115 | 120 |

This table presents guarantee values of ECK honeycomb produced with DuPont® N636 paper and obtained from testing specimens of 12.7mm thickness at RT. Data is based on results gained from experience and tests and is believed to be accurate yet without acceptance of liability for loss or damage incurred and attributable to reliance thereon as conditions of use lie outside our control.

We reserve the right for technical changes without further notice. Our general terms of sales and delivery apply.

A11: Insert Calculation spreadsheet

| | A | B | C | D | E | F | G | H | I | J | K | L | M | N | O | P | Q | R | S |
|----|---|---|---|---|---|---|---|--------------------|--------|---|---|---|---|---|---|---|---|---|---|
| 2 | | | | | | | | | | | | | | | | | | | |
| 3 | | | | | | | | | Modell | | | | | | | | | | |
| 4 | | | | | | | | HX-FC 5056/F40-2.1 | | | | | | | | | | | |
| 5 | | | | | | | | Select from list | | | | | | | | | | | |
| 6 | | | | | | | | | | | | | | | | | | | |
| 7 | | | | | | | | | | | | | | | | | | | |
| 8 | | | | | | | | | | | | | | | | | | | |
| 9 | | | | | | | | | | | | | | | | | | | |
| 10 | | | | | | | | | | | | | | | | | | | |
| 11 | | | | | | | | | | | | | | | | | | | |
| 12 | | | | | | | | | | | | | | | | | | | |
| 13 | | | | | | | | | | | | | | | | | | | |
| 14 | | | | | | | | | | | | | | | | | | | |
| 15 | | | | | | | | | | | | | | | | | | | |
| 16 | | | | | | | | | | | | | | | | | | | |
| 17 | | | | | | | | | | | | | | | | | | | |
| 18 | | | | | | | | | | | | | | | | | | | |
| 19 | | | | | | | | | | | | | | | | | | | |
| 20 | | | | | | | | | | | | | | | | | | | |
| 21 | | | | | | | | | | | | | | | | | | | |
| 22 | | | | | | | | | | | | | | | | | | | |
| 23 | | | | | | | | | | | | | | | | | | | |
| 24 | | | | | | | | | | | | | | | | | | | |
| 25 | | | | | | | | | | | | | | | | | | | |
| 26 | | | | | | | | | | | | | | | | | | | |
| 27 | | | | | | | | | | | | | | | | | | | |
| 28 | | | | | | | | | | | | | | | | | | | |
| 29 | | | | | | | | | | | | | | | | | | | |
| 30 | | | | | | | | | | | | | | | | | | | |
| 31 | | | | | | | | | | | | | | | | | | | |
| 32 | | | | | | | | | | | | | | | | | | | |
| 33 | | | | | | | | | | | | | | | | | | | |
| 34 | | | | | | | | | | | | | | | | | | | |
| 35 | | | | | | | | | | | | | | | | | | | |

Tension Pull-out

Shear

Bending Rotation

Torque

| Load case | Force |
|--------------|----------|
| Out of plane | P = 0 N |
| Shear | Q = 0 N |
| Bending | M = 0 Nm |
| Torque | T = 0 Nm |

| Modell | Hexply |
|------------------|------------------|
| Select from list | Select from list |

| Skin data | |
|-----------------------------|--------|
| E1 [Mpa] | 62500 |
| E2 [Mpa] | 62500 |
| G12 [Mpa] | 2840 |
| v12 | 0,08 |
| v21 | 0,08 |
| Ply thickness [mm] | 0,3 |
| Weight [kg/m ²] | 33,642 |
| Cell size [mm] | 7,62 |

| Compressive strength [MPa] | Plate shear L modulus [GPa] | Plate shear L strength [MPa] | Plate shear W modulus [GPa] | Plate shear W strength [MPa] |
|----------------------------|-----------------------------|------------------------------|-----------------------------|------------------------------|
| 1,65 | 0,12 | 0,38 | 0,07 | 0,38 |
| 448,18 | 0,72 | 0,72 | 0,07 | 0,72 |

| Compressive modulus [MPa] | Compressive strength [MPa] | EI [Mpa] | E2 [Mpa] | G12 [Mpa] | v12 | v21 | Ply thickness [mm] | Weight [g/m ²] | Tensile Strength [Mpa] | Compressive strength [Mpa] |
|---------------------------|----------------------------|----------|----------|-----------|------|------|--------------------|----------------------------|------------------------|----------------------------|
| 62500 | 62500 | 62500 | 62500 | 2840 | 0,08 | 0,08 | 0,3 | 33,642 | 438 | 920 |

Combined loads

$$\left(\frac{P}{F_{critL}}\right)^2 + \left(\frac{Q}{Q_{crit,unarm}}\right)^2 + \left(\frac{M}{M_{crit}}\right)^2 + \left(\frac{T}{T_{crit}}\right)^2 \leq 1$$

| Insert calculations | |
|----------------------------|----------------------------|
| Bearing coefficient | $K_b = 2,2$ |
| Dimpling coefficient | $K_D = 2$ |
| Shear strength, cell walls | $\tau_0 = 200$ MPa |
| Foil thickness, core | $t_f = 0,036$ mm |
| Effective Shear Modulus | $G_c^* = 22,983$ MPa |
| Effective Shear Strength | $\tau_{c,eff} = 0,516$ MPa |
| Minimum potting radius | $b_{p,min} = 26,484$ mm |
| Typical potting radius | $b_{p,typ} = 29,596$ mm |
| Real potting radius, min | $b_{p,min} = 26,167$ mm |
| Real potting radius, typ | $b_{p,typ} = 27,31$ mm |
| Dist. between facesheets | $d = 20,6$ mm |
| $E^* = \sqrt{E1 \cdot E2}$ | $E = 62500,0$ MPa |

| Thickness [mm] | Angle |
|----------------|--------------|
| 90 | INPUT |
| 45 | INPUT |
| 0 | INPUT |
| 0 | INPUT |
| 20 | INPUT |
| 0 | INPUT |
| 0 | INPUT |
| 0 | INPUT |
| 45 | INPUT |
| 90 | INPUT |
| Sum | 21,20 |

| Out of plane capacity | Shear capacity | Dimpling capacity | In-plane bearing capacity | Bending capacity | Torsional capacity |
|-----------------------|------------------------------|-------------------|---------------------------|----------------------|----------------------|
| $P_{crit} = 1767,9$ N | $Q_{crit,unarm} = 29238,2$ N | $Q_d = 7890,2$ N | $Q_b = 18168,1$ N | $M_{crit} = 41,2$ Nm | $T_{crit} = 62,0$ Nm |

| Outerskin |
|-----------------|
| $b_1 = 23,5$ mm |

Used capacity

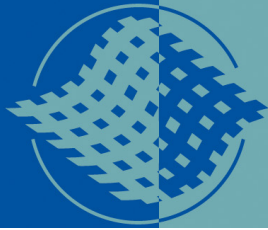
0%

A12: Failure modes

| # | A | B | C | D | E | F | G | H | I | J | K | L | M | N | O | P | Q | R | S | T | U | V | W | X | Y | Z |
|----|------------|---------|--------|------------|------------|---------|----------|---------|------|---------|---------|---------|-----------|-------------|-------------|-------------|-------------|-------------|-------------|------------|-------------|-------------|-------------|-------------|-------------|-------------|
| 1 | Core Model | Density | Total | Total | Core | Core | Cellsize | Faceshe | Core | modulus | shear | Core | modulus | shear | Core | modulus | shear | Core | modulus | shear | Core | modulus | shear | Core | modulus | shear |
| 2 | F40 | 2.1 | 33.642 | 8 | 45234.8974 | 448 | 68.95 | 7.62 | 1.2 | 30 | 31.2 | 0.10093 | 0.256 | 0.356926 | 1.2565119 | 528.0015020 | 430048 | 59.83905983 | 0.57438974 | 2.77993226 | 3324317819 | 9313745312 | 208588.3443 | 413700 | 558.9830457 | 2258.107284 |
| 3 | 2.1 | 33.642 | 6 | 45234.8974 | 448 | 68.95 | 7.62 | 0.9 | 31 | 31.9 | 0.10429 | 0.192 | 0.2962902 | 1.841016701 | 528.0015020 | 430048 | 59.83905983 | 0.57438974 | 2.77993226 | 3324317819 | 9313745312 | 208588.3443 | 413700 | 558.9830457 | 2258.107284 | |
| 4 | 2.1 | 33.642 | 4 | 45234.8974 | 448 | 68.95 | 7.62 | 0.6 | 32 | 32.6 | 0.10765 | 0.128 | 0.2356544 | 1.189898933 | 2884.403072 | 449554 | 114.5194274 | 0.546969352 | 4.18979372 | 2205259403 | 9358033459 | 113868.303 | 441280 | 558.9830457 | 564.5268209 | |
| 5 | 2.1 | 33.642 | 2 | 45234.8974 | 448 | 68.95 | 7.62 | 0.3 | 33 | 33.3 | 0.11402 | 0.064 | 0.1750186 | 0.576479777 | 1504.812715 | 459207 | 224.2242242 | 0.538138138 | 7.105960506 | 1900286653 | 7424.19668 | 59406.59104 | 455070 | 558.9830457 | 141.1370762 | |
| 6 | 3.1 | 49.662 | 8 | 54696.1696 | 862 | 89.635 | 7.62 | 1.2 | 30 | 31.2 | 0.14899 | 0.256 | 0.404966 | 1.78282355 | 6389215761 | 599322 | 59.83905983 | 0.57438974 | 2.77993226 | 3324317819 | 9313745312 | 208588.3443 | 413700 | 558.9830457 | 2258.107284 | |
| 7 | 3.1 | 49.662 | 6 | 54696.1696 | 862 | 89.635 | 7.62 | 0.9 | 31 | 31.9 | 0.15395 | 0.192 | 0.345932 | 1.247140246 | 500843219 | 5718713 | 78.02159526 | 0.56175486 | 2.1690415 | 3526566395 | 10195796700 | 197750.2249 | 555737 | 808.3831856 | 183.855659 | |
| 8 | 3.1 | 49.662 | 4 | 54696.1696 | 862 | 89.635 | 7.62 | 0.6 | 32 | 32.6 | 0.13892 | 0.128 | 0.2869184 | 0.805444807 | 3487374069 | 58420.2 | 114.5194274 | 0.546969352 | 4.18979372 | 2205259403 | 9358033459 | 113868.303 | 441280 | 558.9830457 | 564.5268209 | |
| 9 | 3.1 | 49.662 | 2 | 54696.1696 | 862 | 89.635 | 7.62 | 0.3 | 33 | 33.3 | 0.16388 | 0.064 | 0.2278945 | 0.35518694 | 1811561064 | 596699.1 | 224.2242242 | 0.538138138 | 7.105960506 | 1900286653 | 7424.19668 | 59406.59104 | 455070 | 558.9830457 | 141.1370762 | |
| 10 | 4.1 | 65.682 | 8 | 64524.8974 | 1276 | 117.215 | 7.62 | 1.2 | 30 | 31.2 | 0.19705 | 0.256 | 0.453046 | 1.299189022 | 528.0015020 | 731421.6 | 59.83905983 | 0.57438974 | 2.77993226 | 3324317819 | 9313745312 | 208588.3443 | 413700 | 558.9830457 | 2258.107284 | |
| 11 | 4.1 | 65.682 | 6 | 64524.8974 | 1276 | 117.215 | 7.62 | 0.9 | 31 | 31.9 | 0.20861 | 0.192 | 0.3956142 | 0.94959774 | 414.8833553 | 747831.7 | 78.02159526 | 0.56175486 | 2.8330483 | 3726117356 | 87273232736 | 163546.9068 | 726739 | 945.6690223 | 1270.185347 | |
| 12 | 4.1 | 65.682 | 4 | 64524.8974 | 1276 | 117.215 | 7.62 | 0.6 | 32 | 32.6 | 0.21018 | 0.128 | 0.3381824 | 0.608994854 | 2884.403072 | 764241.8 | 114.5194274 | 0.546969352 | 4.18979372 | 2205259403 | 9358033459 | 113868.303 | 441280 | 558.9830457 | 564.5268209 | |
| 13 | 4.1 | 65.682 | 2 | 64524.8974 | 1276 | 117.215 | 7.62 | 0.3 | 33 | 33.3 | 0.21675 | 0.064 | 0.2807506 | 0.29327032 | 1504.812715 | 860511.9 | 224.2242242 | 0.538138138 | 7.105960506 | 1900286653 | 7424.19668 | 59406.59104 | 455070 | 558.9830457 | 141.1370762 | |
| 14 | F80 | 4.3 | 68.896 | 8 | 54696.1696 | 1345 | 137.9 | 3.81 | 1.2 | 30 | 31.2 | 0.20666 | 0.256 | 0.462658 | 1.238716025 | 6389215761 | 879802 | 78.02159526 | 0.56175486 | 2.3485607 | 393447124 | 9700830660 | 197753.9763 | 854980 | 1082.391797 | 6143.422835 |
| 15 | 4.3 | 68.896 | 6 | 54696.1696 | 1345 | 137.9 | 3.81 | 0.9 | 31 | 31.9 | 0.21355 | 0.192 | 0.4055466 | 0.89910118 | 500843219 | 879802 | 78.02159526 | 0.56175486 | 2.3485607 | 393447124 | 9700830660 | 197753.9763 | 854980 | 1082.391797 | 6143.422835 | |
| 16 | 4.3 | 68.896 | 4 | 54696.1696 | 1345 | 137.9 | 3.81 | 0.6 | 32 | 32.6 | 0.22044 | 0.128 | 0.3484352 | 0.500669512 | 3487374069 | 899108 | 114.5194274 | 0.546969352 | 4.18979372 | 2205259403 | 9358033459 | 113868.303 | 441280 | 558.9830457 | 564.5268209 | |
| 17 | 4.3 | 68.896 | 2 | 54696.1696 | 1345 | 137.9 | 3.81 | 0.3 | 33 | 33.3 | 0.22732 | 0.064 | 0.2913238 | 0.281536733 | 1811561064 | 918414 | 224.2242242 | 0.538138138 | 7.105960506 | 1900286653 | 7424.19668 | 59406.59104 | 455070 | 558.9830457 | 141.1370762 | |
| 18 | 5 | 104.13 | 8 | 72926.2576 | 2827 | 220.64 | 3.81 | 1.2 | 30 | 31.2 | 0.31239 | 0.256 | 0.56889 | 0.81948846 | 528.0015020 | 103255.2 | 59.83905983 | 0.57438974 | 2.17809177 | 4242054194 | 7463280835 | 208597.7983 | | | | |
| 19 | 5 | 104.13 | 6 | 72926.2576 | 2827 | 220.64 | 3.81 | 0.9 | 31 | 31.9 | 0.3228 | 0.192 | 0.514803 | 0.594790011 | 414.8833553 | 105762.4 | 78.02159526 | 0.56175486 | 2.6593253 | 3486197762 | 6771906460 | 163548.5419 | | | | |
| 20 | 5 | 104.13 | 4 | 72926.2576 | 2827 | 220.64 | 3.81 | 0.6 | 32 | 32.6 | 0.3332 | 0.128 | 0.461216 | 0.384135216 | 2884.403072 | 1078929.6 | | | | | | | | | | |
| 21 | 5 | 104.13 | 2 | 72926.2576 | 2827 | 220.64 | 3.81 | 0.3 | 33 | 33.3 | 0.34363 | 0.064 | 0.407629 | | | | | | | | | | | | | |
| 22 | 8 | 128.16 | 8 | 72926.2576 | 2827 | 220.64 | 3.81 | 1.2 | 30 | 31.2 | 0.38448 | 0.256 | 0.64048 | | | | | | | | | | | | | |
| 23 | 8 | 128.16 | 6 | 72926.2576 | 2827 | 220.64 | 3.81 | 0.9 | 31 | 31.9 | 0.3973 | | | | | | | | | | | | | | | |
| 24 | 8 | 128.16 | 4 | 72926.2576 | 2827 | 220.64 | 3.81 | | | | | | | | | | | | | | | | | | | |
| 25 | 8 | 128.16 | 2 | 72926.2576 | 2827 | 220.64 | 3.81 | | | | | | | | | | | | | | | | | | | |
| 26 | WF | 51 | 52 | 8 | 54696.1696 | 75 | 24 | 0 | 1.2 | 30 | 31.2 | 0.1516 | 0.256 | 0.412 | 1.641025641 | 6089312715 | 149760 | 59.83905983 | 0.57438974 | 2.40752727 | 2096319040 | 5088153010 | 252167.9439 | #DIV/0! | | |
| 27 | 51 | 52 | 6 | 54696.1696 | 75 | 24 | 0 | 0.9 | 31 | 31.9 | 0.1612 | | | | | | | | | | | | | | | |
| 28 | 51 | 52 | 4 | 54696.1696 | 75 | 24 | 0 | | | | | | | | | | | | | | | | | | | |
| 29 | 51 | 52 | 2 | 54696.1696 | 75 | 24 | 0 | | | | | | | | | | | | | | | | | | | |
| 30 | 71 | 75 | 8 | 45234.8974 | 105 | 40 | 0 | 1.2 | 30 | 31.2 | 0.225 | | | | | | | | | | | | | | | |
| 31 | 71 | 75 | 6 | 45234.8974 | 105 | 40 | 0 | | | | | | | | | | | | | | | | | | | |
| 32 | 71 | 75 | 4 | 45234.8974 | 105 | 40 | 0 | | | | | | | | | | | | | | | | | | | |
| 33 | 71 | 75 | 2 | 45234.8974 | 105 | 40 | 0 | | | | | | | | | | | | | | | | | | | |
| 34 | 110 | 110 | 8 | 72926 | 45E+09 | 4E+09 | 40 | 0 | 1.2 | 30 | 31.2 | 0.2425 | | | | | | | | | | | | | | |
| 35 | 110 | 110 | 6 | 72926 | 4E+09 | 4E+09 | 40 | 0 | 0.9 | | | | | | | | | | | | | | | | | |
| 36 | 110 | 110 | 4 | 72926 | 3E+09 | 3E+09 | 40 | 0 | | | | | | | | | | | | | | | | | | |
| 37 | 110 | 110</ | | | | | | | | | | | | | | | | | | | | | | | | |

A 13: Suspension Reaction forces

| Chassis reaction forces | 3g bump | | | 2g turn | | | 2g turn 2g bump | | | 2g brake | | | 2g brake 2g bump | | | |
|-------------------------|---------|------|------|---------|------|------|-----------------|------|------|----------|------|------|------------------|------|------|------|
| | X | Y | Z | X | Y | Z | X | Y | Z | X | Y | Z | X | Y | Z | |
| Front upper fore | -789 | 1629 | 333 | -158 | 326 | 67 | -421 | 869 | 178 | 1363 | 2815 | 575 | - | 1627 | 3359 | 687 |
| Front upper aft | 1812 | 5190 | 1061 | 781 | 2238 | 457 | 1385 | 3970 | 812 | 411 | 1178 | 241 | 1016 | 2911 | 595 | |
| Front lower fore | 43 | -117 | -9 | -618 | 1688 | 131 | -604 | 1648 | 128 | 1734 | 4733 | -367 | - | 1747 | 4772 | -370 |
| Front lower aft | -88 | -279 | -22 | 616 | 1946 | 151 | 586 | 1854 | 144 | 1567 | 4954 | 384 | 1537 | 4862 | 377 | |
| Rear upper fore | 2349 | 3717 | 884 | -899 | 1423 | 338 | 1682 | 2662 | 633 | 849 | 1344 | 320 | - | 1631 | 2581 | 614 |
| Rear upper aft | 1277 | 2912 | 692 | 240 | 546 | 130 | 666 | 1518 | 361 | -20 | -45 | -11 | 406 | 925 | 220 | |
| Rear lower fore | 254 | -494 | -43 | -593 | 1154 | 101 | -508 | 989 | 87 | 895 | 1742 | -153 | - | 979 | 1906 | -167 |
| Rear lower aft | -5 | -15 | -1 | 650 | 1955 | 171 | 648 | 1950 | 171 | 461 | 1386 | 121 | 459 | 1381 | 121 | |
| Front bellcrank pivot | 3100 | 6474 | 3166 | 1868 | 3902 | 1908 | 2903 | 6062 | 2965 | 1772 | 3701 | 1810 | 2807 | 5861 | 2867 | |
| Rear bellcrank pivot | 3233 | 6086 | 3557 | 1887 | 3553 | 2076 | 2966 | 5582 | 3262 | 633 | 1192 | -697 | - | 1710 | 3218 | 1881 |
| Front damper | 2118 | 0 | 0 | 1276 | 0 | 0 | 1983 | 0 | 0 | 1211 | 0 | 0 | 1918 | 0 | 0 | |
| Rear damper | 2403 | 0 | 0 | 1403 | 0 | 0 | 2204 | 0 | 0 | -471 | 0 | 0 | - | 1271 | 0 | 0 |
| Steering rod | 4 | 51 | 5 | -29 | -407 | -41 | -28 | -390 | -39 | -37 | -513 | -51 | -36 | -496 | -49 | |
| Tie rod | -7 | 34 | -3 | 118 | 575 | 50 | 116 | 563 | 49 | 51 | 249 | 22 | 49 | 238 | 21 | |



HexPly® 6376C-905-36%

Epoxy Matrix

Product Data Sheet

Description

HexPly® 6376C-905-36% is a Epoxy High Strength Carbon Woven prepreg, whereby 6376 is the resin type; 36% is the resin content by weight; 905 is the reinforcement reference and C represents High Strength Carbon fibre. This data sheet is complementary to the 6376 resin data sheet, which should be consulted for additional information.

Reinforcement Data

| | | | | |
|-----------------------|-------------------|-------------------------|-----|-----|
| Nominal Area Weight | g/m ² | 280 | 0° | 90° |
| Composition | | 5H satin | 140 | 140 |
| Fibre Type | | High Strength Carbon 3K | | |
| Nominal Fibre Density | g/cm ³ | 1,77 | | |

Matrix Properties

| | | |
|--|-------------------|--------------------------------------|
| Glass transition temperature of laminate (Cure cycle: 120min @ 175°C) | °C | 196 (DMA onset, 5°C/min, 1Hz, 30µm), |
| Nominal Resin Density | g/cm ³ | 1,31 |

Prepreg Data

| | | |
|-----------------------|------------------|--------|
| Nominal Area Weight | g/m ² | 438 |
| Nominal Resin Content | weight % | 36 |
| Tack Level | | Medium |

Processing

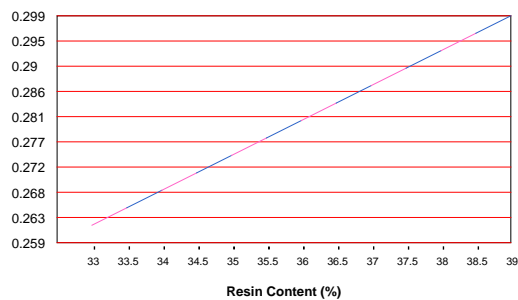
| | | |
|--------------------------|----------|-------------|
| Cure Cycle | @ 175 °C | 120 min |
| Recommended heat up rate | °C/min | 2 - 5°C/min |
| Pressure gauge | bar | 7 |

The optimum cure cycle, heat up rate and dwell period depend on part size, laminate construction, oven capacity and thermal mass of tool. (See prepreg technology brochure on our website for more information),

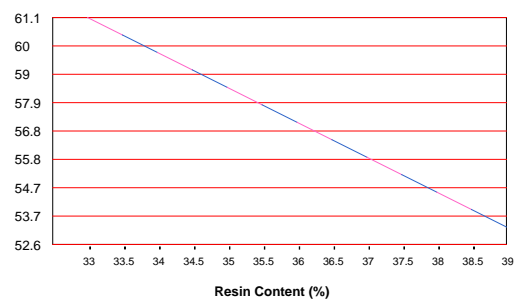
Cured Laminate Properties

(nominal composite density 1,57 g/cm³)

RESIN CONTENT % vs CURED PLY THICKNESS



RESIN CONTENT % vs FIBRE VOLUME %



The above graphs enable the fibre volume content of a laminate to be estimated using the measured cured ply thickness. The calculation assumes no resin loss.



HexPly® 6376C-905-36%

Mechanical Properties

(Normalised to 60% fibre volume, except for ILSS)

Mechanical Properties are based on 175 °C cure for 120 min, at 7 bar pressure and 0,9 bar vacuum.

Data is the result from several tests on Autoclave cured laminates. Some of the values achieved will have been higher, and some lower, than the figure quoted. These are nominal values.

| Warp (RT / Dry) | Tensile | Flexural | ILSS | Compression |
|-----------------|---------|----------|---------|-------------|
| Strength (MPa) | 1006 | - | 83 | 920 |
| Modulus (GPa) | 67 | - | . | - |
| Test Method | EN 2561 | | EN 2563 | EN 2850 |

Prepreg Storage Life

Shelf Life¹: 6 months at -18°C/0°F (from date of manufacture).

¹ Shelf Life: the maximum storage life for HexPly® prepreg, when stored continuously, in a sealed moisture-proof bag, at -18°C/0°F or 5°C/41°F. To accurately establish the exact expiry date, consult the box label.

Out Life²: 21 days at Room Temperature.

² Out Life: the maximum accumulated time allowed at room temperature between removal from the freezer and cure.

Tack Life³: 10 days at Room Temperature.

³ Tack Life: the time, at room temperature, during which prepreg retains enough tack for easy component lay-up.

Prepreg should be stored as received in a cool dry place or in a refrigerator. After removal from refrigerator storage, prepreg should be allowed to reach room temperature before opening the polyethylene bag, thus preventing condensation. (A full reel in its packing can take up to 48 hours).

Precautions for Use

The usual precautions when handling uncured synthetic resins and fine fibrous materials should be observed, and a Safety Data Sheet is available for this product. The use of clean disposable inert gloves provides protection for the operator and avoids contamination of material and components.

Important

All information is believed to be accurate but is given without acceptance of liability. All users should make their own assessment of the suitability of any product for the purposes required. All sales are made subject to our standard terms of sale which include limitations on liability and other terms

© Copyright Hexcel Corporation
HexPly® | 6376C-905-36% | 12/2005 | version : a